NAVAL POSTGRADUATE SCHOOL

MONTEREY, CALIFORNIA

THESIS

NEUTRON PROTECTION FACTOR DETERMINATION AND VALIDATION FOR A VEHICLE SURROGATE USING A CALIFORNIUM FISSION SOURCE

by

Jacob D. Glesmann

June 2017

Thesis Advisor: Joseph Hooper
Co-Advisor: Craig Smith

THIS PAGE INTENTIONALLY LEFT BLANK

REPORT DOCUMENTATION PAGE			*Form Approved OMB No. 0704-0188*
Public reporting burden for this collection of information is estimated to average 1 hour per response, including the time for reviewing instruction, searching existing data sources, gathering and maintaining the data needed, and completing and reviewing the collection of information. Send comments regarding this burden estimate or any other aspect of this collection of information, including suggestions for reducing this burden, to Washington headquarters Services, Directorate for Information Operations and Reports, 1215 Jefferson Davis Highway, Suite 1204, Arlington, VA 22202-4302, and to the Office of Management and Budget, Paperwork Reduction Project (0704-0188) Washington, DC 20503.			
1. AGENCY USE ONLY ***(Leave blank)***	**2. REPORT DATE** June 2017	**3. REPORT TYPE AND DATES COVERED** Master's thesis	
4. TITLE AND SUBTITLE NEUTRON PROTECTION FACTOR DETERMINATION AND VALIDATION FOR A VEHICLE SURROGATE USING A CALIFORNIUM FISSION SOURCE			**5. FUNDING NUMBERS**
6. AUTHOR(S) Jacob D. Glesmann			
7. PERFORMING ORGANIZATION NAME(S) AND ADDRESS(ES) Naval Postgraduate School Monterey, CA 93943-5000			**8. PERFORMING ORGANIZATION REPORT NUMBER**
9. SPONSORING /MONITORING AGENCY NAME(S) AND ADDRESS(ES) N/A			**10. SPONSORING / MONITORING AGENCY REPORT NUMBER**
11. SUPPLEMENTARY NOTES The views expressed in this thesis are those of the author and do not reflect the official policy or position of the Department of Defense or the U.S. Government. IRB number ____N/A____.			
12a. DISTRIBUTION / AVAILABILITY STATEMENT Approved for public release. Distribution is unlimited.			**12b. DISTRIBUTION CODE**

13. ABSTRACT (maximum 200 words)

This thesis describes the work completed to determine and validate the neutron protection factor (NPF) of an armored vehicle surrogate using the Lawrence Livermore National Laboratory's (LLNL) Cf-252 Radiation Calibration Laboratory (RCL). The NPF, a component of the total radiation protection factor (RPF), is used to evaluate the inherent shielding and radiation protection of military personnel from a polyenergetic neutron source. When the NPF is properly combined with the Gamma Protection Factor (GPF), which characterizes the effect of an associated gamma environment, the resultant RPF provides essential information of the total radiation protection afforded by a vehicle or structure to personnel within. To increase personnel survivability, the Navy, Army and Defense Threat Reduction Agency (DTRA) are interested in NPFs for applications involving forward-deployed vehicles or vessels in environments where neutron radiation is present. Such radiation environments can be the result from the detonation of a nuclear weapon or radiological dispersal device, or the conditions following a non-weapon radiation accident calling for humanitarian or disaster-relief missions. NPFs are focused only on the neutron radiation environment and exclude other nuclear weapon effects, such as the thermal destruction zone or firestorms created by nuclear weapons. The results from the fluence measurements at LLNL's Calibration Facility were used to validate computational models, namely the MCNP-6 Monte Carlo code. Through validation, DTRA, the Navy, and the other military services can use computational codes for determining NPFs for a diverse fleet of military vehicles.

14. SUBJECT TERMS radiation protection, radiation shielding, radiation protection factor, neutron protection factor, gamma protection factor, radiation dosimetry, fluence to dose conversion coefficients, flux to dose conversion coefficients.			**15. NUMBER OF PAGES** 209
			16. PRICE CODE
17. SECURITY CLASSIFICATION OF REPORT Unclassified	**18. SECURITY CLASSIFICATION OF THIS PAGE** Unclassified	**19. SECURITY CLASSIFICATION OF ABSTRACT** Unclassified	**20. LIMITATION OF ABSTRACT** UU

NSN 7540-01-280-5500 Standard Form 298 (Rev. 2-89)
Prescribed by ANSI Std. 239-18

THIS PAGE INTENTIONALLY LEFT BLANK

Approved for public release. Distribution is unlimited.

NEUTRON PROTECTION FACTOR DETERMINATION AND VALIDATION FOR A VEHICLE SURROGATE USING A CALIFORNIUM FISSION SOURCE

Jacob D. Glesmann
Ensign, United States Navy
B.S., United States Naval Academy, 2016

Submitted in partial fulfillment of the
requirements for the degree of

MASTER OF SCIENCE IN MECHANICAL ENGINEERING

from the

NAVAL POSTGRADUATE SCHOOL
June 2017

Approved by: Joseph Hooper
Thesis Advisor

Craig Smith
Co-Advisor

Garth Hobson
Chair, Department of Mechanical and Aerospace Engineering

THIS PAGE INTENTIONALLY LEFT BLANK

ABSTRACT

This thesis describes the work completed to determine and validate the neutron protection factor (NPF) of an armored vehicle surrogate using the Lawrence Livermore National Laboratory's (LLNL) Cf-252 Radiation Calibration Laboratory (RCL). The NPF, a component of the total radiation protection factor (RPF), is used to evaluate the inherent shielding and radiation protection of military personnel from a polyenergetic neutron source. When the NPF is properly combined with the Gamma Protection Factor (GPF), which characterizes the effect of an associated gamma environment, the resultant RPF provides essential information of the total radiation protection afforded by a vehicle or structure to personnel within. To increase personnel survivability, the Navy, Army and Defense Threat Reduction Agency (DTRA) are interested in NPFs for applications involving forward-deployed vehicles or vessels in environments where neutron radiation is present. Such radiation environments can be the result from the detonation of a nuclear weapon or radiological dispersal device, or the conditions following a non-weapon radiation accident calling for humanitarian or disaster-relief missions. NPFs are focused only on the neutron radiation environment and exclude other nuclear weapon effects, such as the thermal destruction zone or firestorms created by nuclear weapons. The results from the fluence measurements at LLNL's Calibration Facility were used to validate computational models, namely the MCNP-6 Monte Carlo code. Through validation, DTRA, the Navy, and the other military services can use computational codes for determining NPFs for a diverse fleet of military vehicles.

THIS PAGE INTENTIONALLY LEFT BLANK

TABLE OF CONTENTS

LIST OF FIGURES

LIST OF TABLES

THIS PAGE INTENTIONALLY LEFT BLANK

LIST OF ACRONYMS AND ABBREVIATIONS

AFIT	Air Force Institute of Technology
BRL	Ballistic Research Laboratory
BSS	Bonner Sphere Spectrometer
DNA	Defense Nuclear Agency
DOD	United States Department of Defense
DOT	Discrete Ordinates Transport
DTRA	Defense Threat Reduction Agency
FF	Free Field
GPF	Gamma Protection Factor
GRP	Glass Reinforced Plastic
ICRP	International Commission on Radiation Protection
ICRU	International Commission on Radiation Units
LANL	Los Alamos National Laboratory
LiI(Eu)	Lithium Iodide Europium Doped
LLD	Low Level Discriminator
LLNL	Lawrence Livermore National Laboratory
MASH	Monte Carlo Adjoint Shielding Code System
MCNP	Monte Carlo Neutral Particle Transport Code
MeV	Mega-Electron Volt
NPF	Neutron Protection Factor
NPS	Naval Postgraduate School
NSERC	Nuclear Science and Engineering Research Center
ORNL	Oak Ridge National Laboratory
PMT	Photomultiplier Tube
RCL	Radiation Calibration Laboratory
REM	Roentgen Equivalent Man
ROI	Region of Interest
RPF	Radiation Protection Factor
RSICC	Radiation Safety Information Computational Center
SV	Surrogate Vehicle

Sv	Sieverts
UMG v3.3	Unfolding with MAXED and GRAVEL Version 3.3
USANCA	United States Army Nuclear and Combating Weapons of Mass Destruction Agency
USMA	United States Military Academy
USNA	United States Naval Academy
VCS	Vehicle Code System
WSMR	White Sands Missile Range

ACKNOWLEDGMENTS

The research presented in this thesis produced significant data and results in the field of neutron protection factors. The success of this research is a direct result of the immense collaboration across a number of institutions that all shared a common goal. First and foremost, I would like to personally recognize my mentors Dr. Craig Smith and Major Andrew Decker, United States Army, for their guidance and mentorship throughout the master's program. It is because of their forethought that I was able to undertake such a large research goal and complete it within the allotted one-year program. Secondly, I would like to recognize Ms. Rebecca Becka Hudson and Mr. David Heinrichs at Lawrence Livermore National Laboratory for their incredible generosity of their time to ensure that I had all the tools I needed to succeed, even at a moment's notice. Lastly, I would like to recognize Dr. Luisa Hansen for her mentorship in the computational field of this research. Dr. Hansen maintained constant communication and feedback, and provided insight into efficiently designing the input files for the computational code.

The research was a combined effort that identifies the power that can be held in scientific collaboration, and the progress that can be made within such a short period. It is with much appreciation that I recognize the individuals for their availability, willingness to help, and resources they provided. There is no doubt that the experiences obtained over the course of this research have helped me develop personally and professionally, and I look forward to working with the members of this team again.

THIS PAGE INTENTIONALLY LEFT BLANK

I. INTRODUCTION

The threat of a nuclear incident or attack on the United States has escalated with the rise of hostile nation states seeking to acquire advanced nuclear weapons programs, and with the potential for non-state actors to obtain nuclear or radiological weapons. In the event of such an attack or radiological incident, understanding the degree to which U.S. military vehicles protect their occupants from the harmful effects of ionizing radiation would prove vital to the field commander. The United States Army quantifies protective radiation shielding with a value known as the radiation protection factor (RPF). The RPF is calculated based on the ratio of free field dose to the dose inside the vehicle or platform. Since neutrons and gamma rays are the most penetrating of all the radiation types, RPFs can be further explained through the use of neutron protection factors (NPFs) or gamma ray protection factors (GPFs). The greater the RPF, the more the attenuation provided by the protective walls of the vehicle or platform, and the lower the dose an individual would receive while inside the vehicle during a radiation exposure event.

During the Cold War, RPFs were measured using nuclear reactors located at Aberdeen Proving Grounds and White Sands Missile Range (WSMR), and these measurements were often used to validate legacy RPF computational codes [1], [2]. Today, RPFs can be estimated using the Monte Carlo Neutral-Particle (MCNP6.1) radiation transport code. Following the end of the Cold War, however, the DOD eliminated service requirements to determine RPF values for combat vehicles. Since then, the U.S. military has developed many new platforms and vehicles, such as tanks and other armored vehicles, personnel carriers, and vessels, for which RPF values are unknown. Without accurate determination of these vehicle RPFs, analyses cannot be accurately performed on the survivability of military crews in operations following a nuclear weapon or a radiological dispersal device detonation.

To fill this critical capability gap, the Defense Threat Reduction Agency (DTRA) recently identified MCNP6.1 radiation transport code as the optimal method for computationally determining RPF values today; however, the code must first undergo

extensive verification and validation for this purpose. Specifically, DTRA developed an experimental campaign plan to measure RPFs, as shown in Appendix A. Since 2014, DTRA has developed a methodology for experimentally and computationally determining NPFs and GPFs for a 0.61 meter (2') cubed surrogate vehicle, which is representative of a typical modern military vehicle. NPF and GPF values have been measured using the WSMR Fast Burst Reactor fission source, and these values have also been computed using MCNP6. Experiments performed at WSMR were conducted by measuring the neutron and gamma flux in the free field and within the surrogate vehicle at the same location. Based on the measured neutron and gamma fluence spectra, the free field and shielded dose values were determined and used to calculate NPF and GPF values. In order to validate the accuracy of MCNP6, these same experimental conditions were replicated using MCNP6, and the resultant computational estimates of NPF and GPF differed by less than 5% from the experimental results [1]–[3].

Ongoing research efforts are being made at several service academies and their respective postgraduate institutions. Efforts at the United States Military Academy (USMA) have been made with calculating GPFs using a phantom detector system [4]. The United States Naval Academy (USNA) produced NPFs for a 0.61 meter (2')-cube steel box using its deuterium-tritium neutron generator.[1] The Air Force Institute of Technology (AFIT) has supported several RPF determination experiments on a 0.61 meter (2')-cube iron surrogate [1], [2]. Currently the Naval Postgraduate School (NPS) is working in collaboration with Lawrence Livermore National Laboratory (LLNL) in determining and validating MCNP NPF estimates for a 0.61 meter (2') armored vehicle surrogate using LLNL's Radiation Calibration Laboratory (RCL).

In this thesis, the research validation process is presented through five chapters: Introduction, Background, NPF Determination, Results, and Conclusions. The first chapter provides the reader with introductory comments as well as basic background information on nuclear particle interactions and characteristics, dose calculation and

[1] Based on preliminary independent research I conducted for the United States Naval Academy and Department of Energy as part of the Bowman Scholarship Program. Results remain in an unpublished or pending status.

mechanisms, and RPF determination. Chapter II discusses the background and problem statement that was conceived starting in the 1950s and progressed into the 21st century. Chapter II is also intended to help the reader understand the scientific and historic basis for the standards and computational methods that are commonly used in present day for RPF determination. Chapter III discusses the methodology used in this research for experimental and computational determination of the NPF for a vehicle surrogate. The fourth chapter integrates all research components: code simulation, experimentation, NPF determination, error analysis, and code validation. It is in Chapter IV that the results of the NPS NPF determination are presented and compared. Conclusions, recommendations, and foreword are provided in Chapter V. The general structure of the research is presented in Figure 1 and is representative of the general timeline of NPF determination.

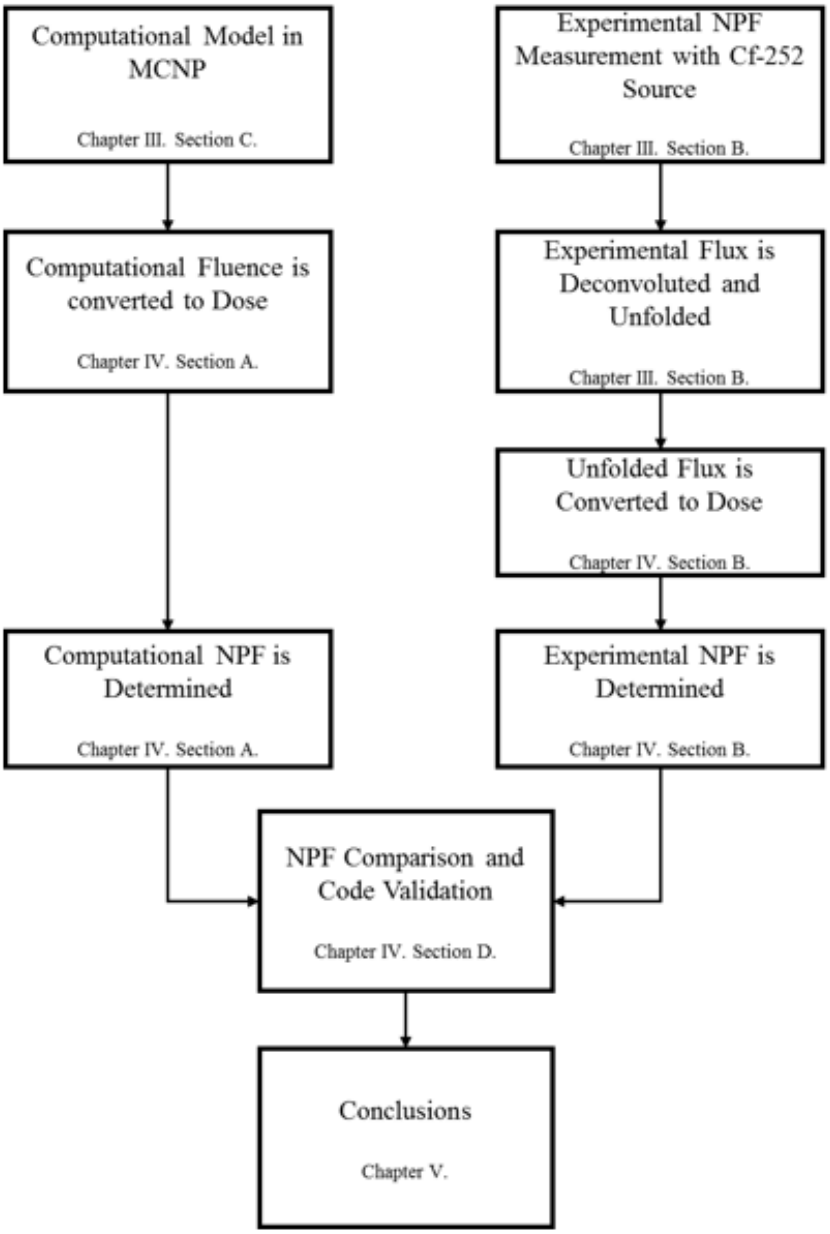

Figure 1. NPS Research Flow Diagram.

A. INTRODUCTION TO NEUTRON AND GAMMA INTERACTIONS

Particle interactions are at the forefront of any radiation discussion. Therefore, it is important to first understand the basic physical interactions that neutrons and photons have with the matter they traverse through to completely understand the complexity of the RPF, dose calculation, and computational methods of particle transport.

1. Photon (Gamma) Interactions

Photons are small packets of electromagnetic energy that contain both wave-like and particle-like properties, and are a function of space, time, and energy. While photons generally encompass a wide range of energy and wave-lengths, such as x-ray and gamma particles, the principal form of concern is gamma radiation. There are three primary modes of gamma interactions with matter: the photoelectric effect, Compton scattering, and pair production. The three, among others, are highly dependent on energy and material type, as depicted in Figure 2.

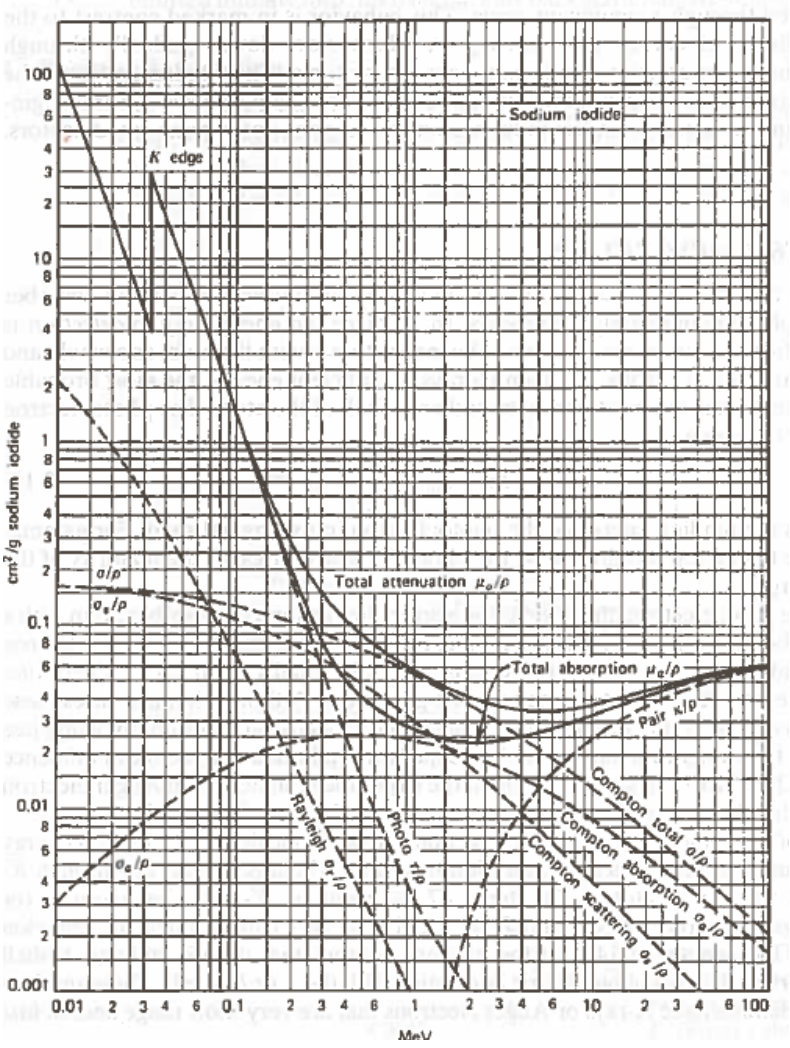

Figure 2. Photon Interactions with Matter Energy Dependency. Source: [5].

a. Photoelectric Effect

The Photoelectric Effect is the process in which an incident gamma particle is directly absorbed by a target atom. The target atom becomes excited and distributes the gamma's energy to its orbiting electrons. Once the electrons gain enough energy to surpass their binding energy, they separate becoming free—unbound—electrons. The residual energy is equivalent to the difference between the energy of the incident gamma particle and the electron's binding energy. The binding energy is described as the energy required by a specific energy state in order to maintain the connection between the electron and the respective atom.

b. Compton Scattering (Figure 3)

Compton Scattering is the process in which a gamma particle interacts with a target electron and is then scattered at some angle (θ). The electron recoils at an angle (φ) with some residual energy from the incident gamma particle. The amount of energy imparted by the gamma particle to the target electron is proportional to the scattering angle (θ); thus, for smaller scattering angles little energy is transferred. It is important to note that the incident gamma particle will always retain some amount of the original energy. In the event that incident gamma interacts with the electron and changes direction, but transfers no energy, coherent Compton Scattering has occurred.

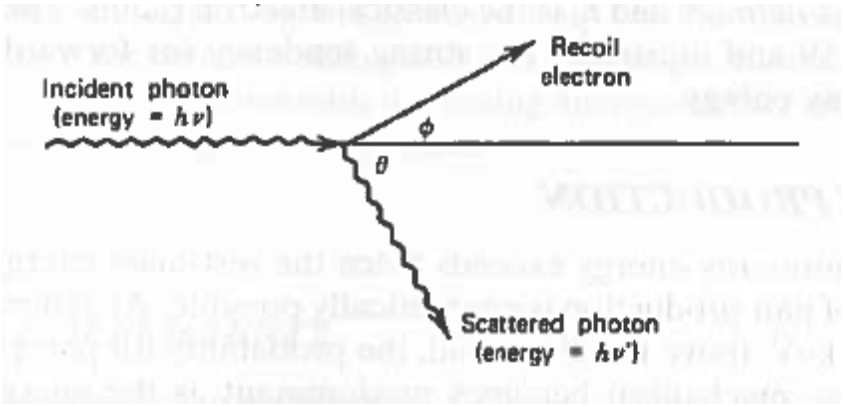

Figure 3. Compton Scattering Interaction with Target Electron. Source: [5].

c. Pair Production (Figure 4)

Pair Production is the process in which a high-energy gamma particle, at or greater than the rest-mass energy of two electrons (1.02 MeV), passes very closely to a target nucleus and splits into an electron-positron pair. Any residual energy above the 1.02 MeV amount is conserved as kinetic energy shared by both the electron and positron. The electron will continue to Compton scatter until it is absorbed in the medium, while the positron will meet another electron and annihilate.

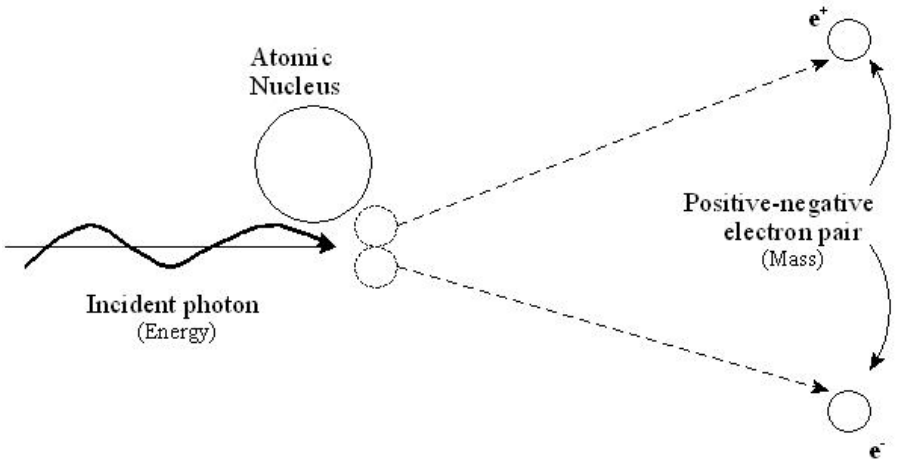

Figure 4. Pair Production Interaction with a Target Nucleus. Source: [6].

2. Neutron Interactions

Neutrons are similar to gammas in that they have no charge and are a function of energy, time, and space, and exhibit the same complexity introduced by wave-like properties. Because neutrons are neutral particles, they interact directly with atomic nuclei and not the surrounding electron cloud. Neutron interactions are directly a function of energy and particle cross-sections for a particular medium. Cross-sections are defined as the probability, or likelihood, that a neutron will undergo a certain reaction at a specific energy value. Combined with the lack of neutron interaction with a nucleus' electron cloud, more energetic neutrons tend to travel deep into materials. Neutron detection can be problematic at higher energies because cross-section values are orders of magnitudes lower, thus making it significantly inefficient. Moderation, or the slowing

down of neutrons through scattering interactions, allows for an increase in probability of absorption interaction and thus an increase in detection efficiency. More discussion on the detection mechanisms of the RPF campaign is provided later in Chapter III.

Neutrons can interact with matter in a variety of ways, but these can be grouped into two primary categories: scattering and absorption. Figure 5 shows a basic flow chart of possible neutron interactions from scatter and absorption.

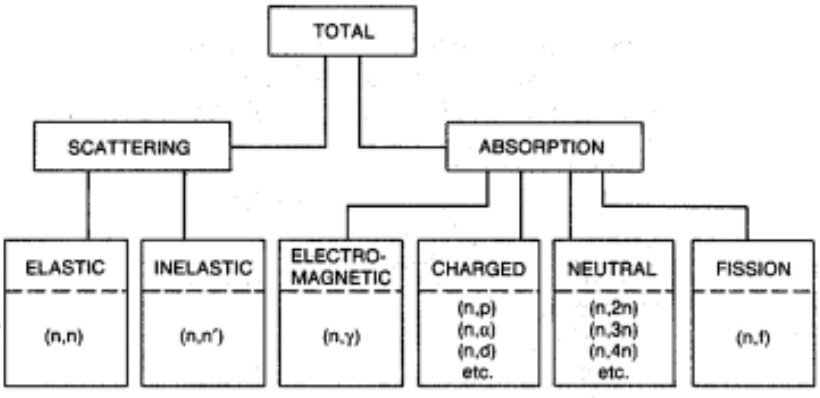

Figure 5. Flow Diagram of Neutron Interactions with Matter. Source: [7].

a. Absorption

Neutron absorption is the process in which the neutron is absorbed by the target nucleus. There are many reactions that result in an absorption process, but the most notable for the RPF campaign is the electromagnetic reaction. Fission, charged, and neutral reactions may occur but can generally be neglected because the probability of these interactions occurring within the materials used in the RPF campaign are extremely low compared to the electromagnetic reaction. The electromagnetic reaction depicted in Figure 5, occurs when a neutron is absorbed in the target nucleus and imparts its kinetic energy. The nucleus will rearrange itself and become excited, thus conserving energy through the release of a gamma particle of commensurate energy to return the electron to its normal state.

b. Scattering

Neutron scattering is a similar process to the gamma scattering described above, but it includes two different variations; inelastic and elastic scattering. During elastic scattering the target nucleus is struck by an incident neutron and the total kinetic energy of the system is unchanged (i.e., the combined kinetic energy of the scattered neutron and the recoil nucleus is the same as that of the incident particle). However, during inelastic scattering, the target nucleus is excited and imparts some residual kinetic energy into a newly formed gamma particle. The total amount of energy the neutron and nucleus contain after the reaction occurs will be less than the energy of the incoming incident neutron. Excited states of the target nucleus must exist in order for inelastic scattering to occur.

B. INTRODUCTION TO THE PROTECTION FACTOR

As aforementioned the Radiation Protection Factor (RPF) is the ratio of free field dose to the dose inside a vehicle or platform for a specified energy spectrum, whether as a result of a nuclear reactor incident or nuclear weapon detonation. Because neutrons and gammas are the most prolific and damaging forms of radiation from such events, the RPF is typically determined by combining the NPFs and GPFs of a particular energy field and application, as expressed below in Equations 1.1 through 1.3.

$$RPF = \frac{Total\ Dose\ in\ Free\ Field}{Total\ Dose\ with\ Surrogate\ Present} \tag{1.1}$$

$$NPF = \frac{Total\ Neutron\ Dose\ in\ Free\ Field}{Total\ Neutron\ Dose\ with\ Surrogate\ Present} \tag{1.2}$$

$$GPF = \frac{Total\ Gamma\ Dose\ in\ Free\ Field}{Total\ Gamma\ Dose\ with\ Surrogate\ Present} \tag{1.3}$$

The equations above reflect a weapon-source scenario, vice a reactor type scenario, and are applied to a vehicle surrogate test article. Because it is incredibly difficult to distinguish between secondary particles that result in higher quantities in reactor scenarios from incident fluxes, reactor applications use “reduction” factors

instead [8]. The higher the protection factor, the greater the degree of incident radiation attenuation, and the higher the protection afforded to personnel within the vehicle. Per the definitions above, additional secondary radiation is included in the determination of the RPF. Secondary gamma or neutron particles are typically delayed and are a subsequent result of a prior neutron or gamma interaction. Residual radiation is generally defined as the additional gamma or neutron flux that is produced from activated isotopes within the environment surrounding the surrogate vehicle. Although the two seem very similar, secondary particles are the direct result of flux interactions with the vehicle surrogate or test article of interest, whereas the residual radiation is created when the incident flux interacts with the environment surrounding the test article. Residual and secondary neutrons are rare and typically produce a flux that is negligible when compared to the incident flux. However, secondary and residual gammas occur much more frequently and, depending on the neutron source, shielding material, and environment, can possess significant flux values and energies. When attempting to measure the delayed gamma fluence, the presence of a strong neutron environment has negatively impacted the electronic detection equipment. For the research conducted in this thesis, the effects of residual and secondary radiation were ignored in the experimental determination, but integrated into the computational determination. This assumption is not unreasonable considering the rarity in secondary and residual neutron effects, low gamma flux produced by the Cf-252 source, and the small room "return" from the RCL. However, this is a source of error and contributed to the difference between the simulated and experimental NPF values [9].

Before determining the RPF value, through some means of combining GPF and NPF, the basics of dosimetry and radiation absorbed dose must be understood. The International Commission on Radiological Protection (ICRP) has defined dose into two separate quantity types: protection and operation. The operational quantities are maintained and defined by the International Commission on Radiation Units (ICRU), like those associated with radiation workers, and will be less applicable for the RPF research campaign, which focuses more heavily on nuclear detonation scenarios.

ICRP has defined two terms in the scope of protection quantities, the effective dose (E) and the equivalent dose (H_T). These definitions can be further explained in ICRP Publication 26 [10] and subsequent publications in the dosimetry field. Dose is a function of energy, particle type, organ (tissue) type and density, and much more. Because the radiation is transported into the vehicle via the air and then directly through the personnel's skin and onto other organs (i.e., it is considered 'external exposure and not inhalation or ingestion of radioactive materials), the definitions of the RPF have been typically limited to only external radiation doses.

In this case, the dose equivalent (H) is typically used, and can be described as a function of the quality factor, absorbed dose, and linear energy transfer. Equation 1.4 shows the integral form of the dose equivalent:

$$H = \int Q(L) * \frac{dD}{dL} dL \tag{1.4}$$

Where dD/dL is the "absorbed dose at 10 mm between linear energy transfer L and L+dL," and the quality factor (Q) is particle and linear energy transfer dependent [11]. To further define the dose equivalent, the quality factor is averaged over an entire spectrum of linear energy transfer, defining the mean quality factor ($\bar{Q}$) as:

$$\overline{Q_n} = \int Q_n(E_n) k_f(E_n) \varphi(E_n) dE / k_f(E_n) \varphi(E_n) dE \tag{1.5}$$

where,

Q_n = Quality Factor for Neutrons
E_n = Neutron Energy
k_f = Kerma Coefficient
φ = Neutron Flux

Since the mean quality factor is defined as a function of particle type (Q_n) and energy (E_n), the dose equivalent can simply be qualitatively explained as a function of:

$$H = H(\text{particle, energy, kerma coefficient, particle geometry and stopping power}) \tag{1.6}$$

Consequently, dose calculation and RPF determination can take significant resources considering the complexity of particle transport, energy transfer, and human tissue response. The ICRP has published credible conversion coefficients that allow for

fluence to be converted directly to an external absorbed dose equivalence. The "fluence-to-dose conversion coefficients" are published in ICRP Publications 60, 72, 74, and 116, and are organized by respective energy ranges or "bins" [10]. ICRP fluence-to-dose conversion coefficients are listed in Appendix B, and are typically presented as ambient dose equivalent per fluence (H*(10)/fluence), where the resultant dose is in international units (Sieverts) per unit area.

Because the dose equivalent value can now be defined by particle type, H_n and H_g for neutrons and gammas respectively, the RPF can further be expanded in Equation 1.7. The equation also considers secondary gamma reactions due to neutron interactions (via elastic scattering and absorption) with the surrogate vehicle. Again, the relatively small magnitude of residual neutrons, created from secondary neutron interactions with the environment, is considerably less than the magnitude of the primary neutron flux, therefore, they may be neglected.

$$\mathrm{RPF} = \frac{\left(\mathrm{H_n} + \mathrm{H_g} + \mathrm{H_{sn}}\right)_{\mathrm{unshielded}}}{\left(\mathrm{H_n} + \mathrm{H_g} + \mathrm{H_{sg}}\right)_{\mathrm{shielded}}} \tag{1.7}$$

where,

H_n = Dose equivalent due to neutrons.
H_g = Dose equivalent due to gammas
H_{sn} = Dose equivalent due to residual neutrons (application dependent)
H_{sg} = Dose equivalent due to secondary gammas.
Unshielded = assembly with the surrogate vehicle not present.
Shielded = assembly with the surrogate vehicle present.

The implication of expressing the RPF as above suggests that there is no readily available method for directly combining the NPF and GPF. Historically, these values have been reported separately, along with the total RPF. By allowing the NPF and GPF to be combined in some manner or approximation, the RPF can be reported as a single value to field commanders, thus eliminating complexity in the RPF application.

Experimentally determining the RPF values is rather difficult because of limitations in detection equipment. Researchers exploring this option should consider the impact of data acquisition in a high-energy mixed particle field, such as those conditions

found after the detonation of a nuclear weapon. For example, neutron detection equipment could be negatively impacted by the associated gamma flux. While it is not impossible to arrange such detection capabilities to account for both neutron and gamma fluxes, it is considerably more challenging and should be accounted for properly. Nevertheless, determining total RPF values in an analytical or computational setting is even more worthwhile, and the need for validating complex particle transport and shielding applications is growing more important.

THIS PAGE INTENTIONALLY LEFT BLANK

II. BACKGROUND

A. COMPUTATIONAL PROGRESSION

The computational methodology for RPF determination significantly changed throughout the Cold War until the present. As one might imagine, assessing radiation dose in an environment characterized by high-energy nuclear physics, large spatial separations, and complex target material compositions is not an easy task. The Vehicle Code System (VCS) [12], developed in 1974, was the first iteration of military vehicle shielding computations to solve personnel survivability problems. Those features the VCS lacked and failed to produce were later introduced by its successor, the Monte Carlo Adjoint Shielding (MASH) code [13]. Meanwhile, Los Alamos National Laboratory (LANL) developed the Monte Carlo N-Particle Transport Code (MCNP) [14] to extend beyond shielding analysis and incorporate a wide breadth of radiation transport applications. With an extensive cross-section library and wide computational capabilities and applications, MCNP took center stage out of the pool of radiation transport codes overseen by the Defense Nuclear Agency (DNA), now DTRA. Later, DNA named MCNP as the superior nuclear transport code and determined that it would be the primary means of determining protection and reduction factors for RPF application [15].

1. Vehicle Code System (VCS)

The VCS is a radiation transport code which focuses on the calculation and determination of protection and reduction factors within predefined radiation environments. VCS couples a discrete ordinates transport (DOT) calculation with an adjoint Monte Carlo calculation. The DOT radiation model solves the radiative transfer equation for a finite number of discrete solid angles or coupling surfaces surrounding some specified vehicle with its environment [9]. As the VCS user manual defines it, the adjoint Monte Carlo method determines the “effectiveness of flux at the surface in causing response in a detector adjacent to the crew members (i.e., dose importance).” The code then uses both the flux with the dose importance to provide a dose response [12]. Like most current codes, the VCS also allows for geometrical changes to

the environment and detection assembly at different distances from the specified source. According to the VCS User Guide, the general structure of the code is depicted in Figure 6.

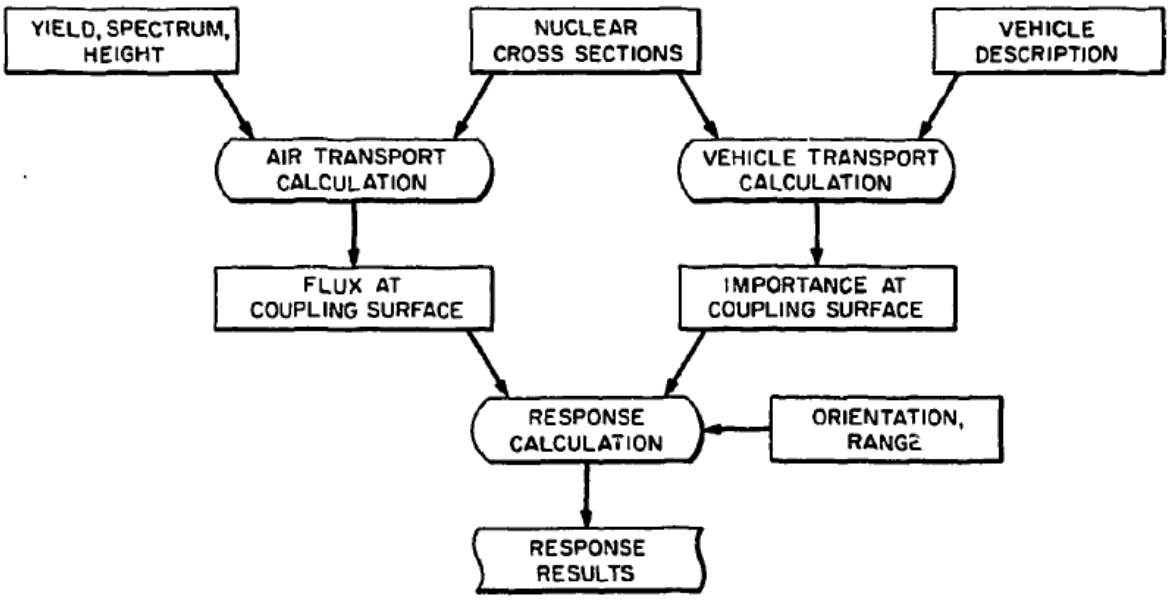

Figure 6. General Structure to VCS. Source: [12].

It is important to note that the coupling transport calculations aforementioned are completed using DOT (Air Transport Calculation) [16] and MORSE (Vehicle Transport Calculation) [17], both created by Oak Ridge National Laboratory (ORNL). The DOT transport code, with the specified environmental details, can determine the scalar, directional, and uncollided fluxes and couple them to characterize a surface within the problem. The MORSE Monte Carlo transport code utilizes the adjoint history data created after the vehicle shielding calculations, considering the detector orientation and range, and the coupling surface flux provided via DOT to provide a full detector response [17]. With the detector response estimated as a function of energy, the dose and subsequent protection or reduction factors can be determined.

A typical VCS problem would consist of the detonation of a tactical nuclear weapon within a kilometer of a structure or vehicle. The DOT code would determine the

air-over-ground neutron and gamma transport of the fluence as a function of energy to the vehicle, while the MORSE code would determine the effectiveness of neutron and gamma radiation impinging on the vehicle's surface to produce the dose-importance. The VCS couples the two codes together to provide the dose received within the vehicle, or post-coupling surface. This scenario is depicted in Figure 7, which is used purely as an illustration of concept [13], and helps provide a general observation of the RPF application.

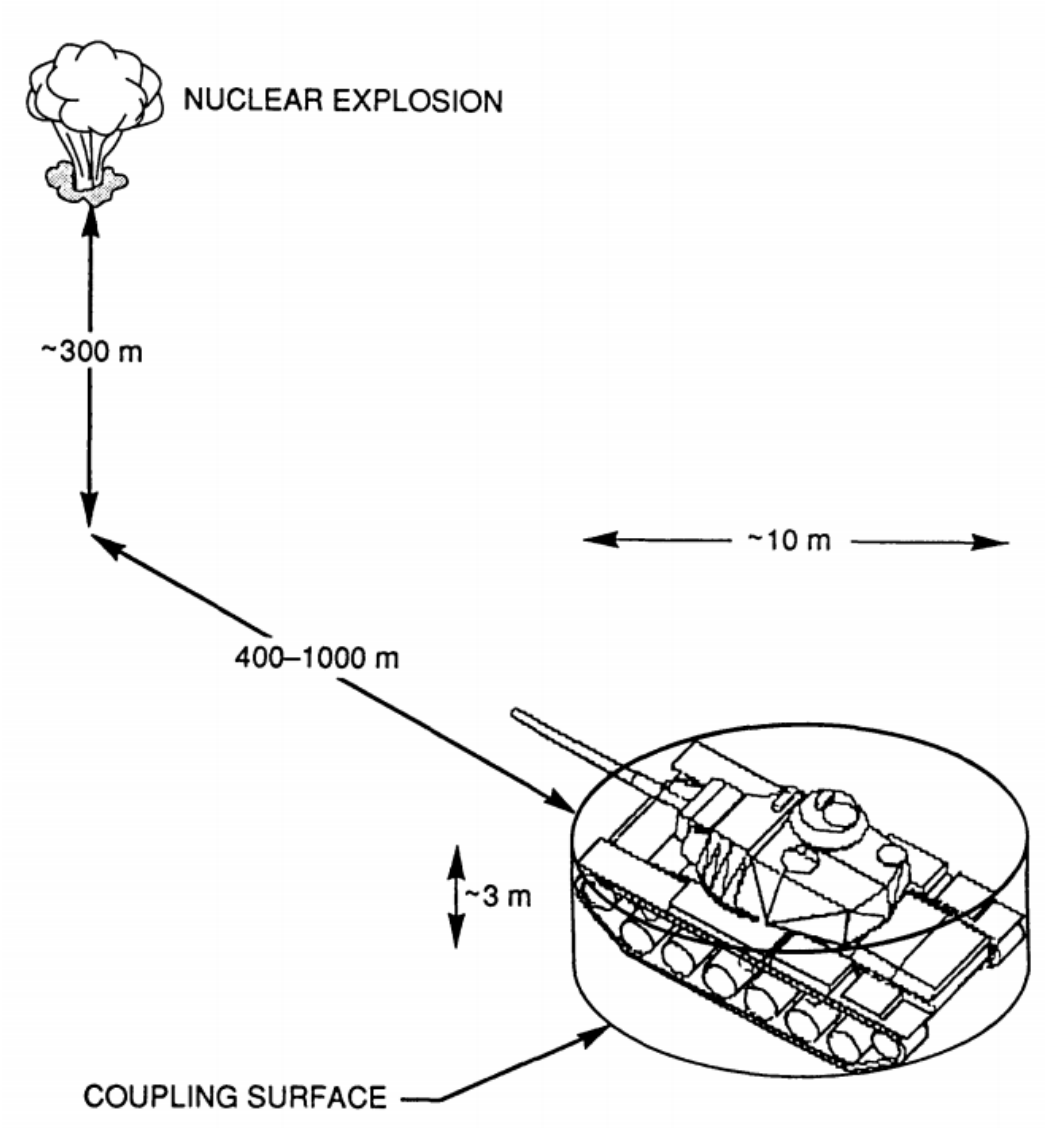

Figure 7. Typical VCS Scenario. Source: [12].

2. Monte Carlo Adjoint Shielding Code System

The Monte Carlo Adjoint Shielding Code System (MASH) [13] was the VCS successor and was also developed by ORNL. It was specifically designed for assessing protection and reduction factors of military vehicles, structures, and other shielding assemblies within large and complex radiation environments. Like VCS, it also couples DOT and adjoint Monte Carlo calculations. However, the primary difference between the two codes is that MASH focuses on optimum computer use and efficiency, thereby reducing run times and computational variance within the problem [13]. In a response to a Defense Nuclear Agency (DNA) concern over disagreement between independent analyses of the code using identical problem sets, the Ballistic Research Laboratory (BRL) and ORNL were tasked in identifying problems with VCS [15]. The following concerns were addressed in the MASH iteration:

- "MORSE did not favorably sample the most important regions of the energy space for calculations involving steel and polyethylene."
- "Cross section libraries had deficiencies for transport in steel and air, especially around the 1 MeV and epithermal energies."
- "Geometry routines used by BRL were not compatible with MORSE, and had to be reviewed."

The corrections and improvements of VCS to create the newly iterative MASH code included:

- "The earlier version of MORSE was replaced and updated with the latest version."
- "Addition of in-group energy biasing into MORSE."
- "Update of the geometry package to the latest version."
- "Modification to MORSE's energy group structures."
- "DOT was updated and replaced with a revised coupling code."
- "And several other similar corrections"

The list continues and can be reviewed within the MASH code User's Guide [13]. The typical structure of MASH remained consistent with VCS, but the user guide

provides a much more detailed flow diagram of the data transfer and response determination as seen in Figure 8.

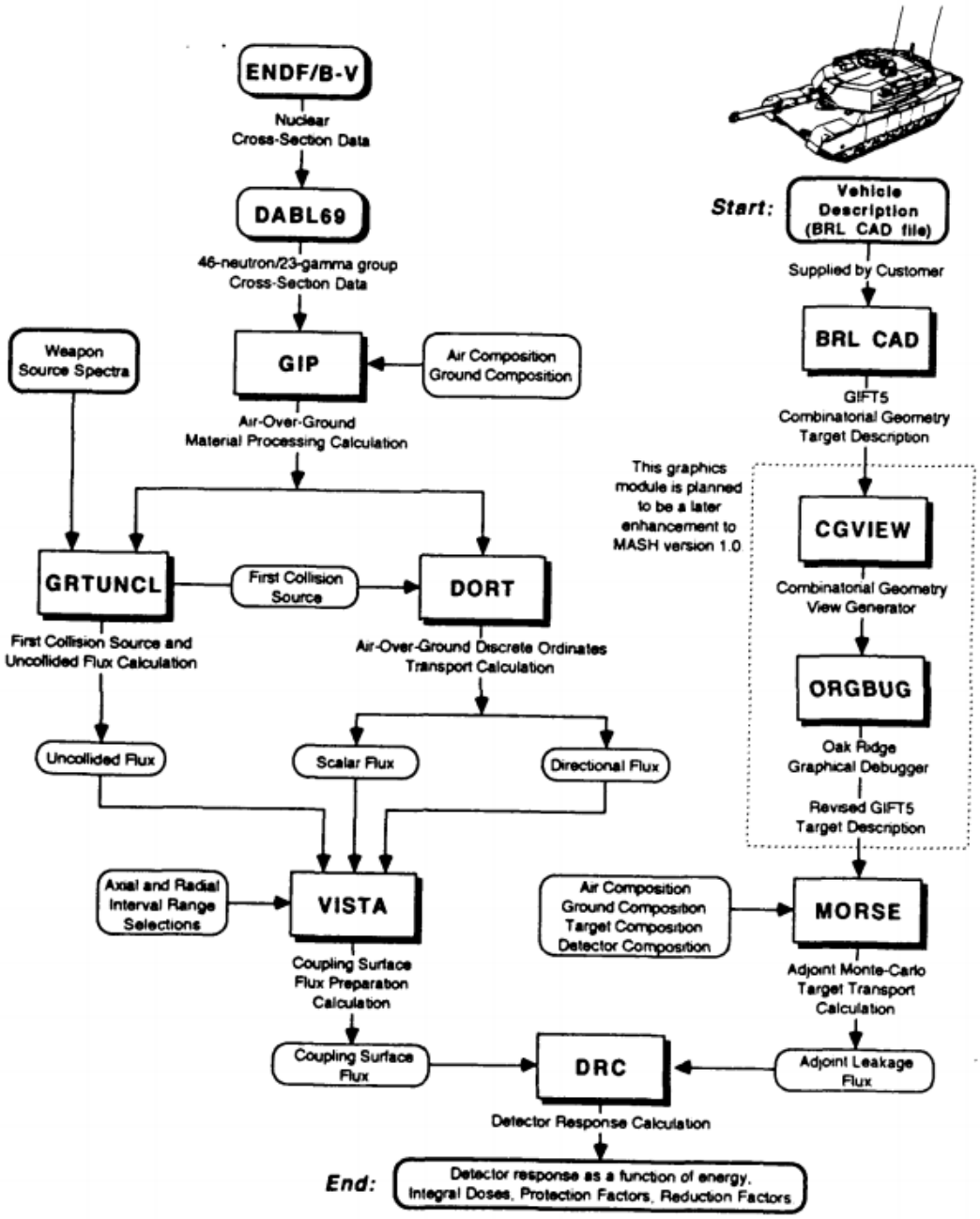

Figure 8. Data Flow of the MASH Code System. Source: [13].

3. Monte Carlo N-Particle Transport Code

MCNP was developed and is maintained by LANL, while being controlled and distributed by the Radiation Safety Information Computational Center (RSICC). The most current version today is MCNP6.1, and is described as a "general-purpose, continuous-energy, generalized-geometry, time-dependent," [18] Monte Carlo radiation-transport code designed to track many particle types over broad ranges of energies. MCNP can be used for applications ranging from reactor design, criticality safety, and nuclear safeguards to high-energy dosimetry and accelerator imaging technology. MCNP has been tested and validated a number of times with applications ranging from criticality safety applications to medical simulations [19].

Today, the RPF research campaign focuses primarily on MCNP as a viable and versatile computational code featuring a wide variety of cross-section files and additional capabilities. LANL's code is well documented, LANL maintains a staff team for consistent monitoring, validation, and updating of packages.

B. EXPERIMENTAL PROGRESSION

The experimental progression originated in Operation JANGLE at the Nevada Test Site from October to November of 1951 [20]. Operation JANGLE aimed to determine the effects of atomic weapons above and below ground, study the laws governing shock wave propagation, and evaluate the suitability of military operations after being subjected to their use. During their assessment of military operations post detonation, a team of scientists measured the dose received by actual personnel inside of an armored vehicle while conducting operations in the vicinity of ground zero. While Operation JANGLE concluded that no further radiation analysis needed to be conducted, analyst Dr. Ralph Rexroad subsequently expanded his analysis of radiation protection to that of other military vehicles [20], [21].

Starting as early as 1953, only two years after Operation JANGLE, Beckelheimer and Rexroad developed a comprehensive gamma attenuation assessment of U.S. military vehicles and rail equipment [21]. Rexroad continued to assess radiation protection of military vehicles and structures through the late 1970s with BRL and the Army

Chemistry Laboratory. Experimental methods continued to run parallel with the DNA sponsored computational code, VCS. While VCS was a first iteration complex and comprehensive shielding code, it still needed to be validated through extensive experimentation. The field expanded from Rexroad's team into new initiatives at BRL and ORNL by the late 1970s. Experimentation took place at the Aberdeen Proving Grounds in Maryland with vehicles ranging from the XM-803 (MBT-70 Pilot II) (1973) Tank to the M60A1 Tank (1977).

In the 1980s, Howell Caton of BRL began to look at merging both computational and experimental methods for smaller test articles that are representative of an Army vehicle [22]. In the late 1980s Caton considered RPFs for light vehicles, specifically in context of residual radiation effects [23]. Other efforts were made at ORNL involving a similar vehicle surrogate test article, but produced different results. Combined with computational differences, these discrepancies were later addressed by DNA and standardized.

After the fall of the Soviet Union in 1990, experimentation slowed and consisted primarily of code improvements with minor efforts in validation requirements [24]. Such efforts included similar surrogate construction to that of Caton at BRL in the late 80's. In 1995, RPFs became a new counter-proliferation focus with former President Clinton's Presidential Decision Directives 39 and 62 [25]. With these new counter-terrorism directives, RPF calculations and determinations appeared sporadically throughout United States Department of Defense (DOD). Efforts were made at DTRA (formerly DNA), Army Health Center, Naval Health Research Center, Army Nuclear and Chemical Agency, and several other organizations.

Experimentation efforts continued into the 21st century, but failed to reach the same level of testing as had taken place during the Cold War. Aberdeen Proving Grounds still remained the focal point for RPF determination and calculations by DTRA, but efforts in DOD declined as a whole. In 2012, the program regained priority and is now supported by both the U.S. Army Nuclear and Combating Weapons of Mass Destruction Agency (USANCA) and DTRA.

Today, service institutions from the U.S. Navy, Army and Air Force seek to validate the Monte Carlo N-Particle Transport Code (MCNP) by comparing NPF and GPF estimates against measured values using known sources and environments. Specifically, efforts have been made at the Air Force Institute of Technology (AFIT), the United States Military Academy at West Point (USMA), the United States Naval Academy (USNA), the Naval Postgraduate School (NPS), and the Nuclear Science and Engineering Research Center (NSERC), as aforementioned in Chapter I.

In this thesis research, NPS, in collaboration with LLNL, measured and analyzed NPFs using LLNL's Californium-252 RCL and modeled the experimental arrangement using MCNP6.1. Additional information about the source, testing facilities, and experimental assembly will be covered in the following chapter.

III. NPF DETERMINATION

A. INTRODUCTION

The United States military currently employs a vast number of vehicles with diverse construction, equipment, and operational capabilities. Experimentally determining protection factors for each vehicle type under a specific radiation field can be costly in time and resources. However, with the advancement in military equipment, analytical technology has made significant progress since World War II and the Cold War. Using computational codes to determine protection factors will allow for the U.S. military to provide vital information to field commanders without expending an unreasonable amount of resources. This will offer the military with methods to assessing the radiological survivability of forward deployed vehicles, structures, and vessels.

However, before complex models can be utilized, the computational codes need to be validated through experimentation. As aforementioned in the Chapter II, DNA stipulated that for the RPF program LANL's MCNP code would be used. The validation process includes testing a number of articles and surrogates within a diverse array of energy spectra and comparing the experimental results with the results produced from MCNP. After the code has been validated, DTRA and other DOD organizations will be able to confidently use the MCNP code to produce NPFs, GPFs, and RPFs for any military vehicle or structure in a specified radiation environment.

B. EXPERIMENTAL DETERMINATION

DTRA's experimental RPF campaign, as described in Appendix A, identifies several experiments in support of the computational code validation requirement. A recent opportunity allowed for DTRA, in collaboration with NPS and LLNL, to characterize a simple geometry, complex composition vehicle surrogate at LLNL's RCL. This opportunity represented a tremendous opportunity for the DTRA RPF research campaign because of the benefits of using the RCL and the Cf-252 source. Specifically, the RCL Cf-252 facility offers a well-characterized and unique polyenergetic spontaneous fission neutron spectrum that differs significantly from the higher-energy

accelerator neutron sources and the lower energy reactor sources used previously in the experimental campaign. Additionally, the Cf-252 source offers a much lower associated gamma flux than other reactor-based neutron sources, thus improving detector efficiency and quality of collected data. A complete experimental plan of the NPS irradiation experiments at the RCL, from 18th of April through the 21st of April, 2017, is found in Appendix B. In subsequent sections, details on the test article, facility, source, detection system, and post-data processing are explained.

1. The Vehicle Surrogate

The vehicle surrogate is a simplified 60.94 x 60.94 x 60.94 cm (24" x 24" x 24") cubic box composed of materials commonly used in the construction of a military vehicle. The surrogate vehicle is composed of aluminum, plastic reinforced with glass (GRP), and rolled homogenous steel at thicknesses 0.635 cm, 1.27 cm, and 1.27 cm (0.25", 0.5", and 0.5"), respectively. As seen in Figures 9 and 10, the plates are supported by a hollow aluminum structure and fastened via four 1.27 cm (0.5") steel bolts on each side. The aluminum plates are the outermost plates (silver), followed by the GRP (green), and then the innermost steel plates (black).

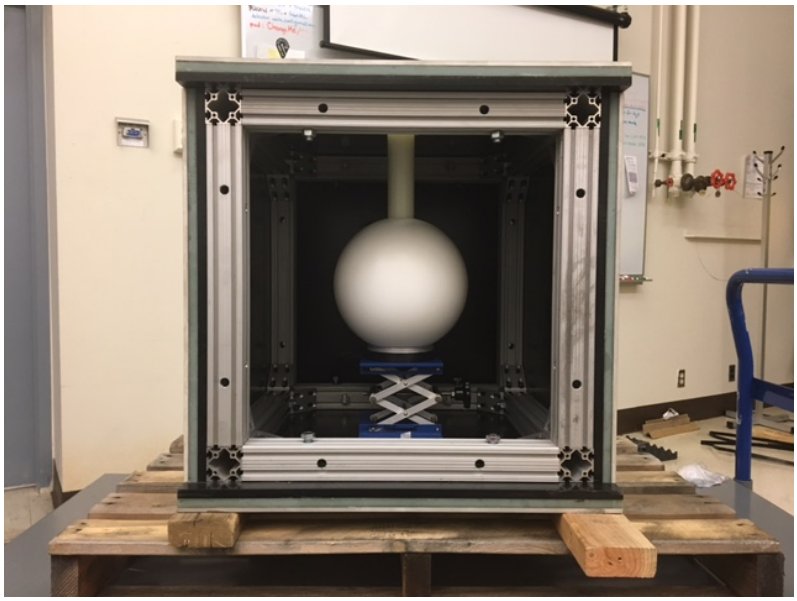

Includes polyethylene detector, 12.7 cm (5") Bonner Sphere, aluminum laboratory jack, and aluminum stability ring.

Figure 9. Primary Vehicle Surrogate Assembly

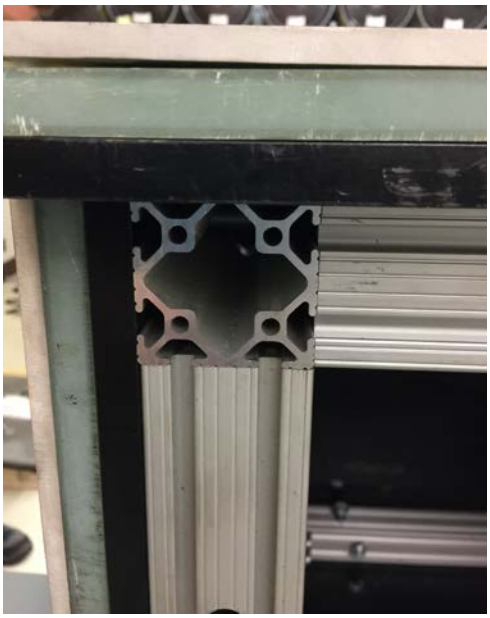

Figure 10. Vehicle Surrogate Primary Plate Assembly

The surrogate's cover plate, which faced the incident neutron flux during irradiations, had two handles mounted to allow easy removal and placement of the internal detection configurations between irradiations. Additionally, two support pins located at the top of the cover plate made it unlike the fixed plates of the other five sides of the surrogate; however, this design allowed for expedited transitions between irradiations to optimize the use of lab time. Figure 11 shows the placement of the front cover plates using a rubber mallet in one of the vehicle surrogate assemblies. The location of the detection equipment within the vehicle surrogate was measured before and after each irradiation to ensure that there was no movement during the placement of the front cover plates. Collectively the vehicle surrogate weighed approximately 317.52 kg (700 lbs) and required the use of a heavy duty steel cart as well as plywood to evenly distribute the weight across the flooring of the RCL.

From left: Ensigns Jacob Glesmann, Mark Schnabel and Donald Puent assembling the front plates of the surrogate vehicle.

Figure 11. Vehicle Surrogate Secondary Assembly

A secondary assembly was tested to evaluate the effects of the aluminum and GRP plates on the NPF, also seen in Figure 11. Due to the presence of the support pins

and the mounted handles, the GRP and aluminum plates could not be removed from the incident plate when the other five wall plates were reconfigured. Although a NPF value could not be assessed for the given secondary assembly, due to time constraints, data was acquired for future research efforts. A hole in the top of the surrogate allowed for the preamplifier to have access to the detector, observed in Figure 12. During irradiations, the hole was filled with standard packing foam, and provided support and stability to the detector. More discussion about the detection assembly and configurations is provided later in this chapter.

Also depicts the northern half of the Radiation Calibration Laboratory.

Figure 12. Primary Assembly with Fabricated Hole in the Top Plate

2. Free Field Assembly

The free field and surrogate assemblies are identical in every manner but exclude the use of the surrogate vehicle. This is to ensure consistency between the detection method, and other constants in the RCL chamber. Figure 13 depicts the free field assembly with the wooden pallets, steel cart, and detection assembly left unchanged. An

aluminum detector stand and four wooden blocks were required in the free field assembly to stabilize the detection equipment. It was assumed that the additional equipment had negligible impact on the neutron transport and fluence measurement.

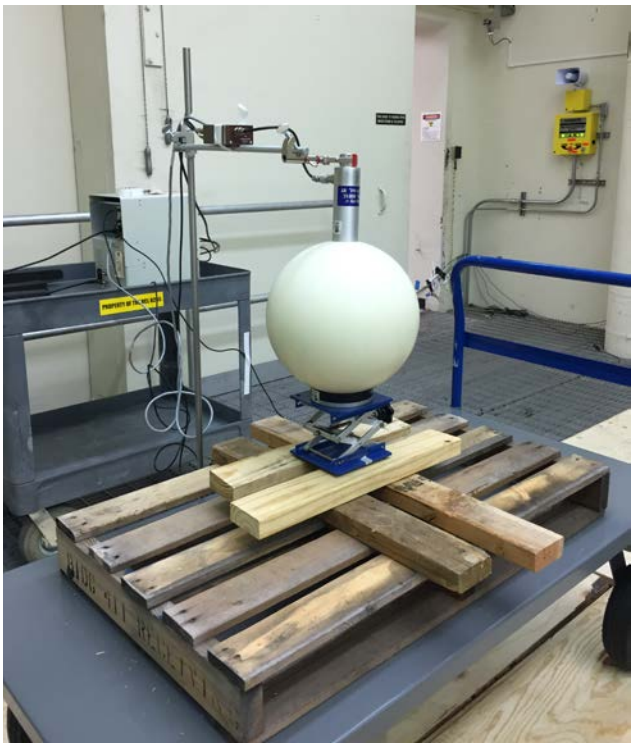

Figure 13. Free Field Assembly

3. The Radiation Calibration Laboratory

The Radiation Calibration Laboratory is a large 9.14 x 12.19 m (30’ x 40’) open room designed for low neutron and gamma residual room return. Figure 14 depicts the vehicle surrogate located on the south side of the facility, approximately 285.2 cm (9.3’) from the source chamber. The flooring located in the facility is grated aluminum and provided a 3 m (9.8’) gap of air between the aluminum flooring and the concrete foundation. The aforementioned cart and wood can also be observed in Figure 14. Dr. Radoslav Radev, of the Global Security Directorate of LLNL, has previously characterized the facility through several neutron detection methods [26]. The approximate neutron dose rate received at 285.2 cm (9.3’), according to Dr. Radev, is

1.38 mSv/hr (138 mRem/hr) on the north side of the source. This previously characterized dose rate will later be compared to the measured dose rate using the detection system and methodology of the RPF research campaign.

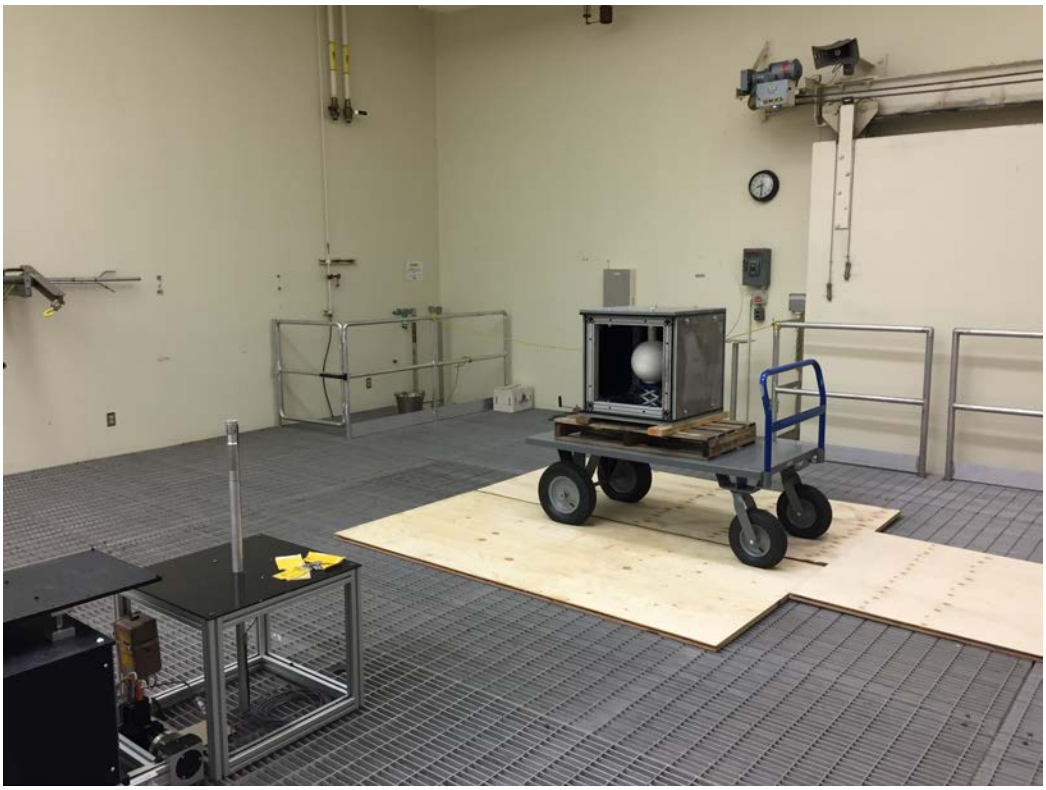

Includes the large steel cart and plywood aforementioned and excludes the auxiliary ORTEC mini-bin data acquisition equipment.

Figure 14. Vehicle Surrogate and Experimental Assembly

Additionally, Figure 15 shows a simplified schematic of the RCL and includes the locations of Dr. Radev's characterization experiments on the north side of the room. Later, in Chapter IV, a comparison between Dr. Radev's results and the results of the NPS experiments will be made to evaluate the Bonner Sphere Spectrometer BSS detection system.

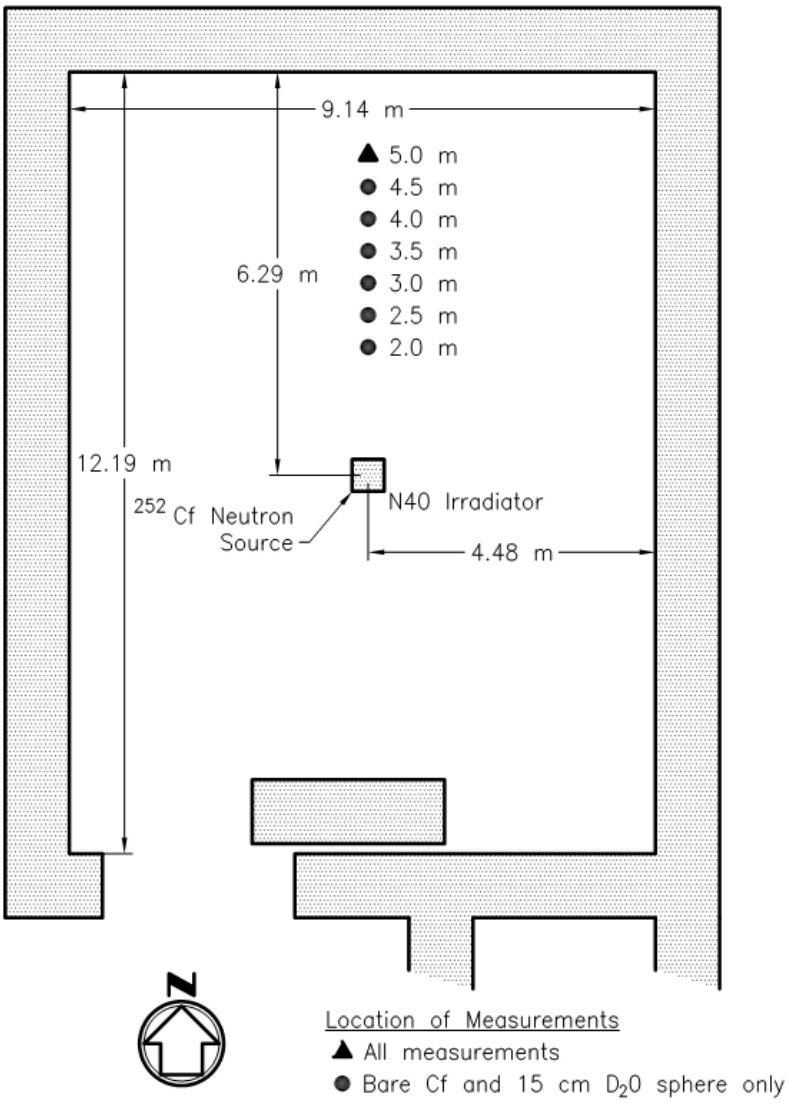

Figure 15. Simplified RCL Schematic. Source: [26].

4. RCL Californium-252 Neutron Source

The LLNL Cf-252 source was purchased from ORNL in 2014. Table 1 shows the isotopic composition of the Cf-252 source as of August 2013, as provided by ORNL. In 2014, the estimated neutron emission of the source was 1.4099×10^9 neutrons per second, which equates to approximately 0.038 Curies. The source is a double encapsulated assembly, which utilizes a N40 Irradiator and pneumatic transport system to move the source from a concrete bunker to its position within the RCL.

Table 1. Isotopic Composition of Cf-252 source SR-CF-3050-OR as of 08/2013. Source: [26].

Source ID	Batch ID	Cf-249 µg	Cf-250 µg	Cf-251 µg	Cf-252 µg	Cm-245 µg	Cm-246 µg	Cm-247 µg	Cm-248 µg
SR-CF-3050OR	CXCF 598	1713.53	2042.972	1346.968	728.84	49.52	2345.77	15.09	31262.97

Cf-252 is a primary alpha emitter (~96%) with a half-life of about 2.65 years. However, because the source is double encapsulated, the alphas are absorbed instantaneously and do not escape the aluminum shielding around the source. The secondary mode of decay for Cf-252 is spontaneous fission (~3%), in which the californium nucleus splits into two different fission fragments and releases an array of neutrons at various energies.

The spontaneous fission of Cf-252 releases polyenergetic neutrons with the majority ranging from 1 and 5 MeV. The Watt Fission Spectrum in Equation 3.1 best mathematically describes the spontaneous fission phenomenon, and was employed to replicate the neutron energy distribution in the MCNP simulation accompanied in Dr. Radev's report [26]. The Watt Fission Spectrum represents the distribution of the number of neutrons with energy (E), with empirical constants (a and b), which are published in the *MCNP6.1 User's Manual* [14].

$$f\left(E\right) = C \cdot \exp\left(-\frac{E}{a}\right) \cdot \sinh\left(\sqrt{b * E}\right) \tag{3.1}$$

5. Detection Methodology

DTRA determined the Bonner Sphere Spectrometer (BSS) system was an excellent approach to be used for the NPF application and determination due to its previous application measuring neutron fields in historic RPF evaluations [25]. The BSS consists of several components, ranging from high-density polyethylene spheres to the lithium-iodide detector itself. The following subsections help to describe each component of the BSS and the detection assembly, as well as their integral roles in the overall

determination of the NPF. The BSS was created and sold via Ludlum Inc. (model 42–5) [27]. Appendix D contains the associated detector settings used in the NPF irradiations at LLNL.

a. Bonner (Polyethylene) Spheres

The Bonner spheres of the BSS range in diameters from 5.08 cm to 30.48 cm (2” to 12”). As seen in Figure 16, they are designed with hollowed central shafts along the primary z-axis to allow the scintillation crystal in the detector to be centered. The spheres contain a high density of neutron-thermalizing hydrogen, thereby providing a variety of moderation thicknesses to incident neutron energies. By using multiple layers of moderation, the spheres can allow for certain neutron energy ranges to be isolated and thermalized, thus expanding the LiI(Eu) detector’s response range and offering energy discrimination between interactions. Additional spheres may be incorporated to widen the response range if the application requires.

12” and 10” polyethylene spheres with LiI(Eu) detector in transport housing. Three additional polyethylene simulation detectors are also present.

Figure 16. Polyethylene Bonner Spheres

b. Lithium Iodide Scintillator

When combined with the polyethylene spheres, a lithium iodide europium doped (LiI(Eu)) scintillation detector allows for continuous energy response from thermal energies to approximately 12 MeV. The detector itself houses a 4 mm x 4 mm (0.157" x 0.157") LiI(Eu) crystal with 96% enrichment of lithium-6. The crystal is connected to a photomultiplier tube (PMT) which amplifies and delivers electrical signals to the output. A schematic of the detector, provided via Ludlum Measurements Inc., can be viewed in Figure 17.

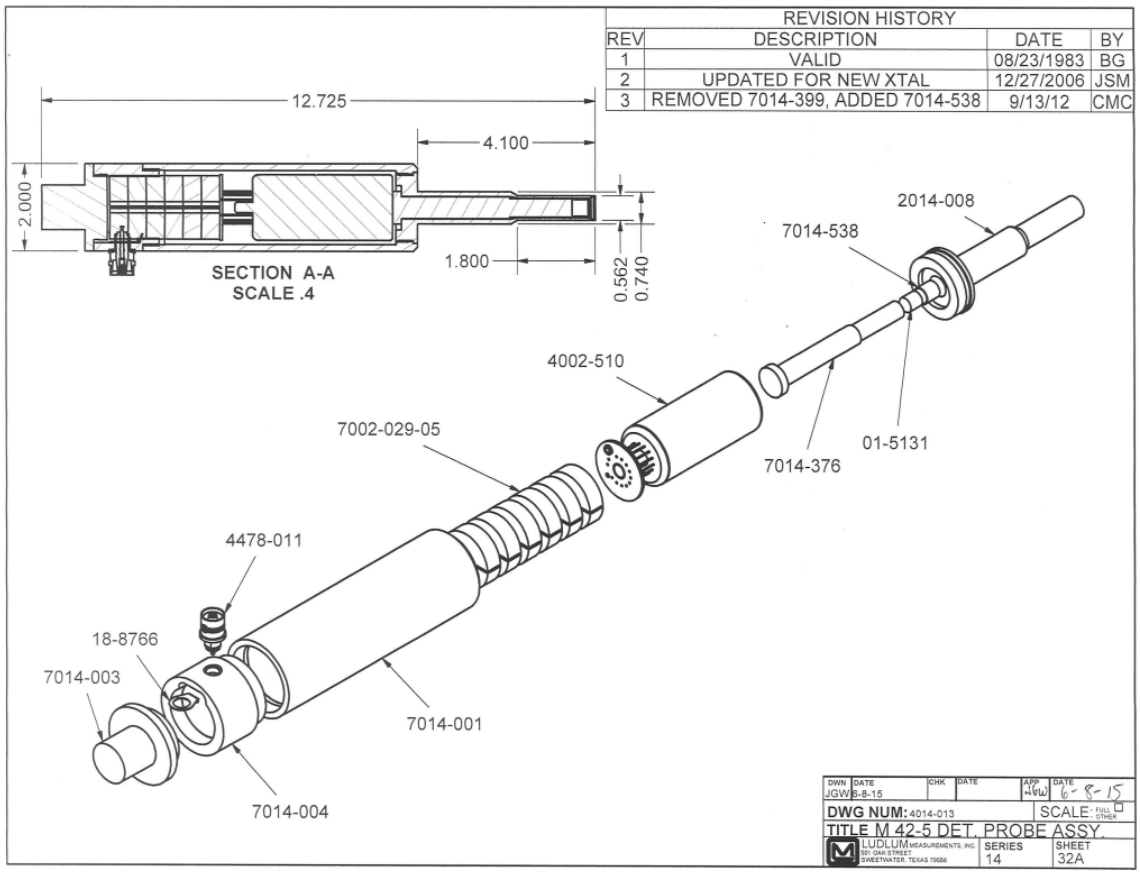

Figure 17. Lithium-6 Iodide, Europium Doped Scintillation Detector. Source: [27].

The primary neutron-detection operation of the LiI(Eu) detector is focused around the Li-6 and neutron absorption interaction. Li-6 has a high thermal neutron absorption

cross section (~940 barns) [5], and provides discrimination between gamma pile-up and alpha reactions. An incident thermal neutron collides with the Li-6 atom and is absorbed. The resultant reaction produces an alpha and triton particle, both of which are exclusively at their respective ground states. Therefore, regardless of incident neutron energy, the total energy produced by the reaction (Q-value) is 4.78 MeV [5]. The alpha and triton particles are produced in opposite directions and interact heavily with the surrounding iodide scintillating material. The drifting particles in the scintillator cause electron-hole pairs, which later recombine to produce photons. The photons are amplified to a detectable electrical signal and carried to the output through the PMT. Equation 3.2 shows the overall interaction with the energy includes in both the triton and alpha particles [5].

$$ {}^{6}_{3}Li + {}^{1}_{0}n \rightarrow {}^{3}_{1}H\left(2.73MeV\right) + {}^{4}_{3}\alpha\left(2.05MeV\right) \tag{3.2} $$

The moderation provided via the polyethylene spheres allow for the LiI(Eu) detector to detect a wide range of neutron energies. Total count rates within the alpha peak are recorded and saved for later spectra convergence algorithms. The unfolding or convergence of the BSS data will be explained later in this chapter.

Helium-3, Boron-10 and LiF detectors have also been explored as detection options for RPF measurements; however, DTRA stipulated a single detection method to be used during the course of the RPF research campaign [1]. By doing so, the detection equipment and test article are held as constants and only the incident energy spectra change.

c. Auxiliary Detection Equipment

Signal amplifiers, low-level discriminator, high-voltage power supply, and more will be further explained in this section. After the electrical signal from the alpha-scintillator reaction has reached the output of the detector, it is then transported through an ORTEC preamplifier (ORTEC 142C), which provides low-noise signal amplification and spectroscopy performance enhancement [28]. The signal then travels to the ORTEC minibin and ORTEC 572A amplifier card. The 572A provides the operator with coarse

and fine gain options, pole adjustments, shaping time, and more. After further signal processing and digitization, the signal travels to the ORTEC 925 ADCAM MCB card which processes it to be received by the ORTEC software. Figure 18 is a simplified block diagram from the LiI(Eu) detector to the ORTEC software.

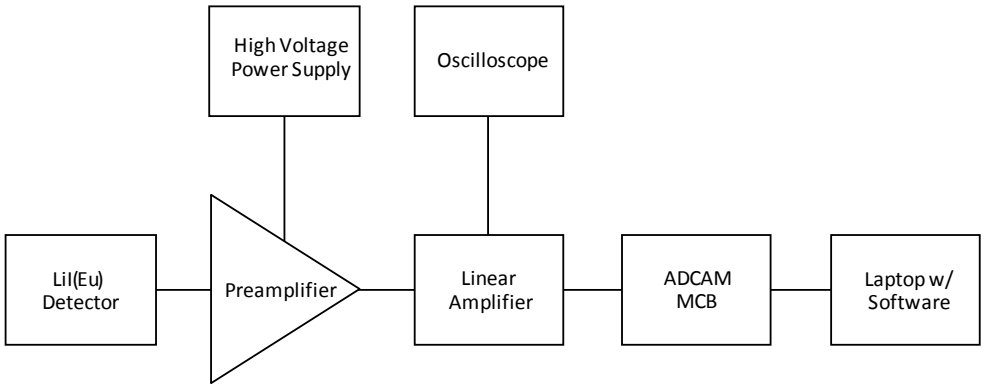

Figure 18. Simplified Block Diagram of Data Acquisition Process. Source: [3].

d. ORTEC Software

The ORTEC software, Maestro, is a multichannel analyzer used for gamma and alpha spectroscopy. The software allows "soft" changes to low level discriminator (LLD) values and preset real time as well as region of interests (ROI). Maestro also provides simple peak calculations to determine net area under the ROI and basic statistical error analysis both of which were used during convergence for a final solution spectrum. The ROI was determined during initialization and the bare configuration, then underwent minor adjustments for further configurations. Figure 19 shows the ORTEC software with a ROI set with the LLD adjusted to remove the first 120 channels. Because the nature of the LiI(Eu) scintillator, a large gamma peak forms within the first 120 channels, and will significantly increase dead time if not adjusted for.

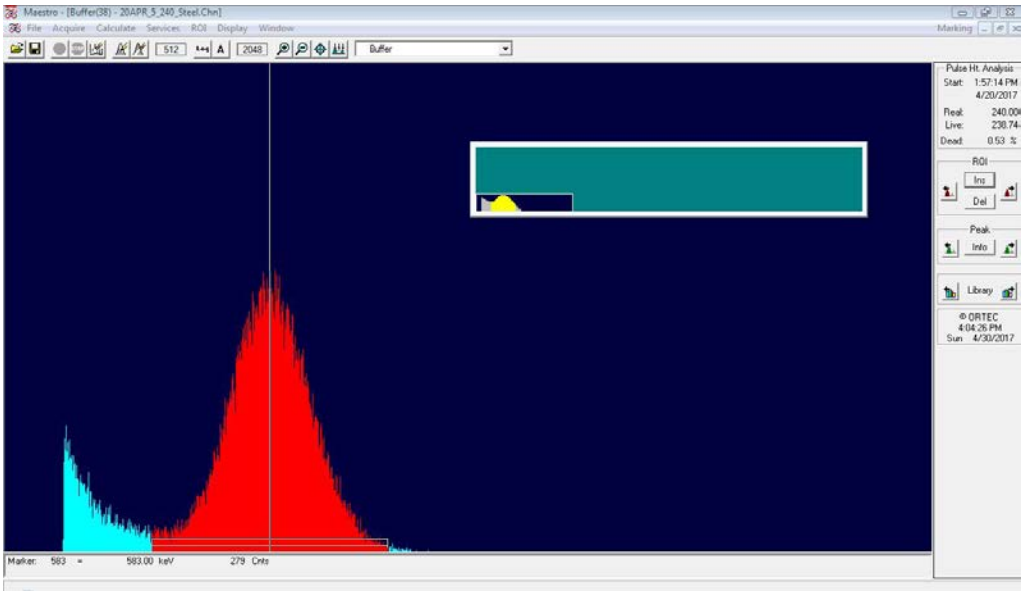

Figure 19. Sample ORTEC Maestro Software Screenshot.

6. Unfolding with MAXED and GRAVEL (UMG v3.3)

The unfolding software used in the RPF campaign is UMG v3.3, which provides a means of converging the measured data received from the BSS system with an initial spectral "guess." The MAXED program employs a "maximum entropy principle," and GRAVEL uses a "modified SAND–II algorithm" to complete the unfolding and convergence process [29]. While the GRAVEL outputs are identical to the MAXED outputs in most aspects, the RPF campaign chose the MAXED program as the standard for unfolding experimental data related to the RPF determination [3]. Additional information of the UMG v3.3 software package can be found through the program's distribution page via the Radiation Safety Information Computational Center (RSICC) [30]. In this section the four primary components of the UMG v3.3 convergence process will be explained: measured data, default spectrum, response functions, and the input file. The respective components for the unfolding process for both the free field and surrogate vehicle assemblies can be found in Appendix E.

a. Measured Data File (.ibu)

The measured data file contains the experimental results and user calculated error. The results are presented per Bonner sphere by counts per second with absolute uncertainty of the total counts, absolute uncertainty as a percent of the total counts (*M*), and absolute uncertainty of raw variance (*R*) as a percent. Tables 2 and 3 contain the averaged results of the free field and surrogate vehicle assemblies, respectively, and were used as the MAXED measured data.

Table 2. Free Field MAXED Measured Data.

	Free Field MAXED Measured Data (Averages)			
Sphere Diameter [cm]	Count Rate [counts/sec]	Abs Uncertainty of M	% Uncertainty of M	Ave % Uncertainty of R
Bare	4.0804E+01	4.1328E-01	1.013	6.39
5.08 (2”)	8.2060E+01	5.8666E-01	0.715	4.19
7.62 (3”)	1.4800E+02	7.8877E-01	0.533	3.21
12.7 (5”)	2.4489E+02	1.0165E+00	0.415	2.35
20.32 (8”)	2.0604E+02	9.3195E-01	0.452	2.69
25.4 (10”)	1.3903E+02	7.6460E-01	0.550	3.44
30.5 (12”)	8.7003E+01	6.0423E-01	0.694	4.51

Table 3. Surrogate Vehicle MAXED Measured Data.

	Surrogate Vehicle MAXED Measured Data (Averages)			
Sphere Diameter [cm]	Count Rate [counts/sec]	Abs Uncertainty of M	% Uncertainty of M	Ave % Uncertainty of R
Bare	9.7780E+00	1.7967E-01	1.837	13.88
5.08 (2”)	5.3725E+01	4.2224E-01	0.786	5.27
7.62 (3”)	1.3349E+02	6.7802E-01	0.508	3.56
12.7 (5”)	2.3381E+02	8.8206E-01	0.377	2.37
20.32 (8”)	1.8437E+02	7.8367E-01	0.425	2.61
25.4 (10”)	1.1651E+02	6.1767E-01	0.530	3.65
30.5 (12”)	7.4871E+01	5.6977E-01	0.761	4.88

As mentioned in the previous section, the ORTEC software, Maestro, receives the alpha peak from the LiI(Eu) detector's operation (Figure 19). A region of interest (ROI) was established to monitor the net count rate and raw statistical variance under the primary alpha peak, thus generating Tables 2 and 3. Minor adjustments were made to the upper and lower boundaries of the ROI due to slight drifts in voltages between Bonner sphere configurations. Maestro has the capability to subtract background radiation from the ROI, thus producing the "net counts" and "net count rate," which is seen in Figure 20.

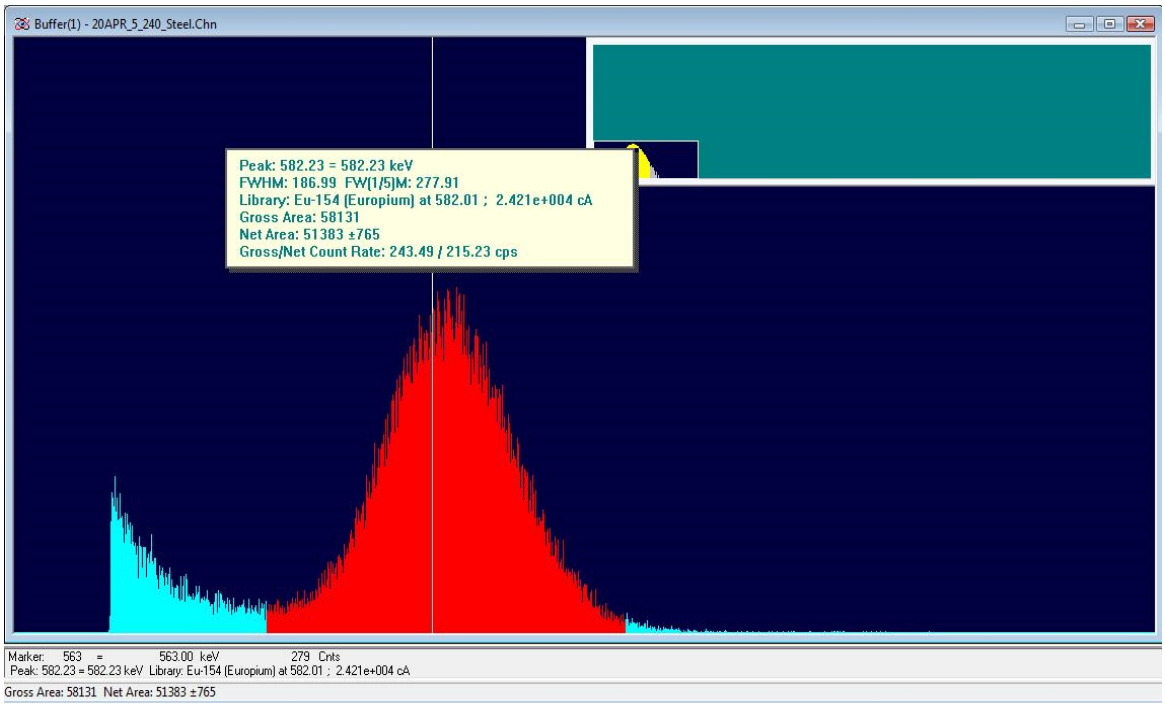

This figure also depicts nuclear forensic and peak identification capabilities based on peak comparison with energy. Because the Li-6(n,α)T reaction produces a fixed energy, this function was ignored and not used.

Figure 20. Maestro Calculated Net Count Rates

b. Default Spectrum (.flu)

The default spectrum, or *a priori*, was produced from the computational method procedures explained later in this chapter. The output from the MCNP code was used as an "initial guess" of the spectra characteristics. Once an initial (theoretical) guess has

been made for a particular spectrum, the MAXED program uses the maximum entropy algorithm to converge the measured data to a solution [29].

c. Response Function (.fmt)

Response functions are generally used to quantitatively describe how the polyethylene spheres and LiI(Eu) detector operate in a particular neutron energy environment with thermalized neutrons. They account for thermal neutrons that interact with the 4 mm x 4 mm (0.157" x 0.157") detection crystal and any polyethylene moderation, at a given thickness, around the detector. MAXED compiles the functions into a response matrix, which is folded with the *a priori* to converge the measured data to a solution spectrum. The response functions used in the BSS system were previously characterized and determined by Andrew Decker, at the Air Force Institute of Technology [3] using MCNP6.1, and have been used as a standard in recent RPF efforts.

d. The Input File (.inp)

Finally, the input file is used to provide general operational information to MAXED, such as the location of the other files or the output spectrum format. Additionally, the input file also allows the user to specify the temperature and reduction factor, the initial χ^2 value, and any modification factors. These additional values were left at default per the UMG v3.3 User's Manual [29].

C. COMPUTATIONAL DETERMINATION

The computational determination is a simulated environment using the MCNP code, as described in Chapter II. The code employs the Monte Carlo (stochastic) mathematical method to solve the overall neutron transport time-independent equation as shown below.

$$\left[\hat{\Omega}*\vec{\nabla}+\sigma\left(\vec{r},\,E\right)\right]\psi\left(\vec{r},\,\hat{\Omega},\,E\right)=q_{ex}\left(\vec{r},\,\hat{\Omega},\,E\right)+\int dE'\int d\Omega'\sigma_s\left(\vec{r},\,E'\rightarrow E,\,\hat{\Omega}'*\hat{\Omega}\right)\psi\left(\vec{r},\,\hat{\Omega}',\,E'\right) \qquad (3.3)$$

where,

$\vec{r}$ = The position vector.
$\hat{\Omega}$ = Unit vector solid angle
E = Energy

$\psi(\vec{r}, \hat{\Omega}, E)$ = Angular neutron flux
$\sigma(\vec{r}, E)$ = Total neutron microscopic cross-section, to include all interaction.
σ_s = neutron microscopic cross-section for scatter
q_{ex} = Emission density from external sources.

Equation 3.3 is presented to indicate the scope and complexity of computationally simulating the problem which includes analysis of neutron transport, interactions and ultimately dosimetry. This section provides a brief introduction to deterministic and stochastic neutron transport calculation methods, the Monte Carlo method, and the applicable MCNP simulation.

1. Deterministic v. Stochastic Methods

Because neutron transport analysis has a wide range of applications, from reactor core to weapon physics, there are two primary methods to solving the neutron transport equation: deterministic and stochastic methods. The deterministic method, used in reactor-based applications, solves the full linearized Boltzmann transport equation through the use of seven different dimensions (space, time, spin, and energy) [31], [32]. Neutron kinetics plays an integral role in reactor based phenomena that are not necessarily represented in weapon based scenarios. For example, neutron transport and interactions in a reactor correlate directly to the output power level and core life. Therefore, a deterministic method to solve the Boltzmann transport equation is needed because it leaves little room for error and better represents an exact solution. This model could be employed in weapons physics prior to detonation, but because the RPF campaign looks at post detonation neutron transport, an exact solution is not needed.

Instead, the RPF research campaign uses a statistical-based method through a set of random processes. The stochastic, or Monte Carlo, method uses a pseudo-random number generator to statistically approximate the interactions between neutrons and the medium they are transporting through. For example, the user first stipulates a large, but finite, number of particle histories. The pseudo-random number generator then determines absorption rates, collision statistics, and scattering angles for all particles of interest. Once the particle has been terminated, via absorption or escaping past the boundary of the specified problem, the particle history is “tallied” and recorded. Tallies

can range from flux or fluence to a specific nuclear interaction or scattering event. Once a tally has been made, the mean quantity is determined via Equation 3.4 and reported to the user. Therefore, the total averaged neutron flux in a specified region or point is simply the summation of all the flux values tabulated at different energy segments (or bins) [31].

$$\hat{x} = \frac{1}{N}\sum_{n=1}^{N} x_n \tag{3.4}$$

The primary consequence of using the deterministic method vice the stochastic method is the exceptionally high computational requirements that follow solving the seven dimension linearized Boltzman transport equation. Because high fidelity is not of concern post detonation of a nuclear weapon, stochastic methods are used with an acceptable margin of error.

2. MCNP6.1 Simulation

The MCNP6.1 simulation begins with an input file called an "input deck." The input deck consists of several "cards," that are used to describe different attributes of neutron transport. Examples of the primary cards are as follows: cell, surface, and data cards. Additional information on the construction and format of the MCNP6.1 simulation can be found in the corresponding user's manual [14].

The NPF MCNP model began with an input deck provided by Dr. Luisa Hansen, who simulated the RCL facility in a number of transport codes for Dr. Radev's RCL characterization report [26]. Slight alterations were made to Dr. Hansen's input deck to better suit the RPF research campaign and to include the surrogate vehicle test article. The complete MCNP input deck used to simulate the irradiation experiment at the RCL facility can be viewed in Appendix F.

a. Cell Card

The cell card in MCNP6.1 contains the information on the relative relationship between objects and surfaces, through utilizing Boolean expressions and union operators. For example, consider Figure 21, which shows the visual editor and plotting component of MCNP. In this example, cell 110 is the cell which contains all of the air in the problem

and is located outside of cell 310, 5100, 5200… 5700, 5800, etc. Each of the cells are generated with their own surfaces in the surface card. The cell card couples information from other cards with the relative relationship between geometries to assemble the modeled problem for simulation.

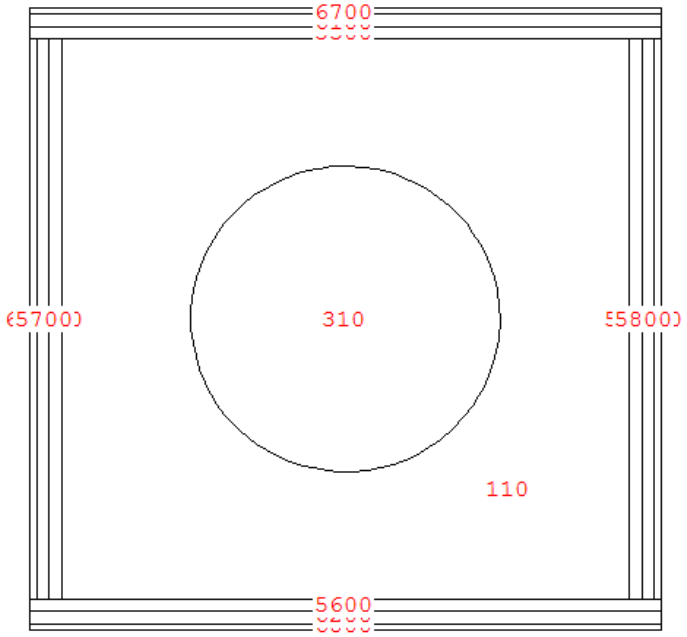

This figure was generated using MCNP's VISED program. The cell numbers depicted have since been changed and altered, but the general structure remains the same.

Figure 21. MCNP Cell Card Example.

A total of 19 cells were incorporated within Dr. Hansen's model, which describe each of the surrogate vehicle plates. A detection sphere composed of air was placed at the center of the surrogate vehicle in the model to simulate the largest polyethylene sphere used during the experimentation. It was assumed that during the experimentation, any neutron that was terminated, via absorption, in the polyethylene sphere made it to the scintillation crystal. This is not an unreasonable assumption considering the average neutron energy from the Cf-252 source, but could be a source of error or difference between the experimental irradiations and the model. The average flux of neutrons entering the air sphere was recorded and "tallied" with its corresponding energy bin.

Because the response functions that were included in the deconvolution procedures accounted for the interactions between neutrons, polyethylene, and the LiI crystal, there is no need to model each of the different Bonner sphere configurations, and allows for the detection sphere (cell 310 in Figure 21) to be air.

As alluded to earlier, the cell card incorporates information from other cards, such as cell material, density, and particle tracking importances. Once the user has defined and selected an appropriate cell number, the material of that cell and its density is defined. The material card is included in the data card, which will be described later in this section. Next the user defines its location relative to other surfaces, which was previously explained. Finally, the user stipulates the cells particle importance. For example, if a neutron travels through the outer walls of the RCL, it is highly unlikely that it will return to interact with the 4 mm x 4 mm (0.157" x 0.157") LiI(Eu) crystal. Therefore, to save computational resources, the importance can be set to "n=0," thus telling MCNP that anything beyond that cell does not need to be tracked. Other more complex applications can allow for the user to filter certain particles, but is beyond the scope of this research.

b. Surface Card

The surface card is used to define the physical geometries of the simulation on a predefined coordinate system. Within MCNP, both physical planes (surfaces) and objects (macrobodies) can be defined and placed at their desired location. Adjustments to Dr. Hansen's MCNP input deck included the addition of the vehicle surrogate test article centered, along all primary axis (x, y, and z), 285.2 cm (11.2") from the source on the south side of the RCL. The surrogate vehicle plates were modeled as rectangular parallelepiped at their respective thicknesses and flush to exclude any air gaps. Because the skeletal structure that the plates were mounted to is hollow, it was assumed that they played a negligible role in altering the neutron kinetics of the problem, thus were removed from the simulation. A spherical macrobody was used for the air detection sphere.

c. Materials Card

Within the materials card, information on the isotopic composition and fractions are defined for use in the cell card. After the user stipulated a material number, the isotopic composition and mass or atom fractions are defined. For example, consider the aluminum plates found on the vehicle surrogate, which were defined as "13027 1.0." The first two digits, "13," represent the atomic number, and the last three digits, "027," represent the atomic mass number (ZZAAA in ZAID notation). In this case, the selected aluminum was solid (1.0) aluminum-27. The materials added to Dr. Hansen's input deck were standard carbon steel and glass reinforced plastic without any boron content. Table 4 lists the material and isotopic mixture of the steel and GRP. Figure 21 was regenerated to create Figure 22, but recolored to indicate material composition.

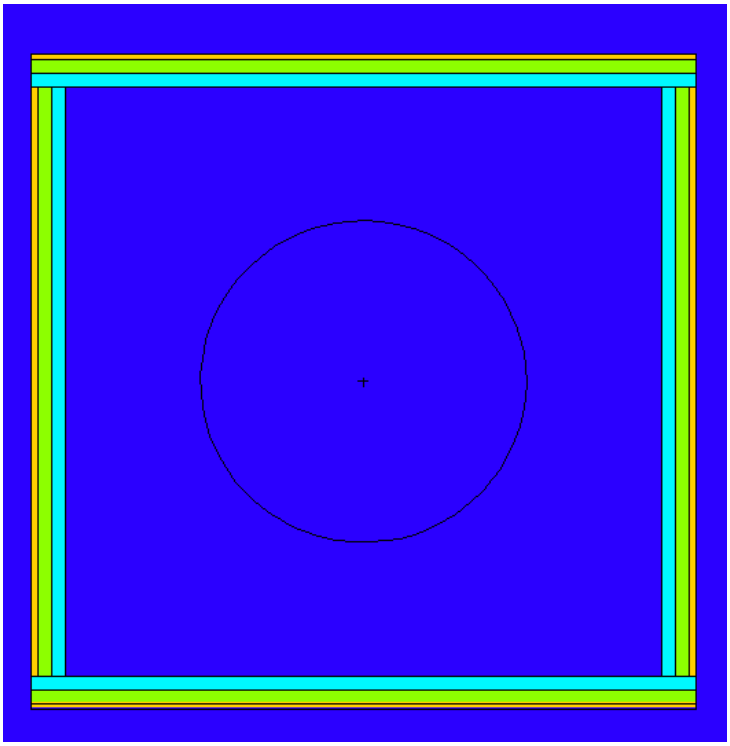

This figure was generated using MCNP's visual editor software. Here the vehicle surrogate is represented by several plates. The aluminum (yellow) is the outer most, followed by the GRP (green), then steel (cyan). The air detection sphere (blue) is the location of the measured flux.

Figure 22. MCNP Material Card Example.

Table 4. Isotopic Mixture of Steel and GRP Plates

Standard Carbon Steel		
Element	**Mass Fraction**	**Mass Number**
Iron	0.977170	56
Carbon	0.022831	12
GRP		
Element	**Mass Fraction**	**Mass Number**
Hydrogen	0.030	1
Carbon	0.060	12
Oxygen	0.390	16
Aluminum	0.010	27
Silicon	0.230	28
Copper	0.140	63
*Copper	0.060	65
Bromine	0.050	79
*Bromine	0.050	81

*Note the different isotopes of copper and bromine, indicated by their respective mass numbers.

d. Source Card

The source card is used to define the location, energy, volume, and mode of the Cf-252 source. Dr. Hansen used the Watt Spontaneous Fission function (Equation 3.1) to define the distribution of output neutron energies from the simulated source. The source is located slightly off center from room and 285.2 cm (11.2”) north of the vehicle surrogate. The simulation dictated “mode n,” which indicated that the particle present within the modelled problem is neutrons. By limiting the model to only track neutrons, two assumptions are inherently made:

1. The flux of residual or delayed neutrons produced from gamma interactions with the iron in the steel plates is negligible when compared to the flux incident to the surrogate vehicle from the Cf-252 source.
2. Gamma particles have no appreciable impact on the LiI(Eu) detector’s operation.

e. Tally Card

The tally card contains the information of how, where, and when neutron histories are recorded when they are terminated. Three primary tallies were used in conjunction with MCNP's internal tally commands. The first and second being a high resolution, 200 logarithmically spaced, fluence tally ("fN4") starting at approximately 0 MeV and ending at 12.5 MeV. The second tally was then modified by MCNP's standard dose function 1, which applies the ICRP-74's fluence to dose conversion coefficients and outputs an absorbed dose solution spectrum in units of pSv/hr/source particle. [11]. Finally, the third tally mimicked the first tally, but had a broader (47) energy bin structure that directly correlated to the ICRP-74's bin structure for the fluence to dose coefficients [11]. The matching energy bin structure allowed for the fluence to dose coefficients to be applied without any additional post processing. However, it was observed that a broader, or low resolution, energy bin structure produced poor results during the deconvolution process.

IV. COMPUTATIONAL AND EXPERIMENTAL RESULTS AND CODE VALIDATION

Computational and experimental results are the two final pieces required in order to assess the suitability of the MCNP code to model neutron transport and radiation protection of military vehicles or structures. In this section, you will find the results of the irradiation experiments conducted on the 18th through the 21st of April, 2017 at the RCL, and the respective computational results from the MCNP model. Additionally, the final code validation comparison is made with an error analysis consideration.

A. COMPUTATIONAL RESULTS

Figure 23 shows the computational results plotted by upper energy bin of both the free field and surrogate vehicle assemblies. Both spectra were normalized and plotted per unit lethargy (u), as per in Equation 4.1.

$$u = \ln\left(\frac{Energy\ of\ Upper\ Energy\ Bin}{Energy\ of\ Lower\ Energy\ Bin}\right) \tag{4.1}$$

The results were determined by applying the fluence to dose conversion coefficients from the ICRP-74 [11] manually and automatically within MCNP6.1. In order for MCNP6.1 to convert directly to dose, "standard dose function 1" was applied to the fluence tally [14]. MCNP6.1 then outputs a dose spectrum, instead of the standard fluence spectrum created from the "f4" tally [14]. In order to produce the dose manually, an unmodified fluence tally (f4) was exported externally to a spreadsheet. The energy bins were summed and grouped to mimic the energy bin structure found in the ICRP-74. Finally, the fluence to dose conversion coefficients were applied directly and plotted in the same manner to produce the dose spectra.

It was observed that there were discrepancies between the two methods, which produced protection factors roughly 0.4% difference. It is suspected that MCNP6.1 interpolates between the tabulated values in the ICRP-74, but its complete methodology is unclear. In order to match experimental procedures, the manual method was used and remained a standard in determining the protection factor quantities.

As aforementioned in Chapter III, there were 200 logarithmically spaced energy bins ranging from 1.00E-09 MeV to 1.25E+01 MeV. The results depicted in Figure 23, show logical radiation protection characteristics, where a shielding assembly reduced the incident flux. The comparative dose effects from both the fast and thermal neutron energy ranges can also be observed in Figure 23. For example, a thermal neutron (e.g., less than 1 eV of energy) is significantly less harmful than a fast neutron (e.g., greater than 100 KeV of energy). As a result, the contribution to dose from thermal energies is negligible when compared to fast energy neutrons. As described in Chapter I, this is primarily because a thermal neutron has less energy to depart on a human's external tissue than a fast neutron. Therefore, the ICRP applies a conversion coefficient of approximately 7 for thermal neutrons, vice up to 600 for a fast neutron.

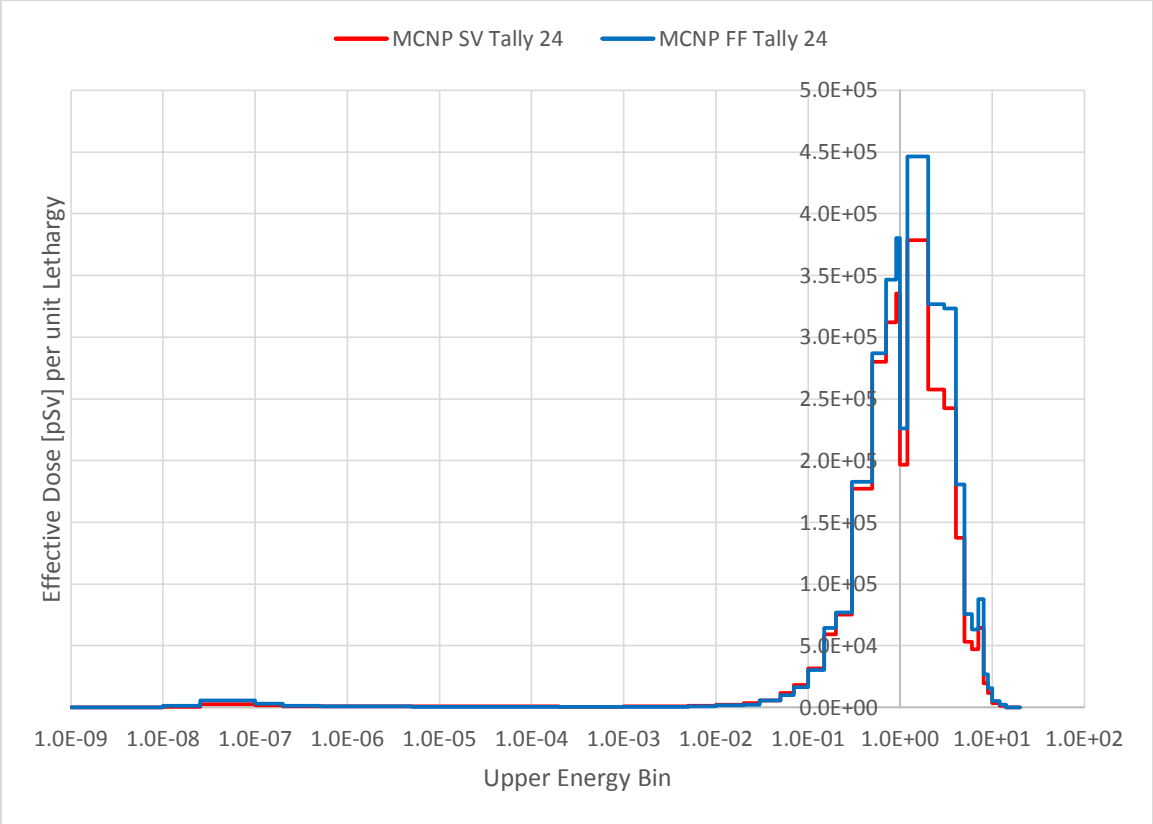

Completed by manually summing and grouping energy bins and applying the ICRP-74 fluence to dose conversion coefficients.

Figure 23. Computational Results

The dose spectra are then integrated over the energy bin to determine the total dose received, independent of time. Table 5 shows the total dose received for both the free field (FF) and surrogate vehicle (SV) assemblies, and subsequently the calculated NPF using equation 1.2. The results are presented per source particle generated, as specified by the user in the tally card (Chapter III, Section C.2.e). The resultant NPF is greater than 1, in which the total integrated dose spectrum for the surrogate vehicle assembly is approximately a factor of 1.16 less than the total integrated dose spectrum for the free field assembly. Additionally, the calculated computational NPF coincides with previously determined NPFs for the similar surrogate vehicle test article but under a different neutron environment [3]. Because of the complexity of the modeled problem and facilities, Appendix G shows only the resultant tally tables and omits the entire MCNP6.1 output file.

Table 5. Computational NPF Calculation Results

Assembly	Units	Dose
Surrogate Vehicle	pSv	8.54E+05
Free Field	pSv	9.90E+05
NPF	**-**	**1.1604E+00**

B. EXPERIMENTAL RESULTS

After the irradiation experimentation, the measured data was combined and unfolded, or deconvoluted, to provide an output spectrum as described in Chapter III. The initial and final χ^2 values are listed in Table 6, and are included in Appendix H with their respective MAXED output files. The significance of the final χ^2 values is that they identify the degree of convergence between the measured data and the *a priori* estimate, and that the values are less than one, which was deemed acceptable by the UMG authors [29]. However, if the initial χ^2 value was set too low, the solution spectrum would not have been consistent with the measured data, and if set too high, the spectrum would not have converged. In regards to this research, the initial χ^2 value was set between 0.9 and 1.0, and was varied slightly. The observed results of varying the χ^2 values had no impact

on the output spectrum, thus only the difference between the initial χ^2 value and the final χ^2 values were considered. If the difference was greater than 5%, arbitrarily determined, the unfolding component files were reexamined for accuracy. However, the difference between the χ^2 values never exceeded the 5% standard, and thus were left unchanged.

Table 6. Initial and Final χ^2 Values During Unfolding

	Assembly	
	Free Field	**Surrogate Vehicle**
Initial χ^2	0.800	0.800
Final χ^2	0.796	0.804
Difference [%]	0.5	0.5

With the χ^2 values listed above, Figure 24 was generated with both free field (FF) and surrogate vehicle (SV) assemblies, in histogram format by upper energy bin. The total energy bin structure is identical to the simulated dose spectra aforementioned, and consists of 200 logarithmically spaced energy bins.

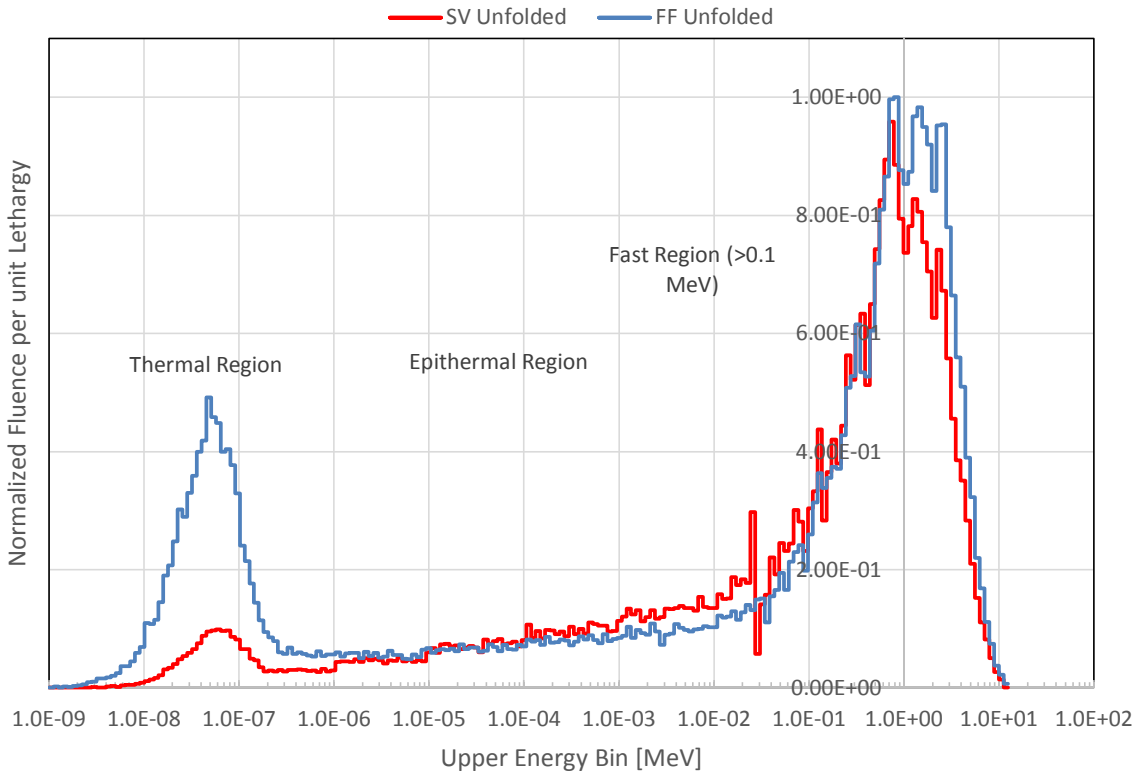

Figure 24. Experimental Fluence Results Normalized.

In Figure 24, key aspects and spectral characteristics can be observed between each assembly. Firstly, the SV (red) assembly shows significant reduction in the thermal energy region (i.e., energies less than 1 eV), with minor "negative" reduction in the epithermal and fast regions. Because the steel plates are composed mostly of iron-56, Figure 25 depicts the inelastic, elastic, and absorption cross sections for iron-56 plotted as a histogram from thermal to fast energy regions.

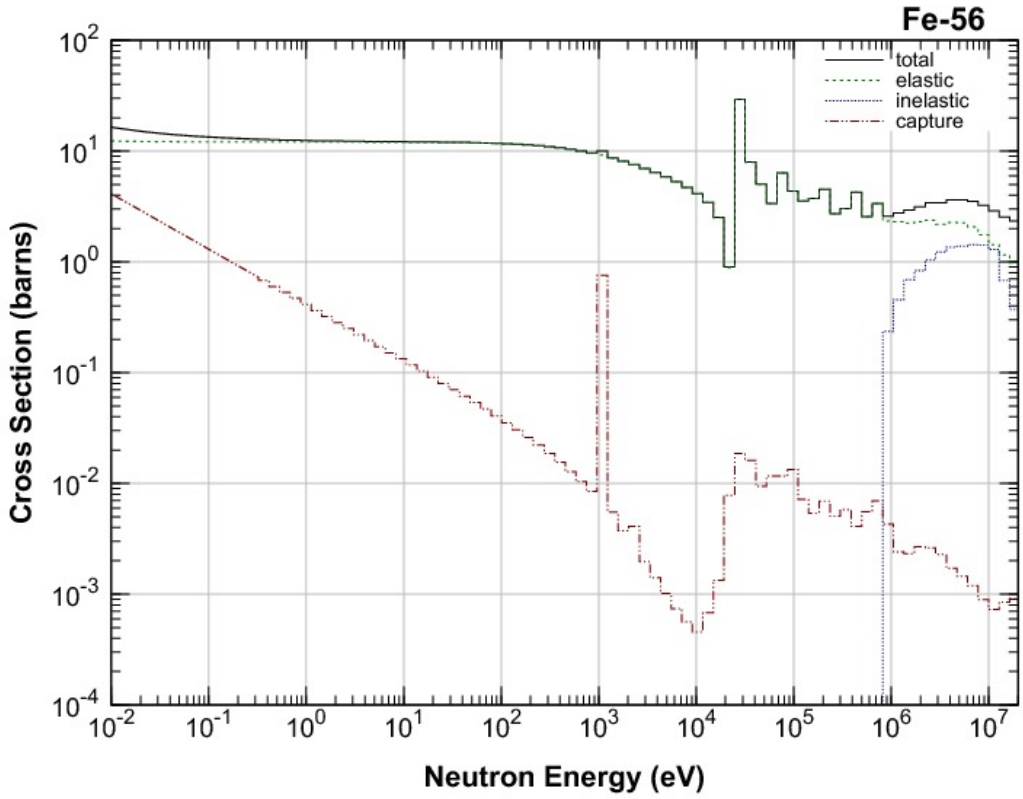

Note: histogram was produced by averaging cross sections into a 70 energy bin structure.

Figure 25. Fe-56 Cross Section Data. Source: [33].

The cross section for neutron capture in iron-56 is approximately three orders of magnitude higher at thermal neutron energies than fast energies. This increase may explain the significant reduction in fluence from the FF to the SV assemblies, where thermal neutrons are more likely to be captured and absorbed by the iron content in the steel plates. It is suspected that the disparity in the fluence spectra in the epithermal energy range is again, primarily due to the iron-56 presence in the steel plates. Here, the SV fluence reduction from the FF fluence is considered to be "negative" because the SV fluence is greater in magnitude than the FF fluence. This implies that for a particular energy range, military personnel would receive a lower dose by leaving the vehicle, post nuclear detonation, than remaining in the vehicle. Fortunately, the NPF considers total dose across all energy bins, and the negative reduction in a limited range of energies is

typically much less of a contributor to the total dose than the positive reduction. From 0.01 to 1 MeV, iron-56 undergoes a nuclear resonance region for neutrons. This nuclear phenomenon occurs when the incident neutron has a certain discrete energy value that corresponds to a specific cross-section probability. The physical system, or nucleus, can then undergo oscillations in the cross-section probabilities, as shown in Figure 26.

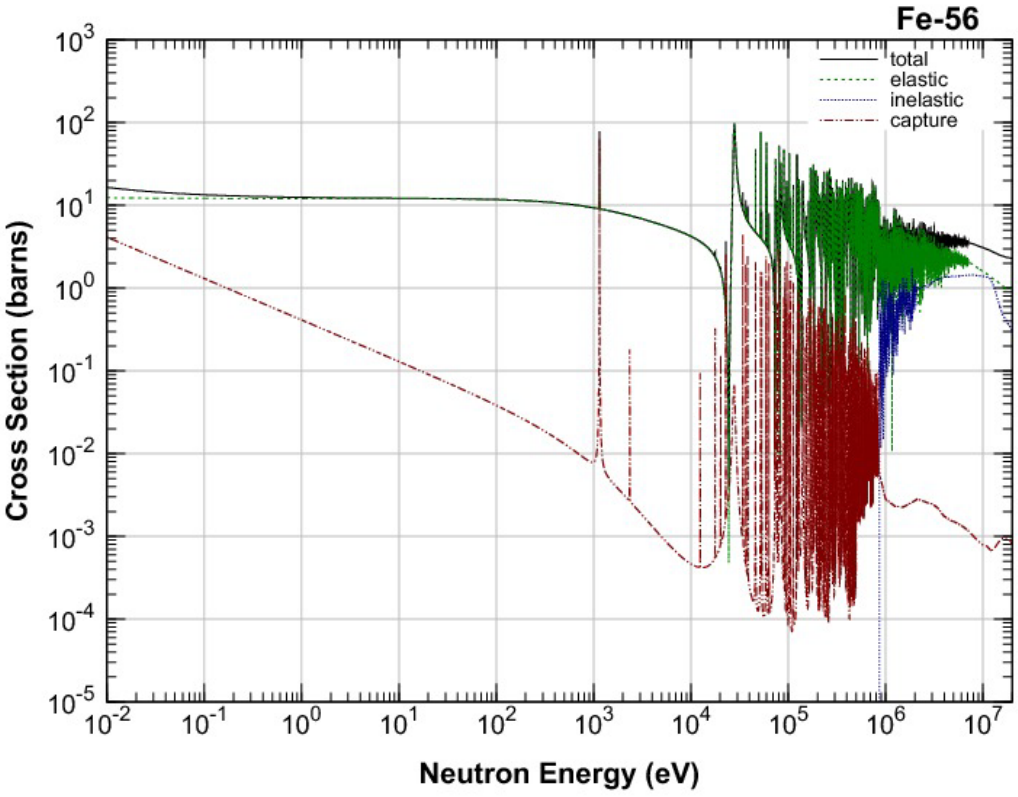

Figure 26. Fe-56 Neutron Cross-Sections and Resonance Region. Source: [33].

The resonance region is problematic in the epithermal neutron energies because at certain discrete energies the likelihood for a capture reaction to occur versus a scattering reaction is as much as six orders of magnitude lower. In a region where scattering reactions significantly dominate, neutrons may become “trapped” inside of the surrogate vehicle, and could account for a NPF of less than one for that specific energy range.

Unlike the simulated model, the UMG v3.3 unfolding code does not contain the capability to directly apply the ICRP's fluence-to-dose coefficients, which were later applied manually. The 200 energy bins, post convergence, were grouped and summed together per the ICRP-74's energy bin structure [11], as shown in Figure 27.

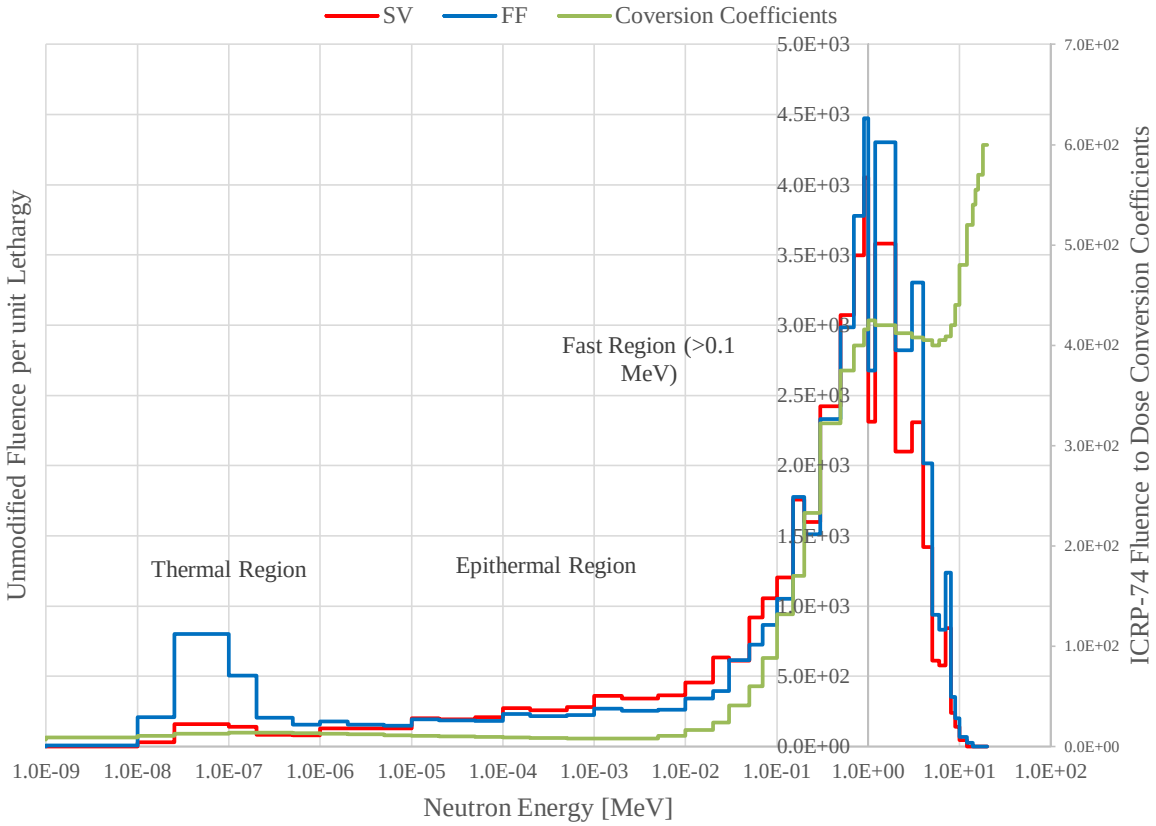

Figure 27. Experimental Fluence per Unit Lethargy with ICRP-74 Energy Bin Grouping

Similar characteristics can be observed in the lower resolution energy bin structure (Figure 27) that are also seen in the higher resolution energy bin structure (Figure 24). The ICRP-74 conversion coefficients were plotted in the same manner as the fluence spectra, so that the overall contribution to dose, per energy bin, could be observed. For example, the conversion coefficients in the epithermal range, where the majority of the surrogate vehicle fluence is higher than the free field fluence, are two

orders of magnitude lower than the coefficients in the fast energy region. While considering the large differences in fluence in conjunction with the increase in conversion coefficients, the thermal and epithermal regions' contribution to the NPF were negligible when compared to the fast region. Applying the conversion coefficients produces the dose spectra in Figure 28, which were integrated to determine the following NPF.

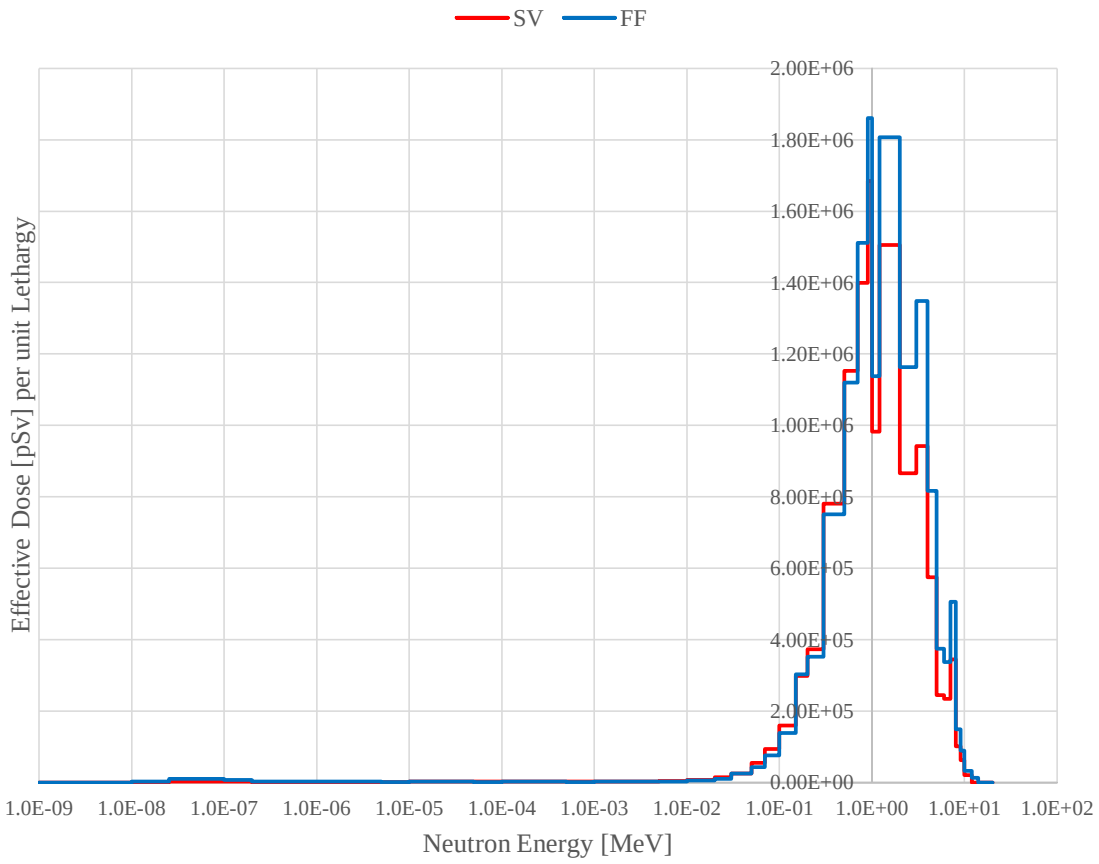

Figure 28. Experimental Effective Dose Spectra for FF and SV Assemblies

Table 7. Experimental NPF Calculation Results

Assembly	Units	Dose
Surrogate Vehicle	pSv	3.57E+06
Free Field	pSv	4.12E+06
NPF		**1.1559E+00**

The units from computational dose values and experimental dose values are different because of the units associated with the unfolding process. The values in the computational code were reported as rem/hr and were compared with published values in Dr. Radev's report as aforementioned. During unfolding, the fluence-to-dose conversion coefficients use international units, pSv. NPF is a ratio of doses and is reported as a unitless value, thus can be directly compared between the computational and experimental procedures.

C. ERROR ANALYSIS

Error in the RPF research campaign is determined via two methods: statistical error introduced by sums or differences of counts in the computational spectra or as determined by the use of a covariance matrix algorithm for the experimental spectra. The sums or difference counts is calculated via Equation 4.2 ([1], [5]), and is simply the square root of the sums of standard deviations from both the free field and surrogate vehicle assemblies as applied to the NPF.

$$\sigma_{total} = \sqrt{\sigma_{FF}^2 + \sigma_{SV}^2} \tag{4.2}$$

The resultant error presented by MCNP is summarized in Table 8, and was assessed for each of the tallies used. Tally 24 was used to produce the data presented earlier in the chapter, and the additional tallies were used to address MCNP's capability of producing dose quantities. Interestingly, the NPF values determined from the tally that was grouped and to which the conversion coefficients were applied manually (Tally 24), and from the tally which used MCNP's standard dose function one (Tally 14), are approximately 0.5% different. It is suspect that MCNP interpolates between the 47 values published by the ICRP-74 for higher energy bin resolution capabilities, but the exact mechanism is unclear and requires additional research. Because the converged solution spectrum required a higher energy bin resolution and subsequently needed manual

grouping, the NPF produced via Tally 24, which used the exact same procedure, was used in the validation component of this research.

Table 8. Statistical Error Presented By MCNP.

MCNP Statistical Error				
Tally	**24 (FF)**	**24 (SV)**	**14 (FF)**	**14 (SV)**
Total Fluence	9.90E+05	8.54E+05	3.43E-01	2.94E-01
Fluence Var.	2.80E-03	3.20E-03	3.90E-03	4.30E-03
σ^2	7.84E-06	1.02E-05	1.52E-05	1.85E-05
$\Sigma\sigma^2$	1.81E-05		3.37E-05	
Sqrt. Sum	4.25E-03		5.81E-03	
NPF	1.1601E+00	+/- 0.00425	1.1654E+00	+/- 0.00581
+	1.1644E+00		1.1712E+00	
-	1.1559E+00		1.1596E+00	

This table was generated based on 1.5E+07 neutron particles (nps) specified in the MCNP6.1 input deck.

The covariance matrix algorithm was employed by UMG's integral quantities software, which evaluates the quantitative sensitivity, or error, of the solution spectrum to that of the *a priori* estimate. For example, if the sensitivity of the calculated solution spectrum is 5% for a specific energy bin or range, then as the *a priori* estimate is changed, the solution spectrum can change as much as 5% for that energy. The result of the integral quantity assessment indicated that the main contributor to the sensitivity of the solution spectrum was primarily due to the statistical error introduced by the *a priori* estimate. The error introduced by the measured data, *a priori*, and the combination of the two are reported in Table 9. Additional information on the covariance matrix solver can be found in the UMG v3.3 user manual [29], and the integral quantities output files which support the data presented in this thesis can be found in Appendix I.

Table 9. Summary of Calculated Error for NPS = 1.5E+07

Unfolded Error		
	FF	**SV**
Measured Data Error	1.28E+00	1.40E+00
***A Priori* Error**	3.30E+00	3.57E+00
Combined	3.60E+00	3.89E+00
$\boldsymbol{\sigma^2}$	1.30E-03	1.51E-03
$\boldsymbol{\Sigma\sigma^2}$	2.81E-03	
$\boldsymbol{\sqrt{\Sigma\sigma^2}}$	0.0530	
NPF	1.1559E+00	
+	1.2090E+00	
-	1.1029E+00	

An additional effort was made to reduce the error in the unfolding process by significantly reducing the statistical error introduced by the *a priori* estimate. Therefore, the number of particles emitted by the simulated Cf-252 source was changed in the MCNP input file from 1.5E+07 to approximately 8.0E+07, and the error was reassessed with the *a priori* spectrum. Because of the computational resources and time required for an increased in emitted particles, it became unreasonable to extend it past 8.0E+07 (approximately 400% increase from the original amount). While the data aforementioned was left unchanged, the reassessment of the sensitivity of the solution spectrum will help to establish a standard for acceptable computational error, and identify the need for further research in this section of the RPF research campaign. Table 10 shows a combined error reduction of approximately 1.60 in both the free field and surrogate vehicle assemblies.

Table 10. Summary of Calculated Error for NPS = 7.957E+07

Reduced Unfolded Error		
	FF	**SV**
Measured Data Error	1.28E+00	1.40E+00
A Priori Error	1.43E+00	1.55E+00
Combined	2.00E+00	2.16E+00
σ^2	3.99E-04	4.65E-04
$\Sigma\sigma^2$	8.65E-04	
Sqrt. Sum	0.029402609	
NPF	1.1559E+00	
+	1.1853E+00	
-	1.1265E+00	
a priori NPS value:	7.957E+07	

D. CODE VALIDATION

The results presented above concluded that the MCNP6.1 code is suitable for modeling a simple geometry but complex composition surrogate vehicle test article in a known neutron environment for the determination of the associated NPF. Without including possible error propagation, the difference in determined NPFs between the computational model and experimental irradiations is approximately 0.3%. Past experiments conducted from accelerator and reactor type sources produced protection factors that faired within 5 to 10 percent of each other [1]–[3], [25]. The significant reduction in difference between the simulation and irradiation experiments can be attributed to the stability and quality of the RCL source, construction, and staff.

Table 11. NPF Results Summary and Validation

MCNP		
	Units	Dose
Surrogate Vehicle	pSv	8.5367E+05
Free Field	pSv	9.9037E+05
NPF		**1.1601E+00**
EXPERIMENTAL		
	Units	Dose
Surrogate Vehicle	pSV	3.5663E+06
Free Field	pSV	4.1223E+06
NPF		**1.1559E+00**
Difference	%	0.36

E. ASSESSMENT OF FREE FIELD ASSEMBLY RESULTS COMPARED TO KNOWN CHARACTERIZATION

To assess the quality of the BSS detection system, the experimental results of the free field assembly were compared to Dr. Radev's RCL report [26], which completely characterized the LLNL Cf-252 source and RCL using the Rospec detection system. Although the two experiments were conducted on opposite sides of the facility, a comparison could be made because it was assumed that the Cf-252 source isotropically emitted neutrons. Both experiments were conducted at approximately 3 meters from the source at an equivalent height, but on opposite sides of the RCL. Figures 29 and 30 depict Dr. Radev's results and the NPS free field assembly results, respectively. Additionally, Figure 30 overlays the data reported by Dr. Radev's experiments with the data presented in this research. It is important to reiterate that both irradiations were bare (free-in-air) and at approximately 3 meters (9.84') from the Cf-252 source.

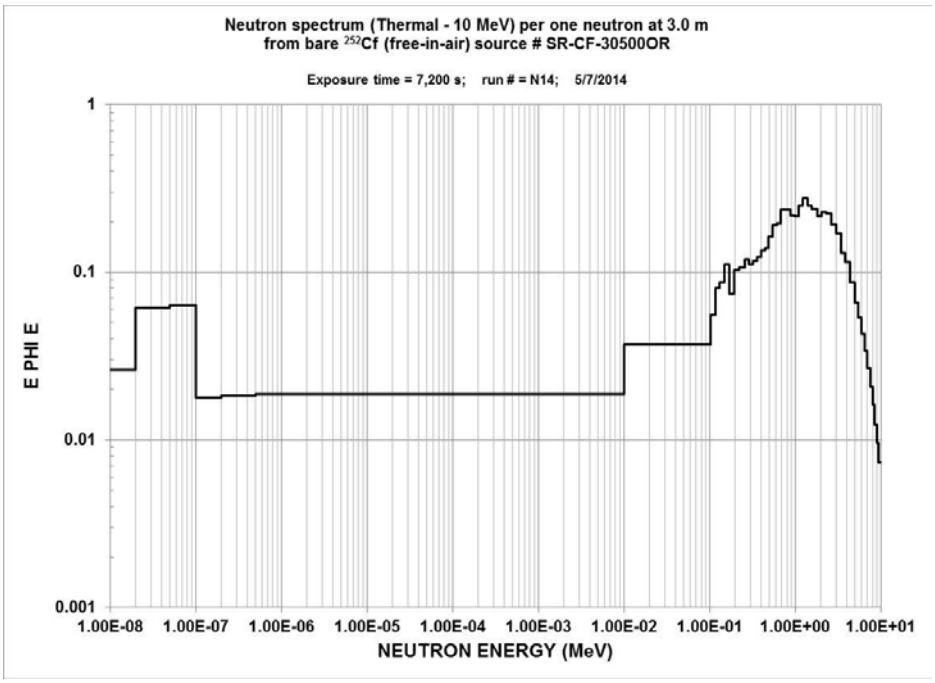

Figure 29. RCL Bare Cf-252 Fluence Spectrum. Source: [26].

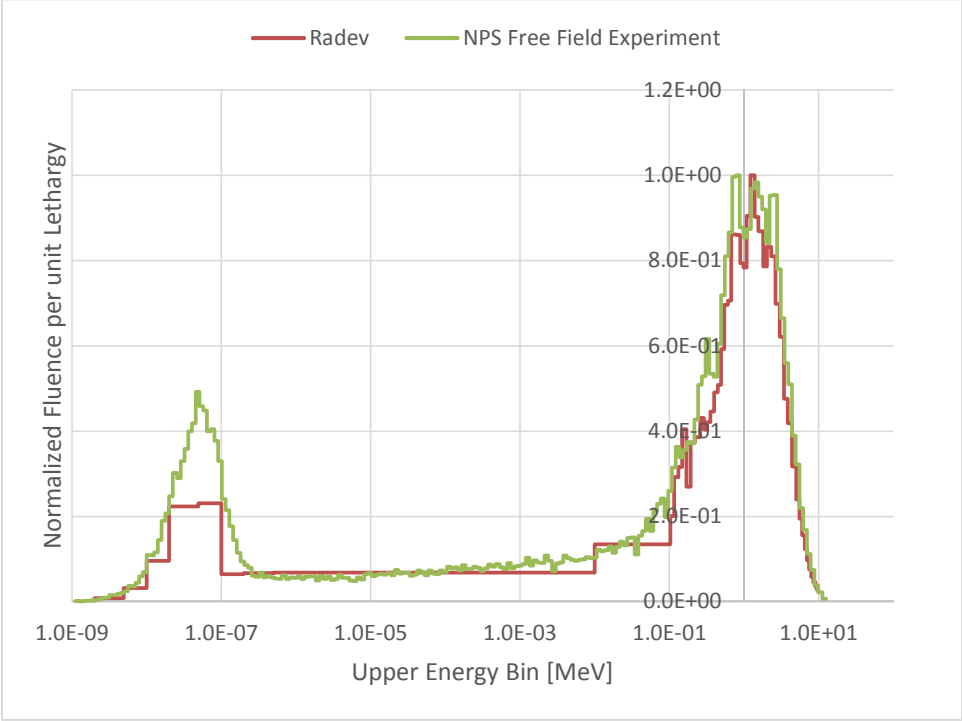

Figure 30. NPS Free Field Experiment and Dr. Radev's Bare Experiment

Both irradiation measurements are very similar and follow the same spectral characteristics. Because fluence-to-dose conversion coefficients dominate in the fast neutron energy region, the discrepancies in spectral values in the thermal energy region are negligible. It is suspected that the finer bin structure produced in the BSS unfolding technique allowed for additional spectral characteristics to be observed. For example, consider the spectral trends from 0.1 eV to 10 KeV from the BSS system compared to Dr. Radev's characterization experiment, which are flattened due to a broader energy bin structure. The data produced by the BSS system provides LLNL's calibration facility with a finer energy bin structure and further characterization of the neutron spectrum emitted from the Cf-252 source.

The finer bin structure from the BSS system is not the only possible contributing factor to spectral discrepancies observed. An additional source that could have attributed a higher thermal fluence is the presence of the large steel cart located directly under the BSS during NPS irradiations. It is suspected that the additional neutron moderation with iron-56 from the surface of the steel cart produced a higher thermal neutron fluence. Because the steel cart and additional wood were present in all NPS irradiations, it was unclear the degree of impact on the resultant fluence spectra. Another source of discrepancy could be the detection mechanisms themselves, and differences in detector efficiencies and overall computational error. The Rospec spectrometer, used in Dr. Radev's characterization irradiations, consists of six gas-filled proportional counters (Figure 31). Four of the six spheres "contain H_2 (or P10), while the other two contain ^{3}He" [26]. The results from the RCL characterization indicated the Rospec detection system was in "good agreement with absolute neutron fluence within 10%, and that the new calibration factors are in good agreement with those derived from the device's manufacturer" [26]. Nevertheless, the two spectra show general agreement, and should both be considered for future calibration uses.

Figure 31. Rospec Detection System. Source: [26].

THIS PAGE INTENTIONALLY LEFT BLANK

V. CONCLUSIONS AND PATH FORWARD

The data presented in this thesis shows significant progress in DTRA's RPF research campaign. The results highlight the need for future collaboration and the use of highly characterized calibrated radiation environments for further determination and validation efforts. With the difference, in this research, between the computational simulation and experimental irradiations less than 1%, the continued use of the LLNL RCL for future NPF determination and validation experiments of more complex vehicle surrogate test articles is recommended.

Furthermore, it is recommended that DTRA begin exploring methods to reduce the total RPF, either through the reduction of the NPF or GPF induced environment. Methods in how to accurately combine the NPF and GPF to determine an approximate optimization of the RPF would simplify testing procedures and experimentation methods used in the RPF research campaign through eliminating the difficulties of measuring neutron and gamma reduction factors in a mixed field. This effort in combining the NPF and GPF have been vaguely addressed before, and a standard in determining the RPF needs to be established.

To increase the NPF, it is recommended that DTRA look at methods to moderate or thermalize neutrons, and also at methods to increase neutron absorption without impacting the functionality of structural materials already in use. Because the fluence-to-dose conversion coefficients presented by the ICRP are energy dependent and significantly increase after neutrons reach 1 MeV, the total external dose received by personnel inside of a vehicle can be decreased by shifting the neutron spectrum to a lower energy value. The results showed that the external dose received from thermal neutrons is negligible in comparison to the external dose received from fast neutrons. By shifting the neutron energy spectrum through thermalization or moderation, the total absorbed external dose will be reduced, thus increasing the NPF and personnel survivability.

Additionally, it is recommended that DTRA continue and enhance its efforts to address the current levels of radiation protection afforded to vehicles and vessels now

employed in the United States' military. With the nuclear threat growing significantly in the most recent years, this knowledge needs to be relayed to field and ship commanders as soon as possible.

Finally, collaboration between the DTRA and the United States Navy in terms of assessing the radiation protection afforded to forward deployed vessels needs to occur. U.S. Navy vessels and U.S. Army vehicles operate in two very different environments and are susceptible to very different radiation fields. DTRA can utilize this opportunity to assess additional types of neutron transport and complexity within a similar problem for further verification and validation attempts.

APPENDIX A. DTRA'S RPF RESEARCH CAMPAIGN

RPF research integration timeline prior to the supported role at NPS. The integration timeline depicts the overall RPF research campaign to include materials, configurations, assemblies, and institutions.

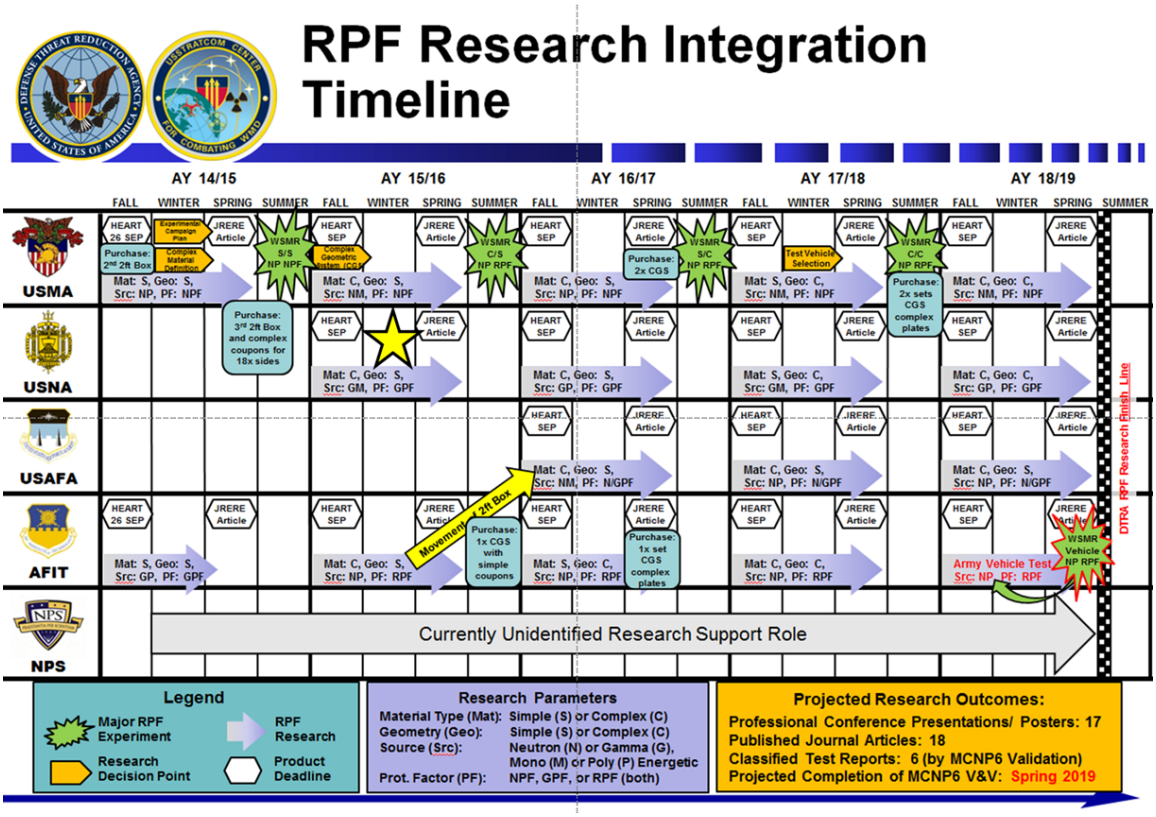

Top to Bottom: United States Military Academy (USMA), United States Naval Academy (USNA), United States Air Force Academy (USAFA), Air Force Institute of Technology (AFIT), and Naval Postgraduate School (NPS).

Figure 32. RPF DTRA's Research Campaign Schedule. Source: [34].

THIS PAGE INTENTIONALLY LEFT BLANK

APPENDIX B. EXCERPTS FROM NPS IRRADIATION EXPERIMENTAL PLAN

The following Appendix contains the experimental plan used from 17 April 2017 to 21 April 2017, in an effort to provide guidance and focus for irradiation experiments.

A. OBJECTIVES

The purpose of this experimental plan is to identify clear objectives to be achieved while conducting experiments at Lawrence Livermore National Laboratory's (LLNL's) Radiation Calibration Lab (RCL). The intent is to conduct experiments that coincide with the Radiation Protection Factor Integrated Timeline and the United States Navy's interests in radiation shielding effects. The following are the intended objectives to be achieved:

Primary Objectives

- Measure the neutron flux within the vehicle surrogate in LLNL's Cf-252 RCL source environment, using the Bonner Sphere Spectrometer (BSS) system.
- Unfold experimental data using UMG v3.3 (MAXED and GRAVEL), FRUIT, or NSDUAZ.
- Apply flux to dose conversion factors from H*(10) or ICRP (74 & 116).
- Calculate NPFs for the vehicle surrogate.
- Model primary assembly within MCNP6.1, apply flux to dose conversion factors, and calculate NPF for code validation.

Secondary Objectives

- Measure and observe the effects on the NPF when altering the primary assembly.
    - Rotating the assembly 45^{o}, while still being centered.
    - Removing glass reinforced with glass (GRP) plates from one or multiple sides to induce a non-symmetric shielding environment.
- Introducing additional materials to enhance neutron protection (i.e., increase NPF)

- Testing and evaluating NPFs or reduction factors (NRF) of ship hull material.

Note: This document only contains brief procedural information regarding the experimentation, and does not include the background, unfolding, and NPF calculations.

B. INFORMATION ON SECONDARY ASSEMBLIES

The secondary assemblies are used to observe and measure the impact of surrogate vehicle alterations on the NPF. There are four goals associated with the secondary assemblies: geometric change, evaluating non-symmetric shielding conditions, introduction of new neutron shielding materials, and free field measurements.

Geometric change

This will consist of simply rotating the box 45 degrees, placing the corner of the vehicle surrogate incident to the source. It is assumed that the same effects will be observed at 45, 135, and 225 degrees as well, because of the symmetric shielding conditions. The objective is to simulate movement within a neutron environment and observing the scattering effects from the corner of the vehicle surrogate.

Non-symmetric shielding conditions

It has been observed elsewhere that neutrons of 1 MeV become trapped within the vehicle surrogate due to the iron resonance cross-section, which inevitably produces a NPF of less than one. If the box is non-symmetric in shielding, this could reduce the effect. It is intended to remove one plate of steel, GRP, and aluminum from different sides of the vehicle surrogate. It is likely that this will better simulate a vehicle in its operational combat capacity.

Introduction to new materials

The current scope of the radiation protection factor (RPF) integrated timeline only includes testing and evaluating material compositions that are typical in a combat environment. It would be advantageous to evaluate the effects of adding a small neutron absorbing material within the vehicle surrogate, while keeping operational capabilities unhindered. The absorbing material is a borated crystalline structure designed by Emil

Kartalov at NPS. The boron content of the structure is roughly 30%, and could prove useful for observing changes in the NPF value.

Lastly, the Navy would like to begin evaluating the radiation protection from typical ship hull material. Cross-section calculations and shielding effects cannot be simply determined because of the complex material composition coating the outer surface of the hull. If the Navy provides a sample of hull material, additional experimental procedures will be written to include it.

Free Field Measurements

Because LLNL's calibration facility has already been fully characterized, the priority of the free field dose measurements is lower than that of the vehicle surrogate. However, for validity purposes and if time permits, the free field measurements will need to be conducted with the BSS system. Like Table 2, Table 4 shows an approximation for the total run time required.

C. ESTIMATED IRRADIATION EXPOSURE TIMES

Table 12. Estimated Time Required for Primary Assembly Experiment.

Process/Task	Estimated Time Required [mins]	Additional Notes
Surrogate Positioning	10	
Detector Setup	30	Initialization and testing
Total Run Time	21	3 minutes for each configuration
*Activation Time	20	~3 minutes between each configuration
Configuration Alteration (2, 3 ,5)	30	10 minutes allotted for configuration alterations for the smaller polyethylene spheres.
Configuration Alteration (8,10,12)	36	12 minutes allotted for configuration alterations for the larger polyethylene spheres.
Total	**147**	
Adjusted Total	**294**	As advised

Table 13. Estimated Time Required for free Field Measurements.

Process/Task	Estimated Time Required [mins]	Additional Notes
Surrogate Positioning	10	
Detector Setup	30	Initialization and testing
Total Run Time	21	3 minutes for each configuration
Configuration Alteration (Bare, 2, 3, 5, 8, 10, 12)	35	5 minutes allotted for configuration alterations for the smaller polyethylene spheres.
Total	**96**	
Adjusted Total	**192**	As advised

D. EXPERIMENTAL SCHEDULE

Tuesday: 18 APR 17	
What	**When**
Equipment Setup [V.S.]	0730 - 1100
Detector Initialization and Testing	1100 - 1200
Bare	1300 - 1330
2” Bonner Sphere	1330 - 1400
3” Bonner Sphere	1400 - 1430
5” Bonner Sphere	1430 - 1500
8” Bonner Sphere	1530 - 1600
*Additional Run Times and Trouble Shooting	1600 - 1700*
*10” / 12” Bonner Spheres	
Tuesday: 18 APR 17 [After Hours]	
What	**When**
10” / 12” Bonner Spheres	1700 - 0800
Wednesday: 19 APR 17	
What	**When**
Equipment Setup [V.S.]	0730 - 0900
Detector Initialization and Testing	0900 - 1000
Bare	1000 - 1030
2” Bonner Sphere	1030 - 1100
3” Bonner Sphere	1130 - 1200

5” Bonner Sphere	1300 - 1330
8” Bonner Sphere	1330 - 1400
10” Bonner Sphere	1400 - 1430
12” Bonner Sphere	1430 - 1500
*Additional Run Time and Trouble Shooting	1500 - 1700*
*Additional Vehicle Surrogate (V.S.) Measurements	
Thursday: 20 APR 17	
What	**When**
Equipment Setup [F.F.]	0730 - 0900
Detector Initialization and Testing	0900 - 1000
Bare	1000 - 1015
2” Bonner Sphere	1015 - 1030
3” Bonner Sphere	1030 - 1045
5” Bonner Sphere	1045 - 1100
8” Bonner Sphere	1100 - 1115
10” Bonner Sphere	1115 - 1130
12” Bonner Sphere	1130 - 1145
*Additional Run Time and Trouble Shooting	1145 - 1200*
Bare	1300 - 1315
2” Bonner Sphere	1315 - 1330
3” Bonner Sphere	1330 - 1345
5” Bonner Sphere	1345 - 1400
8” Bonner Sphere	1415 - 1430
10” Bonner Sphere	1430 - 1445
12” Bonner Sphere	1445 - 1500
*Additional Run Time and Trouble Shooting	1500 - 1700*
*Additional F.F. Measurements if time permits	
Friday: 21 APR 17	
What	**When**
Detection Disassembly	0800 - 1200
Box Deconstruction and Shipping Prep	

THIS PAGE INTENTIONALLY LEFT BLANK

APPENDIX C. ICRP-74 FLUENCE-TO-DOSE CONVERSION COEFFICIENTS

The following coefficients were used to determine total dose values of the deconvoluted spectrum from NPS irradiations at LLNL's RCL. The conversion coefficients are presented per energy bin, and were multiplied directly with the integrated fluence values.

Table A.42. Ambient and personal dose equivalent per unit neutron fluence, $H^*(10)/\Phi$ and $H_{p,slab}(10,\alpha)/\Phi$, in units of pSv cm^2 for monoenergetic neutrons incident in various geometries on the ICRU sphere and slab. See Figs 21 and 31–33

Energy (MeV)	$H^*(10)/\Phi$	$H_{p,slab}(10,0°)/\Phi$	$H_{p,slab}(10,15°)/\Phi$	$H_{p,slab}(10,30°)/\Phi$	$H_{p,slab}(10,45°)/\Phi$	$H_{p,slab}(10,60°)/\Phi$	$H_{p,slab}(10,75°)/\Phi$
1.00×10^{-9}	6.60	8.19	7.64	6.57	4.23	2.61	1.13
1.00×10^{-8}	9.00	9.97	9.35	7.90	5.38	3.37	1.50
2.53×10^{-8}	10.6	11.4	10.6	9.11	6.61	4.04	1.73
1.00×10^{-7}	12.9	12.6	11.7	10.3	7.84	4.70	1.94
2.00×10^{-7}	13.5	13.5	12.6	11.1	8.73	5.21	2.12
5.00×10^{-7}	13.6	14.2	13.5	11.8	9.40	5.65	2.31
1.00×10^{-6}	13.3	14.4	13.9	12.0	9.56	5.82	2.40
2.00×10^{-6}	12.9	14.3	14.0	11.9	9.49	5.85	2.46
5.00×10^{-6}	12.0	13.8	13.9	11.5	9.11	5.71	2.48
1.00×10^{-5}	11.3	13.2	13.4	11.0	8.65	5.47	2.44
2.00×10^{-5}	10.6	12.4	12.6	10.4	8.10	5.14	2.35
5.00×10^{-5}	9.90	11.2	11.2	9.42	7.32	4.57	2.16
1.00×10^{-4}	9.40	10.3	9.85	8.64	6.74	4.10	1.99
2.00×10^{-4}	8.90	9.84	9.41	8.22	6.21	3.91	1.83
5.00×10^{-4}	8.30	9.34	8.66	7.66	5.67	3.58	1.68
1.00×10^{-3}	7.90	8.78	8.20	7.29	5.43	3.46	1.66
2.00×10^{-3}	7.70	8.72	8.22	7.27	5.43	3.46	1.67
5.00×10^{-3}	8.00	9.36	8.79	7.46	5.71	3.59	1.69
1.00×10^{-2}	10.5	11.2	10.8	9.18	7.09	4.32	1.77
2.00×10^{-2}	16.6	17.1	17.0	14.6	11.6	6.64	2.11
3.00×10^{-2}	23.7	24.9	24.1	21.3	16.7	9.81	2.85
5.00×10^{-2}	41.1	39.0	36.0	34.4	27.5	16.7	4.78
7.00×10^{-2}	60.0	59.0	55.8	52.6	42.9	27.3	8.10
1.00×10^{-1}	88.0	90.6	87.8	81.3	67.1	44.6	13.7
1.50×10^{-1}	132	139	137	126	106	73.3	24.2
2.00×10^{-1}	170	180	179	166	141	100	35.5
3.00×10^{-1}	233	246	244	232	201	149	58.5
5.00×10^{-1}	322	335	330	326	291	226	102
7.00×10^{-1}	375	386	379	382	348	279	139
9.00×10^{-1}	400	414	407	415	383	317	171
1.00×10^{0}	416	422	416	426	395	332	180
1.20×10^{0}	425	433	427	440	412	355	210
2.00×10^{0}	420	442	438	457	439	402	274
3.00×10^{0}	412	431	429	449	440	412	306
4.00×10^{0}	408	422	421	440	435	409	320
5.00×10^{0}	405	420	418	437	435	409	331
6.00×10^{0}	400	423	422	440	439	414	345
7.00×10^{0}	405	432	432	449	448	425	361
8.00×10^{0}	409	445	445	462	460	440	379
9.00×10^{0}	420	461	462	478	476	458	399
1.00×10^{1}	440	480	481	497	493	480	421
1.20×10^{1}	480	517	519	536	529	523	464
1.40×10^{1}	520	550	552	570	561	562	503
1.50×10^{1}	540	564	565	584	575	579	520
1.60×10^{1}	555	576	577	597	588	593	535
1.80×10^{1}	570	595	593	617	609	615	561
2.00×10^{1}	600	600	595	619	615	619	570
3.00×10^{1}	515	na[a]	na	na	na	na	na[a]
5.00×10^{1}	400	na	na	na	na	na	na
7.50×10^{1}	330	na	na	na	na	na	na
1.00×10^{2}	285	na	na	na	na	na	na
1.25×10^{2}	260	na	na	na	na	na	na
1.50×10^{2}	245	na	na	na	na	na	na
1.75×10^{2}	250	na	na	na	na	na	na
2.01×10^{2}	260	na	na	na	na	na	na

[a]Not available.

Figure 33. ICRP-74 Fluence-to-Dose Conversion Coefficients. Source: [11].

THIS PAGE INTENTIONALLY LEFT BLANK

APPENDIX D. LII(EU) DETECTOR SETTINGS FOR THE NPS IRRADIATIONS

The following table is representative of the recorded experimental assembly settings that were used during the NPS irradiations at LLNL's RCL from 18 April to 21 April 2017. This information is presented for future reference when using sources similar to the one found at LLNL's RCL.

Table 14. Detection Assembly Settings and Equipment.

Equipment	Model	Setting(s)
High voltage power supply	Ortec 556	700V
Linear amplifier	Ortec 575A	Gain= 1.00
		CG= 20
		Shaping Time= 2 μsec

THIS PAGE INTENTIONALLY LEFT BLANK

APPENDIX E. COMPONENTS FOR UMG V3.3 UNFOLDING CODE

The information presented in this Appendix was used as an input for the multiple components for the unfolding or deconvolution process. The objective of presenting the below data as such is so that they may be directly integrated into UMG v3.3 for further comparison to other UMG input components.

A. FREE FIELD UNFOLDING INPUTS

1. Measured Data File (.ibu)

```
0  *       d       cts / s
  7    0     File 001_Exp.ibu / reference see end of file
0Bare     0.0     4.0804E+01    4.1328E-01    1.013     6.39      1
2in       2.0     8.2060E+01    5.8666E-01    0.715     4.19      2
3in       3.0     1.4800E+02    7.8877E-01    0.533     3.21      3
5in       5.0     2.4489E+02    1.0165E+00    0.415     2.35      4
8in       8.0     2.0604E+02    9.3195E-01    0.452     2.69      5
10in      10.0    1.3903E+02    7.6460E-01    0.550     3.44      6
12in      12.0    8.7003E+01    6.0423E-01    0.694     4.51      7

Dete      Diam      reading M       abs unc   % unc   % unc
ctor      eter      count rate        of M     of M    of R  flag
```

2. Default Spectrum (.flu)

```
File LLNL_SV_DefSpec.flu
         2         1                  fluence  given in n/cm^2/MeV
         2       202         202      1.25E+01
1.00E-10           4.15E-01           4.15E-01
1.00E-09           1.00E-01           1.00E-01
1.12E-09           2.17E-01           2.17E-01
1.26E-09           7.93E-02           7.93E-02
1.41E-09           2.13E-01           2.13E-01
1.59E-09           1.79E-01           1.79E-01
…
```

Please Reference Appendix G, Section A for continuation of the input file.

3. Response Function (.fmt)

```
MAJ Andrew Decker 26NOV13
Neutron Response Functions for Thesis Experiment (units: Counts/N/cm^2)
```

27 1
1.0000E-09 1.0000E-08 2.5120E-08 6.3100E-08
1.0000E-07 2.5120E-07 1.0000E-06 1.0000E-05
1.0000E-04 1.0000E-03 1.0000E-02 2.5120E-02
3.9810E-02 6.3100E-02 1.0000E-01 1.5850E-01
2.5120E-01 3.9810E-01 6.3100E-01 1.0000E+00
1.5850E+00 2.5120E+00 3.9810E+00 6.3100E+00
1.0000E+01 1.5850E+01 2.5120E+01
0
7
0Bare Bare Li6
1.0000E+00 cm^2 0 0 3 1 1 0
7.3079E-02 7.2247E-02 6.9844E-02 6.7591E-02
6.0182E-02 4.3725E-02 1.8752E-02 6.5833E-03
2.1499E-03 6.9408E-04 4.4962E-04 3.5732E-04
3.1509E-04 2.9648E-04 4.1476E-04 1.3838E-03
2.6662E-04 1.4007E-04 1.1041E-04 1.0190E-04
9.0153E-05 5.1723E-05 3.0792E-05 1.9001E-05
1.2217E-05 8.7654E-06
2in 2in sphere
1.0000E+00 cm^2 0 0 3 1 1 0
3.9907E-02 5.0502E-02 6.7800E-02 8.0872E-02
9.9750E-02 1.1346E-01 1.0142E-01 7.5804E-02
5.1565E-02 3.3684E-02 2.8196E-02 2.4987E-02
2.2538E-02 1.9728E-02 1.6145E-02 1.4091E-02
1.0782E-02 7.5478E-03 5.1432E-03 3.4205E-03
2.0297E-03 1.2099E-03 7.4114E-04 3.6405E-04
2.4233E-04 1.2206E-04
3in 3in sphere
1.0000E+00 cm^2 0 0 3 1 1 0
3.0120E-02 3.7938E-02 4.9911E-02 6.2956E-02
8.3796E-02 1.1199E-01 1.2641E-01 1.2023E-01
1.0374E-01 8.6471E-02 7.9456E-02 7.4774E-02
7.3417E-02 6.8600E-02 6.4564E-02 5.8057E-02
4.8588E-02 4.2033E-02 3.1160E-02 2.2527E-02
1.4835E-02 9.3005E-03 5.8399E-03 3.2796E-03
2.1304E-03 9.8677E-04
5in 5in sphere
1.0000E+00 cm^2 0 0 3 1 1 0
1.4466E-02 1.8854E-02 2.4279E-02 3.0806E-02
4.1107E-02 5.8339E-02 7.9836E-02 9.1061E-02
9.6819E-02 1.0263E-01 1.0642E-01 1.0607E-01
1.1009E-01 1.1124E-01 1.1660E-01 1.1793E-01

1.2207E-01 1.1686E-01 1.0752E-01 9.4873E-02
7.2785E-02 5.2416E-02 3.7953E-02 2.2152E-02
1.6255E-02 8.0351E-03
8in 8in sphere
1.0000E+00 cm^2 0 0 3 1 1 0
3.9099E-03 4.8771E-03 6.6752E-03 7.8552E-03
1.0667E-02 1.5337E-02 2.1662E-02 2.6479E-02
3.0960E-02 3.7088E-02 4.1369E-02 4.3148E-02
4.7623E-02 5.1674E-02 5.9482E-02 6.9633E-02
8.3838E-02 9.9173E-02 1.1364E-01 1.1949E-01
1.1628E-01 9.9524E-02 8.1682E-02 5.6714E-02
4.3235E-02 2.5472E-02
10in 10in sphere
1.0000E+00 cm^2 0 0 3 1 1 0
1.5028E-03 1.7580E-03 2.4578E-03 3.0184E-03
4.1487E-03 5.8363E-03 8.1576E-03 1.0171E-02
1.1985E-02 1.4779E-02 1.6493E-02 1.7357E-02
1.9129E-02 2.1765E-02 2.5866E-02 3.2395E-02
4.2731E-02 5.7464E-02 7.5853E-02 9.3716E-02
1.0380E-01 9.7379E-02 8.7536E-02 6.8812E-02
5.5268E-02 3.5116E-02
12in 12in sphere
1.0000E+00 cm^2 0 0 3 1 1 0
5.4037E-04 6.3944E-04 9.2014E-04 1.1243E-03
1.5283E-03 2.1413E-03 2.8637E-03 3.6882E-03
4.4421E-03 5.3334E-03 5.9517E-03 6.3976E-03
7.1512E-03 8.1586E-03 9.9885E-03 1.3056E-02
1.8567E-02 2.7575E-02 4.2229E-02 6.1378E-02
7.8172E-02 8.3129E-02 8.2910E-02 7.3922E-02
6.0233E-02 3.9687E-02

4. Free Field Input File (.inp)

LLNL_FF.ibu File with measured data
c:\U_M_G\FC\$inp\response\AFIT_RF.fmt File with response functions (RF)
FF_LLNLo Name of output file
c:\U_M_G\FC\$inp\def_spec\LLNL_DSFF.flu File with default spectrum (DS)
1.25E+01 Highest energy (use energy units of RF)
1 Requested final CHI^2 P.D.F.
1.0,0.85 Temperature, temp. reduction fact.
2,1 2 = use the DS energy bins, 1 = dF/dE
0 0 = no scaling DS

B. SURROGATE VEHICLE UNFOLDING INPUTS

1. Measured Data File (.ibu)

```
0  *       d       cts / s
  7   0     File 001_Exp.ibu / reference see end of file
0Bare     0.0     9.7780E+00    1.7967E-01    1.837     13.9      1
2in       2.0     5.3725E+01    4.2224E-01    0.786     5.27      2
3in       3.0     1.3349E+02    6.7802E-01    0.508     3.56      3
5in       5.0     2.3381E+02    8.8206E-01    0.377     2.37      4
8in       8.0     1.8437E+02    7.8367E-01    0.425     2.61      5
10in      10.0    1.1651E+02    6.1767E-01    0.530     3.65      6
12in      12.0    7.4871E+01    5.6977E-01    0.761     4.88      7

Dete      Diam      reading M        abs unc   % unc   % unc
ctor      eter      count rate         of M    of M    of R  flag
```

2. Default Spectrum (.flu)

```
File LLNL_SV_DefSpec.flu
         2        1                 fluence  given in n/cm^2/MeV
         2       202        202     1.25E+01
1.00E-10          4.21E-02          4.21E-02
1.00E-09          1.40E-02          1.40E-02
1.12E-09          2.11E-02          2.11E-02
1.26E-09          1.79E-02          1.79E-02
1.41E-09          5.61E-02          5.61E-02
1.59E-09          3.50E-02          3.50E-02
1.78E-09          4.47E-02          4.47E-02
2.00E-09          9.31E-02          9.31E-02
2.25E-09          1.69E-01          1.69E-01
2.52E-09          2.01E-01          2.01E-01
2.83E-09          2.56E-01          2.56E-01
3.18E-09          1.58E-01          1.58E-01
3.57E-09          1.85E-01          1.85E-01
4.01E-09          5.22E-01          5.22E-01
4.50E-09          7.20E-01          7.20E-01
5.05E-09          4.28E-01          4.28E-01
5.67E-09          9.04E-01          9.04E-01
6.36E-09          1.16E+00          1.16E+00
7.14E-09          1.28E+00          1.28E+00
…
```

Please Reference Appendix G, Section B for continuation of the input file.

3. Response Function (.fmt)

Because the response function files were identical in the deconvolution process for both free field and surrogate vehicle assemblies, please refer to Appendix PL, Section A, Subsection 3 for the full response function input component of the UMG unfolding software.

4. Surrogate Vehicle Input File (.inp)

```
LLNL_SV.ibu                                   File with measured data
c:\U_M_G\FC\$inp\response\AFIT_RF.fmt          File with response functions
(RF)
SV_LLNLo                                      Name of output file
c:\U_M_G\FC\$inp\def_spec\LLNL_DSSV.flu       File with default spectrum
(DS)
1.25E+01                                      Highest energy (use energy units of RF)
1.0                                           Requested final CHI^2 P.D.F.
1.0,0.85                                      Temperature, temp. reduction fact.
2,1                                           2 = use the DS energy bins, 1 = dF/dE
0                                             0 = no scaling DS
```

THIS PAGE INTENTIONALLY LEFT BLANK

APPENDIX F. MCNP6.1 INPUT DECK OF THE SURROGATE VEHICLE

Dr. Luisa Hansen created the MCNP6.1 input deck for the characterization of the RCL and calculations required for Dr. Radev's measurements. Modifications to Dr. Hansen's input deck included, but are not limited to, the adjustment of the number of neutron particles, the addition of the surrogate vehicle and associated plates, air detection sphere, and unique tallies used in the NPF and RPF research campaigns. The free field input deck consisted only of the air sphere and the additional tallies for consistency between input decks. Because only slight modifications were made to the free field input deck, it was omitted from the Appendices. The following information presented in this Appendix are done in such a way that it can be directly integrated into MCNP6.1 simulation to produce results immediately. LLNL has approved release of this Appendix and all of its contents.

```
MCNP6 LLNL Radiation Calibration Laboratory, Bldg.255, Rm 183A
C     Cf Source in Hopewell N40 System
C     Hopewell LTS (Linear Transfer System) holds Target exposure to Cf
C
C                         January 31, 2017
C
C    RABBIT revised after conversation with Steve Sherman (ORNL)
C    RADIATION CALIBRATION FACILITY, Bldg-255 Rm 183A,
C
C          ----CALCULATIONS FOR Radev MEAUREMENTS-------
C      --------- At a 2m distance from BARE Cf SOURCE ---------
C
C    Source strength 1.4099e+09 n/s on 5/6/2014,
C
C    Cf-252 half-life =2.645years
C
C    Source Calibration in 2/28/2014
C    Source Strength  1.495e+09 n/s
C
C
```

```
C    ************************CELLS CARDS************************

C
1     0   1000                        imp:n=0  $ outside universe
2     2  -2.3  -1000 #(-1001:-1002:-1003)    imp:n=1  $ Concrete room
3     1  -1.29e-03 -1001  #15 #16 #17 #18 #19 #20 #21 #22 #23 #24 #25
      #26 #27 #28 #29 #30 #31 #32 #33 #34 #35 #36 #37 #38 #39 #40 #41
      #42 #43 #44 #45 #46 #47 #48 #49 #50 #51 #52 #53 #54 #55 #56
      #60 #61 #62 #63 #64 #66 #67 #68 #69 #70 #71 #72 #73 #74 #75 #76
      #80 #81 #82 #83 #84 #85 #86 #87 #88 #91 #92
      #100 #101 #102 #103 #104 #105 #106 #110 #111 #112 #113 #114 #115
                imp:n=1 $ Air Room below grate
C
4     1  -1.29e-03 -1002 #3002 #150 #151 #152 #153 #160 #161 #162 #163
      #165 #166 #167 #168 #170 #171 #172 #175 #176 #177 #178 #179
      #180 #181 #182 #183 #184 #185 #186 #187 #188 #189 #190 #191
      #192 #193 #194 #195 #196 #197 #198 #199
      #201 #202 #203 #204 #205 #206 #207 #208
      #210 #211 #212 #213 #214 #215 #216 #217
      #218 #219 #220 #221 #222 #226 #227 #228 #229
      #230 #231 #232 #233 #234 #235 #236 #237 #240
      #87  #88  #89  #90  #898 #899 #900 #901 #902 #903 #904 #905
      #906 #907 #908 #909 #910 #911 #912 #913 #914 #950 #951
      #922 #923 #924 #925 #926 #927 #928
      #5100 #5200 #5300 #5400 #5500 #5600 #5700 #5800 #5900
      #6000 #6100 #6200 #6300 #6400 #6500 #6600 #6700 #6800 #6900
                              imp:n=1 $ Air above Mzz
C
C  ----DOOR ----
3002  2  -2.3  -3002   imp:n=1   $ Door clossing irradiation facility
C
C
C      ----AlUMINUN GRATE FLOOR---------
10    0  -1003  #87 #88  fill=1                      imp:n=1  $ Grate
11    0  1004 -1005 1006 -1007  lat=1 u=1 fill=2 imp:n=1  $ Grate Unit
12    3 -2.74 -1008 :-1009   u=2         imp:n=1  $ Al filling Grate
13    1 -1.29e-03 #12        u=2         imp:n=1  $ Air filling Grate
C
C       -------Al VERTICAL-BEAMS (AB)
15    3 -2.74  -500:-501:-502:-503  imp:n=1  $ Vert AB-bottom-top plates
16    like 15 but trcl=(0 223.52 0)      imp:n=1
17    like 15 but trcl=(0 436.88 0)      imp:n=1
C
```

```
18      like 15 but trcl=(365.76 0 0) imp:n=1

19      like 15 but trcl=(365.76 223.52 0) imp:n=1
20      like 15 but trcl=(365.76 436.88 0) imp:n=1
C
21      like 15 but trcl=(731.52 0 0) imp:n=1
22      like 15 but trcl=(731.52 223.52 0) imp:n=1
23      like 15 but trcl=(731.52 436.88 0) imp:n=1
C
24      like 15 but trcl=(906.78 0 0) imp:n=1
C
C --------HORIZONTAL BEAMS----------
25      3 -2.7 -504:-505:-506  imp:n=1 $ horizontal al i-beam, Y run
26      like 25 but trcl=(365.76 0 0) imp:n=1
27      like 25 but trcl=(731.52 0 0) imp:n=1
C
28      3 -2.7 -507:-508:-509 imp:n=1 $ horiz al i-beam, 5" X-run, top
29      like 28 but trcl=(0 223.52 0) imp:n=1
30      like 28 but trcl=(0 436.88 0) imp:n=1
31      like 28 but trcl=(0 330.2 0)  imp:n=1
32      like 28 but trcl=(0 556.06 0) imp:n=1
33      like 28 but trcl=(0 111.76 0) imp:n=1
34      like 28 but trcl=(0 -119.18 0) imp:n=1
C
35      like 28 but trcl=(365.76 0 0) imp:n=1 $ horiz i-beam, 5" X-run, bottom
36      like 28 but trcl=(365.76 -119.18 0) imp:n=1
37      like 28 but trcl=(365.76 223.52 0) imp:n=1
38      like 28 but trcl=(365.76 436.88 0) imp:n=1
39      like 28 but trcl=(365.76 330.2 0) imp:n=1
40      like 28 but trcl=(365.76 556.06 0) imp:n=1
41      like 28 but trcl=(365.76 111.76 0) imp:n=1
C
42      3 -2.7 -510:-511:-512 imp:n=1 $ horiz i-beam, 4" X-run, top
43      like 42 but trcl=(0 -119.18 0) imp:n=1
44      like 42 but trcl=(0 223.52 0) imp:n=1
45      like 42 but trcl=(0 436.88 0) imp:n=1
46      like 42 but trcl=(0 330.2 0) imp:n=1
47      like 42 but trcl=(0 556.06 0) imp:n=1
48      like 42 but trcl=(0 111.76 0) imp:n=1
C
49      3 -2.7 -513:-514:-515 imp:n=1
C
50      3 -2.7 -516:-517:-518 imp:n=1
```

```
51      like 50 but trcl=(0 332.54 0) imp:n=1
52      3 -2.7 -519:-520:-521 imp:n=1
C
53      like 52 but trcl=(0 -230.94 0) imp:n=1
54      3 -2.7 -522:-523:-524 imp:n=1
55      like 54 but trcl=(0 106.68 0) imp:n=1
56      3 -2.7 -525:-526:-527 imp:n=1
C
C  --------N40 LOW SCATTER IRRADIATOR-------

C

C  ALL DIMENSIONS TAKEN FROM HOPWEL DESIGNS, INC Drawings.
C Contact Person Ryan Howell (ryan.howell@ryanhopwelldesigns.com
C
C  Al sheet cover 70"x70"x46"  Tickness 0.25" = 0.635cm
60   3 -2.7  -60  61              imp:n=1  $ Al Sheet
C  Concrete bricks 69.5"x69.5"x46"
61   2 -2.3  -61 64 #19  #62 #63 #66 #67 #68 #69 #70 #71 #72 #73 #74 #74
                  #75 #76 #80 #81 #82 #83 #84 #85 #86 imp:n=1 $ Concrete
C  Square Cavity. See dimensions in Pg11 from 11 pgs
62   4 -0.945  -62 #66 #67 #68 #69 #70 #71 #72 #73 #74 #75 #76 #80
               #81 #82 #83 #84 #85 #86  imp:n=1  $ Cavity in Bks C-61
C  Small Cavity West of 62
63   1 -1.29e-03  -63 62 64  #19     imp:n=1
C Al lining of Large aquare cavity
64   3 -2.7  -64  62  #19       imp:n=1
C
C  CARROUSEL SYSTEM IN CAVITY
66 3  -2.7    -66                    imp:n=1  $ Al Base where sits Carrouse
67 4  -0.945  -67                     imp:n=1  $ Lower section Carrousel (WE
C  CILINDER with 8 cyl holes for Sources
68 3  -2.7   -68  #69 #70 #71 #72 #73 #74 #75 #76     imp:n=1  $ Al Cily. abov
69 1 -1.29e-03  -69                   imp:n=1  $ North side hole
70  like 69 but trcl=(5.7158 -5.7158 0) imp:n=1  $ West side hole
71  like 69 but trcl=(5.7158  5.7158 0) imp:n=1  $ East side hole
72  like 69 but trcl=(11.4316 0 0)      imp:n=1  $ South side hole
73  like 69 but trcl=(1.6735 4.0417 0)  imp:n=1  $ NE hole
74  like 69 but trcl=(9.7575 4.0417 0)  imp:n=1  $ SE hole
75  like 69 but trcl=(9.7575 -4.0417 0) imp:n=1  $ SW hole
76  like 69 but trcl=(1.6735 -4.0417 0) imp:n=1  $ NW hole
C
80 3  -2.7    -80   #83 #84  #85 #86     imp:n=1  $ Top section of 68
```

```
81 5  -11.34  -81 68 80  #83 #84 #85 #86 imp:n=1  $ Pb Shield arround 68 & 69
82 3  -2.7    -82 67 81    imp:n=1  $ Al Shield arouund all Carrousel
C
C   DRIVE SHAFT tube
83  1 -1.29e-03  -83      imp:n=1   $ Axel Motor tube-Air from 1011 to 1012
84  6 -7.8       -84  83  imp:n=1   $ Axel Motor tube-SST from 1011 to 1012
C
C Al Stand 17.08cmx17.08cmx 12.25cm Covering Shaft above Cavity Cell 62
100  1 -1.29e-03  -100  92 #83 #84 #87 #88     imp:n=1  $ Air in the box
101  3 -2.7       -101  100 92  #83 #84 #87 #88    imp:n=1  $ Al walls
C
C SST Motor Box over Al Stand
102  6 -7.8   -102  #83 #84 #87 #88            imp:n=1
C
C SST Vertical Plate behind motor box, Lower section, 2.66mm thick
103  6 -7.8  -103 92  #104                imp:n=1
C  Opeing in lower half of the plate
104  1 -1.29e-03   -104  92               imp:n=1
C  Air inside Box enclossing motor
105  1 -1.29e-03 -105 92 #103 #104 #100 #101 #102 #83 #84 #87 #88  imp:n=1
C  SST wall of Box enclosing motor 76.20 x 60.96 x 30.48in cm 1.98mm thick
106  6 -7.8 -106 92 #105 #100 #101 #102 #103 #104 #83 #84 #87 #88 imp:n=1
C
C  STEEL BALLAS TANK,NW of Shaft tube
110  1 -1.29e-03  -110          imp:n=1  $ Air in Tank
111  6 -7.8   -111 110 112 113    imp:n=1  $ Tank walls
112  6 -7.8   -112              imp:n=1  $ Back cover
113  6 -7.8   -113              imp:n=1  $ Front cover
C  Stands wher sits the Tank
114  6  -7.8  -114 92 #111 #110   imp:n=1  $ Front Vertical Support
115  6  -7.8  -115 91 #111 #110   imp:n=1  $ Back Verical Support
C
C  RAILS OVER MEZZANINE
C  EAST
150  3 -2.7  -150       imp:n=1  $ lower plate over mezzanine
151  3 -2.7  -151       imp:n=1  $ upppe horizontal surface
152  3 -2.7  -152       imp:n=1  $ side wall inside rail
153  3 -2.7  -153       imp:n=1  $ side wall outside rail of rail
C  WEST Rail
160  3 -2.7  -160       imp:n=1  $ lower plate over mezzanine
161  3 -2.7  -161       imp:n=1  $ upppe horizontal surface
162  3 -2.7  -162       imp:n=1  $ side wall inside rail
163  3 -2.7  -163       imp:n=1  $ side wall outside rail of rail
```

```
C Transversal pipes joining rails
165  1 -1.29e-03  -165  imp:n=1  $ Air core North bracket
166  3 -2.7  -166  165  imp:n=1  $ North bracket
167  1 -1.29e-03  -167  imp:n=1  $ Air core South bracket
168  3 -2.7  -168  167  imp:n=1  $ South bracket
C
C CHANNEL RAIL attached to inside wall of Left Rail
170  3 -2.7 -170        imp:n=1  $ bottom plate

171  3 -2.7 -171        imp:n=1  $ side plate left of C-170
172  3 -2.7 -172        imp:n=1  $ side plate right of C-170
C
C TABLE with SOURCE TUBE through its center
175  3 -2.7  -175 #89 #90   imp:n=1  $ Metal Plate
C
C LEGS Holding Table KJN Al structure 45x45
176  1 -1.29e-03  -176   imp:n=1  $ N-W leg Air Core
177  3 -2.7  -177  176   imp:n=1  $ N-W leg Al wall
c
178  1 -1.29e-03  -178   imp:n=1  $ N-E leg  Air core
179  3 -2.7  -179  178   imp:n=1  $ N-E leg  Al wall
c
180  1 -1.29e-03  -180  imp:n=1  $ S-W leg Air Core
181  3 -2.7  -181  180  imp:n=1  $ S-W leg Al wall
c
182  1 -1.29e-03  -182  imp:n=1  $ S-E leg  Air core
183  3 -2.7  -183  182  imp:n=1  $ S-E leg  Al wall
C
C Bottom brackets among legs
184  1 -1.29e-03  -184  imp:n=1  $ N, W-E Air core
185  3 -2.7  -185  184  imp:n=1  $ N, W-E Al wall
c
186  1 -1.29e-03  -186  imp:n=1  $ E, N-S Air core
187  3 -2.7  -187  186  imp:n=1  $ E, N-S Al wall
c
188  1 -1.29e-03  -188  imp:n=1  $ S, W-E Air core
189  3 -2.7  -189  188  imp:n=1  $ S, W-E Al wall
c
190  1 -1.29e-03  -190  imp:n=1  $ W, N-S Air core
191  3 -2.7  -191  190  imp:n=1  $ W, N-S Al wall
C
C Top brackets among legs
192  1 -1.29e-03  -192  imp:n=1  $ N, W-E Air core
```

```
193  3 -2.7  -193  192  imp:n=1  $ N, W-E Al wall
c
194  1 -1.29e-03  -194  imp:n=1  $ E, N-S Air core
195  3 -2.7  -195  194  imp:n=1  $ E, N-S Al wall
c
196  1 -1.29e-03  -196  imp:n=1  $ S, W-E Air core
197  3 -2.7  -197  196  imp:n=1  $ S, W-E Al wall
c
198  1 -1.29e-03  -198  imp:n=1  $ W, N-S Air core
199  3 -2.7  -199  198  imp:n=1  $ W, N-S Al wall
C Table enclosing motor sits on Bosh 45x90 E-W BLOCKS over the Rails

C Forward block  9.0cm x 65.085cm x 4.5cm
C
201  3  -2.7  -201  202  imp:n=1  $ S Blck E-W. Al
202  1  -1.29e-03  -202  imp:n=1  $  "   "    "   Air
203  3  -2.7  -203  204  imp:n=1  $ N Blck E-W. Al
204  1  -1.29e-03  -204  imp:n=1  $  "   "    "   Air
205  3  -2.7  -205  206  imp:n=1  $ West Blck N-S. Al
206  1  -1.29e-03  -206  imp:n=1  $  "   "    "   Air
207  3  -2.7  -207  208  imp:n=1  $ Eas Blck N-S. Al
208  1  -1.29e-03  -208  imp:n=1  $  "   "    "   Air
C
C LEGS of Table
210  3  -2.7  -210 211   imp:n=1  $  S-W Leg Al
211  1  -1.27e-03 -211   imp:n=1  $  S-W  " Air
212  3  -2.7  -212 213   imp:n=1  $  S-E Leg Al
213  1  -1.29e-03 -213   imp:n=1  $  S-E  " Air
214  3  -2.7  -214 215   imp:n=1  $  N-E Leg Al
215  1  -1.29e-03 -215   imp:n=1  $  N-E  " Air
216  3  -2.7  -216 217   imp:n=1  $  N-E Leg Al
217  1  -1.29e-03 -217   imp:n=1  $  N-E  " Air
C
C Walls of the Table. All Al plates,0.064"=0.16256=0.163cm thick
218  3  -2.7  -218       imp:n=1  $ North, W-E
219  3  -2.7  -219       imp:n=1  $ East, N-S
220  3  -2.7  -220       imp:n=1  $ South, W-E
221  3  -2.7  -221       imp:n=1  $ West, N-S
222  3  -2.7  -222 #230 #231 #232 #233     imp:n=1  $ Top surface
C
C  4 Al blocks where sits Instrument Platform 5.5x5.5x2.5cm
226  3  -2.7  -226 230   imp:n=1  $ N-W block
227  3  -2.7  -227 231   imp:n=1  $ N-E block
```

```
228  3  -2.7  -228 232   imp:n=1  $ S-E block
229  3  -2.7  -229 233   imp:n=1  $ S-W block
C
C Tubes through blocks, rasing Inst. Platform
230  3  -2.7  -230       imp:n=1  $ Tube through block 226
231  3  -2.7  -231       imp:n=1  $ Tube through block 227
232  3  -2.7  -232       imp:n=1  $ Tube through block 228
233  3  -2.7  -233       imp:n=1  $ Tube through block 229
C
C Upper blocks at end of tubes & under Inst. Platform 5.5x5.5x1.25cm
234  3  -2.7  -234 230  imp:n=1  $ N-W block
235  3  -2.7  -235 231  imp:n=1  $ N-E block
236  3  -2.7  -236 232  imp:n=1  $ S-E block
237  3  -2.7  -237 233  imp:n=1  $ S-W block
C
C Instrument Platform Table 42cm x 61.9cm 0.55cm.
240  3  -2.7   -240      imp:n=1
C
C      ----------SOURCE TUBE -----------
C  I  SST LOWER EXPOSURE TUBE
85  1 -1.29e-03  -85      imp:n=1   $ Air
86  6 -7.8       -86  85   imp:n=1   $ SST  wall
C  Al shell around large Cavity, Cell 62
91   3 -2.7  -91 60 61  #19 #62 #64 #83 #84 #85 #86 imp:n=1 $ Al cover over 61
92   3 -2.7  -92 62 64  #83 #84 #85 #86         imp:n=1 $ Al cover over 62,64
C  II Al TRANSFER TUBE

87  1 -1.29e-03  -87       imp:n=1   $ Air
88  6 -7.8       -88  87   imp:n=1   $ AL  wall
C  III Al EXPOSURE TUBE

89  1 -1.29e-03 -89  #898 #899 #900 #905 #906 #907 #908 #909 #910 #911
                #912 #913 #914 #922 #923 #924 #925 #926 #927 #928
                #950 #951 imp:n=1
90  3 -2.7  -90  89       imp:n=1  $ Al wall,
C  Al TUBE
901 3 -2.70  -901 89       imp:n=1    $ Lower truncade wall section
902 3 -2.70  -902 89       imp:n=1    $ Cyl thiner wall sectionr
903 3 -2.70  -903 89       imp:n=1    $ Upper truncade wall section
904 3 -2.70  -904 89 #905 #906 imp:n=1    $  Cyl wall section as in Cell 90
905 1 -1.29e-03 -905 915 -916 #906 #922 #923
                    imp:n=1 $ Vent hole N-S in Cell 904
906 1 -1.29e-03 -906 917 -918  #922 #923  imp:n=1 $ Vent hole W-E in Cell 904
```

```
C
C   SOURCE RABBIT
C  Central Cavity for Cf Oxide,
C Air
898  1 -1.29e-03 -898  #899 #900      imp:n=1
C  Platinum Filter above & below CfO source, with a density 70% of solid Pt AN
899  10 14.35  -899 #900    imp:n=1
C  ORNL Californium-252 Newsletter Vol 5, #1, 2001 Cf metal, 15.1gr/cm3
900  7 -15.1 -900        imp:n=1   $ Cf2O3 Source
C PRIMARY CAPSULE, Pt-Rh 90-10 wgt%), J.S ACKEN, NBS Journal of Research,
Vol
907  8  -18.5 -907 898 imp:n=1
C  SECONDARY CAPSULE Zircaloy-2 or SST or Zircoloide
908  17 -6.55 -908 907 imp:n=1
C  Zircaloide cup above 908
909  17 -6.55  -909 908 imp:n=1
C  HOPEWELL CAPSULE AL Lower section
910  3 -2.70  -910 908    imp:n=1
C  Lower Extenal ring around 909
911  3 -2.70  -911 910 908 imp:n=1
C  Middle section

912  3 -2.70  -912 908    imp:n=1
C  Upper External Ring
913  3 -2.70  -913 912 908   imp:n=1
950  3 -2.70  -950 908       imp:n=1
951  3 -2.70 -951 908 909   imp:n=1
C  Upper section
914  3 -2.70  (-914 950 908 -920):(-914 951 908 909 920 -921) imp:n=1
C RABBIT CUP (Pg. 1/3 from "1.125"Source Rabbit"
922  3 -2.70  -922  914     imp:n=1
923  3 -2.70  -923  922     imp:n=1
C  SUCTION CUP Chloroprene C4H5Cl  Density=0.9598g/cc
924  9 -0.9598  -924  923  imp:n=1   $ Chlorop-rubber connical bottom section
925  9 -0.9598 -925 924    imp:n=1   $ Neck conn. section
926  1 -1.29e-03  -926     imp:n=1   $ Air gap
927  9 -0.9598 -927 928    imp:n=1   $ Chorop=rubber neck
928  1 -1.29e-03 -928      imp:n=1   $ Hole in neck
C
C --------SURROGATE VEHICLE CELLS--------

5100    18    -7.82     -2001       imp:n=1        $ Lt Steel plate
5200    19    -1.8      -2002       imp:n=1        $ Lt GRP plate
```

```
5300    3     -2.6989   -2003       imp:n=1        $ Lt Al plate
5400    18    -7.82     -2004       imp:n=1        $ Rt Steel plate
5500    19    -1.8      -2005       imp:n=1        $ Rt GRP plate
5600    3     -2.6989   -2006       imp:n=1        $ Rt Al plate
5700    18    -7.82     -2007       imp:n=1        $ Fr Steel plate
5800    19    -1.8      -2008       imp:n=1        $ Fr GRP plate
5900    3     -2.698    -2009       imp:n=1        $ Fr Al plate
6000    18    -7.82     -2010       imp:n=1        $ R Steel plate
6100    19    -1.8      -2011       imp:n=1        $ R GRP plate
6200    3     -2.698    -2012       imp:n=1        $ R Al plate
6300    18    -7.82     -2013       imp:n=1        $ Tp Steel plate
6400    19    -1.8      -2014       imp:n=1        $ Tp GRP plate
6500    3     -2.698    -2015       imp:n=1        $ Tp Al plate
6600    18    -7.82     -2016       imp:n=1        $ Bt Steel plate
6700    19    -1.8      -2017       imp:n=1        $ Bt GRP plate
6800    3     -2.69     -2018       imp:n=1        $ Bt Al plate
6900    1     -1.2e-3   -2019       imp:n=1        $ Air Detector
C 7000    1     -1.2e-3   -2020 2019  imp:n=1        $ Air Btw. Detector and P
C  Follows blank line

C
C    **********SURFACES**********
C
C
C  ROOM DIMENSIONS
C   Dimensions taken from Winstom Wong Mechanical Drawings
C   The room has 2'(60.96cm) thick walls all around
C   Dimensions inside the room: 40'( N-S); 30'(E-W); 24.25'Floor-Ceiling
C   Add 2'=60.96cm to each side of the wall for the Out Room surfaces
C
1000  RPP  -671 671  -518 518  -61  800 $ out room surfaces $ outside World
1001  RPP  -609 607  -457 457   0.0  268.984  $ Air below Latt.
1002  RPP  -609 607  -457 457   272  738      $ Air in room above Latt.
C
C  CONCRETE DOOR, 233.05cm long; 45.88cm thick at 38cm from WEST wall
3002  RPP   561 607   -419 -186   272 738
C
C  MEZZANINE, Al GRATE FLOOR

1003  RPP   -609 607 -457 457  268.984 272.00   $ Al Lattice
1004  px  100
1005  px  103.992  $ 103.016
1006  py  100
```

```
1007  py  110.992  $ 110.16
C
1008  px  100.2363 $ 100.4763
1009  py  100.2363 $ 100.4763
C
1010  pz  272.00
1011  pz   44.69
1012  pz  268.984
1013  pz  272.00
1014  pz  421.709
C
915  px   20.095
916  px   23.905
917  py  -13.005
918  py  -9.195
C  Upper Section Rabit secondary shielding
920  pz  373.73
C  End Rabbit
921  pz  374.81
C
C Vertical Al Beams (VB)97" Tall with bottom and top plates 0.5" thick
500     rpp -380.4 -360.08 -228.4 -208.08  247.7115 248.6640 $ vert i-beam top
501     rpp -377.86 -376.9075 -225.86 -210.62  0 247.7115
502     rpp -363.5725 -362.62 -225.86 -210.62  0 247.7115
503     rpp -376.9075 -363.5725 -218.7163 -217.7638  0.0 247.7115
C
504     rpp -376.59   -363.89   -457 457  248.6640  249.6165 $ horiz Al i-beam
505     rpp -376.59   -363.89   -457 457  268.0315  268.9840
506     rpp -370.7163 -369.7638 -457 457  249.6165  268.0315
C
507     rpp -363.89 -10.83  -224.59   -211.89   268.0315 268.9840
508     rpp -363.89 -10.83  -224.59   -211.89   248.6640 249.6165
509     rpp -369.605 -5.115 -218.7163 -217.7638 249.6165 268.0315
C
510     rpp -609 -376.59  -223.32   -213.16   268.0315 268.9840 $ 4"i=beam
511     rpp -609 -370.875 -223.32   -213.16   253.744  254.6965
512     rpp -609 -370.875 -218.5575 -217.9225 254.6965 268.0315
C
513     rpp 367.63  544.23  -224.59  -211.89  268.0315 268.9840
514     rpp 367.63  544.23  -224.59  -211.89  248.6640 249.6165
515     rpp 361.915 549.945 -218.875 -217.605 249.6165 268.0315
C
516     rpp 367.63  607 -1.07   11.63    268.0315  268.9840
```

```
517     rpp 367.63  607 -1.07   11.63    248.6640  249.6165
518     rpp 361.915 607  4.80375 5.75625 249.6165  268.0315
C
519     rpp 367.63 544.23 -111.56   -101.4    268.0315 268.9840
520     rpp 367.63 544.23 -111.56   -101.4    253.744  254.6965
521     rpp 367.63 544.23 -106.7975 -106.1625 254.6965 268.0315
C
522     rpp 367.63 607 106.88   117.04   268.0315 268.9840
523     rpp 367.63 607 106.88   117.04   253.744  254.6965
524     rpp 367.63 607 111.6425 112.2775 254.6965 268.0315
C
525     rpp 544.23   556.93   -457 -1.07  268.0315 268.9840
526     rpp 544.23   556.93   -457 -1.07  248.6640 249.6165
527     rpp 550.1038 551.0563 -457  4.645 249.6165 268.0315
C
C  ------N40 Low SCATTER IRRADIATOR-------
C Position of the N$) on the bottom floor (given by Jeff Debisschop):
C  220" from N-wall x1= -609cm +558.8cm = -50.20cm
C  N40 is 70" wide, x2= -50.20 + 177.80 =127.60
C  N40 is 188.7"  from S-wall, versus 188" measutrd by J.D.
C  N40 is 139" from W-wall: y1 = -457 +353.06 = -103.94
C  N40 is 70"depth, y2= -103.94 +177.80 = 73.86
C  N40 is 383.14cm = 150.84 versus 149.0 from J.D.
C  N40 is 40" =116.84cm height
C
C  Thickness Al Sheet 0.0403" -0.102cm thick R.H. Private Comm.
60   RPP  -55.30 122.70  -103.94 73.86  0 116.738  $ Al sheet 0.102cm thick
61   RPP  -55.20 122.60  -103.84 73.76  0 116.738  $ Concrete Bricks70"x70"x46
C  Center Bricks: x=38.70 y=-15.04  z=58.42. Square Cavity 61.2775x61.2775
62   RPP   3.1613 64.4388  -45.6788 15.60  0.0 121.92  $ larger square cavity
C  additional opening
63   RPP  -17.3587  3.1613  -8.53 20.68  0  116.738  $ west of 62 N to S
C  Al wall of Cavity 62
64   RPP 2.2088 65.3913  -46.6313 16.5525  0  121.92
C
C SECTION A-A inside Cavity 62, Lined with 0.375"=0.9525cm Al shield
66 RCC 33.70 -15.04  0       0 0  0.9525  15.5     $ Al disc where sits Carrou
67 RCC 33.70 -15.04  0.9525  0 0 30.1625  12.5     $ Carrousel base
68 RCC 33.70 -15.04  31.115  0 0 13.574    7.7788  $ Cyl above carrousel base
C HOLES in 68 for 8 different Sources
69 RCC 27.9842 -15.04   31.115  0 0 13.574  1.5088  $ North hole
70 RCC 39.4158 -15.04   31.115  0 0 13.574  1.5088  $ South hole
71 RCC 33.70   -20.7558 31.115  0 0 13.574  1.5088  $ West Hole
```

```
72 RCC 33.70    -9.3242 31.115  0 0 13.574  1.5088  $ East Hole
73 RCC 29.6583 -10.9983 31.115  0 0 13.574  1.5088  $ NE hole
74 RCC 37.7417 -10.9983 31.115  0 0 13.574  1.5088  $ SE hole
75 RCC 37.7417 -19.0817 31.115  0 0 13.574  1.5088  $ SW hole
76 RCC 29.6583 -19.0817 31.115  0 0 13.574  1.5088  $ NW hole
C
80 RCC 33.90 -15.04  44.689  0 0 1.905     8.0     $ Plate above 68
81 RCC 33.90 -15.04  31.115  0 0 20.0025   12.5    $ Pb Shield
82 RCC 33.90 -15.04  0.9525  0 0 50.1650   13.4525 $ Al shield 0.375" =0.9525c
C
C  TUBES ABOVE CARROUSEL
C SHAFT Tube
83 RCC  33.70 -15.04    44.69    0 0  99.76  1.346  $ air in MOTOR Axel tube
84 RCC  33.70 -15.04    44.69    0 0  99.76   1.5875  $ SST wall Motor Axel
C Al Stand 8.54x8.54 12.25 in cm  0.307cm thick
100 RPP  26.123 38.123  -23.273 -6.807  122.022   133.965  $ Air inside Al Sta
101 RPP  26.430 38.430  -23.580 -6.500  122.022   134.272 $ Al Stand wall
C  SST Motor box over Al Stand 12 x 12 x 20.28 in cm
102 RPP  27.70 39.70   -21.04  -9.04   134.272 154.552   $ Motor
C SST Vertical Plate behind motor box, Lower section, 2.66mm thick
103 RPP  24.772 25.038  -30.082 0.002 122.022 198.024  $ above cell 92
C  Opeing in lower half of the plate
104 RPP  24.772 25.038  -30.082 0.002 122.022 160.122  $ above cell 92
C  Air inside Box enclossing motor
105 RPP  24.772 39.292  -30.082 0.002 122.022 198.024  $ above cell 92
C  SST Box of Box enclosing motor 76.20 x 60.96 x 30.48in cm 1.98mm thick
106 RPP  24.970 39.490   -30.28  0.20  122.022 198.222  $ above cell 92
C
C STEEL BALLAS TANK:l23"=58.42cm long, r=7"=17.78cm,1/8"=0.3175cm thick
110 RCC  -37.42   -32.94  144.882  58.42   0 0  17.4625  $ Air
111 RCC  -37.42   -32.94  144.882  58.42   0 0  17.7800  $ Still wall
112 RCC  -37.7375 -32.94  144.882   0.3175 0 0  17.7800  $ back cover
113 RCC   21.00   -32.94  144.882   0.3175 0 0  17.7800  $ forward cap
C  Support plates for the TANK, 3/16 = 0.4763cm=0.48cm cm thick
114 RPP   10.45 10.93  -44.73 -21.15  121.92 130.00     $ Front vertical stand
115 RPP  -26.87 -26.39 -44.73 -21.15  116.738 130.00    $ Back stand
C
C   RAILS over MEZZANINE.  They are 11.9125cm behind Table N edge
C East Rail (Lookin toward door)

150 4 RPP  -578.375  -8.375   6.263 10.143   272    272.48  $ lower plate on M
151 4 RPP  -578.375  -8.375   6.263 10.143   281.48 281.96  $ upper plat
152 4 RPP  -578.375  -8.375   5.783  6.263   272    281.96  $ in side-wall
```

```
153 4 RPP  -578.375  -8.375  10.143 10.623   272    281.96  $ out side-wall
C West Rail
160 4 RPP  -578.375  -8.375  -40.223  -36.343  272.00 272.48  $ lower plate on
161 4 RPP  -578.375  -8.375  -40.223  -36.343  281.48 281.96  $ upper plate
162 4 RPP  -578.375  -8.375  -36.343  -35.863  272    281.96  $ in side-wall
163 4 RPP  -578.375  -8.375  -40.703  -40.223  272    281.96  $ out side-wall
C Transversal pipes joining the rails at their extremes
165 4 RPP  -577.343  -573.763  -35.863  5.783  278.88 281.16  $ Air core
166 4 RPP  -577.803  -573.303  -35.863  5.783  278.42 281.62  $ North bracket
C
167 4 RPP   -12.843  -9.263  -35.863  5.783  278.88 281.16  $ Air core
168 4 RPP   -13.303  -8.803  -35.863  5.783  278.42 281.62  $ South bracket
C CHANNEL attached to the in-wall of left rail
170 4 RPP  -573.763  -12.843   -1.137  5.780  272.00 272.40 $ bottom plate

171 4 RPP  -573.763  -12.843   -1.137 -0.737  272.40 277.48 $ side plate touch
172 4 RPP  -573.763  -12.843    5.380  5.780  272.40 277.48 $ side plate towar
C
C TABLE with SOURCE TUBE through its center

175 4 RPP   3.5375  63.8625  -45.2025 15.1225  324.07 324.705  $ Metal plate
C
C LEGS Hol+ding Table KJN Al structure 45x45 wall thickness 0.46cm
C Legs are indented 0.47cm from Table edge
176 4  RPP  4.4675  8.0475   10.6125 14.1925   272 324.07 $ N-E Air core
177 4  RPP  4.0075  8.5075   10.1525 14.6525   272 324.07 $ N-E Al wall
C
C tr2   22.0  -11.10  0  Puts Legs on Table centered at Source tube

178 2 RPP  -29.2325 -25.6525  -29.2325 -25.6525   272 324.07 $ N-W Air core
179 2 RPP  -29.6925 -25.1925  -29.6925 -25.1925   272 324.07 $ N-W Al wall
c
180 2 RPP   25.6525 29.2325    25.6525 29.3225   272 324.07 $ S-E Air core
181 2 RPP   25.1925 29.6925    25.1925 29.6925   272 324.07 $ S-E Al wall
c
182 2 RPP   25.6525 29.2325   -29.3225 -25.6525  272 324.07 $ S-W Air core
183 2 RPP   25.1925 29.6925   -29.6925 -25.1925  272 324.07 $ S-W Al wall
C
C Bottom brackets among legs

184 2 RPP  -29.2325 -25.6525  -25.1925 25.1925   272.46 276.04  $ N, W-E Air
185 2 RPP  -29.6925 -25.1925  -25.1925 25.1925   272.00 276.50  $ N, W-E Al
c
```

```
186 2 RPP  -25.1925 25.1925    25.6525 29.3225   272.46 276.04  $ E, N-S Air
187 2 RPP  -25.1925 25.1925    25.1925 29.6925   272.00 276.50  $ E, N-S Al
c
188 2 RPP   25.6525 29.2325   -25.1925 25.1925   272.46 276.04  $ S, W-E Air
189 2 RPP   25.1925 29.6925   -25.1925 25.1925   272.00 276.50  $ S, W-E Al
c
190 2 RPP   -25.1925 25.1925  -29.3225 -25.6525  272.46 276.04  $ W, N-S Air
191 2 RPP   -25.1925 25.1925  -29.6925 -25.1925  272.00 276.50  $ W, N-S Al
C
C Top brackets among legs
192 2 RPP  -29.2325 -25.6525  -25.1925 25.1925   320.03 323.61  $ N, W-E Air
193 2 RPP  -29.6925 -25.1925  -25.1925 25.1925   319.57 324.07 $ N, W-E Al
c
194 2 RPP  -25.1925 25.1925    25.6525 29.3225   320.03 323.61 $ E, N-S Air
195 2 RPP  -25.1925 25.1925    25.1925 29.6925   319.57 324.07  $ E, N-S Al
c
196 2 RPP   25.6525 29.2325   -25.1925 25.1925   320.03 323.61  $ S, W-E Air
197 2 RPP   25.1925 29.6925   -25.1925 25.1925   319.57 324.07  $ S, W-E Al
c
198 2 RPP   -25.1925 25.1925  -29.3225 -25.6525  320.03 323.61  $ W, N-S Air
199 2 RPP   -25.1925 25.1925  -29.6925 -25.1925  319.57 324.07  $ W, N-S Al
C
C   CENTER OF TABLE MOVED  BACK to ALIGNED WITH NRD at 2m from Cf:=:
-178cm
C Box enclosing motor sits on Bosh 45x90 E-W BLOCKs over the Rails
C Forward block  9.0cm x 65.085cm x 4.5cm.  Set 6cm behind end of rail
C Thickness Al wall =0.46
201 1 RPP   -17.375  -8.375  -49.330 19.250   281.96 286.46  $ S Blck E-W. Al
202 1 RPP   -16.915  -8.835  -49.330 19.250   282.42 286.00  $  "   "    "  Ai
C
203 1 RPP  -50.375 -41.375  -49.330 19.250   281.96 286.46  $ N blck E-W. Al
204 1 RPP  -49.915 -41.835  -49.330 19.250   282.42 286.00  $  "   "    "  Air
c
205 1 RPP  -41.375 -17.375  -49.330 -40.330  281.96 286.46  $ West Blck N-S.AL
206 1 RPP  -41.375 -17.375  -48.870 -40.790  282.48 285.98  $  "    "    " Air
c
207 1 RPP  -41.375 -17.375   10.250  19.250  281.96 286.46  $ East Blck E-W.Al
208 1 RPP  -41.375 -17.375   10.710  18.790  282.48 285.98  $  "   "     " Air
C
C Legs Bosh 4.50x4.50 40.64cm high, indented 3.175cm from ends of Blocks
210 1 RPP  -12.875 -8.375   -46.790 -42.290   286.46 327.10 $ S-W Leg Al
211 1 RPP  -12.415 -8.835   -46.330 -41.830   286.46 327.10 $ S-W  "  Air
```

```
c

212 1 RPP   -12.875 -8.375   12.210  16.710   286.46 327.10 $ S-E Leg Al
213 1 RPP   -12.415 -8.835   12.670  16.250   286.46 327.10 $ S-E  "  Air
c
214 1 RPP   -50.375 -45.875   12.210  16.710  286.46 327.10 $ N-E Leg Al
215 1 RPP   -49.915 -46.335   12.670  16.250  286.46 327.10
c
216 1 RPP   -50.375 -45.875  -46.790  -42.290   286.46 327.10 $ N-W Leg Al
217 1 RPP   -49.915 -46.335  -46.330  -41.830   286.46 327.10 $ N-W  "  Air
C
C Walls of the Table. All Al plates,0.064"=0.16256 =0.163cm thick
218 1 RPP   -50.538  -50.375  -46.790  16.710  286.46 328.42 $ North W-E
219 1 RPP   -50.375  -8.375    16.710  16.837  286.46 328.42 $ East N-S
220 1 RPP    -8.375  -7.915   -46.790  16.710  286.46 328.42 $ South W-E
221 1 RPP   -50.375  -8.375   -46.953 -46.790  286.46 328.42 $ West N-S
C  Top Cover 63.5cm x 42cm x 1.27cm
222 1 RPP    -50.375  -8.375   -46.790 16.710  327.10 328.37 $
C
C  4 Al blocks where sits Instrument Platform
226 1 RPP   -45.175 -39.675  -34.590 -29.090  328.37 330.087 $ N-W block
227 1 RPP   -45.175 -39.675   -0.990   4.510  328.37 330.087 $ N-E
228 1 RPP   -19.075 -13.575   -0.990   4.510  328.37 330.087 $ S-E
229 1 RPP   -19.075 -13.575  -34.590 -29.090  328.37 330.087 $ S-W
C
C  Tubes centered at the blocks.
C The height will be adjust  to position object aligned with Source
230 3 RCC  -42.425 -31.84  286.46  0  0  56.91   0.90  $ tube through 226
231 3 RCC  -42.425   1.76  286.46  0  0  56.91   0.90  $ through 227
232 3 RCC  -16.325   1.76  286.46  0  0  56.91   0.90  $ through 228
233 3 RCC  -16.325 -31.84  286.46  0  0  56.91   0.90  $ tube through 229
C
C Upper blocks at top of tubes below Inst. Platform

234 3 RPP   -45.175 -39.675  -34.590 -29.090  342.12 343.37 $ N-W block
235 3 RPP   -45.175 -39.675   -0.990   4.510  342.12 343.37 $ N-E  "
236 3 RPP   -19.075 -13.575   -0.990   4.510  342.12 343.37 $ S-E
237 3 RPP   -19.075 -13.575  -34.590 -29.090  342.12 343.37 $ S-W
C
C Instrument Platform Table 42cm x 61.9cm 0.55cm.
C 15"=3.81cm forward than No side of Cell 222 (Box enclosing motor)
240 3 RPP   -46.565 15.335  -36.04 5.96  343.37 343.92
C
```

```
C       ----------SOURCE TUBE  ----------
C
C I  SST LOWER EXPOSURE TUBE from the Carrousel to top of 62)
85 RCC  29.66 -11.10  44.69   0 0 77.23    1.346  $ Air
86 RCC  29.66 -11.10  44.69   0 0 77.23    1.746  $ SST wall SOURCE
91 RPP  -55.10 122.70  -103.94  73.86   116.738 116.840   $ Al Top over bricks
92 RPP  3.1613  64.4388  -45.6788 15.60  121.92 122.022 $ Al over Cell 62 & 64
C II Al TRANSFER TUBE, outside r=1.5875cm, wall tickness 0.1245cm
C 11.7475cm behind the Axis of the Shaft; 4.313cm East; 187.488cm above C-63
87 RCC  29.00 -11.10 122.022   0 0  187.488   1.4630  $ air
88 RCC  29.00 -11.10 122.022   0 0  187.488  1.5875  $ SST wall
C III Al EXPOSE TUBE 60.44cm; out r=1.905cm, wall tickness==0.442cm
C From this high up the TUBE is encased in an Al tube r=1.905cm
89 RCC  29.00 -11.10 309.51   0 0  67.15  1.4630  $ air -tube
90 RCC  29.00 -11.10 309.51   0 0  60.44  1.9050  $ SST wall
C IV Lower truncade segment ro change r=1.905cm to r=1.598cm
901   TRC 29.00 -11.10 369.95  0   0  0.26 1.905 1.598

C V Tube, Thinner walls r=1.598cm
902 RCC 29.00 -11.10 370.21  0 0 3.11  1.598
C VI Upper truncade section change r=1.598cm back to 1.905cm
903 TRC  29.00 -11.10 373.58   0  0  -0.26  1.905 1.598
C VII  Upper section of Expose Tube
904  RCC 29.00 -11.10  373.58   0 0 3.08  1.905   $ TOP of Exp. Tube=376.66
C
C TUBE LENGTH ABOVE TABLE 324.705 to 376.66 =51.995cm = 20.455"
C Vent Holes, 0.9"=2.286cm from Tube top r=0.125"=0.3175cm
C  Vent hole through x-direction in cell 904
905  c/x   -11.10  375.11  0.29

C  Vent hole through the y-direction in cell 904
906  c/y    29.00  375.11  0.29
C
C   SOURCE RABBIT
C  Air Cavity
898 RCC 29.00 -11.10  369.54  0 0 4.20  0.159
C Pt Filters
899 RCC 29.00 -11.10  370.20  0 0 3.30  0.159
C  Central Cavity for Cf Oxide,
900 RCC 29.00 -11.10  370.87  0 0 1.96  0.159
C  PRIMARY Capsule  Pt-Rd (90-10)
907 RCC 29.00 -11.10  369.54  0 0 4.20  0.284    $ 0.298  $
C  SECONDARY Capsule 304-SST
```

```
908 RCC 29.00 -11.10  368.90  0 0 5.07  0.391    $ 0.471
909 RCC 29.00 -11.10  373.97  0 0 0.54  0.200    $ 0.412  $
C  HOPEWELL Capsule Al
910  RCC 29.00 -11.10  368.50  0 0 2.04  1.118  $ Lower section
911  RCC 29.00 -11.10  370.54  0 0 0.40  1.429  $ Lower Ring
912  RCC 29.00 -11.10  370.94  0 0 2.06  1.0325 $ Middle section
913  RCC 29.00 -11.10  373.00  0 0 0.40  1.429  $ Upper ring
950  RCC 29.00 -11.10  373.40  0 0 0.33  0.857  $ SSt Lip around Prim. caps.
951  RCC 29.00 -11.10  373.73  0 0 1.08  0.768  $ Annodize section
914  RCC 29.00 -11.10  373.40  0 0 1.41  1.118  $ Upper section
C  Rabbit Cup Pg. 1/3  "1.125Source Rabbit"
922  RCC 29.00 -11.10  374.81  0 0 0.10  0.673  $ Cap neck
923  RCC 29.00 -11.10  374.91  0 0 0.60  1.113  $ Cap
C  RABBIT LENGTH = 2.73"=6.934cm (from 368.50 to 375.50 =7.00cm
C Suction Cup Piab F-20 outerdiam=2.21cm, height 0.79cm
924  TRC 29.00 -11.10  375.45  0 0 0.19  1.10 0.71 $ Si connicall bottom secti
925  RCC 29.00 -11.10  375.64  0 0 0.10  0.72      $ Si neck of conn.bottom
926  RCC 29.00 -11.10  375.74  0 0 0.16  0.68      $ air gap
927  RCC 29.00 -11.10  375.90  0 0 0.20  0.72      $ top Si dection
928  RCC 29.00 -11.10  375.90  0 0 0.20  0.36      $ Centered air hole
C
C Plane through one point  Chris result
1015   p   1 0 1  209.85     $ vary last value to move relative to origin
C
C          -----BOX GEOMETRY -----
C Source located at pos=29.00 -11.10 371.85 (x,y,z)
C
C LEFT PLATES
2001   rpp  286.27   342.13   -40.31  -39.04  344.02  399.89  $ Lt Steel plate
2002   rpp  286.27   342.13   -41.58  -40.31  344.02  399.89  $ Lt GRP plate
2003   rpp  286.27   342.13   -42.22  -41.58  344.02  399.89  $ Lt Al plate
C RIGHT PLATES
2004   rpp  286.27   342.13    16.84   18.11  344.02  399.89  $ Rt Steel plate
2005   rpp  286.27   342.13    18.11   19.38  344.02  399.89  $ Rt GRP plate
2006   rpp  286.27   342.13    19.38   20.02  344.02  399.89  $ Rt Al plate
C FRONT PLATES
2007   rpp  285.00  286.27    -42.22   20.02  344.02  399.89  $ Fr Steel plate
2008   rpp  283.73  285.00    -42.22   20.02  344.02  399.89  $ Fr GRP plate
2009   rpp  283.09  283.73    -42.22   20.02  344.02  399.89  $ Fr Al plate
C REAR PLATES
2010   rpp  342.13  343.40    -42.22   20.02  344.02  399.89  $ R Steel plate
2011   rpp  343.40  344.67    -42.22   20.02  344.02  399.89  $ R GRP plate
2012   rpp  344.67  345.31    -42.22   20.02  344.02  399.89  $ R Al plate
```

```
C TOP PLATES
2013   rpp  283.72  344.68    -42.22   20.02  399.89  401.16  $ Tp Steel plate
2014   rpp  283.72  344.68    -42.22   20.02  401.16  402.43  $ Tp GRP plate
2015   rpp  283.72  344.68    -42.22   20.02  402.43  403.07  $ Tp Al plate
C BOTTOM PLATES
2016   rpp  283.72  344.68    -42.22   20.02  342.75  344.02  $ Bt Steel plate
2017   rpp  283.72  344.68    -42.22   20.02  341.48  342.75  $ Bt GRP plate
2018   rpp  283.72  344.68    -42.22   20.02  340.84  341.48  $ Bt Al plate
C AIR DETECTION SPHERE
2019   SPH    314.2    -11.10    371.95    15.24   $ Air detector (12" Sphere)
C AIR INSIDE BOX
C 2020   RPP  283.72  341.50    -39.04   16.84  340.83  399.98 $ Air within Bo
C   ----End Geometry follows blank line

C
C   Transformations:
TR1   -155.40   3.94   0
TR2    29.0   -11.10   0  $ Puts Legs on Table centered at Source tube
TR3   -155.40   3.94  17.50
TR4      -4.7  3.94   0
C  TR5  dx dy dz  xx' yx' zx'  xy' yy' zy'  xz' yz' zz'
*TR5    0 0 0 -45 90 -135  90 0 90  45 45 -45  -1
C
C      ----------------  Materials  -------------
C
C      Moist Air @ den = 1.2e-3 g/cm2

m1     8016   -0.2403 7014  -0.7460   18000 -1.239e-2
       6000  -1.21e-4 1001  -1.3367e-3

mt1    lwtr.60t
C      ANSI.ANS 6.6.1-1987 Concrete Composition @ den = 2.3 g/cm3
m2      1001 7.86e+21  8016 4.38e+22 11023 1.05e+21
       12000 1.40e+20 13027 2.39e+21 14000 1.58e+22
       19000 6.90e+20 20000 2.92e+21 26000 3.10e+20
mt2    lwtr.01t
C
C      Al  aluminum, den = 2.7 g/cm3
m3     13027 1
C     WEP Shielding has 3% Boron. HOPEWELL Designs den= 0.945g/cm3
m4    1001 -0.118  5010 -0.006   6012 -0.586  8016 -0.285 11023 -0.005
mt4   lwtr.01t
C
```

```
C       Pb shielding den = 11.34 g/cm3
m5      82000  1
C     Stainless Steel   SS304 (density=7.8g/cc)
m6   6012  -.0008   14028 -9.223e-3  14029 -4.67e-4   14030 -3.1e-4
     15031 -4.5e-4  16000 -3e-4      24050 -8.265e-3  24052 -0.159
     24053 -0.018   24054 -4.484e-3  25055 -0.02      26054 -0.034
     26056 -0.627   26057 -.0145     26058 -1.914e-3  28058 -0.095
C    Cf2O3  Nominal density =12.0g/cc  $ Cf density=15.1g/cc
m7   98252.66c 2   8016 3
C   Pt-Rh (90% and 10% by weight)  Pt den.=21.45g/cc; Rh den=12.41g/cc
m8   78000 0.90  45103  10
C   CHLOROPRENE C4H5Cl  Density=0.9598g/cc
m9   12000 4  1001 5  17000 1
C   Si-Glass SiO2
m10  14028 -46.743  8016 -53.257
C   POLYETHYLENE   density0.917g/cc Average value 0.857min to 0.975 max
m11  1001  4  6000 2
mt11 poly.01t
C   TUNGTEN Carbide WC, 30% W by weight.  Density 1.314g/cc
m12  6000  0.70  74000 0.30
C  FLEX BORON 5% B by weight  1.96g/cc
m13  5010  0.05  14028  0.95
C  FLEX BORON 35% B by weight, density=
m14  5010  0.35  14028  0.65
C   He3 at 600 torr = 0.7895at  density=0.000098gr/cc
m15  2003  1
C  CERAMIC Al2O3  density = 3.69
m16 13027 2  8016 3
C  Zircaloy-2  density -6.55
m17 40000 -0.982  50000 -0.015  26000 -0.0012  24000 -0.0010 28000 -0.005
                8016 -0.0013
C -----ADDED MATERIALS FOR NPF-----
m18  26056.70c -0.977170 06000.70c -0.022831        $ Shield, carbon steel
m19  01001.70c -0.030000 06000.70c -0.040000        $ GRP w/out Boron
     08016.70c -0.390000 13027.70c -0.010000
     14028.70c -0.230000 29063.70c -0.140000
     29065.70c -0.060000 35079.70c -0.050000
     35081.70c -0.050000
C       -----------------  SOURCE   ------------------
C
C   Cf Spontaneous Fission.Coef Watt Spec:a=1.18000 [MeV]; b=1.03419 [1/MeV]
mode  n              $ Transport neutrons
sdef  par sf erg=d1 cell=900  pos=29.00 -11.10 371.85 rad=d2 ext=d3
```

```
          wgt=1.4099e+09
C
C  Watt Spontaneous Fission Spectrum

sp1   -3  1.1800  1.03419     $ MCNP6 App. H 1.2.2
C  Radial sampling in Source volume
si2   h 0 0.156
sp2   -21  1
C Linear Sampling along Z-axis
Si3  -0.98  0.98   $  370.87   372.83
sp3   -21  1
C
C
lost 15
C
C  ----------------------TALLIES----------------
C
C fc5:n  Neutron Fluence rate in n/cm2/s at 2m from Cf Source
C f5:n   -171 -11.10   371.85   0.5
C
C fc25:n  Neutron Fluence rate at 2m from Cf Source
C f25:n   -171 -11.10   371.85   0.5
C
C ---------------UNMODIFIED FLUX TALLY (ICRP74 Bins)----------
f4:n 6900
E4     1.00E-09 1.00E-08 2.53E-08 1.00E-07 2.00E-07      $ Result energy bins
       5.00E-07 1.00E-06 2.00E-06 5.00E-06 1.00E-05
       2.00E-05 5.00E-05 1.00E-04 2.00E-04 5.00E-04
       1.00E-03 2.00E-03 5.00E-03 1.00E-02 2.00E-02
       3.00E-02 5.00E-02 7.00E-02 1.00E-01 1.50E-01
       2.00E-01 3.00E-01 5.00E-01 7.00E-01 9.00E-01
       1.00E+00 1.20E+00 2.00E+00 3.00E+00 4.00E+00
       5.00E+00 6.00E+00 7.00E+00 8.00E+00 9.00E+00
       1.00E+01 1.20E+01 1.40E+01 1.50E+01 1.60E+01
       1.80E+01 2.00E+01
C
C ---------------MODIFIED FLUX TALLY ICRP74----------
f14:n 6900
e14 1e-9 200ILOG 12.5
DF14 IC 40 IU=1 $ rem/hr/source neutron
C ---------------UNMODIFIED FLUX TALLY----------
f24:n 6900
e24 1e-9 200ILOG 12.5
```

```
C
C  ------------------  ICRP-74 NEUTRON CONVERSION FACTORS---------
C
C    Fluence in n/s.x H*(10) neutron fluence to dose conversion factor
C    units:  pSv/n/cm^2 = pSv.      1Sievert=100Rem

C
C de25      2.5e-08 1.0e-07 1.0e-06 1.0e-05 1.0e-04 1.0e-03 2.0e-03 5.0e-03
C           1.0e-02 2.0e-02 3.0e-02 5.0e-02 7.0e-02 1.0e-01 1.5e-01 2.0e-01
C           2.5e-01 3.0e-01 3.5e-01 4.0e-01 4.5e-01 5.0e-01 5.5e-01 6.0e-01
C           6.5e-01 7.0e-01 7.5e-01 8.0e-01 8.5e-01 9.0e-01 9.5e-01 1.00
C           1.20 1.40 1.6 1.8 2.0 2.2 2.4 2.6 2.8 3.0 3.2 3.4 3.6 3.8 4.0
C           4.2 4.4 4.6 4.8 5.0 5.5 6.0 6.5 7.0 8.0 9.0 10.0 11.0 12.0 13.0
C           14.0 15.0 16.0 17.0 18.0 19.0 20.0
C C
C df25     10.6 12.9 13.3 11.3 9.4 7.9 7.7 8.0 10.5 16.6 23.7 41.1 60.0
C          88.0 132.0 170.0 210.0 233.0 270.0 280.0 310.0 322.0 340.0
C          350.0 365.0 375.0 385.0 390.0 395.0 400.0 400.0 416.0 425.0
C           425.0 420.0 420.0 420.0 418.0 416.0 415.0 412.0 412.0 410.0
C          410.0 410.0 408.0 408.0 408.0 408.0 408.0 405.0 405.0 402.0
C          400.0 402.0 405.0 409.0 420.0 440.0 460.0 480.0 500.0 520.0
C          540.0 540.0 562.0 570.0 585.0 600.0
C
C Fc35:n  Neutron Fluence rate at a RING  2m from Cf Source
C f35x:n   -171   10   0.05
C      ------------  ICRP-74 NEUTRON CONVERSION FACTORS---------
C
C     Fluence in n/s.x H*(10) neutron fluence to dose conversion factor
C     units:  pSv/n/cm^2 = pSv.      1Sievert=100Rem
C
C de35      2.5e-08 1.0e-07 1.0e-06 1.0e-05 1.0e-04 1.0e-03 2.0e-03 5.0e-03
C           1.0e-02 2.0e-02 3.0e-02 5.0e-02 7.0e-02 1.0e-01 1.5e-01 2.0e-01
C           2.5e-01 3.0e-01 3.5e-01 4.0e-01 4.5e-01 5.0e-01 5.5e-01 6.0e-01
C           6.5e-01 7.0e-01 7.5e-01 8.0e-01 8.5e-01 9.0e-01 9.5e-01 1.00
C           1.20 1.40 1.6 1.8 2.0 2.2 2.4 2.6 2.8 3.0 3.2 3.4 3.6 3.8 4.0
C           4.2 4.4 4.6 4.8 5.0 5.5 6.0 6.5 7.0 8.0 9.0 10.0 11.0 12.0 13.0
C           14.0 15.0 16.0 17.0 18.0 19.0 20.0
C
C df35     10.6 12.9 13.3 11.3 9.4 7.9 7.7 8.0 10.5 16.6 23.7 41.1 60.0
C          88.0 132.0 170.0 210.0 233.0 270.0 280.0 310.0 322.0 340.0
C          350.0 365.0 375.0 385.0 390.0 395.0 400.0 400.0 416.0 425.0
C           425.0 420.0 420.0 420.0 418.0 416.0 415.0 412.0 412.0 410.0
C          410.0 410.0 408.0 408.0 408.0 408.0 408.0 405.0 405.0 402.0
```

```
C         400.0 402.0 405.0 409.0 420.0 440.0 460.0 480.0 500.0 520.0
C         540.0 540.0 562.0 570.0 585.0 600.0
C
C
C       ----------------ROSPEC ENERGY SPECTRUM---------
C e0    0.1000000E-08 0.2000000E-08  0.5000000E-08
C       0.1000000E-07   0.2000000E-07
C         0.5000000E-07  0.1000000E-06
C         0.2000000E-06  0.5000000E-06
C         0.1000000E-01  0.1026900E+00
C         0.1165500E+00  0.1316700E+00
C         0.1493100E+00  0.1707300E+00
C         0.1934100E+00  0.2198700E+00
C       0.2606250E+00  0.2906250E+00
C         0.3243750E+00  0.3581250E+00
C         0.3993750E+00  0.4443750E+00
C         0.4931250E+00  0.5456250E+00
C         0.6093750E+00  0.6768750E+00
C       0.7946400E+00  0.8870400E+00
C         0.9871400E+00  0.1094940E+01
C         0.1218140E+01  0.1391000E+01
C         0.1573000E+01  0.1807000E+01
C         0.2041000E+01  0.2327000E+01
C         0.2639000E+01  0.3003000E+01
C         0.3419000E+01  0.3861000E+01
C         0.4407000E+01  0.5000000E+01
C         0.5500000E+01  0.6000000E+01
C         0.6500000E+01  0.7000000E+01
C         0.7500000E+01  0.8000000E+01
C         0.8500000E+01  0.9000000E+01
C         0.9500000E+01  0.1000000E+02
C
print
dbcn  7j  1 0 0 0 0 154913 j
C
C          ndp     ndm  mct ndmp  dmmp
prdmp   1.0e+03 2.5e+03  1   4    0
C
C ctme    10      $ 1200
C
nps  1.5e+07
```

THIS PAGE INTENTIONALLY LEFT BLANK

APPENDIX G. MCNP OUTPUT TALLIES

The computational results of the free field and surrogate vehicle assemblies are listed below. Tally types 4 and 24 were unmodified fluence tallies, which differed in energy bin structure. Tally type 14 had a similar tally to tally 24, but instead extended to 18.0 MeV and applied standard dose function 1. The standard dose function one in MCNP6.1 utilizes the published fluence to dose conversion coefficients and applies them to all energy bins.

A. FREE FIELD ASSEMBLY

```
1tally       24        nps =    15000000
         tally type 4    track length estimate of particle flux.       units   1/cm**2
         particle(s): neutrons

         volumes
               cell:     6900
                    1.48267E+04

 cell  6900
     energy
   1.0000E-09   4.15079E-01 0.2110
   1.1226E-09   1.00481E-01 0.5078
   1.2603E-09   2.16855E-01 0.2823
   1.4148E-09   7.93181E-02 0.4046
   1.5883E-09   2.12914E-01 0.2859
   1.7831E-09   1.78869E-01 0.3256
   2.0017E-09   3.13509E-01 0.2367
   2.2472E-09   4.72365E-01 0.2042
   2.5227E-09   6.55368E-01 0.1720
   2.8320E-09   1.02234E+00 0.1410
   3.1793E-09   1.12378E+00 0.1307
   3.5692E-09   1.70669E+00 0.1089
   4.0068E-09   1.78607E+00 0.1058
   4.4982E-09   1.92747E+00 0.1017
   5.0497E-09   2.27284E+00 0.0911
   5.6689E-09   2.74751E+00 0.0838
   6.3641E-09   4.04073E+00 0.0713
```

7.1444E-09 4.05279E+00 0.0699
8.0205E-09 5.03244E+00 0.0612
9.0040E-09 6.57736E+00 0.0562
1.0108E-08 7.68469E+00 0.0510
1.1348E-08 1.23825E+01 0.0409
1.2739E-08 1.30595E+01 0.0400
1.4301E-08 1.40997E+01 0.0376
1.6055E-08 1.73409E+01 0.0345
1.8023E-08 2.06976E+01 0.0313
2.0233E-08 2.41858E+01 0.0295
2.2714E-08 2.93844E+01 0.0263
2.5500E-08 3.58420E+01 0.0239
2.8626E-08 3.55357E+01 0.0241
3.2137E-08 4.10816E+01 0.0227
3.6077E-08 4.56434E+01 0.0215
4.0501E-08 4.90367E+01 0.0209
4.5468E-08 5.22439E+01 0.0203
5.1043E-08 5.97000E+01 0.0191
5.7302E-08 5.76424E+01 0.0196
6.4328E-08 5.59424E+01 0.0199
7.2216E-08 5.25807E+01 0.0208
8.1072E-08 5.33376E+01 0.0208
9.1013E-08 4.90453E+01 0.0219
1.0217E-07 4.29975E+01 0.0237
1.1470E-07 3.55539E+01 0.0263
1.2877E-07 2.92663E+01 0.0296
1.4456E-07 2.47310E+01 0.0335
1.6228E-07 1.87990E+01 0.0389
1.8218E-07 1.63054E+01 0.0430
2.0452E-07 1.38138E+01 0.0480
2.2960E-07 1.17029E+01 0.0537
2.5775E-07 1.10325E+01 0.0558
2.8936E-07 8.55749E+00 0.0637
3.2484E-07 8.64972E+00 0.0640
3.6467E-07 9.91134E+00 0.0598
4.0939E-07 8.17537E+00 0.0658
4.5959E-07 9.02250E+00 0.0628
5.1594E-07 8.21338E+00 0.0661
5.7921E-07 7.88407E+00 0.0676
6.5023E-07 7.74355E+00 0.0686
7.2997E-07 9.14517E+00 0.0628
8.1948E-07 7.81057E+00 0.0687
9.1996E-07 8.38920E+00 0.0647
1.0328E-06 7.83240E+00 0.0682
1.1594E-06 8.50526E+00 0.0661

1.3016E-06 7.04175E+00 0.0726
1.4612E-06 7.94840E+00 0.0685
1.6403E-06 8.11562E+00 0.0670
1.8415E-06 7.94537E+00 0.0677
2.0673E-06 6.93153E+00 0.0734
2.3208E-06 8.00683E+00 0.0683
2.6054E-06 7.43132E+00 0.0703
2.9248E-06 7.62931E+00 0.0683
3.2835E-06 7.03366E+00 0.0720
3.6861E-06 7.37727E+00 0.0710
4.1381E-06 8.42139E+00 0.0664
4.6455E-06 7.55373E+00 0.0698
5.2152E-06 7.40410E+00 0.0705
5.8547E-06 6.56476E+00 0.0757
6.5726E-06 6.60835E+00 0.0735
7.3785E-06 7.68838E+00 0.0698
8.2833E-06 6.95719E+00 0.0724
9.2990E-06 8.83859E+00 0.0648
1.0439E-05 8.43822E+00 0.0662
1.1719E-05 7.51225E+00 0.0710
1.3156E-05 8.20806E+00 0.0678
1.4770E-05 7.61870E+00 0.0694
1.6581E-05 7.49739E+00 0.0696
1.8614E-05 7.84627E+00 0.0701
2.0896E-05 7.63494E+00 0.0699
2.3459E-05 9.08994E+00 0.0642
2.6335E-05 7.59236E+00 0.0689
2.9565E-05 8.54923E+00 0.0660
3.3190E-05 8.13610E+00 0.0673
3.7260E-05 7.43960E+00 0.0708
4.1828E-05 7.48243E+00 0.0709
4.6957E-05 9.11240E+00 0.0650
5.2715E-05 8.20898E+00 0.0676
5.9180E-05 7.53784E+00 0.0702
6.6436E-05 8.75463E+00 0.0658
7.4583E-05 8.01437E+00 0.0682
8.3728E-05 7.79973E+00 0.0690
9.3995E-05 8.94159E+00 0.0644
1.0552E-04 8.41275E+00 0.0662
1.1846E-04 8.00072E+00 0.0695
1.3299E-04 9.16898E+00 0.0641
1.4929E-04 8.70803E+00 0.0655
1.6760E-04 8.47293E+00 0.0664
1.8815E-04 9.03299E+00 0.0652
2.1122E-04 8.40828E+00 0.0665

2.3712E-04	8.62908E+00	0.0658
2.6620E-04	9.05708E+00	0.0650
2.9884E-04	8.92601E+00	0.0652
3.3548E-04	7.78182E+00	0.0691
3.7662E-04	8.92218E+00	0.0653
4.2280E-04	9.47996E+00	0.0630
4.7465E-04	8.98027E+00	0.0641
5.3285E-04	9.66652E+00	0.0624
5.9819E-04	8.88093E+00	0.0654
6.7154E-04	8.43401E+00	0.0679
7.5389E-04	9.90799E+00	0.0615
8.4633E-04	8.61657E+00	0.0661
9.5011E-04	9.16289E+00	0.0639
1.0666E-03	9.27467E+00	0.0628
1.1974E-03	8.79739E+00	0.0651
1.3442E-03	9.99277E+00	0.0610
1.5091E-03	9.18576E+00	0.0638
1.6941E-03	9.75353E+00	0.0620
1.9018E-03	9.83582E+00	0.0621
2.1350E-03	9.68152E+00	0.0615
2.3968E-03	1.09061E+01	0.0591
2.6907E-03	9.59319E+00	0.0627
3.0207E-03	7.49492E+00	0.0701
3.3911E-03	9.26710E+00	0.0635
3.8069E-03	9.60225E+00	0.0626
4.2737E-03	1.08573E+01	0.0586
4.7978E-03	1.06595E+01	0.0600
5.3861E-03	1.00956E+01	0.0607
6.0465E-03	9.74301E+00	0.0618
6.7880E-03	1.00813E+01	0.0615
7.6203E-03	1.02339E+01	0.0596
8.5547E-03	1.06709E+01	0.0592
9.6037E-03	1.06157E+01	0.0594
1.0781E-02	1.06942E+01	0.0586
1.2103E-02	1.19973E+01	0.0562
1.3588E-02	1.21774E+01	0.0555
1.5254E-02	1.23850E+01	0.0549
1.7124E-02	1.22694E+01	0.0561
1.9224E-02	1.18246E+01	0.0569
2.1581E-02	1.34422E+01	0.0532
2.4227E-02	1.39246E+01	0.0520
2.7198E-02	1.35252E+01	0.0526
3.0533E-02	1.47921E+01	0.0496
3.4277E-02	1.54678E+01	0.0487
3.8481E-02	1.10415E+01	0.0585

4.3199E-02	1.54435E+01	0.0493
4.8496E-02	1.66002E+01	0.0481
5.4443E-02	1.93201E+01	0.0440
6.1119E-02	1.67775E+01	0.0470
6.8613E-02	2.13848E+01	0.0421
7.7027E-02	2.29275E+01	0.0405
8.6472E-02	2.42560E+01	0.0395
9.7075E-02	1.96705E+01	0.0440
1.0898E-01	2.58833E+01	0.0383
1.2234E-01	3.05420E+01	0.0353
1.3734E-01	3.72937E+01	0.0318
1.5418E-01	3.50418E+01	0.0328
1.7309E-01	3.65178E+01	0.0321
1.9432E-01	3.76509E+01	0.0319
2.1814E-01	3.84004E+01	0.0313
2.4489E-01	4.39733E+01	0.0294
2.7492E-01	5.18020E+01	0.0269
3.0863E-01	5.44673E+01	0.0265
3.4648E-01	6.10960E+01	0.0250
3.8896E-01	5.62133E+01	0.0261
4.3666E-01	5.56887E+01	0.0263
4.9020E-01	6.28352E+01	0.0246
5.5031E-01	7.61056E+01	0.0224
6.1779E-01	8.66686E+01	0.0210
6.9355E-01	9.47078E+01	0.0200
7.7859E-01	1.08599E+02	0.0187
8.7406E-01	1.09092E+02	0.0187
9.8124E-01	9.63554E+01	0.0199
1.1016E+00	9.69962E+01	0.0199
1.2366E+00	1.06060E+02	0.0190
1.3883E+00	1.08195E+02	0.0188
1.5585E+00	1.12258E+02	0.0184
1.7496E+00	1.10169E+02	0.0186
1.9642E+00	1.06204E+02	0.0190
2.2050E+00	1.05187E+02	0.0190
2.4754E+00	1.10420E+02	0.0185
2.7789E+00	1.06120E+02	0.0189
3.1197E+00	8.84107E+01	0.0207
3.5022E+00	7.51905E+01	0.0224
3.9317E+00	6.43499E+01	0.0243
4.4138E+00	5.60354E+01	0.0261
4.9550E+00	4.36170E+01	0.0296
5.5626E+00	3.44835E+01	0.0333
6.2447E+00	2.39646E+01	0.0399
7.0104E+00	1.73287E+01	0.0472

7.8700E+00 1.13121E+01 0.0581
8.8351E+00 7.52510E+00 0.0703
9.9184E+00 3.77644E+00 0.1010
1.1135E+01 2.00256E+00 0.1388
1.2500E+01 6.28483E-01 0.2495
total 4.64444E+03 0.0028

****
ICRP Dose: 200 Energy Bin // rem/hr/source neutron
****

1tally 14 nps = 15000000
tally type 4 track length estimate of particle flux.
particle(s): neutrons
this tally is modified by standard dose function 1.

volumes
cell: 6900
1.48267E+04

cell 6900
energy
1.0000E-09 9.86228E-07 0.2110
1.1247E-09 2.41367E-07 0.5083
1.2649E-09 5.29521E-07 0.2824
1.4225E-09 2.66678E-07 0.3544
1.5999E-09 4.90011E-07 0.2998
1.7993E-09 5.93673E-07 0.2812
2.0236E-09 7.66939E-07 0.2513
2.2759E-09 1.37879E-06 0.2001
2.5596E-09 1.79137E-06 0.1674
2.8787E-09 2.75061E-06 0.1429
3.2375E-09 3.61710E-06 0.1231
3.6411E-09 5.24858E-06 0.1040
4.0950E-09 5.28676E-06 0.1033
4.6055E-09 5.62807E-06 0.1021
5.1796E-09 7.15024E-06 0.0871
5.8253E-09 9.05146E-06 0.0847
6.5515E-09 1.25523E-05 0.0687
7.3682E-09 1.39940E-05 0.0657
8.2867E-09 1.72681E-05 0.0603
9.3197E-09 2.32235E-05 0.0522
1.0482E-08 2.75471E-05 0.0494
1.1788E-08 4.31330E-05 0.0397
1.3258E-08 4.60901E-05 0.0389
1.4910E-08 5.48718E-05 0.0359

1.6769E-08	6.47805E-05	0.0332
1.8860E-08	7.90028E-05	0.0306
2.1211E-08	9.85997E-05	0.0278
2.3855E-08	1.28431E-04	0.0244
2.6828E-08	1.31489E-04	0.0244
3.0173E-08	1.52977E-04	0.0232
3.3934E-08	1.70158E-04	0.0220
3.8164E-08	1.96937E-04	0.0210
4.2922E-08	2.07444E-04	0.0205
4.8273E-08	2.45710E-04	0.0192
5.4290E-08	2.46859E-04	0.0194
6.1058E-08	2.44766E-04	0.0197
6.8670E-08	2.47084E-04	0.0200
7.7230E-08	2.37682E-04	0.0208
8.6858E-08	2.41403E-04	0.0208
9.7685E-08	2.09433E-04	0.0229
1.0986E-07	1.80461E-04	0.0252
1.2356E-07	1.45267E-04	0.0284
1.3896E-07	1.31353E-04	0.0314
1.5628E-07	9.71206E-05	0.0368
1.7577E-07	8.31926E-05	0.0417
1.9768E-07	7.04235E-05	0.0462
2.2232E-07	6.12134E-05	0.0513
2.5003E-07	5.51739E-05	0.0549
2.8120E-07	4.61341E-05	0.0600
3.1626E-07	4.09459E-05	0.0652
3.5568E-07	4.98081E-05	0.0591
4.0002E-07	4.18763E-05	0.0638
4.4989E-07	4.33434E-05	0.0638
5.0597E-07	4.14356E-05	0.0650
5.6905E-07	3.97322E-05	0.0661
6.3998E-07	3.72343E-05	0.0695
7.1976E-07	4.54971E-05	0.0619
8.0949E-07	3.98590E-05	0.0666
9.1040E-07	4.13225E-05	0.0642
1.0239E-06	3.76588E-05	0.0681
1.1515E-06	4.01492E-05	0.0665
1.2951E-06	3.55376E-05	0.0704
1.4565E-06	3.74553E-05	0.0684
1.6381E-06	3.82547E-05	0.0671
1.8423E-06	3.76824E-05	0.0670
2.0720E-06	3.27746E-05	0.0727
2.3303E-06	3.79863E-05	0.0672
2.6207E-06	3.33058E-05	0.0711
2.9474E-06	3.56793E-05	0.0672

3.3149E-06	3.26284E-05	0.0709
3.7281E-06	3.24781E-05	0.0713
4.1928E-06	3.77331E-05	0.0657
4.7155E-06	3.33960E-05	0.0692
5.3034E-06	3.24312E-05	0.0704
5.9645E-06	2.85982E-05	0.0747
6.7080E-06	2.77516E-05	0.0740
7.5442E-06	3.46380E-05	0.0674
8.4847E-06	3.02241E-05	0.0705
9.5424E-06	3.55278E-05	0.0656
1.0732E-05	3.45186E-05	0.0661
1.2070E-05	3.20215E-05	0.0691
1.3574E-05	3.13106E-05	0.0693
1.5267E-05	3.09189E-05	0.0677
1.7170E-05	2.91871E-05	0.0705
1.9310E-05	3.15475E-05	0.0681
2.1717E-05	3.08469E-05	0.0677
2.4425E-05	3.39893E-05	0.0645
2.7469E-05	2.93082E-05	0.0674
3.0894E-05	3.17480E-05	0.0657
3.4745E-05	2.85160E-05	0.0700
3.9076E-05	3.03600E-05	0.0669
4.3948E-05	2.76018E-05	0.0709
4.9426E-05	3.17850E-05	0.0654
5.5587E-05	2.95034E-05	0.0674
6.2517E-05	2.88600E-05	0.0671
7.0310E-05	2.89272E-05	0.0676
7.9075E-05	2.82270E-05	0.0673
8.8933E-05	2.87250E-05	0.0665
1.0002E-04	3.06345E-05	0.0644
1.1249E-04	2.65241E-05	0.0692
1.2651E-04	3.07976E-05	0.0641
1.4228E-04	2.92041E-05	0.0651
1.6002E-04	2.87297E-05	0.0650
1.7997E-04	2.84493E-05	0.0662
2.0240E-04	2.89861E-05	0.0645
2.2763E-04	2.68312E-05	0.0665
2.5601E-04	2.89598E-05	0.0643
2.8792E-04	2.98081E-05	0.0635
3.2381E-04	2.43108E-05	0.0691
3.6418E-04	2.62303E-05	0.0663
4.0958E-04	2.91650E-05	0.0625
4.6064E-04	3.01850E-05	0.0617
5.1806E-04	2.78878E-05	0.0631
5.8264E-04	2.78259E-05	0.0638

6.5527E-04	2.49411E-05	0.0673
7.3696E-04	2.85135E-05	0.0623
8.2883E-04	2.65791E-05	0.0640
9.3215E-04	2.54814E-05	0.0647
1.0484E-03	2.66206E-05	0.0627
1.1790E-03	2.57135E-05	0.0641
1.3260E-03	2.74927E-05	0.0615
1.4913E-03	2.75930E-05	0.0619
1.6772E-03	2.66959E-05	0.0631
1.8863E-03	2.82561E-05	0.0609
2.1215E-03	2.78614E-05	0.0607
2.3859E-03	3.06362E-05	0.0587
2.6834E-03	2.72365E-05	0.0623
3.0179E-03	2.14166E-05	0.0694
3.3941E-03	2.61993E-05	0.0635
3.8172E-03	2.79125E-05	0.0618
4.2930E-03	3.17480E-05	0.0580
4.8282E-03	3.10551E-05	0.0595
5.4301E-03	2.96939E-05	0.0603
6.1070E-03	2.97997E-05	0.0620
6.8683E-03	3.27927E-05	0.0607
7.7245E-03	3.47408E-05	0.0596
8.6874E-03	3.93063E-05	0.0580
9.7704E-03	4.00364E-05	0.0584
1.0988E-02	4.34001E-05	0.0579
1.2358E-02	5.14214E-05	0.0558
1.3899E-02	5.86051E-05	0.0544
1.5631E-02	6.15357E-05	0.0555
1.7580E-02	6.42630E-05	0.0565
1.9772E-02	7.65618E-05	0.0538
2.2236E-02	8.56515E-05	0.0531
2.5008E-02	9.67018E-05	0.0520
2.8126E-02	1.01780E-04	0.0529
3.1632E-02	1.40760E-04	0.0474
3.5575E-02	1.39929E-04	0.0511
4.0010E-02	1.36581E-04	0.0555
4.4998E-02	2.16642E-04	0.0478
5.0607E-02	2.50005E-04	0.0464
5.6916E-02	2.84357E-04	0.0459
6.4011E-02	3.61852E-04	0.0441
7.1990E-02	4.63993E-04	0.0415
8.0965E-02	6.16073E-04	0.0384
9.1058E-02	5.99840E-04	0.0416
1.0241E-01	6.69239E-04	0.0419
1.1518E-01	1.03715E-03	0.0358

1.2953E-01	1.29708E-03	0.0341
1.4568E-01	1.65216E-03	0.0317
1.6384E-01	1.77340E-03	0.0322
1.8427E-01	2.09532E-03	0.0314
2.0724E-01	2.30467E-03	0.0314
2.3307E-01	2.75204E-03	0.0303
2.6212E-01	3.61167E-03	0.0277
2.9480E-01	4.28180E-03	0.0266
3.3155E-01	5.29429E-03	0.0249
3.7288E-01	5.55075E-03	0.0254
4.1937E-01	5.73809E-03	0.0260
4.7164E-01	6.21871E-03	0.0259
5.3044E-01	8.68417E-03	0.0225
5.9656E-01	1.00412E-02	0.0216
6.7093E-01	1.23250E-02	0.0200
7.5457E-01	1.43197E-02	0.0190
8.4863E-01	1.62605E-02	0.0181
9.5442E-01	1.43120E-02	0.0196
1.0734E+00	1.44120E-02	0.0199
1.2072E+00	1.61626E-02	0.0189
1.3577E+00	1.68979E-02	0.0186
1.5270E+00	1.71741E-02	0.0184
1.7173E+00	1.72178E-02	0.0184
1.9314E+00	1.64183E-02	0.0188
2.1722E+00	1.62606E-02	0.0188
2.4429E+00	1.65667E-02	0.0185
2.7475E+00	1.62505E-02	0.0187
3.0900E+00	1.35754E-02	0.0204
3.4752E+00	1.14006E-02	0.0222
3.9084E+00	9.76420E-03	0.0240
4.3956E+00	8.35464E-03	0.0259
4.9435E+00	6.55426E-03	0.0292
5.5598E+00	5.12896E-03	0.0329
6.2529E+00	3.49413E-03	0.0397
7.0324E+00	2.52229E-03	0.0471
7.9090E+00	1.65775E-03	0.0580
8.8950E+00	1.11066E-03	0.0707
1.0004E+01	5.84309E-04	0.1009
1.1251E+01	2.87384E-04	0.1478
1.2653E+01	1.14455E-04	0.2418
1.4231E+01	3.04526E-05	0.4769
1.6005E+01	3.13813E-05	0.4842
1.8000E+01	9.24704E-06	1.0000
total	3.42950E-01	0.0039

****

ICRP Flux: 47 Energy Bin
****

1tally 4 nps = 15000000
tally type 4 track length estimate of particle flux. units 1/cm**2
particle(s): neutrons

volumes
cell: 6900
1.48267E+04

cell 6900
energy

1.0000E-09	4.15079E-01	0.2110
1.0000E-08	4.14547E+01	0.0219
2.5300E-08	1.65377E+02	0.0112
1.0000E-07	5.89786E+02	0.0062
2.0000E-07	1.43313E+02	0.0138
5.0000E-07	7.56363E+01	0.0215
1.0000E-06	4.89055E+01	0.0272
2.0000E-06	4.66098E+01	0.0282
5.0000E-06	6.02533E+01	0.0249
1.0000E-05	4.41187E+01	0.0290
2.0000E-05	4.68446E+01	0.0283
5.0000E-05	6.45348E+01	0.0241
1.0000E-04	4.97339E+01	0.0274
2.0000E-04	5.16603E+01	0.0271
5.0000E-04	7.00035E+01	0.0233
1.0000E-03	5.44610E+01	0.0264
2.0000E-03	5.67051E+01	0.0257
5.0000E-03	7.79075E+01	0.0220
1.0000E-02	6.10305E+01	0.0248
2.0000E-02	7.24943E+01	0.0229
3.0000E-02	4.81690E+01	0.0279
5.0000E-02	6.63500E+01	0.0239
7.0000E-02	5.55586E+01	0.0260
1.0000E-01	7.00609E+01	0.0233
1.5000E-01	1.14274E+02	0.0182
2.0000E-01	9.16405E+01	0.0203
3.0000E-01	1.65011E+02	0.0152
5.0000E-01	2.63472E+02	0.0121
7.0000E-01	2.52638E+02	0.0123
9.0000E-01	2.34217E+02	0.0128
1.0000E+00	8.69289E+01	0.0210
1.2000E+00	1.58769E+02	0.0155
2.0000E+00	4.81848E+02	0.0089

3.0000E+00 3.64314E+02 0.0102
4.0000E+00 1.77582E+02 0.0146
5.0000E+00 9.50652E+01 0.0200
6.0000E+00 4.72061E+01 0.0285
7.0000E+00 2.45356E+01 0.0395
8.0000E+00 1.29000E+01 0.0544
9.0000E+00 6.87695E+00 0.0737
1.0000E+01 3.38052E+00 0.1069
1.2000E+01 2.17939E+00 0.1335
1.4000E+01 4.07580E-01 0.3093
1.5000E+01 1.28644E-01 0.4900
1.6000E+01 4.96358E-02 1.0000
1.8000E+01 4.57270E-02 1.0000
2.0000E+01 0.00000E+00 0.0000

B. SURROGATE VEHICLE ASSEMBLY

****
200 Energy Bin for Unfolding
****
1tally 24 nps = 15000000
tally type 4 track length estimate of particle flux. units 1/cm**2
particle(s): neutrons

volumes
cell: 6900
1.48267E+04

cell 6900
energy
1.0000E-09 4.21271E-02 0.5010
1.1226E-09 1.40015E-02 0.8425
1.2603E-09 2.10769E-02 1.0000
1.4148E-09 1.78536E-02 0.8393
1.5883E-09 5.60590E-02 0.5307
1.7831E-09 3.50466E-02 0.7279
2.0017E-09 4.47285E-02 0.4542
2.2472E-09 9.31247E-02 0.4386
2.5227E-09 1.68778E-01 0.3088
2.8320E-09 2.01139E-01 0.2935
3.1793E-09 2.56365E-01 0.3035
3.5692E-09 1.58454E-01 0.3263
4.0068E-09 1.85251E-01 0.2851
4.4982E-09 5.21717E-01 0.1939
5.0497E-09 7.20415E-01 0.1552
5.6689E-09 4.28431E-01 0.1932

6.3641E-09	9.04448E-01	0.1333
7.1444E-09	1.16373E+00	0.1236
8.0205E-09	1.28247E+00	0.1097
9.0040E-09	1.76981E+00	0.0963
1.0108E-08	2.16686E+00	0.0903
1.1348E-08	2.80151E+00	0.0812
1.2739E-08	3.75941E+00	0.0678
1.4301E-08	4.47058E+00	0.0631
1.6055E-08	5.72803E+00	0.0558
1.8023E-08	7.58443E+00	0.0480
2.0233E-08	8.78261E+00	0.0442
2.2714E-08	1.07132E+01	0.0414
2.5500E-08	1.27736E+01	0.0376
2.8626E-08	1.45303E+01	0.0359
3.2137E-08	1.62415E+01	0.0334
3.6077E-08	1.83590E+01	0.0317
4.0501E-08	2.03215E+01	0.0296
4.5468E-08	2.41641E+01	0.0277
5.1043E-08	2.53621E+01	0.0270
5.7302E-08	2.69554E+01	0.0266
6.4328E-08	2.72131E+01	0.0261
7.2216E-08	2.73898E+01	0.0266
8.1072E-08	2.78406E+01	0.0263
9.1013E-08	2.43646E+01	0.0281
1.0217E-07	2.27854E+01	0.0306
1.1470E-07	1.95248E+01	0.0327
1.2877E-07	1.79555E+01	0.0349
1.4456E-07	1.37579E+01	0.0410
1.6228E-07	1.21974E+01	0.0446
1.8218E-07	1.00641E+01	0.0492
2.0452E-07	8.23657E+00	0.0580
2.2960E-07	8.14662E+00	0.0596
2.5775E-07	7.46496E+00	0.0630
2.8936E-07	7.18437E+00	0.0642
3.2484E-07	6.84615E+00	0.0658
3.6467E-07	7.40142E+00	0.0654
4.0939E-07	7.36461E+00	0.0648
4.5959E-07	7.81022E+00	0.0653
5.1594E-07	7.34719E+00	0.0667
5.7921E-07	6.88091E+00	0.0678
6.5023E-07	7.21861E+00	0.0667
7.2997E-07	6.54313E+00	0.0702
8.1948E-07	7.77418E+00	0.0644
9.1996E-07	6.86986E+00	0.0691
1.0328E-06	6.32750E+00	0.0718

1.1594E-06	7.67030E+00	0.0658
1.3016E-06	7.37654E+00	0.0675
1.4612E-06	7.51488E+00	0.0673
1.6403E-06	7.37125E+00	0.0685
1.8415E-06	8.00372E+00	0.0688
2.0673E-06	7.43944E+00	0.0674
2.3208E-06	8.17883E+00	0.0651
2.6054E-06	7.89949E+00	0.0673
2.9248E-06	7.80779E+00	0.0673
3.2835E-06	7.87742E+00	0.0689
3.6861E-06	7.02428E+00	0.0713
4.1381E-06	7.63184E+00	0.0684
4.6455E-06	7.59363E+00	0.0675
5.2152E-06	8.46666E+00	0.0670
5.8547E-06	7.29945E+00	0.0692
6.5726E-06	8.04494E+00	0.0668
7.3785E-06	7.39255E+00	0.0705
8.2833E-06	7.82438E+00	0.0687
9.2990E-06	7.53201E+00	0.0685
1.0439E-05	8.75927E+00	0.0667
1.1719E-05	8.89605E+00	0.0642
1.3156E-05	7.89213E+00	0.0678
1.4770E-05	8.96998E+00	0.0644
1.6581E-05	9.16232E+00	0.0639
1.8614E-05	8.62095E+00	0.0645
2.0896E-05	9.16945E+00	0.0634
2.3459E-05	8.41180E+00	0.0666
2.6335E-05	8.27935E+00	0.0667
2.9565E-05	9.23097E+00	0.0648
3.3190E-05	8.46631E+00	0.0666
3.7260E-05	7.64130E+00	0.0684
4.1828E-05	1.00377E+01	0.0613
4.6957E-05	9.62454E+00	0.0626
5.2715E-05	9.83602E+00	0.0616
5.9180E-05	1.05268E+01	0.0595
6.6436E-05	9.16897E+00	0.0643
7.4583E-05	9.57827E+00	0.0617
8.3728E-05	9.75107E+00	0.0618
9.3995E-05	8.85028E+00	0.0650
1.0552E-04	9.75499E+00	0.0627
1.1846E-04	1.01427E+01	0.0606
1.3299E-04	9.50274E+00	0.0621
1.4929E-04	1.00443E+01	0.0612
1.6760E-04	9.32876E+00	0.0638
1.8815E-04	9.87175E+00	0.0616

2.1122E-04	1.02599E+01	0.0617
2.3712E-04	9.76416E+00	0.0620
2.6620E-04	1.00700E+01	0.0621
2.9884E-04	9.36424E+00	0.0629
3.3548E-04	1.06622E+01	0.0589
3.7662E-04	9.91352E+00	0.0623
4.2280E-04	1.04307E+01	0.0604
4.7465E-04	9.69951E+00	0.0618
5.3285E-04	1.16349E+01	0.0571
5.9819E-04	1.13096E+01	0.0580
6.7154E-04	1.12669E+01	0.0591
7.5389E-04	1.09791E+01	0.0602
8.4633E-04	1.00332E+01	0.0607
9.5011E-04	1.02364E+01	0.0600
1.0666E-03	1.16871E+01	0.0571
1.1974E-03	1.10644E+01	0.0588
1.3442E-03	1.19695E+01	0.0561
1.5091E-03	1.26064E+01	0.0550
1.6941E-03	1.22460E+01	0.0559
1.9018E-03	1.11311E+01	0.0597
2.1350E-03	1.19450E+01	0.0575
2.3968E-03	1.22155E+01	0.0562
2.6907E-03	1.08985E+01	0.0596
3.0207E-03	1.15248E+01	0.0574
3.3911E-03	1.28432E+01	0.0551
3.8069E-03	1.28983E+01	0.0542
4.2737E-03	1.25822E+01	0.0544
4.7978E-03	1.35302E+01	0.0532
5.3861E-03	1.29131E+01	0.0548
6.0465E-03	1.27517E+01	0.0554
6.7880E-03	1.23886E+01	0.0561
7.6203E-03	1.46360E+01	0.0516
8.5547E-03	1.30042E+01	0.0546
9.6037E-03	1.30058E+01	0.0541
1.0781E-02	1.30279E+01	0.0534
1.2103E-02	1.43327E+01	0.0520
1.3588E-02	1.42095E+01	0.0522
1.5254E-02	1.43050E+01	0.0519
1.7124E-02	1.62588E+01	0.0486
1.9224E-02	1.63655E+01	0.0487
2.1581E-02	1.75945E+01	0.0465
2.4227E-02	1.60547E+01	0.0489
2.7198E-02	2.79694E+01	0.0371
3.0533E-02	5.16836E+00	0.0857
3.4277E-02	1.33449E+01	0.0540

3.8481E-02	1.44131E+01	0.0520
4.3199E-02	1.99501E+01	0.0444
4.8496E-02	1.74765E+01	0.0466
5.4443E-02	2.22135E+01	0.0417
6.1119E-02	2.14318E+01	0.0424
6.8613E-02	2.23443E+01	0.0418
7.7027E-02	2.73526E+01	0.0378
8.6472E-02	2.57577E+01	0.0386
9.7075E-02	2.09899E+01	0.0427
1.0898E-01	2.74926E+01	0.0378
1.2234E-01	2.94392E+01	0.0362
1.3734E-01	4.08356E+01	0.0307
1.5418E-01	2.66117E+01	0.0381
1.7309E-01	3.45481E+01	0.0334
1.9432E-01	3.91212E+01	0.0315
2.1814E-01	3.63291E+01	0.0325
2.4489E-01	4.21538E+01	0.0302
2.7492E-01	5.28040E+01	0.0267
3.0863E-01	4.94716E+01	0.0277
3.4648E-01	5.61050E+01	0.0261
3.8896E-01	6.12563E+01	0.0251
4.3666E-01	5.07396E+01	0.0275
4.9020E-01	6.33364E+01	0.0248
5.5031E-01	7.38471E+01	0.0228
6.1779E-01	8.29682E+01	0.0215
6.9355E-01	9.45924E+01	0.0201
7.7859E-01	1.02070E+02	0.0195
8.7406E-01	9.39007E+01	0.0204
9.8124E-01	8.48994E+01	0.0213
1.1016E+00	8.44267E+01	0.0213
1.2366E+00	9.61839E+01	0.0201
1.3883E+00	9.36592E+01	0.0202
1.5585E+00	9.30668E+01	0.0203
1.7496E+00	9.18969E+01	0.0204
1.9642E+00	8.57980E+01	0.0212
2.2050E+00	8.25800E+01	0.0214
2.4754E+00	9.05961E+01	0.0206
2.7789E+00	8.02095E+01	0.0218
3.1197E+00	6.79217E+01	0.0238
3.5022E+00	5.54295E+01	0.0263
3.9317E+00	4.75769E+01	0.0283
4.4138E+00	4.15638E+01	0.0302
4.9550E+00	3.42687E+01	0.0334
5.5626E+00	2.43076E+01	0.0394
6.2447E+00	1.80109E+01	0.0457

```
   7.0104E+00   1.22393E+01 0.0561
   7.8700E+00   8.86846E+00 0.0652
   8.8351E+00   5.46577E+00 0.0824
   9.9184E+00   2.82778E+00 0.1173
   1.1135E+01   1.37401E+00 0.1660
   1.2500E+01   3.55163E-01 0.3290
         total      3.92595E+03 0.0032


1**********************************************************************
ICRP Dose: 200 Energy Bin // rem/hr/source neutron
**********************************************************************
1tally       14        nps =    15000000
         tally type 4    track length estimate of particle flux.
         particle(s): neutrons
         this tally is modified by standard dose function 1.

         volumes
               cell:     6900
                    1.48267E+04

 cell  6900
     energy
   1.0000E-09   1.00094E-07 0.5010
   1.1247E-09   3.36527E-08 0.8438
   1.2649E-09   5.14646E-08 1.0000
   1.4225E-09   4.43375E-08 0.8386
   1.5999E-09   1.41852E-07 0.5302
   1.7993E-09   9.05015E-08 0.7277
   2.0236E-09   1.74308E-07 0.4478
   2.2759E-09   2.35206E-07 0.4152
   2.5596E-09   5.06319E-07 0.3035
   2.8787E-09   7.14403E-07 0.3009
   3.2375E-09   4.56304E-07 0.3255
   3.6411E-09   4.69310E-07 0.3151
   4.0950E-09   1.01476E-06 0.2287
   4.6055E-09   1.41640E-06 0.1872
   5.1796E-09   2.15332E-06 0.1553
   5.8253E-09   1.43875E-06 0.1863
   6.5515E-09   2.74764E-06 0.1367
   7.3682E-09   4.21924E-06 0.1129
   8.2867E-09   3.89345E-06 0.1084
   9.3197E-09   6.42913E-06 0.0913
   1.0482E-08   7.55809E-06 0.0877
   1.1788E-08   9.94035E-06 0.0773
```

1.3258E-08	1.47763E-05	0.0638
1.4910E-08	1.66330E-05	0.0616
1.6769E-08	2.27279E-05	0.0512
1.8860E-08	2.96180E-05	0.0465
2.1211E-08	3.60753E-05	0.0420
2.3855E-08	4.39423E-05	0.0398
2.6828E-08	5.34142E-05	0.0365
3.0173E-08	5.99257E-05	0.0345
3.3934E-08	6.65505E-05	0.0331
3.8164E-08	7.98788E-05	0.0303
4.2922E-08	9.39158E-05	0.0283
4.8273E-08	1.04474E-04	0.0271
5.4290E-08	1.15485E-04	0.0264
6.1058E-08	1.13594E-04	0.0265
6.8670E-08	1.25317E-04	0.0260
7.7230E-08	1.25449E-04	0.0264
8.6858E-08	1.17885E-04	0.0271
9.7685E-08	1.10178E-04	0.0290
1.0986E-07	9.87012E-05	0.0316
1.2356E-07	8.90638E-05	0.0333
1.3896E-07	7.23487E-05	0.0394
1.5628E-07	6.07530E-05	0.0428
1.7577E-07	5.31373E-05	0.0471
1.9768E-07	4.20492E-05	0.0548
2.2232E-07	4.14627E-05	0.0586
2.5003E-07	3.67863E-05	0.0610
2.8120E-07	3.69451E-05	0.0626
3.1626E-07	3.34436E-05	0.0658
3.5568E-07	3.47510E-05	0.0661
4.0002E-07	3.54899E-05	0.0652
4.4989E-07	3.88366E-05	0.0640
5.0597E-07	3.72933E-05	0.0654
5.6905E-07	3.45464E-05	0.0670
6.3998E-07	3.59982E-05	0.0656
7.1976E-07	3.36813E-05	0.0678
8.0949E-07	3.67002E-05	0.0651
9.1040E-07	3.42933E-05	0.0680
1.0239E-06	3.10778E-05	0.0703
1.1515E-06	3.65033E-05	0.0650
1.2951E-06	3.47572E-05	0.0676
1.4565E-06	3.63808E-05	0.0665
1.6381E-06	3.54357E-05	0.0676
1.8423E-06	3.77530E-05	0.0685
2.0720E-06	3.49773E-05	0.0669
2.3303E-06	3.82965E-05	0.0646

2.6207E-06	3.74266E-05	0.0663
2.9474E-06	3.49381E-05	0.0677
3.3149E-06	3.66102E-05	0.0682
3.7281E-06	3.05637E-05	0.0716
4.1928E-06	3.58477E-05	0.0662
4.7155E-06	3.30138E-05	0.0682
5.3034E-06	3.55739E-05	0.0671
5.9645E-06	3.41648E-05	0.0667
6.7080E-06	3.24229E-05	0.0685
7.5442E-06	3.30377E-05	0.0679
8.4847E-06	3.17577E-05	0.0681
9.5424E-06	3.08440E-05	0.0695
1.0732E-05	3.67288E-05	0.0642
1.2070E-05	3.80837E-05	0.0617
1.3574E-05	3.14738E-05	0.0675
1.5267E-05	3.64431E-05	0.0632
1.7170E-05	3.38748E-05	0.0652
1.9310E-05	3.60192E-05	0.0622
2.1717E-05	3.44807E-05	0.0641
2.4425E-05	3.32253E-05	0.0651
2.7469E-05	3.17753E-05	0.0650
3.0894E-05	3.36497E-05	0.0650
3.4745E-05	2.97376E-05	0.0677
3.9076E-05	3.34815E-05	0.0638
4.3948E-05	3.53279E-05	0.0624
4.9426E-05	3.87139E-05	0.0593
5.5587E-05	3.29088E-05	0.0633
6.2517E-05	3.60868E-05	0.0609
7.0310E-05	2.96673E-05	0.0651
7.9075E-05	3.66106E-05	0.0595
8.8933E-05	3.27370E-05	0.0621
1.0002E-04	3.34582E-05	0.0618
1.1249E-04	3.32747E-05	0.0611
1.2651E-04	3.38365E-05	0.0616
1.4228E-04	3.34397E-05	0.0613
1.6002E-04	3.21468E-05	0.0623
1.7997E-04	3.07129E-05	0.0641
2.0240E-04	3.24373E-05	0.0619
2.2763E-04	3.29722E-05	0.0614
2.5601E-04	3.06941E-05	0.0622
2.8792E-04	3.18580E-05	0.0609
3.2381E-04	3.07906E-05	0.0615
3.6418E-04	3.50117E-05	0.0582
4.0958E-04	2.98383E-05	0.0627
4.6064E-04	3.01516E-05	0.0611

5.1806E-04	3.27868E-05	0.0585
5.8264E-04	3.56605E-05	0.0565
6.5527E-04	3.25494E-05	0.0596
7.3696E-04	3.37456E-05	0.0578
8.2883E-04	3.06385E-05	0.0601
9.3215E-04	2.99307E-05	0.0598
1.0484E-03	3.28461E-05	0.0576
1.1790E-03	3.15777E-05	0.0588
1.3260E-03	3.40133E-05	0.0560
1.4913E-03	3.55013E-05	0.0551
1.6772E-03	3.47971E-05	0.0554
1.8863E-03	3.24557E-05	0.0579
2.1215E-03	3.31784E-05	0.0577
2.3859E-03	3.41149E-05	0.0561
2.6834E-03	3.15545E-05	0.0587
3.0179E-03	3.30371E-05	0.0569
3.3941E-03	3.65380E-05	0.0549
3.8172E-03	3.73155E-05	0.0536
4.2930E-03	3.62486E-05	0.0542
4.8282E-03	3.94135E-05	0.0528
5.4301E-03	3.76342E-05	0.0551
6.1070E-03	4.10514E-05	0.0537
6.8683E-03	4.02894E-05	0.0558
7.7245E-03	5.11529E-05	0.0506
8.6874E-03	4.47351E-05	0.0554
9.7704E-03	4.85918E-05	0.0535
1.0988E-02	5.14764E-05	0.0534
1.2358E-02	6.70355E-05	0.0500
1.3899E-02	6.32384E-05	0.0531
1.5631E-02	7.43996E-05	0.0508
1.7580E-02	8.71512E-05	0.0482
1.9772E-02	9.90192E-05	0.0473
2.2236E-02	1.12083E-04	0.0461
2.5008E-02	1.32101E-04	0.0449
2.8126E-02	1.65123E-04	0.0423
3.1632E-02	7.23151E-05	0.0676
3.5575E-02	1.38766E-04	0.0534
4.0010E-02	1.89437E-04	0.0487
4.4998E-02	2.45069E-04	0.0457
5.0607E-02	2.83559E-04	0.0442
5.6916E-02	3.50241E-04	0.0418
6.4011E-02	4.18622E-04	0.0416
7.1990E-02	5.40386E-04	0.0386
8.0965E-02	6.78309E-04	0.0370
9.1058E-02	5.92450E-04	0.0418

1.0241E-01	7.21626E-04	0.0404
1.1518E-01	1.05946E-03	0.0357
1.2953E-01	1.35317E-03	0.0338
1.4568E-01	1.54421E-03	0.0332
1.6384E-01	1.53841E-03	0.0353
1.8427E-01	2.23499E-03	0.0305
2.0724E-01	1.96782E-03	0.0343
2.3307E-01	2.64334E-03	0.0313
2.6212E-01	3.56081E-03	0.0281
2.9480E-01	4.02343E-03	0.0274
3.3155E-01	4.95577E-03	0.0260
3.7288E-01	5.76476E-03	0.0252
4.1937E-01	5.65939E-03	0.0267
4.7164E-01	6.25116E-03	0.0258
5.3044E-01	8.32101E-03	0.0232
5.9656E-01	9.68764E-03	0.0221
6.7093E-01	1.25144E-02	0.0199
7.5457E-01	1.37649E-02	0.0195
8.4863E-01	1.36728E-02	0.0200
9.5442E-01	1.27851E-02	0.0208
1.0734E+00	1.25292E-02	0.0215
1.2072E+00	1.46886E-02	0.0200
1.3577E+00	1.42494E-02	0.0203
1.5270E+00	1.49132E-02	0.0198
1.7173E+00	1.38771E-02	0.0205
1.9314E+00	1.37818E-02	0.0206
2.1722E+00	1.25151E-02	0.0214
2.4429E+00	1.36884E-02	0.0205
2.7475E+00	1.24418E-02	0.0214
3.0900E+00	1.03606E-02	0.0235
3.4752E+00	8.43072E-03	0.0259
3.9084E+00	7.12097E-03	0.0280
4.3956E+00	6.22024E-03	0.0299
4.9435E+00	5.15596E-03	0.0329
5.5598E+00	3.63089E-03	0.0389
6.2529E+00	2.61891E-03	0.0456
7.0324E+00	1.78799E-03	0.0559
7.9090E+00	1.30983E-03	0.0649
8.8950E+00	7.94036E-04	0.0833
1.0004E+01	4.50980E-04	0.1153
1.1251E+01	1.91989E-04	0.1799
1.2653E+01	6.74785E-05	0.3122
1.4231E+01	3.41833E-05	0.4592
1.6005E+01	2.12071E-05	0.5311
1.8000E+01	7.85447E-06	1.0000

total 2.94268E-01 0.0043

****
ICRP Flux: 47 Energy Bin
****

1tally 4 nps = 15000000
tally type 4 track length estimate of particle flux. units 1/cm**2
particle(s): neutrons

volumes
cell: 6900
1.48267E+04

cell 6900
energy

1.0000E-09	4.21271E-02	0.5010
1.0000E-08	9.91495E+00	0.0421
2.5300E-08	5.61599E+01	0.0184
1.0000E-07	2.72418E+02	0.0088
2.0000E-07	8.41674E+01	0.0173
5.0000E-07	5.88328E+01	0.0238
1.0000E-06	4.23135E+01	0.0288
2.0000E-06	4.48165E+01	0.0293
5.0000E-06	6.12021E+01	0.0255
1.0000E-05	4.64625E+01	0.0294
2.0000E-05	5.23512E+01	0.0282
5.0000E-05	7.16738E+01	0.0245
1.0000E-04	5.72419E+01	0.0271
2.0000E-04	5.84946E+01	0.0267
5.0000E-04	7.93699E+01	0.0230
1.0000E-03	6.64482E+01	0.0252
2.0000E-03	7.10786E+01	0.0242
5.0000E-03	9.74625E+01	0.0208
1.0000E-02	7.80738E+01	0.0231
2.0000E-02	9.04863E+01	0.0210
3.0000E-02	5.93261E+01	0.0257
5.0000E-02	7.24533E+01	0.0240
7.0000E-02	6.41572E+01	0.0249
1.0000E-01	7.60460E+01	0.0228
1.5000E-01	1.11584E+02	0.0189
2.0000E-01	8.77504E+01	0.0212
3.0000E-01	1.58105E+02	0.0158
5.0000E-01	2.58690E+02	0.0125
7.0000E-01	2.46746E+02	0.0126
9.0000E-01	2.10828E+02	0.0137

1.0000E+00	7.63792E+01	0.0225
1.2000E+00	1.42627E+02	0.0165
2.0000E+00	4.00911E+02	0.0099
3.0000E+00	2.86728E+02	0.0116
4.0000E+00	1.31586E+02	0.0171
5.0000E+00	7.20733E+01	0.0231
6.0000E+00	3.40754E+01	0.0333
7.0000E+00	1.77860E+01	0.0466
8.0000E+00	1.01631E+01	0.0611
9.0000E+00	4.77678E+00	0.0877
1.0000E+01	2.61267E+00	0.1217
1.2000E+01	1.41107E+00	0.1655
1.4000E+01	3.17862E-01	0.3747
1.5000E+01	1.05885E-01	0.5255
1.6000E+01	3.87675E-02	1.0000
1.8000E+01	3.88674E-02	1.0000
2.0000E+01	0.00000E+00	0.0000

THIS PAGE INTENTIONALLY LEFT BLANK

APPENDIX H. UMG V3.3 MAXED OUTPUT FILES FOR NPS IRRADIATION EXPERIMENT

The results from the MAXED unfolding algorithm provides two primary output files: a text file containing information of the unfolding process and a ".flu" file containing a table of the solution spectrum. The text file includes information on initial and final chi-squared values, count rates, and scaling factors used during the deconvolution.

A. FREE FIELD MAXED OUTPUT FILES

UMG package, version 3.3, release date: March 1, 2004

Deconvolution Using the MAXED (Maximum Entropy) Algorithm
==========

File with Input Data : LLNL_FF.ibu

File with Default Spectrum : c:\U_M_G\FC\$inp\def_spec\LLNL_DSFF.flu
Default Spectrum Fluence Format : fluence rate per bin
Energy of Default Sp. in Units of : MeV

File with Response Function : c:\U_M_G\FC\$inp\response\AFIT_RF.fmt
Response Functions in Units of : cm^
Energy of Final Spect. in Units of : MeV

Chi-squared P.D.F. Using the Default Spectrum = 290.617
Final Chi-squared P.D.F. = 0.990
NOTE: Chi-squared Per Degree of Freedom was set to: 1.000

*** RESULTS FOR THE FINAL SPECTRUM: ***

DN	M	C	(C-M)/S	(C-M)/M
1	4.080400E+01	4.306687E+01	0.86911	0.05546
2	8.206000E+01	8.585729E+01	1.11187	0.04627
3	1.480000E+02	1.476424E+02	-0.07448	-0.00242
4	2.448900E+02	2.377207E+02	-1.25262	-0.02928
5	2.060400E+02	1.975628E+02	-1.55905	-0.04114
6	1.390300E+02	1.387885E+02	-0.05043	-0.00174
7	8.700300E+01	9.082705E+01	0.96532	0.04395

Note 1: DN = detector number
M = measured count rate
C = calculated count rate
S = estimated standard uncertainty
Note 2: M<0 indicates data not used for the deconvolution

*** RESULTS FOR THE DEFAULT SPECTRUM: ***

DN	M	C	(C-M)/S	(C-M)/M
1	4.080400E+01	7.517509E+01	13.20101	0.84235
2	8.206000E+01	1.453156E+02	18.52160	0.77085
3	1.480000E+02	2.350236E+02	18.12522	0.58800
4	2.448900E+02	3.637691E+02	20.77062	0.48544
5	2.060400E+02	3.032747E+02	17.88261	0.47192
6	1.390300E+02	2.146665E+02	15.79556	0.54403
7	8.700300E+01	1.412862E+02	13.70296	0.62392

Note 1: DN = detector number
M = measured count rate
C = calculated count rate
S = estimated standard uncertainty
Note 2: M<0 indicates data not used for the deconvolution

Scaling Factor/Default Spectrum for best fit = 6.3995E-01
Scaling Factor/Default Spectrum used = 1.0000E+00

Bin Structure Used : Default Spectrum Bin Structure

Lowest and highest energy bin edges
of the solution spectrum (MeV) : 1.0000E-10 1.2500E+01

Parameter EUPPER (MeV) was set to 1.2500E+02
Highest energy of default spectrum (MeV) = 1.2500E+01
Highest energy of response functions (MeV) = 2.5120E+01

Choice of solution spectrum representation : ~ dF/dE

Temperature parameter set to: 1.0000E+00
Temperature reduction factor parameter set to: 8.5000E-01

*** MAXED PARAMETER LAMBDA ***

DN	LAMBDA
1	7.857371E-01
2	7.604548E-01
3	-3.178617E-02
4	-5.131439E-01
5	-6.703540E-01
6	-2.844508E-02
7	5.601600E-01
--	1.527839E-03

Note: DN = detector number

INPUT DATA WITH STANDARD DEVIATIONS:

1	0Bare	4.080400E+01	+- 2.603672E+00	+-	6.381%
2	2in	8.206000E+01	+- 3.415237E+00	+-	4.162%
3	3in	1.480000E+02	+- 4.801246E+00	+-	3.244%
4	5in	2.448900E+02	+- 5.723423E+00	+-	2.337%
5	8in	2.060400E+02	+- 5.437389E+00	+-	2.639%
6	10in	1.390300E+02	+- 4.788469E+00	+-	3.444%
7	12in	8.700300E+01	+- 3.961421E+00	+-	4.553%

Note: count rates < 0 indicate data not used for the deconvolution

Calculated / measured ratios

d	C_M	sC_MpR	sC_M	nC_M	nsC_MpR	nsC_M
0.0	1.05546	0.09278	0.01473	-	-	-
2.0	1.04627	0.06024	0.01035	-	-	-
3.0	0.99758	0.04582	0.00753	-	-	-
5.0	0.97072	0.03257	0.00578	-	-	-
8.0	0.95886	0.03656	0.00627	-	-	-
10.0	0.99826	0.04867	0.00777	-	-	-
12.0	1.04395	0.06582	0.01004	-	-	-

d : sphere identifier
C_M : (calculated / measured) readings
sC_MpR : stand. dev. of C_M from total uncertainty
sC_M : stand. dev. of C_M from stat. uncertainty only
nC_M +
nsC_MpR | same as above, measurements not used for the unfolding
nsC_M +

Fluence spectrum from program MXD_FC33

1	1			
1	202	202	12.5000000000000	0
1.000000000000000E-010			461111111.111111	0.000000000000000E+000
1.000000000000000E-009			542232880.875584	0.000000000000000E+000
1.120000000000000E-009			1008553158.42859	0.000000000000000E+000
1.260000000000000E-009			343992539.627471	0.000000000000000E+000
1.410000000000000E-009			769970690.843330	0.000000000000000E+000
1.590000000000000E-009			613008541.116187	0.000000000000000E+000
1.780000000000000E-009			928697043.245092	0.000000000000000E+000
2.000000000000000E-009			1228482814.91173	0.000000000000000E+000
2.250000000000000E-009			1578500164.32670	0.000000000000000E+000
2.520000000000000E-009			2140945310.29586	0.000000000000000E+000
2.830000000000000E-009			2082174262.56224	0.000000000000000E+000
3.180000000000000E-009			2852979157.83769	0.000000000000000E+000
3.570000000000000E-009			2647082336.63808	0.000000000000000E+000
4.010000000000000E-009			2562880310.42419	0.000000000000000E+000
4.500000000000000E-009			2685531577.28199	0.000000000000000E+000
5.050000000000000E-009			2886078236.91843	0.000000000000000E+000
5.670000000000000E-009			3809775371.71715	0.000000000000000E+000
6.360000000000000E-009			3378527950.07095	0.000000000000000E+000
7.140000000000000E-009			3719224623.82389	0.000000000000000E+000
8.020000000000000E-009			4368847783.05471	0.000000000000000E+000
9.000000000000000E-009			4525263878.21573	0.000000000000000E+000
1.010000000000000E-008			6441671859.65750	0.000000000000000E+000
1.130000000000000E-008			5833126822.22443	0.000000000000000E+000
1.270000000000000E-008			5493603219.02242	0.000000000000000E+000
1.430000000000000E-008			5991447482.36962	0.000000000000000E+000
1.610000000000000E-008			6791643845.24161	0.000000000000000E+000
1.800000000000000E-008			6857263592.53863	0.000000000000000E+000
2.020000000000000E-008			7331038168.02311	0.000000000000000E+000
2.270000000000000E-008			7900761261.02031	0.000000000000000E+000
2.550000000000000E-008			6691447477.85734	0.000000000000000E+000
2.860000000000000E-008			6861628355.36261	0.000000000000000E+000
3.210000000000000E-008			6661288841.33743	0.000000000000000E+000
3.610000000000000E-008			6507239896.84079	0.000000000000000E+000
4.050000000000000E-008			6100338202.06691	0.000000000000000E+000
4.550000000000000E-008			6342566887.20645	0.000000000000000E+000
5.100000000000000E-008			5342387040.67162	0.000000000000000E+000
5.730000000000000E-008			4622590827.62290	0.000000000000000E+000
6.430000000000000E-008			3683002229.89198	0.000000000000000E+000
7.220000000000000E-008			3312687975.69235	0.000000000000000E+000
8.110000000000000E-008			2737815729.90588	0.000000000000000E+000
9.099999999999999E-008			2135147146.55178	0.000000000000000E+000
1.020000000000000E-007			1413018621.47987	0.000000000000000E+000

1.150000000000000E-007	1079893244.22488	0.000000000000000E+000
1.290000000000000E-007	796559479.208542	0.000000000000000E+000
1.450000000000000E-007	570624175.627362	0.000000000000000E+000
1.620000000000000E-007	420531806.027505	0.000000000000000E+000
1.820000000000000E-007	309593967.627611	0.000000000000000E+000
2.050000000000000E-007	241483294.749537	0.000000000000000E+000
2.300000000000000E-007	200689107.835155	0.000000000000000E+000
2.580000000000000E-007	136720278.811475	0.000000000000000E+000
2.890000000000000E-007	118969180.825860	0.000000000000000E+000
3.250000000000000E-007	122668916.044606	0.000000000000000E+000
3.650000000000000E-007	92049512.2690465	0.000000000000000E+000
4.090000000000000E-007	87570378.3243186	0.000000000000000E+000
4.600000000000000E-007	72589865.9886273	0.000000000000000E+000
5.160000000000000E-007	61930777.5331312	0.000000000000000E+000
5.790000000000000E-007	53976345.4291582	0.000000000000000E+000
6.500000000000000E-007	56630705.4393615	0.000000000000000E+000
7.300000000000000E-007	43449210.7306601	0.000000000000000E+000
8.190000000000000E-007	41130259.6882535	0.000000000000000E+000
9.200000000000000E-007	35985297.3160197	0.000000000000000E+000
1.030000000000000E-006	34981301.9858633	0.000000000000000E+000
1.160000000000000E-006	26871653.1622142	0.000000000000000E+000
1.300000000000000E-006	26551979.7314848	0.000000000000000E+000
1.460000000000000E-006	24106451.4794864	0.000000000000000E+000
1.640000000000000E-006	21241583.7851878	0.000000000000000E+000
1.840000000000000E-006	16101085.6583376	0.000000000000000E+000
2.070000000000000E-006	17121518.1000609	0.000000000000000E+000
2.320000000000000E-006	13691170.4640161	0.000000000000000E+000
2.610000000000000E-006	13152630.0897531	0.000000000000000E+000
2.920000000000000E-006	10435243.4667974	0.000000000000000E+000
3.280000000000000E-006	9618830.39329261	0.000000000000000E+000
3.690000000000000E-006	9998833.56932391	0.000000000000000E+000
4.140000000000000E-006	7910911.70690187	0.000000000000000E+000
4.650000000000000E-006	6937557.98346641	0.000000000000000E+000
5.220000000000000E-006	5564332.22045851	0.000000000000000E+000
5.850000000000000E-006	4905900.37806050	0.000000000000000E+000
6.570000000000000E-006	5073306.29111249	0.000000000000000E+000
7.380000000000000E-006	4132534.53934052	0.000000000000000E+000
8.280000000000000E-006	4631288.70788162	0.000000000000000E+000
9.300000000000001E-006	4264782.87860676	0.000000000000000E+000
1.040000000000000E-005	3440045.63498675	0.000000000000000E+000
1.170000000000000E-005	3259263.83153250	0.000000000000000E+000
1.320000000000000E-005	2835976.36985509	0.000000000000000E+000
1.480000000000000E-005	2481169.17747602	0.000000000000000E+000
1.660000000000000E-005	2337261.36518241	0.000000000000000E+000
1.860000000000000E-005	1975442.17295395	0.000000000000000E+000

2.090000000000000E-005	2081891.79906988	0.000000000000000E+000
2.350000000000000E-005	1614177.77631797	0.000000000000000E+000
2.630000000000000E-005	1542836.10672145	0.000000000000000E+000
2.960000000000000E-005	1346447.80697699	0.000000000000000E+000
3.320000000000000E-005	1080579.43495151	0.000000000000000E+000
3.730000000000000E-005	989821.090534433	0.000000000000000E+000
4.180000000000000E-005	1043236.20954492	0.000000000000000E+000
4.700000000000000E-005	857701.008298025	0.000000000000000E+000
5.270000000000000E-005	690757.499009323	0.000000000000000E+000
5.920000000000000E-005	723674.343430505	0.000000000000000E+000
6.640000000000000E-005	581682.881314622	0.000000000000000E+000
7.460000000000000E-005	510411.945080781	0.000000000000000E+000
8.370000000000000E-005	516854.037591510	0.000000000000000E+000
9.399999999999999E-005	438016.738626103	0.000000000000000E+000
1.060000000000000E-004	437313.653374632	0.000000000000000E+000
1.180000000000000E-004	401016.620144537	0.000000000000000E+000
1.330000000000000E-004	357093.930083723	0.000000000000000E+000
1.490000000000000E-004	292424.735059194	0.000000000000000E+000
1.680000000000000E-004	296170.671747969	0.000000000000000E+000
1.880000000000000E-004	239857.032057434	0.000000000000000E+000
2.110000000000000E-004	217731.740112870	0.000000000000000E+000
2.370000000000000E-004	204934.225840043	0.000000000000000E+000
2.660000000000000E-004	177509.587483430	0.000000000000000E+000
2.990000000000000E-004	141762.509302276	0.000000000000000E+000
3.350000000000000E-004	139315.635289347	0.000000000000000E+000
3.770000000000000E-004	135186.959804071	0.000000000000000E+000
4.230000000000000E-004	113281.055979929	0.000000000000000E+000
4.750000000000000E-004	109366.112796535	0.000000000000000E+000
5.330000000000001E-004	89615.6594300015	0.000000000000000E+000
5.980000000000000E-004	74727.4479313814	0.000000000000000E+000
6.720000000000000E-004	79276.4324074865	0.000000000000000E+000
7.540000000000000E-004	61461.5819362390	0.000000000000000E+000
8.460000000000000E-004	57775.8615131484	0.000000000000000E+000
9.500000000000000E-004	52679.6180243106	0.000000000000000E+000
1.070000000000000E-003	47459.8309765692	0.000000000000000E+000
1.200000000000000E-003	50029.2877347973	0.000000000000000E+000
1.340000000000000E-003	37901.2433607668	0.000000000000000E+000
1.510000000000000E-003	37976.8533856070	0.000000000000000E+000
1.690000000000000E-003	32852.0648188460	0.000000000000000E+000
1.900000000000000E-003	28278.1492902058	0.000000000000000E+000
2.140000000000000E-003	29392.7362298071	0.000000000000000E+000
2.400000000000000E-003	23185.0200934517	0.000000000000000E+000
2.690000000000000E-003	15913.0982857732	0.000000000000000E+000
3.020000000000000E-003	17565.6763850932	0.000000000000000E+000
3.390000000000000E-003	16025.3974726078	0.000000000000000E+000

3.810000000000000E-003	16613.2856951083	0.000000000000000E+000
4.270000000000000E-003	14154.5079091784	0.000000000000000E+000
4.800000000000000E-003	12002.0720478111	0.000000000000000E+000
5.390000000000000E-003	10346.7007545682	0.000000000000000E+000
6.050000000000000E-003	9569.21960568724	0.000000000000000E+000
6.790000000000000E-003	8616.06460500147	0.000000000000000E+000
7.620000000000000E-003	8066.54751813388	0.000000000000000E+000
8.550000000000000E-003	7077.88388373511	0.000000000000000E+000
9.599999999999999E-003	6323.50298279185	0.000000000000000E+000
1.080000000000000E-002	6583.80946962579	0.000000000000000E+000
1.210000000000000E-002	5801.06767712583	0.000000000000000E+000
1.360000000000000E-002	5202.50042403763	0.000000000000000E+000
1.530000000000000E-002	4873.84784348687	0.000000000000000E+000
1.710000000000000E-002	4007.76338349443	0.000000000000000E+000
1.920000000000000E-002	3982.29031114171	0.000000000000000E+000
2.160000000000000E-002	3813.12298449161	0.000000000000000E+000
2.420000000000000E-002	3238.71281291923	0.000000000000000E+000
2.720000000000000E-002	3240.72214852812	0.000000000000000E+000
3.050000000000000E-002	2947.42065962329	0.000000000000000E+000
3.430000000000000E-002	1892.50666009606	0.000000000000000E+000
3.850000000000000E-002	2365.86291314424	0.000000000000000E+000
4.320000000000000E-002	2260.85364760963	0.000000000000000E+000
4.850000000000000E-002	2361.26934463946	0.000000000000000E+000
5.440000000000000E-002	1809.98389483152	0.000000000000000E+000
6.110000000000000E-002	2067.81874681504	0.000000000000000E+000
6.859999999999999E-002	1978.52485242682	0.000000000000000E+000
7.700000000000000E-002	1856.38470640020	0.000000000000000E+000
8.649999999999999E-002	1348.79415250717	0.000000000000000E+000
9.710000000000001E-002	1575.36911141198	0.000000000000000E+000
0.109000000000000	1696.73332175058	0.000000000000000E+000
0.122000000000000	1798.35188571990	0.000000000000000E+000
0.137000000000000	1488.93666614564	0.000000000000000E+000
0.154000000000000	1376.35474202728	0.000000000000000E+000
0.173000000000000	1282.48212000039	0.000000000000000E+000
0.194000000000000	1143.00793718868	0.000000000000000E+000
0.218000000000000	1164.17475084032	0.000000000000000E+000
0.245000000000000	1220.85043439818	0.000000000000000E+000
0.275000000000000	1130.33117588390	0.000000000000000E+000
0.309000000000000	1164.46813031550	0.000000000000000E+000
0.346000000000000	921.628679700852	0.000000000000000E+000
0.389000000000000	798.996645278570	0.000000000000000E+000
0.437000000000000	811.319468930170	0.000000000000000E+000
0.490000000000000	868.443421984090	0.000000000000000E+000
0.550000000000000	873.008170588476	0.000000000000000E+000
0.618000000000000	824.736746067278	0.000000000000000E+000

0.694000000000000	842.843959908878	0.000000000000000E+000
0.779000000000000	754.123543076365	0.000000000000000E+000
0.874000000000000	592.151539697621	0.000000000000000E+000
0.981000000000000	514.530739449473	0.000000000000000E+000
1.10000000000000	474.273983938163	0.000000000000000E+000
1.24000000000000	451.007713027989	0.000000000000000E+000
1.39000000000000	412.686796234761	0.000000000000000E+000
1.56000000000000	356.115321447607	0.000000000000000E+000
1.75000000000000	309.628687056431	0.000000000000000E+000
1.96000000000000	257.634435833747	0.000000000000000E+000
2.21000000000000	249.909946575945	0.000000000000000E+000
2.48000000000000	223.336075513486	0.000000000000000E+000
2.78000000000000	164.930966059125	0.000000000000000E+000
3.12000000000000	125.534500482249	0.000000000000000E+000
3.50000000000000	94.8574339678150	0.000000000000000E+000
3.93000000000000	76.9099408162270	0.000000000000000E+000
4.41000000000000	52.4983452043610	0.000000000000000E+000
4.96000000000000	38.0793616304568	0.000000000000000E+000
5.56000000000000	23.3735212053955	0.000000000000000E+000
6.24000000000000	16.0082137962093	0.000000000000000E+000
7.01000000000000	9.43070279555622	0.000000000000000E+000
7.87000000000000	5.57169465956236	0.000000000000000E+000
8.84000000000000	2.51207216058622	0.000000000000000E+000
9.92000000000000	1.29456562472917	0.000000000000000E+000
11.1000000000000	0.344169357242350	0.000000000000000E+000
12.5000000000000	0.000000000000000E+000	0.000000000000000E+000

B. SURROGATE VEHICLE MAXED OUTPUT FILES

UMG package, version 3.3, release date: March 1, 2004

Deconvolution Using the MAXED (Maximum Entropy) Algorithm
==========

File with Input Data : LLNL_SV.ibu

File with Default Spectrum : c:\U_M_G\FC\$inp\def_spec\LLNL_DSSV.flu
Default Spectrum Fluence Format : fluence rate per bin
Energy of Default Sp. in Units of : MeV

File with Response Function : c:\U_M_G\FC\$inp\response\AFIT_RF.fmt
Response Functions in Units of : cm^
Energy of Final Spect. in Units of : MeV

Chi-squared P.D.F. Using the Default Spectrum = 334.600
Final Chi-squared P.D.F. = 0.998

NOTE: Chi-squared Per Degree of Freedom was set to: 1.000

*** RESULTS FOR THE FINAL SPECTRUM: ***

DN	M	C	(C-M)/S	(C-M)/M
1	9.778000E+00	1.170965E+01	1.50467	0.19755
2	5.372500E+01	5.577427E+01	0.72529	0.03814
3	1.334900E+02	1.300553E+02	-0.72753	-0.02573
4	2.338100E+02	2.269744E+02	-1.25438	-0.02924
5	1.843700E+02	1.786452E+02	-1.17861	-0.03105
6	1.165100E+02	1.200362E+02	0.83173	0.03027
7	7.487100E+01	7.528601E+01	0.11406	0.00554

Note 1: DN = detector number
M = measured count rate
C = calculated count rate
S = estimated standard uncertainty
Note 2: M<0 indicates data not used for the deconvolution

*** RESULTS FOR THE DEFAULT SPECTRUM: ***

DN	M	C	(C-M)/S	(C-M)/M
1	9.778000E+00	3.860148E+01	22.45224	2.94779
2	5.372500E+01	1.124623E+02	20.78877	1.09330
3	1.334900E+02	2.133821E+02	16.92232	0.59849
4	2.338100E+02	3.407696E+02	19.62780	0.45746
5	1.843700E+02	2.710275E+02	17.84088	0.47002
6	1.165100E+02	1.859977E+02	16.39027	0.59641
7	7.487100E+01	1.190436E+02	12.13968	0.58998

Note 1: DN = detector number
M = measured count rate
C = calculated count rate
S = estimated standard uncertainty
Note 2: M<0 indicates data not used for the deconvolution

Scaling Factor/Default Spectrum for best fit = 6.1468E-01
Scaling Factor/Default Spectrum used = 1.0000E+00

Bin Structure Used : Default Spectrum Bin Structure

Lowest and highest energy bin edges

of the solution spectrum (MeV) : 1.0000E-10 1.1100E+01

Parameter EUPPER (MeV) was set to 1.2500E+01
Highest energy of default spectrum (MeV) = 1.2500E+01
Highest energy of response functions (MeV) = 2.5120E+01

Choice of solution spectrum representation : ~ dF/dE

Temperature parameter set to: 1.0000E+00
Temperature reduction factor parameter set to: 8.5000E-01

*** MAXED PARAMETER LAMBDA ***

DN	LAMBDA
1	7.738399E+00
2	1.678196E+00
3	-1.023108E+00
4	-1.518605E+00
5	-1.601450E+00
6	1.290969E+00
7	2.133871E-01
--	2.048614E-03

Note: DN = detector number

INPUT DATA WITH STANDARD DEVIATIONS:

1	0Bare	9.778000E+00	+- 1.283768E+00	+-	13.129%
2	2in	5.372500E+01	+- 2.825434E+00	+-	5.259%
3	3in	1.334900E+02	+- 4.721106E+00	+-	3.537%
4	5in	2.338100E+02	+- 5.449393E+00	+-	2.331%
5	8in	1.843700E+02	+- 4.857240E+00	+-	2.635%
6	10in	1.165100E+02	+- 4.239571E+00	+-	3.639%
7	12in	7.487100E+01	+- 3.638694E+00	+-	4.860%

Note: count rates < 0 indicate data not used for the deconvolution

Calculated / measured ratios

d	C_M	sC_MpR	sC_M	nC_M	nsC_MpR	nsC_M
0.0	1.19755	0.20484	0.02867	-	-	-
2.0	1.03814	0.07581	0.01133	-	-	-
3.0	0.97427	0.04938	0.00709	-	-	-
5.0	0.97076	0.03248	0.00526	-	-	-

8.0	0.96895	0.03668	0.00592	-	-	-
10.0	1.03027	0.05225	0.00761	-	-	-
12.0	1.00554	0.06892	0.01079	-	-	-

d : sphere identifier
C_M : (calculated / measured) readings
sC_MpR : stand. dev. of C_M from total uncertainty
sC_M : stand. dev. of C_M from stat. uncertainty only
nC_M +
nsC_MpR | same as above, measurements not used for the unfolding
nsC_M +

Fluence spectrum from program MXD_FC33

1	1			
1	201	201	11.1000000000000	0
1.000000000000000E-010	46777777.7777778	0.000000000000000E+000		
1.000000000000000E-009	34100076.0587509	0.000000000000000E+000		
1.120000000000000E-009	44051730.9085497	0.000000000000000E+000		
1.260000000000000E-009	34879506.3686652	0.000000000000000E+000		
1.410000000000000E-009	91095917.4712346	0.000000000000000E+000		
1.590000000000000E-009	53842225.3559225	0.000000000000000E+000		
1.780000000000000E-009	59387275.3179026	0.000000000000000E+000		
2.000000000000000E-009	108847442.779533	0.000000000000000E+000		
2.250000000000000E-009	182949614.410441	0.000000000000000E+000		
2.520000000000000E-009	189514708.418680	0.000000000000000E+000		
2.830000000000000E-009	213786599.290781	0.000000000000000E+000		
3.180000000000000E-009	118413450.929289	0.000000000000000E+000		
3.570000000000000E-009	122893131.250693	0.000000000000000E+000		
4.010000000000000E-009	311374455.440257	0.000000000000000E+000		
4.500000000000000E-009	382629424.867024	0.000000000000000E+000		
5.050000000000000E-009	201771878.614913	0.000000000000000E+000		
5.670000000000000E-009	382937500.088333	0.000000000000000E+000		
6.360000000000000E-009	434682288.221441	0.000000000000000E+000		
7.140000000000000E-009	425143805.407804	0.000000000000000E+000		
8.020000000000000E-009	527904967.556757	0.000000000000000E+000		
9.000000000000000E-009	574376697.591079	0.000000000000000E+000		
1.010000000000000E-008	653609874.409174	0.000000000000000E+000		
1.130000000000000E-008	752318304.421989	0.000000000000000E+000		
1.270000000000000E-008	782581108.555984	0.000000000000000E+000		
1.430000000000000E-008	891710614.372518	0.000000000000000E+000		
1.610000000000000E-008	1117525454.44095	0.000000000000000E+000		
1.800000000000000E-008	1117927538.43751	0.000000000000000E+000		
2.020000000000000E-008	1198907255.34483	0.000000000000000E+000		
2.270000000000000E-008	1270926871.23318	0.000000000000000E+000		
2.550000000000000E-008	1239452376.31855	0.000000000000000E+000		

2.860000000000000E-008	1226508341.64961	0.000000000000000E+000
3.210000000000000E-008	1218937302.50363	0.000000000000000E+000
3.610000000000000E-008	1222550753.00512	0.000000000000000E+000
4.050000000000000E-008	1282534031.32990	0.000000000000000E+000
4.550000000000000E-008	1223755236.50562	0.000000000000000E+000
5.100000000000000E-008	1135655871.89779	0.000000000000000E+000
5.730000000000000E-008	1022881963.35733	0.000000000000000E+000
6.430000000000000E-008	884324949.267920	0.000000000000000E+000
7.220000000000000E-008	796421903.379892	0.000000000000000E+000
8.110000000000000E-008	628409928.558890	0.000000000000000E+000
9.099999999999999E-008	528469492.929159	0.000000000000000E+000
1.020000000000000E-007	382402841.033282	0.000000000000000E+000
1.150000000000000E-007	327773863.742813	0.000000000000000E+000
1.290000000000000E-007	219881633.594137	0.000000000000000E+000
1.450000000000000E-007	182953516.102197	0.000000000000000E+000
1.620000000000000E-007	128742289.814538	0.000000000000000E+000
1.820000000000000E-007	91333316.2351953	0.000000000000000E+000
2.050000000000000E-007	83108884.1178999	0.000000000000000E+000
2.300000000000000E-007	70319789.4230485	0.000000000000000E+000
2.580000000000000E-007	68113443.5177328	0.000000000000000E+000
2.890000000000000E-007	55957481.1629161	0.000000000000000E+000
3.250000000000000E-007	54405375.8459885	0.000000000000000E+000
3.650000000000000E-007	49192084.3030068	0.000000000000000E+000
4.090000000000000E-007	45035080.5889953	0.000000000000000E+000
4.600000000000000E-007	38598408.5393837	0.000000000000000E+000
5.160000000000000E-007	32115743.0991335	0.000000000000000E+000
5.790000000000000E-007	29905353.1486895	0.000000000000000E+000
6.500000000000000E-007	24041294.4616733	0.000000000000000E+000
7.300000000000000E-007	25674447.0284440	0.000000000000000E+000
8.190000000000000E-007	20003475.0902832	0.000000000000000E+000
9.200000000000000E-007	18800707.1323149	0.000000000000000E+000
1.030000000000000E-006	25518983.1735862	0.000000000000000E+000
1.160000000000000E-006	22800253.7313639	0.000000000000000E+000
1.300000000000000E-006	20301648.6900034	0.000000000000000E+000
1.460000000000000E-006	17709501.5055866	0.000000000000000E+000
1.640000000000000E-006	17301005.5414143	0.000000000000000E+000
1.840000000000000E-006	13991247.9595785	0.000000000000000E+000
2.070000000000000E-006	14152222.5328769	0.000000000000000E+000
2.320000000000000E-006	11782581.3601011	0.000000000000000E+000
2.610000000000000E-006	10896843.0063263	0.000000000000000E+000
2.920000000000000E-006	9467494.69905173	0.000000000000000E+000
3.280000000000000E-006	7405674.32321516	0.000000000000000E+000
3.690000000000000E-006	7333704.01561062	0.000000000000000E+000
4.140000000000000E-006	6436991.76761444	0.000000000000000E+000
4.650000000000000E-006	6427171.79542892	0.000000000000000E+000

5.220000000000000E-006	5011799.22429859	0.000000000000000E+000
5.850000000000000E-006	4829864.04697817	0.000000000000000E+000
6.570000000000000E-006	3946124.41206950	0.000000000000000E+000
7.380000000000000E-006	3758162.87038500	0.000000000000000E+000
8.280000000000000E-006	3193053.22859926	0.000000000000000E+000
9.300000000000001E-006	3816844.78222472	0.000000000000000E+000
1.040000000000000E-005	3926971.50242165	0.000000000000000E+000
1.170000000000000E-005	3017149.56556845	0.000000000000000E+000
1.320000000000000E-005	3215759.45854907	0.000000000000000E+000
1.480000000000000E-005	2918999.79093864	0.000000000000000E+000
1.660000000000000E-005	2472227.11551331	0.000000000000000E+000
1.860000000000000E-005	2286928.54325200	0.000000000000000E+000
2.090000000000000E-005	1855383.72670596	0.000000000000000E+000
2.350000000000000E-005	1696224.76934457	0.000000000000000E+000
2.630000000000000E-005	1604349.03158179	0.000000000000000E+000
2.960000000000000E-005	1349559.40115995	0.000000000000000E+000
3.320000000000000E-005	1068859.43990276	0.000000000000000E+000
3.730000000000000E-005	1274672.39778980	0.000000000000000E+000
4.180000000000000E-005	1061164.77116001	0.000000000000000E+000
4.700000000000000E-005	990219.189019864	0.000000000000000E+000
5.270000000000000E-005	926588.781470276	0.000000000000000E+000
5.920000000000000E-005	730546.617983278	0.000000000000000E+000
6.640000000000000E-005	670135.695959978	0.000000000000000E+000
7.460000000000000E-005	614574.191791509	0.000000000000000E+000
8.370000000000000E-005	492852.701378434	0.000000000000000E+000
9.399999999999999E-005	508759.593923760	0.000000000000000E+000
1.060000000000000E-004	575317.410639805	0.000000000000000E+000
1.180000000000000E-004	432912.110976487	0.000000000000000E+000
1.330000000000000E-004	427215.898989955	0.000000000000000E+000
1.490000000000000E-004	335656.786322212	0.000000000000000E+000
1.680000000000000E-004	337329.673842468	0.000000000000000E+000
1.880000000000000E-004	306109.478928454	0.000000000000000E+000
2.110000000000000E-004	256592.441485659	0.000000000000000E+000
2.370000000000000E-004	238062.376816471	0.000000000000000E+000
2.660000000000000E-004	193878.342523441	0.000000000000000E+000
2.990000000000000E-004	203164.894186334	0.000000000000000E+000
3.350000000000000E-004	161284.173675827	0.000000000000000E+000
3.770000000000000E-004	154540.707808540	0.000000000000000E+000
4.230000000000000E-004	127507.514467771	0.000000000000000E+000
4.750000000000000E-004	136709.087676785	0.000000000000000E+000
5.330000000000001E-004	118831.745442129	0.000000000000000E+000
5.980000000000000E-004	104379.235861329	0.000000000000000E+000
6.720000000000000E-004	91695.1197832097	0.000000000000000E+000
7.540000000000000E-004	74298.4172156443	0.000000000000000E+000
8.460000000000000E-004	67040.0333799620	0.000000000000000E+000

9.500000000000000E-004	70726.6144392129	0.000000000000000E+000
1.070000000000000E-003	64624.0560144036	0.000000000000000E+000
1.200000000000000E-003	64873.5697441888	0.000000000000000E+000
1.340000000000000E-003	56096.5573670339	0.000000000000000E+000
1.510000000000000E-003	51298.1745940160	0.000000000000000E+000
1.690000000000000E-003	40005.3680089165	0.000000000000000E+000
1.900000000000000E-003	37527.5580534093	0.000000000000000E+000
2.140000000000000E-003	35514.1208727803	0.000000000000000E+000
2.400000000000000E-003	28447.4331694345	0.000000000000000E+000
2.690000000000000E-003	26375.3654768041	0.000000000000000E+000
3.020000000000000E-003	26183.2065273844	0.000000000000000E+000
3.390000000000000E-003	23246.3624916677	0.000000000000000E+000
3.810000000000000E-003	20731.3364182516	0.000000000000000E+000
4.270000000000000E-003	19278.4664805845	0.000000000000000E+000
4.800000000000000E-003	16548.2580449160	0.000000000000000E+000
5.390000000000000E-003	14678.4642653518	0.000000000000000E+000
6.050000000000000E-003	12682.4906617018	0.000000000000000E+000
6.790000000000000E-003	13313.4113009159	0.000000000000000E+000
7.620000000000000E-003	10579.7398686760	0.000000000000000E+000
8.550000000000000E-003	9370.62674082729	0.000000000000000E+000
9.599999999999999E-003	8342.62011014736	0.000000000000000E+000
1.080000000000000E-002	8544.68259533318	0.000000000000000E+000
1.210000000000000E-002	7353.60562749886	0.000000000000000E+000
1.360000000000000E-002	6534.16904349008	0.000000000000000E+000
1.530000000000000E-002	7034.25890423893	0.000000000000000E+000
1.710000000000000E-002	6066.35474300711	0.000000000000000E+000
1.920000000000000E-002	5696.45506355545	0.000000000000000E+000
2.160000000000000E-002	4810.11852394630	0.000000000000000E+000
2.420000000000000E-002	7326.08017179920	0.000000000000000E+000
2.720000000000000E-002	1235.42354254581	0.000000000000000E+000
3.050000000000000E-002	2759.98876526192	0.000000000000000E+000
3.430000000000000E-002	2703.66246393004	0.000000000000000E+000
3.850000000000000E-002	3367.85363243178	0.000000000000000E+000
4.320000000000000E-002	2616.94446563848	0.000000000000000E+000
4.850000000000000E-002	2982.17613391791	0.000000000000000E+000
5.440000000000000E-002	2531.46133298692	0.000000000000000E+000
6.110000000000000E-002	2365.61255723816	0.000000000000000E+000
6.859999999999999E-002	2598.82913311006	0.000000000000000E+000
7.700000000000000E-002	2163.72742884215	0.000000000000000E+000
8.649999999999999E-002	1578.41020204040	0.000000000000000E+000
9.710000000000001E-002	1840.60513612534	0.000000000000000E+000
0.109000000000000	1801.09444198338	0.000000000000000E+000
0.122000000000000	2166.21426763715	0.000000000000000E+000
0.137000000000000	1246.13537022380	0.000000000000000E+000
0.154000000000000	1414.88962649263	0.000000000000000E+000

0.173000000000000	1441.03283742711	0.000000000000000E+000
0.194000000000000	1170.60883628590	0.000000000000000E+000
0.218000000000000	1209.66496213688	0.000000000000000E+000
0.245000000000000	1351.57043283652	0.000000000000000E+000
0.275000000000000	1115.75562027000	0.000000000000000E+000
0.309000000000000	1161.99414147038	0.000000000000000E+000
0.346000000000000	1092.53364518052	0.000000000000000E+000
0.389000000000000	777.980001477021	0.000000000000000E+000
0.437000000000000	871.557990868748	0.000000000000000E+000
0.490000000000000	897.580812397056	0.000000000000000E+000
0.550000000000000	890.712666534622	0.000000000000000E+000
0.618000000000000	852.432477829832	0.000000000000000E+000
0.694000000000000	811.094282095851	0.000000000000000E+000
0.779000000000000	668.085553410531	0.000000000000000E+000
0.874000000000000	536.307667834407	0.000000000000000E+000
0.981000000000000	444.309266785563	0.000000000000000E+000
1.10000000000000	424.293992682714	0.000000000000000E+000
1.24000000000000	385.716465420086	0.000000000000000E+000
1.39000000000000	338.158731847039	0.000000000000000E+000
1.56000000000000	283.025228054780	0.000000000000000E+000
1.75000000000000	237.133194408165	0.000000000000000E+000
1.96000000000000	191.762815394127	0.000000000000000E+000
2.21000000000000	194.755078857366	0.000000000000000E+000
2.48000000000000	157.463306269228	0.000000000000000E+000
2.78000000000000	117.836955969544	0.000000000000000E+000
3.12000000000000	86.0234440214843	0.000000000000000E+000
3.50000000000000	65.3174399907903	0.000000000000000E+000
3.93000000000000	52.8582345901448	0.000000000000000E+000
4.41000000000000	38.1856600142039	0.000000000000000E+000
4.96000000000000	24.7984133182622	0.000000000000000E+000
5.56000000000000	16.2081132799099	0.000000000000000E+000
6.24000000000000	10.4880736014075	0.000000000000000E+000
7.01000000000000	6.88077829162863	0.000000000000000E+000
7.87000000000000	3.76207966613738	0.000000000000000E+000
8.84000000000000	1.74813543427343	0.000000000000000E+000
9.92000000000000	0.833166945677385	0.000000000000000E+000
11.1000000000000	0.000000000000000E+000	0.000000000000000E+000

THIS PAGE INTENTIONALLY LEFT BLANK

APPENDIX I. UMG V3.3 INTEGRAL QUANTITIES OUTPUT FILES

The following tables support the data presented in Chapter IV, and were used to assess the error from both the a priori (default spectrum) and detection assembly. Although a total of five tables were presented in the integral quantities output files, the first two were omitted due to initialization procedures. Tables 3, 4, and 5 were reported results and were used in this appendix.

A. INTEGRAL QUANTITIES OUTPUT FOR FREE FIELD

*** Table 3: Fluence rate uncertainty due to measurement uncertainty ***

	Energy	Fluence Rate	Fluence rate unc.	% Fluence rate unc.
1	1.000E-10	4.150E-01	0.000E+00	0.000E+00
2	1.000E-09	6.511E-02	6.081E-04	9.339E-01
3	1.120E-09	1.413E-01	1.320E-03	9.339E-01
4	1.260E-09	5.163E-02	4.822E-04	9.339E-01
5	1.410E-09	1.387E-01	1.295E-03	9.339E-01
6	1.590E-09	1.166E-01	1.088E-03	9.339E-01
7	1.780E-09	2.044E-01	1.909E-03	9.339E-01
8	2.000E-09	3.073E-01	2.870E-03	9.339E-01
9	2.250E-09	4.265E-01	3.983E-03	9.339E-01
10	2.520E-09	6.642E-01	6.203E-03	9.339E-01
11	2.830E-09	7.293E-01	6.811E-03	9.339E-01
12	3.180E-09	1.113E+00	1.040E-02	9.339E-01
13	3.570E-09	1.165E+00	1.088E-02	9.339E-01
14	4.010E-09	1.257E+00	1.174E-02	9.339E-01
15	4.500E-09	1.478E+00	1.380E-02	9.339E-01
16	5.050E-09	1.791E+00	1.672E-02	9.339E-01
17	5.670E-09	2.631E+00	2.457E-02	9.339E-01
18	6.360E-09	2.637E+00	2.463E-02	9.339E-01
19	7.140E-09	3.275E+00	3.059E-02	9.339E-01
20	8.020E-09	4.284E+00	4.001E-02	9.339E-01
21	9.000E-09	4.981E+00	4.698E-02	9.432E-01
22	1.010E-08	7.736E+00	8.014E-02	1.036E+00
23	1.130E-08	8.172E+00	8.466E-02	1.036E+00
24	1.270E-08	8.796E+00	9.113E-02	1.036E+00
25	1.430E-08	1.079E+01	1.118E-01	1.036E+00
26	1.610E-08	1.291E+01	1.338E-01	1.036E+00
27	1.800E-08	1.510E+01	1.564E-01	1.036E+00
28	2.020E-08	1.834E+01	1.900E-01	1.036E+00

29	2.270E-08	2.214E+01	2.339E-01	1.057E+00
30	2.550E-08	2.076E+01	2.468E-01	1.189E+00
31	2.860E-08	2.404E+01	2.857E-01	1.189E+00
32	3.210E-08	2.667E+01	3.170E-01	1.189E+00
33	3.610E-08	2.866E+01	3.406E-01	1.189E+00
34	4.050E-08	3.053E+01	3.629E-01	1.189E+00
35	4.550E-08	3.491E+01	4.150E-01	1.189E+00
36	5.100E-08	3.368E+01	4.004E-01	1.189E+00
37	5.730E-08	3.238E+01	3.925E-01	1.212E+00
38	6.430E-08	2.912E+01	3.856E-01	1.324E+00
39	7.220E-08	2.951E+01	3.907E-01	1.324E+00
40	8.110E-08	2.713E+01	3.592E-01	1.324E+00
41	9.100E-08	2.351E+01	3.190E-01	1.357E+00
42	1.020E-07	1.839E+01	2.768E-01	1.506E+00
43	1.150E-07	1.513E+01	2.279E-01	1.506E+00
44	1.290E-07	1.276E+01	1.921E-01	1.506E+00
45	1.450E-07	9.709E+00	1.462E-01	1.506E+00
46	1.620E-07	8.418E+00	1.268E-01	1.506E+00
47	1.820E-07	7.127E+00	1.073E-01	1.506E+00
48	2.050E-07	6.042E+00	9.098E-02	1.506E+00
49	2.300E-07	5.624E+00	8.673E-02	1.542E+00
50	2.580E-07	4.242E+00	7.020E-02	1.655E+00
51	2.890E-07	4.286E+00	7.094E-02	1.655E+00
52	3.250E-07	4.911E+00	8.127E-02	1.655E+00
53	3.650E-07	4.053E+00	6.708E-02	1.655E+00
54	4.090E-07	4.470E+00	7.397E-02	1.655E+00
55	4.600E-07	4.068E+00	6.733E-02	1.655E+00
56	5.160E-07	3.905E+00	6.462E-02	1.655E+00
57	5.790E-07	3.835E+00	6.347E-02	1.655E+00
58	6.500E-07	4.534E+00	7.504E-02	1.655E+00
59	7.300E-07	3.870E+00	6.405E-02	1.655E+00
60	8.190E-07	4.157E+00	6.880E-02	1.655E+00
61	9.200E-07	3.961E+00	6.464E-02	1.632E+00
62	1.030E-06	4.550E+00	7.143E-02	1.570E+00
63	1.160E-06	3.764E+00	5.909E-02	1.570E+00
64	1.300E-06	4.250E+00	6.673E-02	1.570E+00
65	1.460E-06	4.341E+00	6.815E-02	1.570E+00
66	1.640E-06	4.250E+00	6.673E-02	1.570E+00
67	1.840E-06	3.705E+00	5.817E-02	1.570E+00
68	2.070E-06	4.282E+00	6.723E-02	1.570E+00
69	2.320E-06	3.972E+00	6.236E-02	1.570E+00
70	2.610E-06	4.079E+00	6.404E-02	1.570E+00
71	2.920E-06	3.758E+00	5.900E-02	1.570E+00
72	3.280E-06	3.945E+00	6.194E-02	1.570E+00
73	3.690E-06	4.501E+00	7.067E-02	1.570E+00

74	4.140E-06	4.036E+00	6.337E-02	1.570E+00
75	4.650E-06	3.956E+00	6.211E-02	1.570E+00
76	5.220E-06	3.507E+00	5.506E-02	1.570E+00
77	5.850E-06	3.534E+00	5.548E-02	1.570E+00
78	6.570E-06	4.111E+00	6.454E-02	1.570E+00
79	7.380E-06	3.721E+00	5.842E-02	1.570E+00
80	8.280E-06	4.726E+00	7.420E-02	1.570E+00
81	9.300E-06	4.693E+00	7.047E-02	1.502E+00
82	1.040E-05	4.473E+00	6.183E-02	1.382E+00
83	1.170E-05	4.889E+00	6.759E-02	1.382E+00
84	1.320E-05	4.538E+00	6.273E-02	1.382E+00
85	1.480E-05	4.467E+00	6.175E-02	1.382E+00
86	1.660E-05	4.675E+00	6.463E-02	1.382E+00
87	1.860E-05	4.544E+00	6.282E-02	1.382E+00
88	2.090E-05	5.414E+00	7.484E-02	1.382E+00
89	2.350E-05	4.520E+00	6.249E-02	1.382E+00
90	2.630E-05	5.092E+00	7.039E-02	1.382E+00
91	2.960E-05	4.848E+00	6.702E-02	1.382E+00
92	3.320E-05	4.431E+00	6.125E-02	1.382E+00
93	3.730E-05	4.455E+00	6.158E-02	1.382E+00
94	4.180E-05	5.426E+00	7.500E-02	1.382E+00
95	4.700E-05	4.889E+00	6.759E-02	1.382E+00
96	5.270E-05	4.490E+00	6.208E-02	1.382E+00
97	5.920E-05	5.211E+00	7.204E-02	1.382E+00
98	6.640E-05	4.770E+00	6.595E-02	1.382E+00
99	7.460E-05	4.645E+00	6.422E-02	1.382E+00
100	8.370E-05	5.324E+00	7.360E-02	1.382E+00
101	9.400E-05	5.256E+00	6.781E-02	1.290E+00
102	1.060E-04	5.247E+00	6.284E-02	1.198E+00
103	1.180E-04	6.015E+00	7.204E-02	1.198E+00
104	1.330E-04	5.713E+00	6.842E-02	1.198E+00
105	1.490E-04	5.556E+00	6.654E-02	1.198E+00
106	1.680E-04	5.923E+00	7.094E-02	1.198E+00
107	1.880E-04	5.516E+00	6.606E-02	1.198E+00
108	2.110E-04	5.660E+00	6.779E-02	1.198E+00
109	2.370E-04	5.942E+00	7.117E-02	1.198E+00
110	2.660E-04	5.857E+00	7.015E-02	1.198E+00
111	2.990E-04	5.103E+00	6.112E-02	1.198E+00
112	3.350E-04	5.851E+00	7.007E-02	1.198E+00
113	3.770E-04	6.218E+00	7.447E-02	1.198E+00
114	4.230E-04	5.890E+00	7.054E-02	1.198E+00
115	4.750E-04	6.343E+00	7.596E-02	1.198E+00
116	5.330E-04	5.824E+00	6.976E-02	1.198E+00
117	5.980E-04	5.529E+00	6.622E-02	1.198E+00
118	6.720E-04	6.500E+00	7.785E-02	1.198E+00

119	7.540E-04	5.654E+00	6.771E-02	1.198E+00
120	8.460E-04	6.008E+00	7.196E-02	1.198E+00
121	9.500E-04	6.320E+00	7.124E-02	1.127E+00
122	1.070E-03	6.168E+00	6.641E-02	1.077E+00
123	1.200E-03	7.002E+00	7.539E-02	1.077E+00
124	1.340E-03	6.441E+00	6.935E-02	1.077E+00
125	1.510E-03	6.834E+00	7.358E-02	1.077E+00
126	1.690E-03	6.897E+00	7.426E-02	1.077E+00
127	1.900E-03	6.785E+00	7.305E-02	1.077E+00
128	2.140E-03	7.640E+00	8.226E-02	1.077E+00
129	2.400E-03	6.722E+00	7.237E-02	1.077E+00
130	2.690E-03	5.250E+00	5.652E-02	1.077E+00
131	3.020E-03	6.497E+00	6.996E-02	1.077E+00
132	3.390E-03	6.729E+00	7.245E-02	1.077E+00
133	3.810E-03	7.640E+00	8.226E-02	1.077E+00
134	4.270E-03	7.500E+00	8.075E-02	1.077E+00
135	4.800E-03	7.079E+00	7.622E-02	1.077E+00
136	5.390E-03	6.827E+00	7.351E-02	1.077E+00
137	6.050E-03	7.079E+00	7.622E-02	1.077E+00
138	6.790E-03	7.149E+00	7.698E-02	1.077E+00
139	7.620E-03	7.500E+00	8.075E-02	1.077E+00
140	8.550E-03	7.430E+00	7.999E-02	1.077E+00
141	9.600E-03	7.586E+00	8.054E-02	1.062E+00
142	1.080E-02	8.556E+00	9.020E-02	1.054E+00
143	1.210E-02	8.698E+00	9.170E-02	1.054E+00
144	1.360E-02	8.841E+00	9.320E-02	1.054E+00
145	1.530E-02	8.770E+00	9.245E-02	1.054E+00
146	1.710E-02	8.413E+00	8.869E-02	1.054E+00
147	1.920E-02	9.554E+00	1.007E-01	1.054E+00
148	2.160E-02	9.911E+00	1.045E-01	1.054E+00
149	2.420E-02	9.713E+00	1.006E-01	1.036E+00
150	2.720E-02	1.069E+01	1.099E-01	1.028E+00
151	3.050E-02	1.120E+01	1.151E-01	1.028E+00
152	3.430E-02	7.946E+00	8.168E-02	1.028E+00
153	3.850E-02	1.111E+01	1.159E-01	1.043E+00
154	4.320E-02	1.198E+01	1.255E-01	1.048E+00
155	4.850E-02	1.393E+01	1.460E-01	1.048E+00
156	5.440E-02	1.212E+01	1.271E-01	1.048E+00
157	6.110E-02	1.550E+01	1.623E-01	1.047E+00
158	6.860E-02	1.661E+01	1.739E-01	1.047E+00
159	7.700E-02	1.763E+01	1.845E-01	1.047E+00
160	8.650E-02	1.429E+01	1.496E-01	1.047E+00
161	9.710E-02	1.874E+01	2.010E-01	1.073E+00
162	1.090E-01	2.205E+01	2.384E-01	1.081E+00
163	1.220E-01	2.696E+01	2.915E-01	1.081E+00

164	1.370E-01	2.530E+01	2.736E-01	1.081E+00
165	1.540E-01	2.614E+01	2.926E-01	1.119E+00
166	1.730E-01	2.692E+01	3.045E-01	1.131E+00
167	1.940E-01	2.742E+01	3.101E-01	1.131E+00
168	2.180E-01	3.142E+01	3.554E-01	1.131E+00
169	2.450E-01	3.661E+01	4.332E-01	1.183E+00
170	2.750E-01	3.841E+01	4.599E-01	1.197E+00
171	3.090E-01	4.306E+01	5.155E-01	1.197E+00
172	3.460E-01	3.961E+01	4.742E-01	1.197E+00
173	3.890E-01	3.834E+01	4.875E-01	1.272E+00
174	4.370E-01	4.298E+01	5.541E-01	1.289E+00
175	4.900E-01	5.209E+01	6.715E-01	1.289E+00
176	5.500E-01	5.934E+01	7.650E-01	1.289E+00
177	6.180E-01	6.267E+01	8.624E-01	1.376E+00
178	6.940E-01	7.163E+01	9.986E-01	1.394E+00
179	7.790E-01	7.163E+01	9.986E-01	1.394E+00
180	8.740E-01	6.335E+01	8.832E-01	1.394E+00
181	9.810E-01	6.123E+01	9.032E-01	1.475E+00
182	1.100E+00	6.641E+01	9.897E-01	1.490E+00
183	1.240E+00	6.766E+01	1.008E+00	1.490E+00
184	1.390E+00	7.017E+01	1.046E+00	1.490E+00
185	1.560E+00	6.769E+01	1.007E+00	1.488E+00
186	1.750E+00	6.505E+01	9.680E-01	1.488E+00
187	1.960E+00	6.444E+01	9.589E-01	1.488E+00
188	2.210E+00	6.750E+01	1.005E+00	1.488E+00
189	2.480E+00	6.704E+01	9.061E-01	1.352E+00
190	2.780E+00	5.611E+01	7.492E-01	1.335E+00
191	3.120E+00	4.773E+01	6.373E-01	1.335E+00
192	3.500E+00	4.081E+01	5.450E-01	1.335E+00
193	3.930E+00	3.694E+01	4.388E-01	1.188E+00
194	4.410E+00	2.889E+01	3.381E-01	1.170E+00
195	4.960E+00	2.286E+01	2.676E-01	1.170E+00
196	5.560E+00	1.590E+01	1.861E-01	1.170E+00
197	6.240E+00	1.233E+01	1.145E-01	9.282E-01
198	7.010E+00	8.115E+00	7.336E-02	9.040E-01
199	7.870E+00	5.408E+00	4.888E-02	9.040E-01
200	8.840E+00	2.715E+00	2.454E-02	9.040E-01
201	9.920E+00	1.528E+00	1.112E-02	7.276E-01
	1.110E+01			

*** Table 4: Fluence rate uncertainty due to default spectrum uncertainty ***

Energy Fluence Rate Fluence rate unc. % Fluence rate unc. % Default sp. unc.

1	1.000E-10	4.150E-01	8.756E-02	2.110E+01
2.110E+01				
2	1.000E-09	6.511E-02	3.306E-02	5.078E+01
5.078E+01				
3	1.120E-09	1.413E-01	3.989E-02	2.823E+01
2.823E+01				
4	1.260E-09	5.163E-02	2.089E-02	4.046E+01
4.046E+01				
5	1.410E-09	1.387E-01	3.965E-02	2.859E+01
2.859E+01				
6	1.590E-09	1.166E-01	3.795E-02	3.256E+01
3.256E+01				
7	1.780E-09	2.044E-01	4.839E-02	2.367E+01
2.367E+01				
8	2.000E-09	3.073E-01	6.276E-02	2.042E+01
2.042E+01				
9	2.250E-09	4.265E-01	7.336E-02	1.720E+01
1.720E+01				
10	2.520E-09	6.642E-01	9.364E-02	1.410E+01
1.410E+01				
11	2.830E-09	7.293E-01	9.531E-02	1.307E+01
1.307E+01				
12	3.180E-09	1.113E+00	1.212E-01	1.089E+01
1.089E+01				
13	3.570E-09	1.165E+00	1.233E-01	1.058E+01
1.058E+01				
14	4.010E-09	1.257E+00	1.278E-01	1.017E+01
1.017E+01				
15	4.500E-09	1.478E+00	1.347E-01	9.110E+00
9.110E+00				
16	5.050E-09	1.791E+00	1.500E-01	8.380E+00
8.380E+00				
17	5.670E-09	2.631E+00	1.875E-01	7.129E+00
7.130E+00				
18	6.360E-09	2.637E+00	1.843E-01	6.990E+00
6.990E+00				
19	7.140E-09	3.275E+00	2.004E-01	6.120E+00
6.120E+00				
20	8.020E-09	4.284E+00	2.408E-01	5.619E+00
5.620E+00				
21	9.000E-09	4.981E+00	2.540E-01	5.099E+00
5.100E+00				
22	1.010E-08	7.736E+00	3.163E-01	4.089E+00
4.090E+00				

23	1.130E-08	8.172E+00	3.268E-01	3.999E+00
4.000E+00				
24	1.270E-08	8.796E+00	3.307E-01	3.759E+00
3.760E+00				
25	1.430E-08	1.079E+01	3.722E-01	3.449E+00
3.450E+00				
26	1.610E-08	1.291E+01	4.041E-01	3.129E+00
3.130E+00				
27	1.800E-08	1.510E+01	4.452E-01	2.949E+00
2.950E+00				
28	2.020E-08	1.834E+01	4.822E-01	2.629E+00
2.630E+00				
29	2.270E-08	2.214E+01	5.288E-01	2.389E+00
2.390E+00				
30	2.550E-08	2.076E+01	5.001E-01	2.409E+00
2.410E+00				
31	2.860E-08	2.404E+01	5.453E-01	2.269E+00
2.270E+00				
32	3.210E-08	2.667E+01	5.729E-01	2.149E+00
2.150E+00				
33	3.610E-08	2.866E+01	5.984E-01	2.088E+00
2.090E+00				
34	4.050E-08	3.053E+01	6.191E-01	2.028E+00
2.030E+00				
35	4.550E-08	3.491E+01	6.660E-01	1.908E+00
1.910E+00				
36	5.100E-08	3.368E+01	6.594E-01	1.958E+00
1.960E+00				
37	5.730E-08	3.238E+01	6.437E-01	1.988E+00
1.990E+00				
38	6.430E-08	2.912E+01	6.050E-01	2.078E+00
2.080E+00				
39	7.220E-08	2.951E+01	6.130E-01	2.077E+00
2.080E+00				
40	8.110E-08	2.713E+01	5.933E-01	2.187E+00
2.190E+00				
41	9.100E-08	2.351E+01	5.564E-01	2.367E+00
2.370E+00				
42	1.020E-07	1.839E+01	4.831E-01	2.627E+00
2.630E+00				
43	1.150E-07	1.513E+01	4.474E-01	2.957E+00
2.960E+00				
44	1.290E-07	1.276E+01	4.268E-01	3.346E+00
3.350E+00				

45	1.450E-07	9.709E+00	3.773E-01	3.886E+00
3.890E+00				
46	1.620E-07	8.418E+00	3.616E-01	4.295E+00
4.300E+00				
47	1.820E-07	7.127E+00	3.417E-01	4.795E+00
4.800E+00				
48	2.050E-07	6.042E+00	3.242E-01	5.365E+00
5.370E+00				
49	2.300E-07	5.624E+00	3.135E-01	5.575E+00
5.580E+00				
50	2.580E-07	4.242E+00	2.700E-01	6.365E+00
6.370E+00				
51	2.890E-07	4.286E+00	2.741E-01	6.395E+00
6.400E+00				
52	3.250E-07	4.911E+00	2.934E-01	5.974E+00
5.980E+00				
53	3.650E-07	4.053E+00	2.665E-01	6.575E+00
6.580E+00				
54	4.090E-07	4.470E+00	2.804E-01	6.274E+00
6.280E+00				
55	4.600E-07	4.068E+00	2.687E-01	6.605E+00
6.610E+00				
56	5.160E-07	3.905E+00	2.637E-01	6.755E+00
6.760E+00				
57	5.790E-07	3.835E+00	2.629E-01	6.855E+00
6.860E+00				
58	6.500E-07	4.534E+00	2.845E-01	6.274E+00
6.280E+00				
59	7.300E-07	3.870E+00	2.657E-01	6.864E+00
6.870E+00				
60	8.190E-07	4.157E+00	2.688E-01	6.465E+00
6.470E+00				
61	9.200E-07	3.961E+00	2.699E-01	6.814E+00
6.820E+00				
62	1.030E-06	4.550E+00	3.004E-01	6.604E+00
6.610E+00				
63	1.160E-06	3.764E+00	2.730E-01	7.254E+00
7.260E+00				
64	1.300E-06	4.250E+00	2.909E-01	6.844E+00
6.850E+00				
65	1.460E-06	4.341E+00	2.906E-01	6.694E+00
6.700E+00				
66	1.640E-06	4.250E+00	2.875E-01	6.764E+00
6.770E+00				

67	1.840E-06	3.705E+00	2.717E-01	7.334E+00
7.340E+00				
68	2.070E-06	4.282E+00	2.922E-01	6.824E+00
6.830E+00				
69	2.320E-06	3.972E+00	2.790E-01	7.024E+00
7.030E+00				
70	2.610E-06	4.079E+00	2.784E-01	6.824E+00
6.830E+00				
71	2.920E-06	3.758E+00	2.704E-01	7.194E+00
7.200E+00				
72	3.280E-06	3.945E+00	2.799E-01	7.094E+00
7.100E+00				
73	3.690E-06	4.501E+00	2.986E-01	6.634E+00
6.640E+00				
74	4.140E-06	4.036E+00	2.815E-01	6.974E+00
6.980E+00				
75	4.650E-06	3.956E+00	2.787E-01	7.044E+00
7.050E+00				
76	5.220E-06	3.507E+00	2.653E-01	7.564E+00
7.570E+00				
77	5.850E-06	3.534E+00	2.595E-01	7.345E+00
7.350E+00				
78	6.570E-06	4.111E+00	2.867E-01	6.974E+00
6.980E+00				
79	7.380E-06	3.721E+00	2.692E-01	7.234E+00
7.240E+00				
80	8.280E-06	4.726E+00	3.059E-01	6.473E+00
6.480E+00				
81	9.300E-06	4.693E+00	3.104E-01	6.614E+00
6.620E+00				
82	1.040E-05	4.473E+00	3.173E-01	7.094E+00
7.100E+00				
83	1.170E-05	4.889E+00	3.312E-01	6.774E+00
6.780E+00				
84	1.320E-05	4.538E+00	3.147E-01	6.934E+00
6.940E+00				
85	1.480E-05	4.467E+00	3.106E-01	6.954E+00
6.960E+00				
86	1.660E-05	4.675E+00	3.274E-01	7.004E+00
7.010E+00				
87	1.860E-05	4.544E+00	3.174E-01	6.984E+00
6.990E+00				
88	2.090E-05	5.414E+00	3.472E-01	6.413E+00
6.420E+00				

89	2.350E-05	4.520E+00	3.112E-01	6.884E+00
6.890E+00				
90	2.630E-05	5.092E+00	3.357E-01	6.594E+00
6.600E+00				
91	2.960E-05	4.848E+00	3.260E-01	6.724E+00
6.730E+00				
92	3.320E-05	4.431E+00	3.134E-01	7.074E+00
7.080E+00				
93	3.730E-05	4.455E+00	3.156E-01	7.084E+00
7.090E+00				
94	4.180E-05	5.426E+00	3.523E-01	6.493E+00
6.500E+00				
95	4.700E-05	4.889E+00	3.302E-01	6.754E+00
6.760E+00				
96	5.270E-05	4.490E+00	3.150E-01	7.014E+00
7.020E+00				
97	5.920E-05	5.211E+00	3.425E-01	6.573E+00
6.580E+00				
98	6.640E-05	4.770E+00	3.250E-01	6.814E+00
6.820E+00				
99	7.460E-05	4.645E+00	3.202E-01	6.894E+00
6.900E+00				
100	8.370E-05	5.324E+00	3.425E-01	6.434E+00
6.440E+00				
101	9.400E-05	5.256E+00	3.476E-01	6.614E+00
6.620E+00				
102	1.060E-04	5.247E+00	3.644E-01	6.944E+00
6.950E+00				
103	1.180E-04	6.015E+00	3.852E-01	6.404E+00
6.410E+00				
104	1.330E-04	5.713E+00	3.739E-01	6.544E+00
6.550E+00				
105	1.490E-04	5.556E+00	3.686E-01	6.634E+00
6.640E+00				
106	1.680E-04	5.923E+00	3.858E-01	6.514E+00
6.520E+00				
107	1.880E-04	5.516E+00	3.665E-01	6.644E+00
6.650E+00				
108	2.110E-04	5.660E+00	3.721E-01	6.574E+00
6.580E+00				
109	2.370E-04	5.942E+00	3.859E-01	6.494E+00
6.500E+00				
110	2.660E-04	5.857E+00	3.815E-01	6.514E+00
6.520E+00				

111	2.990E-04	5.103E+00	3.523E-01	6.905E+00
6.910E+00				
112	3.350E-04	5.851E+00	3.817E-01	6.524E+00
6.530E+00				
113	3.770E-04	6.218E+00	3.913E-01	6.294E+00
6.300E+00				
114	4.230E-04	5.890E+00	3.772E-01	6.404E+00
6.410E+00				
115	4.750E-04	6.343E+00	3.954E-01	6.234E+00
6.240E+00				
116	5.330E-04	5.824E+00	3.806E-01	6.534E+00
6.540E+00				
117	5.980E-04	5.529E+00	3.751E-01	6.784E+00
6.790E+00				
118	6.720E-04	6.500E+00	3.993E-01	6.144E+00
6.150E+00				
119	7.540E-04	5.654E+00	3.734E-01	6.604E+00
6.610E+00				
120	8.460E-04	6.008E+00	3.836E-01	6.384E+00
6.390E+00				
121	9.500E-04	6.320E+00	3.966E-01	6.274E+00
6.280E+00				
122	1.070E-03	6.168E+00	4.012E-01	6.505E+00
6.510E+00				
123	1.200E-03	7.002E+00	4.267E-01	6.094E+00
6.100E+00				
124	1.340E-03	6.441E+00	4.106E-01	6.375E+00
6.380E+00				
125	1.510E-03	6.834E+00	4.233E-01	6.194E+00
6.200E+00				
126	1.690E-03	6.897E+00	4.279E-01	6.204E+00
6.210E+00				
127	1.900E-03	6.785E+00	4.169E-01	6.145E+00
6.150E+00				
128	2.140E-03	7.640E+00	4.511E-01	5.904E+00
5.910E+00				
129	2.400E-03	6.722E+00	4.211E-01	6.264E+00
6.270E+00				
130	2.690E-03	5.250E+00	3.678E-01	7.005E+00
7.010E+00				
131	3.020E-03	6.497E+00	4.122E-01	6.345E+00
6.350E+00				
132	3.390E-03	6.729E+00	4.208E-01	6.254E+00
6.260E+00				

133	3.810E-03	7.640E+00	4.472E-01	5.854E+00
5.860E+00				
134	4.270E-03	7.500E+00	4.495E-01	5.994E+00
6.000E+00				
135	4.800E-03	7.079E+00	4.293E-01	6.064E+00
6.070E+00				
136	5.390E-03	6.827E+00	4.215E-01	6.174E+00
6.180E+00				
137	6.050E-03	7.079E+00	4.350E-01	6.144E+00
6.150E+00				
138	6.790E-03	7.149E+00	4.257E-01	5.954E+00
5.960E+00				
139	7.620E-03	7.500E+00	4.435E-01	5.914E+00
5.920E+00				
140	8.550E-03	7.430E+00	4.409E-01	5.934E+00
5.940E+00				
141	9.600E-03	7.586E+00	4.441E-01	5.854E+00
5.860E+00				
142	1.080E-02	8.556E+00	4.803E-01	5.614E+00
5.620E+00				
143	1.210E-02	8.698E+00	4.822E-01	5.544E+00
5.550E+00				
144	1.360E-02	8.841E+00	4.848E-01	5.484E+00
5.490E+00				
145	1.530E-02	8.770E+00	4.914E-01	5.603E+00
5.610E+00				
146	1.710E-02	8.413E+00	4.782E-01	5.684E+00
5.690E+00				
147	1.920E-02	9.554E+00	5.076E-01	5.313E+00
5.320E+00				
148	2.160E-02	9.911E+00	5.147E-01	5.193E+00
5.200E+00				
149	2.420E-02	9.713E+00	5.103E-01	5.254E+00
5.260E+00				
150	2.720E-02	1.069E+01	5.295E-01	4.954E+00
4.960E+00				
151	3.050E-02	1.120E+01	5.445E-01	4.863E+00
4.870E+00				
152	3.430E-02	7.946E+00	4.644E-01	5.844E+00
5.850E+00				
153	3.850E-02	1.111E+01	5.472E-01	4.923E+00
4.930E+00				
154	4.320E-02	1.198E+01	5.752E-01	4.802E+00
4.810E+00				

155	4.850E-02	1.393E+01	6.116E-01	4.392E+00
4.400E+00				
156	5.440E-02	1.212E+01	5.688E-01	4.693E+00
4.700E+00				
157	6.110E-02	1.550E+01	6.513E-01	4.201E+00
4.210E+00				
158	6.860E-02	1.661E+01	6.713E-01	4.041E+00
4.050E+00				
159	7.700E-02	1.763E+01	6.947E-01	3.941E+00
3.950E+00				
160	8.650E-02	1.429E+01	6.276E-01	4.392E+00
4.400E+00				
161	9.710E-02	1.874E+01	7.158E-01	3.820E+00
3.830E+00				
162	1.090E-01	2.205E+01	7.759E-01	3.519E+00
3.530E+00				
163	1.220E-01	2.696E+01	8.542E-01	3.168E+00
3.180E+00				
164	1.370E-01	2.530E+01	8.269E-01	3.269E+00
3.280E+00				
165	1.540E-01	2.614E+01	8.358E-01	3.198E+00
3.210E+00				
166	1.730E-01	2.692E+01	8.552E-01	3.177E+00
3.190E+00				
167	1.940E-01	2.742E+01	8.547E-01	3.117E+00
3.130E+00				
168	2.180E-01	3.142E+01	9.193E-01	2.926E+00
2.940E+00				
169	2.450E-01	3.661E+01	9.789E-01	2.674E+00
2.690E+00				
170	2.750E-01	3.841E+01	1.011E+00	2.633E+00
2.650E+00				
171	3.090E-01	4.306E+01	1.069E+00	2.482E+00
2.500E+00				
172	3.460E-01	3.961E+01	1.027E+00	2.593E+00
2.610E+00				
173	3.890E-01	3.834E+01	1.001E+00	2.611E+00
2.630E+00				
174	4.370E-01	4.298E+01	1.049E+00	2.440E+00
2.460E+00				
175	4.900E-01	5.209E+01	1.155E+00	2.218E+00
2.240E+00				
176	5.500E-01	5.934E+01	1.232E+00	2.076E+00
2.100E+00				

177	6.180E-01	6.267E+01	1.237E+00	1.973E+00
2.000E+00				
178	6.940E-01	7.163E+01	1.319E+00	1.841E+00
1.870E+00				
179	7.790E-01	7.163E+01	1.319E+00	1.841E+00
1.870E+00				
180	8.740E-01	6.335E+01	1.243E+00	1.963E+00
1.990E+00				
181	9.810E-01	6.123E+01	1.201E+00	1.961E+00
1.990E+00				
182	1.100E+00	6.641E+01	1.242E+00	1.870E+00
1.900E+00				
183	1.240E+00	6.766E+01	1.251E+00	1.850E+00
1.880E+00				
184	1.390E+00	7.017E+01	1.270E+00	1.809E+00
1.840E+00				
185	1.560E+00	6.769E+01	1.239E+00	1.831E+00
1.860E+00				
186	1.750E+00	6.505E+01	1.217E+00	1.871E+00
1.900E+00				
187	1.960E+00	6.444E+01	1.206E+00	1.872E+00
1.900E+00				
188	2.210E+00	6.750E+01	1.229E+00	1.821E+00
1.850E+00				
189	2.480E+00	6.704E+01	1.250E+00	1.865E+00
1.890E+00				
190	2.780E+00	5.611E+01	1.149E+00	2.048E+00
2.070E+00				
191	3.120E+00	4.773E+01	1.059E+00	2.220E+00
2.240E+00				
192	3.500E+00	4.081E+01	9.839E-01	2.411E+00
2.430E+00				
193	3.930E+00	3.694E+01	9.585E-01	2.595E+00
2.610E+00				
194	4.410E+00	2.889E+01	8.514E-01	2.947E+00
2.960E+00				
195	4.960E+00	2.286E+01	7.586E-01	3.318E+00
3.330E+00				
196	5.560E+00	1.590E+01	6.330E-01	3.980E+00
3.990E+00				
197	6.240E+00	1.233E+01	5.814E-01	4.714E+00
4.720E+00				
198	7.010E+00	8.115E+00	4.711E-01	5.805E+00
5.810E+00				

199	7.870E+00	5.408E+00	3.800E-01	7.026E+00 7.030E+00
200	8.840E+00	2.715E+00	2.741E-01	1.010E+01 1.010E+01
201	9.920E+00	1.528E+00	2.121E-01	1.388E+01 1.388E+01
	1.110E+01			

*** Table 5: Fluence rate uncertainty due to measurement and default spectrum uncertainty ***

	Energy	Fluence Rate	Fluence rate unc.	% Fluence rate unc.
1	1.000E-10	4.150E-01	8.756E-02	2.110E+01
2	1.000E-09	6.511E-02	3.307E-02	5.079E+01
3	1.120E-09	1.413E-01	3.991E-02	2.825E+01
4	1.260E-09	5.163E-02	2.090E-02	4.047E+01
5	1.410E-09	1.387E-01	3.967E-02	2.861E+01
6	1.590E-09	1.166E-01	3.796E-02	3.257E+01
7	1.780E-09	2.044E-01	4.843E-02	2.369E+01
8	2.000E-09	3.073E-01	6.282E-02	2.044E+01
9	2.250E-09	4.265E-01	7.346E-02	1.723E+01
10	2.520E-09	6.642E-01	9.385E-02	1.413E+01
11	2.830E-09	7.293E-01	9.556E-02	1.310E+01
12	3.180E-09	1.113E+00	1.217E-01	1.093E+01
13	3.570E-09	1.165E+00	1.238E-01	1.062E+01
14	4.010E-09	1.257E+00	1.283E-01	1.021E+01
15	4.500E-09	1.478E+00	1.354E-01	9.158E+00
16	5.050E-09	1.791E+00	1.510E-01	8.432E+00
17	5.670E-09	2.631E+00	1.891E-01	7.190E+00
18	6.360E-09	2.637E+00	1.860E-01	7.052E+00
19	7.140E-09	3.275E+00	2.028E-01	6.191E+00
20	8.020E-09	4.284E+00	2.441E-01	5.696E+00
21	9.000E-09	4.981E+00	2.583E-01	5.186E+00
22	1.010E-08	7.736E+00	3.263E-01	4.218E+00
23	1.130E-08	8.172E+00	3.376E-01	4.131E+00
24	1.270E-08	8.796E+00	3.430E-01	3.899E+00
25	1.430E-08	1.079E+01	3.886E-01	3.601E+00
26	1.610E-08	1.291E+01	4.256E-01	3.296E+00
27	1.800E-08	1.510E+01	4.718E-01	3.125E+00
28	2.020E-08	1.834E+01	5.182E-01	2.826E+00
29	2.270E-08	2.214E+01	5.782E-01	2.612E+00
30	2.550E-08	2.076E+01	5.577E-01	2.686E+00
31	2.860E-08	2.404E+01	6.156E-01	2.561E+00
32	3.210E-08	2.667E+01	6.548E-01	2.455E+00

33	3.610E-08	2.866E+01	6.885E-01	2.403E+00
34	4.050E-08	3.053E+01	7.176E-01	2.351E+00
35	4.550E-08	3.491E+01	7.848E-01	2.248E+00
36	5.100E-08	3.368E+01	7.714E-01	2.290E+00
37	5.730E-08	3.238E+01	7.539E-01	2.328E+00
38	6.430E-08	2.912E+01	7.174E-01	2.464E+00
39	7.220E-08	2.951E+01	7.269E-01	2.463E+00
40	8.110E-08	2.713E+01	6.936E-01	2.557E+00
41	9.100E-08	2.351E+01	6.413E-01	2.728E+00
42	1.020E-07	1.839E+01	5.568E-01	3.028E+00
43	1.150E-07	1.513E+01	5.021E-01	3.318E+00
44	1.290E-07	1.276E+01	4.680E-01	3.669E+00
45	1.450E-07	9.709E+00	4.046E-01	4.168E+00
46	1.620E-07	8.418E+00	3.832E-01	4.552E+00
47	1.820E-07	7.127E+00	3.582E-01	5.026E+00
48	2.050E-07	6.042E+00	3.367E-01	5.572E+00
49	2.300E-07	5.624E+00	3.253E-01	5.784E+00
50	2.580E-07	4.242E+00	2.789E-01	6.576E+00
51	2.890E-07	4.286E+00	2.831E-01	6.605E+00
52	3.250E-07	4.911E+00	3.044E-01	6.199E+00
53	3.650E-07	4.053E+00	2.748E-01	6.780E+00
54	4.090E-07	4.470E+00	2.900E-01	6.489E+00
55	4.600E-07	4.068E+00	2.770E-01	6.809E+00
56	5.160E-07	3.905E+00	2.715E-01	6.954E+00
57	5.790E-07	3.835E+00	2.704E-01	7.051E+00
58	6.500E-07	4.534E+00	2.942E-01	6.489E+00
59	7.300E-07	3.870E+00	2.733E-01	7.061E+00
60	8.190E-07	4.157E+00	2.774E-01	6.673E+00
61	9.200E-07	3.961E+00	2.776E-01	7.007E+00
62	1.030E-06	4.550E+00	3.088E-01	6.788E+00
63	1.160E-06	3.764E+00	2.793E-01	7.422E+00
64	1.300E-06	4.250E+00	2.984E-01	7.021E+00
65	1.460E-06	4.341E+00	2.985E-01	6.876E+00
66	1.640E-06	4.250E+00	2.951E-01	6.944E+00
67	1.840E-06	3.705E+00	2.779E-01	7.500E+00
68	2.070E-06	4.282E+00	2.998E-01	7.002E+00
69	2.320E-06	3.972E+00	2.859E-01	7.197E+00
70	2.610E-06	4.079E+00	2.856E-01	7.003E+00
71	2.920E-06	3.758E+00	2.767E-01	7.364E+00
72	3.280E-06	3.945E+00	2.867E-01	7.266E+00
73	3.690E-06	4.501E+00	3.069E-01	6.817E+00
74	4.140E-06	4.036E+00	2.885E-01	7.149E+00
75	4.650E-06	3.956E+00	2.855E-01	7.217E+00
76	5.220E-06	3.507E+00	2.709E-01	7.725E+00
77	5.850E-06	3.534E+00	2.654E-01	7.511E+00

78	6.570E-06	4.111E+00	2.939E-01	7.148E+00
79	7.380E-06	3.721E+00	2.754E-01	7.403E+00
80	8.280E-06	4.726E+00	3.148E-01	6.661E+00
81	9.300E-06	4.693E+00	3.183E-01	6.782E+00
82	1.040E-05	4.473E+00	3.232E-01	7.227E+00
83	1.170E-05	4.889E+00	3.380E-01	6.913E+00
84	1.320E-05	4.538E+00	3.209E-01	7.071E+00
85	1.480E-05	4.467E+00	3.167E-01	7.090E+00
86	1.660E-05	4.675E+00	3.337E-01	7.139E+00
87	1.860E-05	4.544E+00	3.235E-01	7.119E+00
88	2.090E-05	5.414E+00	3.552E-01	6.561E+00
89	2.350E-05	4.520E+00	3.174E-01	7.022E+00
90	2.630E-05	5.092E+00	3.430E-01	6.737E+00
91	2.960E-05	4.848E+00	3.328E-01	6.865E+00
92	3.320E-05	4.431E+00	3.194E-01	7.208E+00
93	3.730E-05	4.455E+00	3.215E-01	7.218E+00
94	4.180E-05	5.426E+00	3.602E-01	6.639E+00
95	4.700E-05	4.889E+00	3.371E-01	6.894E+00
96	5.270E-05	4.490E+00	3.210E-01	7.149E+00
97	5.920E-05	5.211E+00	3.500E-01	6.717E+00
98	6.640E-05	4.770E+00	3.317E-01	6.953E+00
99	7.460E-05	4.645E+00	3.266E-01	7.031E+00
100	8.370E-05	5.324E+00	3.504E-01	6.580E+00
101	9.400E-05	5.256E+00	3.542E-01	6.739E+00
102	1.060E-04	5.247E+00	3.698E-01	7.047E+00
103	1.180E-04	6.015E+00	3.918E-01	6.515E+00
104	1.330E-04	5.713E+00	3.801E-01	6.653E+00
105	1.490E-04	5.556E+00	3.745E-01	6.741E+00
106	1.680E-04	5.923E+00	3.923E-01	6.623E+00
107	1.880E-04	5.516E+00	3.724E-01	6.751E+00
108	2.110E-04	5.660E+00	3.782E-01	6.682E+00
109	2.370E-04	5.942E+00	3.924E-01	6.603E+00
110	2.660E-04	5.857E+00	3.879E-01	6.623E+00
111	2.990E-04	5.103E+00	3.576E-01	7.008E+00
112	3.350E-04	5.851E+00	3.881E-01	6.633E+00
113	3.770E-04	6.218E+00	3.984E-01	6.407E+00
114	4.230E-04	5.890E+00	3.837E-01	6.515E+00
115	4.750E-04	6.343E+00	4.026E-01	6.348E+00
116	5.330E-04	5.824E+00	3.869E-01	6.643E+00
117	5.980E-04	5.529E+00	3.809E-01	6.889E+00
118	6.720E-04	6.500E+00	4.069E-01	6.259E+00
119	7.540E-04	5.654E+00	3.795E-01	6.712E+00
120	8.460E-04	6.008E+00	3.902E-01	6.495E+00
121	9.500E-04	6.320E+00	4.029E-01	6.375E+00
122	1.070E-03	6.168E+00	4.067E-01	6.593E+00

123	1.200E-03	7.002E+00	4.333E-01	6.189E+00
124	1.340E-03	6.441E+00	4.164E-01	6.465E+00
125	1.510E-03	6.834E+00	4.297E-01	6.287E+00
126	1.690E-03	6.897E+00	4.343E-01	6.297E+00
127	1.900E-03	6.785E+00	4.232E-01	6.238E+00
128	2.140E-03	7.640E+00	4.585E-01	6.001E+00
129	2.400E-03	6.722E+00	4.272E-01	6.356E+00
130	2.690E-03	5.250E+00	3.721E-01	7.087E+00
131	3.020E-03	6.497E+00	4.181E-01	6.435E+00
132	3.390E-03	6.729E+00	4.270E-01	6.346E+00
133	3.810E-03	7.640E+00	4.547E-01	5.952E+00
134	4.270E-03	7.500E+00	4.567E-01	6.090E+00
135	4.800E-03	7.079E+00	4.360E-01	6.159E+00
136	5.390E-03	6.827E+00	4.279E-01	6.268E+00
137	6.050E-03	7.079E+00	4.416E-01	6.238E+00
138	6.790E-03	7.149E+00	4.326E-01	6.051E+00
139	7.620E-03	7.500E+00	4.508E-01	6.011E+00
140	8.550E-03	7.430E+00	4.481E-01	6.031E+00
141	9.600E-03	7.586E+00	4.513E-01	5.950E+00
142	1.080E-02	8.556E+00	4.887E-01	5.712E+00
143	1.210E-02	8.698E+00	4.909E-01	5.643E+00
144	1.360E-02	8.841E+00	4.937E-01	5.584E+00
145	1.530E-02	8.770E+00	5.000E-01	5.702E+00
146	1.710E-02	8.413E+00	4.863E-01	5.781E+00
147	1.920E-02	9.554E+00	5.175E-01	5.417E+00
148	2.160E-02	9.911E+00	5.252E-01	5.299E+00
149	2.420E-02	9.713E+00	5.201E-01	5.355E+00
150	2.720E-02	1.069E+01	5.408E-01	5.059E+00
151	3.050E-02	1.120E+01	5.565E-01	4.971E+00
152	3.430E-02	7.946E+00	4.715E-01	5.934E+00
153	3.850E-02	1.111E+01	5.593E-01	5.032E+00
154	4.320E-02	1.198E+01	5.888E-01	4.915E+00
155	4.850E-02	1.393E+01	6.288E-01	4.515E+00
156	5.440E-02	1.212E+01	5.829E-01	4.808E+00
157	6.110E-02	1.550E+01	6.712E-01	4.330E+00
158	6.860E-02	1.661E+01	6.935E-01	4.175E+00
159	7.700E-02	1.763E+01	7.188E-01	4.078E+00
160	8.650E-02	1.429E+01	6.452E-01	4.515E+00
161	9.710E-02	1.874E+01	7.435E-01	3.968E+00
162	1.090E-01	2.205E+01	8.117E-01	3.682E+00
163	1.220E-01	2.696E+01	9.026E-01	3.348E+00
164	1.370E-01	2.530E+01	8.710E-01	3.443E+00
165	1.540E-01	2.614E+01	8.855E-01	3.388E+00
166	1.730E-01	2.692E+01	9.078E-01	3.372E+00
167	1.940E-01	2.742E+01	9.092E-01	3.316E+00

168	2.180E-01	3.142E+01	9.856E-01	3.137E+00
169	2.450E-01	3.661E+01	1.070E+00	2.924E+00
170	2.750E-01	3.841E+01	1.111E+00	2.892E+00
171	3.090E-01	4.306E+01	1.187E+00	2.755E+00
172	3.460E-01	3.961E+01	1.131E+00	2.856E+00
173	3.890E-01	3.834E+01	1.113E+00	2.904E+00
174	4.370E-01	4.298E+01	1.186E+00	2.759E+00
175	4.900E-01	5.209E+01	1.336E+00	2.565E+00
176	5.500E-01	5.934E+01	1.450E+00	2.444E+00
177	6.180E-01	6.267E+01	1.508E+00	2.406E+00
178	6.940E-01	7.163E+01	1.654E+00	2.309E+00
179	7.790E-01	7.163E+01	1.654E+00	2.309E+00
180	8.740E-01	6.335E+01	1.525E+00	2.407E+00
181	9.810E-01	6.123E+01	1.503E+00	2.454E+00
182	1.100E+00	6.641E+01	1.588E+00	2.391E+00
183	1.240E+00	6.766E+01	1.607E+00	2.375E+00
184	1.390E+00	7.017E+01	1.645E+00	2.344E+00
185	1.560E+00	6.769E+01	1.597E+00	2.359E+00
186	1.750E+00	6.505E+01	1.555E+00	2.391E+00
187	1.960E+00	6.444E+01	1.541E+00	2.391E+00
188	2.210E+00	6.750E+01	1.588E+00	2.352E+00
189	2.480E+00	6.704E+01	1.544E+00	2.303E+00
190	2.780E+00	5.611E+01	1.372E+00	2.445E+00
191	3.120E+00	4.773E+01	1.236E+00	2.590E+00
192	3.500E+00	4.081E+01	1.125E+00	2.756E+00
193	3.930E+00	3.694E+01	1.054E+00	2.854E+00
194	4.410E+00	2.889E+01	9.161E-01	3.171E+00
195	4.960E+00	2.286E+01	8.044E-01	3.519E+00
196	5.560E+00	1.590E+01	6.598E-01	4.149E+00
197	6.240E+00	1.233E+01	5.926E-01	4.805E+00
198	7.010E+00	8.115E+00	4.768E-01	5.875E+00
199	7.870E+00	5.408E+00	3.831E-01	7.084E+00
200	8.840E+00	2.715E+00	2.752E-01	1.014E+01
201	9.920E+00	1.528E+00	2.124E-01	1.390E+01
	1.110E+01			

B. INTEGRAL QUANTITIES OUTPUT FILE FOR THE VEHICLE SURROGATE ASSEMBLY.

*** Table 3: Fluence rate uncertainty due to measurement uncertainty ***

	Energy	Fluence Rate	Fluence rate unc.	% Fluence rate unc.
1	1.000E-10	4.210E-02	0.000E+00	0.000E+00
2	1.000E-09	4.092E-03	6.165E-05	1.507E+00
3	1.120E-09	6.167E-03	9.291E-05	1.507E+00
4	1.260E-09	5.232E-03	7.882E-05	1.507E+00

5	1.410E-09	1.640E-02	2.470E-04	1.507E+00
6	1.590E-09	1.023E-02	1.541E-04	1.507E+00
7	1.780E-09	1.306E-02	1.968E-04	1.507E+00
8	2.000E-09	2.721E-02	4.100E-04	1.507E+00
9	2.250E-09	4.940E-02	7.442E-04	1.507E+00
10	2.520E-09	5.875E-02	8.851E-04	1.507E+00
11	2.830E-09	7.483E-02	1.127E-03	1.507E+00
12	3.180E-09	4.618E-02	6.957E-04	1.507E+00
13	3.570E-09	5.407E-02	8.146E-04	1.507E+00
14	4.010E-09	1.526E-01	2.299E-03	1.507E+00
15	4.500E-09	2.104E-01	3.171E-03	1.507E+00
16	5.050E-09	1.251E-01	1.885E-03	1.507E+00
17	5.670E-09	2.642E-01	3.981E-03	1.507E+00
18	6.360E-09	3.391E-01	5.108E-03	1.507E+00
19	7.140E-09	3.741E-01	5.636E-03	1.507E+00
20	8.020E-09	5.173E-01	7.794E-03	1.507E+00
21	9.000E-09	6.318E-01	9.581E-03	1.516E+00
22	1.010E-08	7.843E-01	1.267E-02	1.615E+00
23	1.130E-08	1.053E+00	1.701E-02	1.615E+00
24	1.270E-08	1.252E+00	2.022E-02	1.615E+00
25	1.430E-08	1.605E+00	2.592E-02	1.615E+00
26	1.610E-08	2.123E+00	3.429E-02	1.615E+00
27	1.800E-08	2.459E+00	3.971E-02	1.615E+00
28	2.020E-08	2.997E+00	4.840E-02	1.615E+00
29	2.270E-08	3.559E+00	5.822E-02	1.636E+00
30	2.550E-08	3.842E+00	6.802E-02	1.770E+00
31	2.860E-08	4.293E+00	7.599E-02	1.770E+00
32	3.210E-08	4.876E+00	8.631E-02	1.770E+00
33	3.610E-08	5.379E+00	9.522E-02	1.770E+00
34	4.050E-08	6.413E+00	1.135E-01	1.770E+00
35	4.550E-08	6.731E+00	1.191E-01	1.770E+00
36	5.100E-08	7.155E+00	1.267E-01	1.770E+00
37	5.730E-08	7.160E+00	1.284E-01	1.793E+00
38	6.430E-08	6.986E+00	1.331E-01	1.905E+00
39	7.220E-08	7.088E+00	1.350E-01	1.905E+00
40	8.110E-08	6.221E+00	1.185E-01	1.905E+00
41	9.100E-08	5.813E+00	1.123E-01	1.932E+00
42	1.020E-07	4.971E+00	1.022E-01	2.056E+00
43	1.150E-07	4.589E+00	9.434E-02	2.056E+00
44	1.290E-07	3.518E+00	7.233E-02	2.056E+00
45	1.450E-07	3.110E+00	6.394E-02	2.056E+00
46	1.620E-07	2.575E+00	5.294E-02	2.056E+00
47	1.820E-07	2.101E+00	4.319E-02	2.056E+00
48	2.050E-07	2.078E+00	4.272E-02	2.056E+00
49	2.300E-07	1.969E+00	4.072E-02	2.068E+00

50	2.580E-07	2.111E+00	4.446E-02	2.106E+00
51	2.890E-07	2.014E+00	4.242E-02	2.106E+00
52	3.250E-07	2.176E+00	4.583E-02	2.106E+00
53	3.650E-07	2.164E+00	4.558E-02	2.106E+00
54	4.090E-07	2.297E+00	4.837E-02	2.106E+00
55	4.600E-07	2.162E+00	4.552E-02	2.106E+00
56	5.160E-07	2.023E+00	4.261E-02	2.106E+00
57	5.790E-07	2.123E+00	4.471E-02	2.106E+00
58	6.500E-07	1.923E+00	4.050E-02	2.106E+00
59	7.300E-07	2.285E+00	4.812E-02	2.106E+00
60	8.190E-07	2.020E+00	4.255E-02	2.106E+00
61	9.200E-07	2.068E+00	4.202E-02	2.032E+00
62	1.030E-06	3.317E+00	6.085E-02	1.834E+00
63	1.160E-06	3.192E+00	5.855E-02	1.834E+00
64	1.300E-06	3.248E+00	5.958E-02	1.834E+00
65	1.460E-06	3.188E+00	5.847E-02	1.834E+00
66	1.640E-06	3.460E+00	6.347E-02	1.834E+00
67	1.840E-06	3.218E+00	5.903E-02	1.834E+00
68	2.070E-06	3.538E+00	6.490E-02	1.834E+00
69	2.320E-06	3.417E+00	6.268E-02	1.834E+00
70	2.610E-06	3.378E+00	6.196E-02	1.834E+00
71	2.920E-06	3.408E+00	6.252E-02	1.834E+00
72	3.280E-06	3.036E+00	5.570E-02	1.834E+00
73	3.690E-06	3.300E+00	6.054E-02	1.834E+00
74	4.140E-06	3.283E+00	6.022E-02	1.834E+00
75	4.650E-06	3.663E+00	6.720E-02	1.834E+00
76	5.220E-06	3.157E+00	5.792E-02	1.834E+00
77	5.850E-06	3.478E+00	6.379E-02	1.834E+00
78	6.570E-06	3.196E+00	5.863E-02	1.834E+00
79	7.380E-06	3.382E+00	6.204E-02	1.834E+00
80	8.280E-06	3.257E+00	5.974E-02	1.834E+00
81	9.300E-06	4.199E+00	7.246E-02	1.726E+00
82	1.040E-05	5.105E+00	7.843E-02	1.536E+00
83	1.170E-05	4.526E+00	6.953E-02	1.536E+00
84	1.320E-05	5.145E+00	7.905E-02	1.536E+00
85	1.480E-05	5.254E+00	8.072E-02	1.536E+00
86	1.660E-05	4.944E+00	7.596E-02	1.536E+00
87	1.860E-05	5.260E+00	8.081E-02	1.536E+00
88	2.090E-05	4.824E+00	7.411E-02	1.536E+00
89	2.350E-05	4.749E+00	7.296E-02	1.536E+00
90	2.630E-05	5.294E+00	8.134E-02	1.536E+00
91	2.960E-05	4.858E+00	7.464E-02	1.536E+00
92	3.320E-05	4.382E+00	6.733E-02	1.536E+00
93	3.730E-05	5.736E+00	8.812E-02	1.536E+00
94	4.180E-05	5.518E+00	8.477E-02	1.536E+00

95	4.700E-05	5.644E+00	8.671E-02	1.536E+00
96	5.270E-05	6.023E+00	9.253E-02	1.536E+00
97	5.920E-05	5.260E+00	8.081E-02	1.536E+00
98	6.640E-05	5.495E+00	8.442E-02	1.536E+00
99	7.460E-05	5.593E+00	8.592E-02	1.536E+00
100	8.370E-05	5.076E+00	7.799E-02	1.536E+00
101	9.400E-05	6.105E+00	8.650E-02	1.417E+00
102	1.060E-04	6.904E+00	8.956E-02	1.297E+00
103	1.180E-04	6.494E+00	8.424E-02	1.297E+00
104	1.330E-04	6.835E+00	8.868E-02	1.297E+00
105	1.490E-04	6.378E+00	8.274E-02	1.297E+00
106	1.680E-04	6.747E+00	8.752E-02	1.297E+00
107	1.880E-04	7.040E+00	9.134E-02	1.297E+00
108	2.110E-04	6.671E+00	8.655E-02	1.297E+00
109	2.370E-04	6.904E+00	8.956E-02	1.297E+00
110	2.660E-04	6.398E+00	8.300E-02	1.297E+00
111	2.990E-04	7.314E+00	9.488E-02	1.297E+00
112	3.350E-04	6.774E+00	8.788E-02	1.297E+00
113	3.770E-04	7.109E+00	9.222E-02	1.297E+00
114	4.230E-04	6.630E+00	8.602E-02	1.297E+00
115	4.750E-04	7.929E+00	1.029E-01	1.297E+00
116	5.330E-04	7.724E+00	1.002E-01	1.297E+00
117	5.980E-04	7.724E+00	1.002E-01	1.297E+00
118	6.720E-04	7.519E+00	9.755E-02	1.297E+00
119	7.540E-04	6.835E+00	8.868E-02	1.297E+00
120	8.460E-04	6.972E+00	9.045E-02	1.297E+00
121	9.500E-04	8.487E+00	1.029E-01	1.212E+00
122	1.070E-03	8.401E+00	9.672E-02	1.151E+00
123	1.200E-03	9.082E+00	1.046E-01	1.151E+00
124	1.340E-03	9.536E+00	1.098E-01	1.151E+00
125	1.510E-03	9.234E+00	1.063E-01	1.151E+00
126	1.690E-03	8.401E+00	9.672E-02	1.151E+00
127	1.900E-03	9.007E+00	1.037E-01	1.151E+00
128	2.140E-03	9.234E+00	1.063E-01	1.151E+00
129	2.400E-03	8.250E+00	9.498E-02	1.151E+00
130	2.690E-03	8.704E+00	1.002E-01	1.151E+00
131	3.020E-03	9.688E+00	1.115E-01	1.151E+00
132	3.390E-03	9.764E+00	1.124E-01	1.151E+00
133	3.810E-03	9.536E+00	1.098E-01	1.151E+00
134	4.270E-03	1.022E+01	1.176E-01	1.151E+00
135	4.800E-03	9.764E+00	1.124E-01	1.151E+00
136	5.390E-03	9.688E+00	1.115E-01	1.151E+00
137	6.050E-03	9.385E+00	1.080E-01	1.151E+00
138	6.790E-03	1.105E+01	1.272E-01	1.151E+00
139	7.620E-03	9.839E+00	1.133E-01	1.151E+00

140	8.550E-03	9.839E+00	1.133E-01	1.151E+00
141	9.600E-03	1.001E+01	1.134E-01	1.133E+00
142	1.080E-02	1.111E+01	1.249E-01	1.124E+00
143	1.210E-02	1.103E+01	1.240E-01	1.124E+00
144	1.360E-02	1.111E+01	1.249E-01	1.124E+00
145	1.530E-02	1.266E+01	1.423E-01	1.124E+00
146	1.710E-02	1.274E+01	1.432E-01	1.124E+00
147	1.920E-02	1.367E+01	1.537E-01	1.124E+00
148	2.160E-02	1.251E+01	1.406E-01	1.124E+00
149	2.420E-02	2.198E+01	2.426E-01	1.104E+00
150	2.720E-02	4.077E+00	4.464E-02	1.095E+00
151	3.050E-02	1.049E+01	1.148E-01	1.095E+00
152	3.430E-02	1.136E+01	1.243E-01	1.095E+00
153	3.850E-02	1.583E+01	1.757E-01	1.110E+00
154	4.320E-02	1.387E+01	1.547E-01	1.115E+00
155	4.850E-02	1.759E+01	1.962E-01	1.115E+00
156	5.440E-02	1.696E+01	1.892E-01	1.115E+00
157	6.110E-02	1.774E+01	1.977E-01	1.114E+00
158	6.860E-02	2.183E+01	2.431E-01	1.114E+00
159	7.700E-02	2.055E+01	2.289E-01	1.114E+00
160	8.650E-02	1.673E+01	1.863E-01	1.114E+00
161	9.710E-02	2.190E+01	2.502E-01	1.142E+00
162	1.090E-01	2.341E+01	2.696E-01	1.151E+00
163	1.220E-01	3.249E+01	3.741E-01	1.151E+00
164	1.370E-01	2.118E+01	2.439E-01	1.151E+00
165	1.540E-01	2.688E+01	3.223E-01	1.199E+00
166	1.730E-01	3.026E+01	3.673E-01	1.214E+00
167	1.940E-01	2.809E+01	3.410E-01	1.214E+00
168	2.180E-01	3.266E+01	3.964E-01	1.214E+00
169	2.450E-01	4.055E+01	5.135E-01	1.266E+00
170	2.750E-01	3.794E+01	4.856E-01	1.280E+00
171	3.090E-01	4.299E+01	5.504E-01	1.280E+00
172	3.460E-01	4.698E+01	6.014E-01	1.280E+00
173	3.890E-01	3.734E+01	5.090E-01	1.363E+00
174	4.370E-01	4.619E+01	6.385E-01	1.382E+00
175	4.900E-01	5.385E+01	7.444E-01	1.382E+00
176	5.500E-01	6.057E+01	8.372E-01	1.382E+00
177	6.180E-01	6.478E+01	9.597E-01	1.481E+00
178	6.940E-01	6.894E+01	1.035E+00	1.502E+00
179	7.790E-01	6.347E+01	9.531E-01	1.502E+00
180	8.740E-01	5.738E+01	8.618E-01	1.502E+00
181	9.810E-01	5.287E+01	8.427E-01	1.594E+00
182	1.100E+00	5.940E+01	9.571E-01	1.611E+00
183	1.240E+00	5.786E+01	9.322E-01	1.611E+00
184	1.390E+00	5.749E+01	9.262E-01	1.611E+00

185	1.560E+00	5.377E+01	8.677E-01	1.614E+00
186	1.750E+00	4.980E+01	8.037E-01	1.614E+00
187	1.960E+00	4.794E+01	7.737E-01	1.614E+00
188	2.210E+00	5.258E+01	8.487E-01	1.614E+00
189	2.480E+00	4.724E+01	6.934E-01	1.468E+00
190	2.780E+00	4.006E+01	5.811E-01	1.450E+00
191	3.120E+00	3.269E+01	4.741E-01	1.450E+00
192	3.500E+00	2.809E+01	4.074E-01	1.450E+00
193	3.930E+00	2.537E+01	3.276E-01	1.291E+00
194	4.410E+00	2.100E+01	2.672E-01	1.272E+00
195	4.960E+00	1.488E+01	1.893E-01	1.272E+00
196	5.560E+00	1.102E+01	1.402E-01	1.272E+00
197	6.240E+00	8.076E+00	8.154E-02	1.010E+00
198	7.010E+00	5.918E+00	5.819E-02	9.834E-01
199	7.870E+00	3.649E+00	3.588E-02	9.834E-01
200	8.840E+00	1.888E+00	1.857E-02	9.834E-01
201	9.920E+00	9.831E-01	7.784E-03	7.917E-01
	1.110E+01			

*** Table 4: Fluence rate uncertainty due to default spectrum uncertainty ***

	Energy	Fluence Rate	Fluence rate unc.	% Fluence rate unc.	% Default sp. unc.
1	1.000E-10	4.210E-02	2.109E-02	5.010E+01	5.010E+01
2	1.000E-09	4.092E-03	3.448E-03	8.425E+01	8.425E+01
3	1.120E-09	6.167E-03	6.167E-03	1.000E+02	1.000E+02
4	1.260E-09	5.232E-03	4.391E-03	8.393E+01	8.393E+01
5	1.410E-09	1.640E-02	8.702E-03	5.307E+01	5.307E+01
6	1.590E-09	1.023E-02	7.446E-03	7.279E+01	7.279E+01
7	1.780E-09	1.306E-02	5.934E-03	4.542E+01	4.542E+01
8	2.000E-09	2.721E-02	1.194E-02	4.386E+01	4.386E+01
9	2.250E-09	4.940E-02	1.525E-02	3.088E+01	3.088E+01
10	2.520E-09	5.875E-02	1.724E-02	2.935E+01	2.935E+01

11	2.830E-09	7.483E-02	2.271E-02	3.035E+01
3.035E+01				
12	3.180E-09	4.618E-02	1.507E-02	3.263E+01
3.263E+01				
13	3.570E-09	5.407E-02	1.542E-02	2.851E+01
2.851E+01				
14	4.010E-09	1.526E-01	2.959E-02	1.939E+01
1.939E+01				
15	4.500E-09	2.104E-01	3.267E-02	1.552E+01
1.552E+01				
16	5.050E-09	1.251E-01	2.417E-02	1.932E+01
1.932E+01				
17	5.670E-09	2.642E-01	3.523E-02	1.333E+01
1.333E+01				
18	6.360E-09	3.391E-01	4.191E-02	1.236E+01
1.236E+01				
19	7.140E-09	3.741E-01	4.105E-02	1.097E+01
1.097E+01				
20	8.020E-09	5.173E-01	4.984E-02	9.633E+00
9.630E+00				
21	9.000E-09	6.318E-01	5.707E-02	9.033E+00
9.030E+00				
22	1.010E-08	7.843E-01	6.372E-02	8.124E+00
8.120E+00				
23	1.130E-08	1.053E+00	7.146E-02	6.785E+00
6.780E+00				
24	1.270E-08	1.252E+00	7.908E-02	6.316E+00
6.310E+00				
25	1.430E-08	1.605E+00	8.967E-02	5.586E+00
5.580E+00				
26	1.610E-08	2.123E+00	1.021E-01	4.808E+00
4.800E+00				
27	1.800E-08	2.459E+00	1.089E-01	4.428E+00
4.420E+00				
28	2.020E-08	2.997E+00	1.243E-01	4.148E+00
4.140E+00				
29	2.270E-08	3.559E+00	1.341E-01	3.770E+00
3.760E+00				
30	2.550E-08	3.842E+00	1.384E-01	3.602E+00
3.590E+00				
31	2.860E-08	4.293E+00	1.439E-01	3.353E+00
3.340E+00				
32	3.210E-08	4.876E+00	1.552E-01	3.184E+00
3.170E+00				

33	3.610E-08	5.379E+00	1.600E-01	2.975E+00
2.960E+00				
34	4.050E-08	6.413E+00	1.786E-01	2.786E+00
2.770E+00				
35	4.550E-08	6.731E+00	1.828E-01	2.716E+00
2.700E+00				
36	5.100E-08	7.155E+00	1.915E-01	2.676E+00
2.660E+00				
37	5.730E-08	7.160E+00	1.881E-01	2.627E+00
2.610E+00				
38	6.430E-08	6.986E+00	1.871E-01	2.679E+00
2.660E+00				
39	7.220E-08	7.088E+00	1.878E-01	2.649E+00
2.630E+00				
40	8.110E-08	6.221E+00	1.759E-01	2.828E+00
2.810E+00				
41	9.100E-08	5.813E+00	1.788E-01	3.076E+00
3.060E+00				
42	1.020E-07	4.971E+00	1.634E-01	3.287E+00
3.270E+00				
43	1.150E-07	4.589E+00	1.608E-01	3.505E+00
3.490E+00				
44	1.290E-07	3.518E+00	1.447E-01	4.112E+00
4.100E+00				
45	1.450E-07	3.110E+00	1.390E-01	4.471E+00
4.460E+00				
46	1.620E-07	2.575E+00	1.269E-01	4.930E+00
4.920E+00				
47	1.820E-07	2.101E+00	1.220E-01	5.807E+00
5.800E+00				
48	2.050E-07	2.078E+00	1.240E-01	5.966E+00
5.960E+00				
49	2.300E-07	1.969E+00	1.242E-01	6.305E+00
6.300E+00				
50	2.580E-07	2.111E+00	1.356E-01	6.424E+00
6.420E+00				
51	2.890E-07	2.014E+00	1.326E-01	6.584E+00
6.580E+00				
52	3.250E-07	2.176E+00	1.424E-01	6.543E+00
6.540E+00				
53	3.650E-07	2.164E+00	1.403E-01	6.484E+00
6.480E+00				
54	4.090E-07	2.297E+00	1.500E-01	6.533E+00
6.530E+00				

55	4.600E-07	2.162E+00	1.442E-01	6.673E+00
6.670E+00				
56	5.160E-07	2.023E+00	1.372E-01	6.783E+00
6.780E+00				
57	5.790E-07	2.123E+00	1.417E-01	6.673E+00
6.670E+00				
58	6.500E-07	1.923E+00	1.351E-01	7.023E+00
7.020E+00				
59	7.300E-07	2.285E+00	1.472E-01	6.443E+00
6.440E+00				
60	8.190E-07	2.020E+00	1.397E-01	6.913E+00
6.910E+00				
61	9.200E-07	2.068E+00	1.485E-01	7.181E+00
7.180E+00				
62	1.030E-06	3.317E+00	2.182E-01	6.577E+00
6.580E+00				
63	1.160E-06	3.192E+00	2.154E-01	6.747E+00
6.750E+00				
64	1.300E-06	3.248E+00	2.185E-01	6.727E+00
6.730E+00				
65	1.460E-06	3.188E+00	2.183E-01	6.847E+00
6.850E+00				
66	1.640E-06	3.460E+00	2.379E-01	6.875E+00
6.880E+00				
67	1.840E-06	3.218E+00	2.168E-01	6.737E+00
6.740E+00				
68	2.070E-06	3.538E+00	2.302E-01	6.507E+00
6.510E+00				
69	2.320E-06	3.417E+00	2.298E-01	6.726E+00
6.730E+00				
70	2.610E-06	3.378E+00	2.272E-01	6.726E+00
6.730E+00				
71	2.920E-06	3.408E+00	2.347E-01	6.886E+00
6.890E+00				
72	3.280E-06	3.036E+00	2.164E-01	7.126E+00
7.130E+00				
73	3.690E-06	3.300E+00	2.256E-01	6.836E+00
6.840E+00				
74	4.140E-06	3.283E+00	2.215E-01	6.747E+00
6.750E+00				
75	4.650E-06	3.663E+00	2.453E-01	6.695E+00
6.700E+00				
76	5.220E-06	3.157E+00	2.184E-01	6.917E+00
6.920E+00				

77	5.850E-06	3.478E+00	2.322E-01	6.676E+00
6.680E+00				
78	6.570E-06	3.196E+00	2.252E-01	7.046E+00
7.050E+00				
79	7.380E-06	3.382E+00	2.322E-01	6.866E+00
6.870E+00				
80	8.280E-06	3.257E+00	2.230E-01	6.846E+00
6.850E+00				
81	9.300E-06	4.199E+00	2.798E-01	6.664E+00
6.670E+00				
82	1.040E-05	5.105E+00	3.274E-01	6.413E+00
6.420E+00				
83	1.170E-05	4.526E+00	3.065E-01	6.774E+00
6.780E+00				
84	1.320E-05	5.145E+00	3.310E-01	6.433E+00
6.440E+00				
85	1.480E-05	5.254E+00	3.354E-01	6.383E+00
6.390E+00				
86	1.660E-05	4.944E+00	3.186E-01	6.443E+00
6.450E+00				
87	1.860E-05	5.260E+00	3.331E-01	6.333E+00
6.340E+00				
88	2.090E-05	4.824E+00	3.209E-01	6.653E+00
6.660E+00				
89	2.350E-05	4.749E+00	3.165E-01	6.663E+00
6.670E+00				
90	2.630E-05	5.294E+00	3.427E-01	6.472E+00
6.480E+00				
91	2.960E-05	4.858E+00	3.232E-01	6.653E+00
6.660E+00				
92	3.320E-05	4.382E+00	2.995E-01	6.834E+00
6.840E+00				
93	3.730E-05	5.736E+00	3.512E-01	6.122E+00
6.130E+00				
94	4.180E-05	5.518E+00	3.450E-01	6.252E+00
6.260E+00				
95	4.700E-05	5.644E+00	3.473E-01	6.152E+00
6.160E+00				
96	5.270E-05	6.023E+00	3.579E-01	5.942E+00
5.950E+00				
97	5.920E-05	5.260E+00	3.378E-01	6.422E+00
6.430E+00				
98	6.640E-05	5.495E+00	3.387E-01	6.163E+00
6.170E+00				

99	7.460E-05	5.593E+00	3.452E-01	6.172E+00
6.180E+00				
100	8.370E-05	5.076E+00	3.296E-01	6.493E+00
6.500E+00				
101	9.400E-05	6.105E+00	3.823E-01	6.262E+00
6.270E+00				
102	1.060E-04	6.904E+00	4.178E-01	6.052E+00
6.060E+00				
103	1.180E-04	6.494E+00	4.028E-01	6.203E+00
6.210E+00				
104	1.330E-04	6.835E+00	4.178E-01	6.112E+00
6.120E+00				
105	1.490E-04	6.378E+00	4.064E-01	6.372E+00
6.380E+00				
106	1.680E-04	6.747E+00	4.151E-01	6.152E+00
6.160E+00				
107	1.880E-04	7.040E+00	4.338E-01	6.162E+00
6.170E+00				
108	2.110E-04	6.671E+00	4.131E-01	6.192E+00
6.200E+00				
109	2.370E-04	6.904E+00	4.282E-01	6.202E+00
6.210E+00				
110	2.660E-04	6.398E+00	4.020E-01	6.283E+00
6.290E+00				
111	2.990E-04	7.314E+00	4.302E-01	5.882E+00
5.890E+00				
112	3.350E-04	6.774E+00	4.215E-01	6.222E+00
6.230E+00				
113	3.770E-04	7.109E+00	4.288E-01	6.032E+00
6.040E+00				
114	4.230E-04	6.630E+00	4.093E-01	6.172E+00
6.180E+00				
115	4.750E-04	7.929E+00	4.521E-01	5.701E+00
5.710E+00				
116	5.330E-04	7.724E+00	4.473E-01	5.792E+00
5.800E+00				
117	5.980E-04	7.724E+00	4.558E-01	5.901E+00
5.910E+00				
118	6.720E-04	7.519E+00	4.520E-01	6.011E+00
6.020E+00				
119	7.540E-04	6.835E+00	4.144E-01	6.062E+00
6.070E+00				
120	8.460E-04	6.972E+00	4.178E-01	5.992E+00
6.000E+00				

121	9.500E-04	8.487E+00	4.839E-01	5.702E+00
5.710E+00				
122	1.070E-03	8.401E+00	4.933E-01	5.872E+00
5.880E+00				
123	1.200E-03	9.082E+00	5.088E-01	5.602E+00
5.610E+00				
124	1.340E-03	9.536E+00	5.237E-01	5.492E+00
5.500E+00				
125	1.510E-03	9.234E+00	5.154E-01	5.582E+00
5.590E+00				
126	1.690E-03	8.401E+00	5.009E-01	5.962E+00
5.970E+00				
127	1.900E-03	9.007E+00	5.171E-01	5.741E+00
5.750E+00				
128	2.140E-03	9.234E+00	5.182E-01	5.612E+00
5.620E+00				
129	2.400E-03	8.250E+00	4.910E-01	5.952E+00
5.960E+00				
130	2.690E-03	8.704E+00	4.989E-01	5.732E+00
5.740E+00				
131	3.020E-03	9.688E+00	5.330E-01	5.501E+00
5.510E+00				
132	3.390E-03	9.764E+00	5.284E-01	5.412E+00
5.420E+00				
133	3.810E-03	9.536E+00	5.180E-01	5.432E+00
5.440E+00				
134	4.270E-03	1.022E+01	5.427E-01	5.311E+00
5.320E+00				
135	4.800E-03	9.764E+00	5.342E-01	5.471E+00
5.480E+00				
136	5.390E-03	9.688E+00	5.358E-01	5.531E+00
5.540E+00				
137	6.050E-03	9.385E+00	5.257E-01	5.601E+00
5.610E+00				
138	6.790E-03	1.105E+01	5.692E-01	5.151E+00
5.160E+00				
139	7.620E-03	9.839E+00	5.364E-01	5.451E+00
5.460E+00				
140	8.550E-03	9.839E+00	5.315E-01	5.401E+00
5.410E+00				
141	9.600E-03	1.001E+01	5.338E-01	5.332E+00
5.340E+00				
142	1.080E-02	1.111E+01	5.766E-01	5.191E+00
5.200E+00				

143	1.210E-02	1.103E+01	5.748E-01	5.211E+00
5.220E+00				
144	1.360E-02	1.111E+01	5.755E-01	5.181E+00
5.190E+00				
145	1.530E-02	1.266E+01	6.141E-01	4.850E+00
4.860E+00				
146	1.710E-02	1.274E+01	6.191E-01	4.860E+00
4.870E+00				
147	1.920E-02	1.367E+01	6.343E-01	4.640E+00
4.650E+00				
148	2.160E-02	1.251E+01	6.103E-01	4.880E+00
4.890E+00				
149	2.420E-02	2.198E+01	8.126E-01	3.698E+00
3.710E+00				
150	2.720E-02	4.077E+00	3.492E-01	8.565E+00
8.570E+00				
151	3.050E-02	1.049E+01	5.655E-01	5.391E+00
5.400E+00				
152	3.430E-02	1.136E+01	5.894E-01	5.191E+00
5.200E+00				
153	3.850E-02	1.583E+01	7.011E-01	4.429E+00
4.440E+00				
154	4.320E-02	1.387E+01	6.449E-01	4.650E+00
4.660E+00				
155	4.850E-02	1.759E+01	7.317E-01	4.158E+00
4.170E+00				
156	5.440E-02	1.696E+01	7.172E-01	4.229E+00
4.240E+00				
157	6.110E-02	1.774E+01	7.395E-01	4.168E+00
4.180E+00				
158	6.860E-02	2.183E+01	8.223E-01	3.767E+00
3.780E+00				
159	7.700E-02	2.055E+01	7.909E-01	3.848E+00
3.860E+00				
160	8.650E-02	1.673E+01	7.125E-01	4.259E+00
4.270E+00				
161	9.710E-02	2.190E+01	8.249E-01	3.766E+00
3.780E+00				
162	1.090E-01	2.341E+01	8.443E-01	3.606E+00
3.620E+00				
163	1.220E-01	3.249E+01	9.921E-01	3.053E+00
3.070E+00				
164	1.370E-01	2.118E+01	8.042E-01	3.796E+00
3.810E+00				

165	1.540E-01	2.688E+01	8.936E-01	3.324E+00
3.340E+00				
166	1.730E-01	3.026E+01	9.479E-01	3.132E+00
3.150E+00				
167	1.940E-01	2.809E+01	9.084E-01	3.233E+00
3.250E+00				
168	2.180E-01	3.266E+01	9.805E-01	3.002E+00
3.020E+00				
169	2.450E-01	4.055E+01	1.074E+00	2.649E+00
2.670E+00				
170	2.750E-01	3.794E+01	1.043E+00	2.749E+00
2.770E+00				
171	3.090E-01	4.299E+01	1.112E+00	2.587E+00
2.610E+00				
172	3.460E-01	4.698E+01	1.168E+00	2.486E+00
2.510E+00				
173	3.890E-01	3.734E+01	1.018E+00	2.727E+00
2.750E+00				
174	4.370E-01	4.619E+01	1.133E+00	2.454E+00
2.480E+00				
175	4.900E-01	5.385E+01	1.213E+00	2.252E+00
2.280E+00				
176	5.500E-01	6.057E+01	1.284E+00	2.120E+00
2.150E+00				
177	6.180E-01	6.478E+01	1.281E+00	1.977E+00
2.010E+00				
178	6.940E-01	6.894E+01	1.321E+00	1.915E+00
1.950E+00				
179	7.790E-01	6.347E+01	1.273E+00	2.007E+00
2.040E+00				
180	8.740E-01	5.738E+01	1.204E+00	2.099E+00
2.130E+00				
181	9.810E-01	5.287E+01	1.110E+00	2.100E+00
2.130E+00				
182	1.100E+00	5.940E+01	1.175E+00	1.977E+00
2.010E+00				
183	1.240E+00	5.786E+01	1.150E+00	1.988E+00
2.020E+00				
184	1.390E+00	5.749E+01	1.149E+00	1.998E+00
2.030E+00				
185	1.560E+00	5.377E+01	1.082E+00	2.012E+00
2.040E+00				
186	1.750E+00	4.980E+01	1.042E+00	2.093E+00
2.120E+00				

187	1.960E+00	4.794E+01	1.014E+00	2.114E+00
2.140E+00				
188	2.210E+00	5.258E+01	1.069E+00	2.032E+00
2.060E+00				
189	2.480E+00	4.724E+01	1.020E+00	2.158E+00
2.180E+00				
190	2.780E+00	4.006E+01	9.456E-01	2.360E+00
2.380E+00				
191	3.120E+00	3.269E+01	8.539E-01	2.612E+00
2.630E+00				
192	3.500E+00	2.809E+01	7.902E-01	2.814E+00
2.830E+00				
193	3.930E+00	2.537E+01	7.630E-01	3.007E+00
3.020E+00				
194	4.410E+00	2.100E+01	6.990E-01	3.328E+00
3.340E+00				
195	4.960E+00	1.488E+01	5.848E-01	3.930E+00
3.940E+00				
196	5.560E+00	1.102E+01	5.028E-01	4.562E+00
4.570E+00				
197	6.240E+00	8.076E+00	4.526E-01	5.605E+00
5.610E+00				
198	7.010E+00	5.918E+00	3.856E-01	6.516E+00
6.520E+00				
199	7.870E+00	3.649E+00	3.006E-01	8.237E+00
8.240E+00				
200	8.840E+00	1.888E+00	2.214E-01	1.173E+01
1.173E+01				
201	9.920E+00	9.831E-01	1.632E-01	1.660E+01
1.660E+01				
1.110E+01				

*** Table 5: Fluence rate uncertainty due to measurement and default spectrum uncertainty ***

	Energy	Fluence Rate	Fluence rate unc.	% Fluence rate unc.
1	1.000E-10	4.210E-02	2.109E-02	5.010E+01
2	1.000E-09	4.092E-03	3.448E-03	8.426E+01
3	1.120E-09	6.167E-03	6.168E-03	1.000E+02
4	1.260E-09	5.232E-03	4.392E-03	8.394E+01
5	1.410E-09	1.640E-02	8.705E-03	5.309E+01
6	1.590E-09	1.023E-02	7.448E-03	7.281E+01
7	1.780E-09	1.306E-02	5.938E-03	4.545E+01
8	2.000E-09	2.721E-02	1.194E-02	4.389E+01

9	2.250E-09	4.940E-02	1.527E-02	3.092E+01
10	2.520E-09	5.875E-02	1.727E-02	2.939E+01
11	2.830E-09	7.483E-02	2.274E-02	3.039E+01
12	3.180E-09	4.618E-02	1.509E-02	3.267E+01
13	3.570E-09	5.407E-02	1.544E-02	2.855E+01
14	4.010E-09	1.526E-01	2.967E-02	1.945E+01
15	4.500E-09	2.104E-01	3.282E-02	1.559E+01
16	5.050E-09	1.251E-01	2.424E-02	1.938E+01
17	5.670E-09	2.642E-01	3.545E-02	1.342E+01
18	6.360E-09	3.391E-01	4.222E-02	1.245E+01
19	7.140E-09	3.741E-01	4.144E-02	1.108E+01
20	8.020E-09	5.173E-01	5.044E-02	9.750E+00
21	9.000E-09	6.318E-01	5.787E-02	9.160E+00
22	1.010E-08	7.843E-01	6.497E-02	8.283E+00
23	1.130E-08	1.053E+00	7.346E-02	6.975E+00
24	1.270E-08	1.252E+00	8.162E-02	6.519E+00
25	1.430E-08	1.605E+00	9.334E-02	5.815E+00
26	1.610E-08	2.123E+00	1.077E-01	5.071E+00
27	1.800E-08	2.459E+00	1.159E-01	4.714E+00
28	2.020E-08	2.997E+00	1.334E-01	4.452E+00
29	2.270E-08	3.559E+00	1.462E-01	4.109E+00
30	2.550E-08	3.842E+00	1.542E-01	4.013E+00
31	2.860E-08	4.293E+00	1.628E-01	3.792E+00
32	3.210E-08	4.876E+00	1.776E-01	3.643E+00
33	3.610E-08	5.379E+00	1.862E-01	3.462E+00
34	4.050E-08	6.413E+00	2.117E-01	3.300E+00
35	4.550E-08	6.731E+00	2.182E-01	3.242E+00
36	5.100E-08	7.155E+00	2.296E-01	3.208E+00
37	5.730E-08	7.160E+00	2.278E-01	3.181E+00
38	6.430E-08	6.986E+00	2.296E-01	3.287E+00
39	7.220E-08	7.088E+00	2.313E-01	3.263E+00
40	8.110E-08	6.221E+00	2.121E-01	3.409E+00
41	9.100E-08	5.813E+00	2.111E-01	3.632E+00
42	1.020E-07	4.971E+00	1.927E-01	3.877E+00
43	1.150E-07	4.589E+00	1.865E-01	4.064E+00
44	1.290E-07	3.518E+00	1.617E-01	4.597E+00
45	1.450E-07	3.110E+00	1.530E-01	4.921E+00
46	1.620E-07	2.575E+00	1.375E-01	5.341E+00
47	1.820E-07	2.101E+00	1.294E-01	6.160E+00
48	2.050E-07	2.078E+00	1.311E-01	6.311E+00
49	2.300E-07	1.969E+00	1.307E-01	6.636E+00
50	2.580E-07	2.111E+00	1.427E-01	6.761E+00
51	2.890E-07	2.014E+00	1.393E-01	6.913E+00
52	3.250E-07	2.176E+00	1.496E-01	6.874E+00
53	3.650E-07	2.164E+00	1.476E-01	6.817E+00

54	4.090E-07	2.297E+00	1.576E-01	6.864E+00
55	4.600E-07	2.162E+00	1.512E-01	6.997E+00
56	5.160E-07	2.023E+00	1.437E-01	7.103E+00
57	5.790E-07	2.123E+00	1.486E-01	6.997E+00
58	6.500E-07	1.923E+00	1.410E-01	7.332E+00
59	7.300E-07	2.285E+00	1.549E-01	6.779E+00
60	8.190E-07	2.020E+00	1.460E-01	7.226E+00
61	9.200E-07	2.068E+00	1.543E-01	7.463E+00
62	1.030E-06	3.317E+00	2.265E-01	6.828E+00
63	1.160E-06	3.192E+00	2.232E-01	6.992E+00
64	1.300E-06	3.248E+00	2.265E-01	6.973E+00
65	1.460E-06	3.188E+00	2.260E-01	7.088E+00
66	1.640E-06	3.460E+00	2.462E-01	7.116E+00
67	1.840E-06	3.218E+00	2.247E-01	6.982E+00
68	2.070E-06	3.538E+00	2.392E-01	6.760E+00
69	2.320E-06	3.417E+00	2.382E-01	6.972E+00
70	2.610E-06	3.378E+00	2.355E-01	6.972E+00
71	2.920E-06	3.408E+00	2.429E-01	7.126E+00
72	3.280E-06	3.036E+00	2.234E-01	7.359E+00
73	3.690E-06	3.300E+00	2.336E-01	7.078E+00
74	4.140E-06	3.283E+00	2.295E-01	6.992E+00
75	4.650E-06	3.663E+00	2.543E-01	6.942E+00
76	5.220E-06	3.157E+00	2.259E-01	7.156E+00
77	5.850E-06	3.478E+00	2.408E-01	6.923E+00
78	6.570E-06	3.196E+00	2.327E-01	7.281E+00
79	7.380E-06	3.382E+00	2.404E-01	7.107E+00
80	8.280E-06	3.257E+00	2.308E-01	7.088E+00
81	9.300E-06	4.199E+00	2.890E-01	6.884E+00
82	1.040E-05	5.105E+00	3.367E-01	6.594E+00
83	1.170E-05	4.526E+00	3.143E-01	6.946E+00
84	1.320E-05	5.145E+00	3.403E-01	6.614E+00
85	1.480E-05	5.254E+00	3.449E-01	6.565E+00
86	1.660E-05	4.944E+00	3.275E-01	6.624E+00
87	1.860E-05	5.260E+00	3.428E-01	6.516E+00
88	2.090E-05	4.824E+00	3.294E-01	6.828E+00
89	2.350E-05	4.749E+00	3.248E-01	6.838E+00
90	2.630E-05	5.294E+00	3.522E-01	6.652E+00
91	2.960E-05	4.858E+00	3.317E-01	6.828E+00
92	3.320E-05	4.382E+00	3.070E-01	7.004E+00
93	3.730E-05	5.736E+00	3.621E-01	6.312E+00
94	4.180E-05	5.518E+00	3.553E-01	6.438E+00
95	4.700E-05	5.644E+00	3.579E-01	6.341E+00
96	5.270E-05	6.023E+00	3.697E-01	6.138E+00
97	5.920E-05	5.260E+00	3.473E-01	6.604E+00
98	6.640E-05	5.495E+00	3.490E-01	6.351E+00

99	7.460E-05	5.593E+00	3.557E-01	6.361E+00
100	8.370E-05	5.076E+00	3.387E-01	6.672E+00
101	9.400E-05	6.105E+00	3.920E-01	6.420E+00
102	1.060E-04	6.904E+00	4.273E-01	6.190E+00
103	1.180E-04	6.494E+00	4.115E-01	6.337E+00
104	1.330E-04	6.835E+00	4.271E-01	6.248E+00
105	1.490E-04	6.378E+00	4.147E-01	6.503E+00
106	1.680E-04	6.747E+00	4.242E-01	6.288E+00
107	1.880E-04	7.040E+00	4.433E-01	6.297E+00
108	2.110E-04	6.671E+00	4.221E-01	6.327E+00
109	2.370E-04	6.904E+00	4.374E-01	6.336E+00
110	2.660E-04	6.398E+00	4.104E-01	6.415E+00
111	2.990E-04	7.314E+00	4.405E-01	6.023E+00
112	3.350E-04	6.774E+00	4.305E-01	6.356E+00
113	3.770E-04	7.109E+00	4.386E-01	6.170E+00
114	4.230E-04	6.630E+00	4.182E-01	6.307E+00
115	4.750E-04	7.929E+00	4.636E-01	5.847E+00
116	5.330E-04	7.724E+00	4.584E-01	5.935E+00
117	5.980E-04	7.724E+00	4.667E-01	6.042E+00
118	6.720E-04	7.519E+00	4.624E-01	6.150E+00
119	7.540E-04	6.835E+00	4.238E-01	6.200E+00
120	8.460E-04	6.972E+00	4.275E-01	6.131E+00
121	9.500E-04	8.487E+00	4.947E-01	5.829E+00
122	1.070E-03	8.401E+00	5.027E-01	5.984E+00
123	1.200E-03	9.082E+00	5.194E-01	5.719E+00
124	1.340E-03	9.536E+00	5.351E-01	5.611E+00
125	1.510E-03	9.234E+00	5.262E-01	5.699E+00
126	1.690E-03	8.401E+00	5.101E-01	6.072E+00
127	1.900E-03	9.007E+00	5.274E-01	5.856E+00
128	2.140E-03	9.234E+00	5.289E-01	5.728E+00
129	2.400E-03	8.250E+00	5.001E-01	6.062E+00
130	2.690E-03	8.704E+00	5.089E-01	5.846E+00
131	3.020E-03	9.688E+00	5.445E-01	5.620E+00
132	3.390E-03	9.764E+00	5.402E-01	5.533E+00
133	3.810E-03	9.536E+00	5.295E-01	5.552E+00
134	4.270E-03	1.022E+01	5.553E-01	5.435E+00
135	4.800E-03	9.764E+00	5.459E-01	5.591E+00
136	5.390E-03	9.688E+00	5.473E-01	5.650E+00
137	6.050E-03	9.385E+00	5.367E-01	5.718E+00
138	6.790E-03	1.105E+01	5.832E-01	5.278E+00
139	7.620E-03	9.839E+00	5.482E-01	5.572E+00
140	8.550E-03	9.839E+00	5.434E-01	5.523E+00
141	9.600E-03	1.001E+01	5.457E-01	5.451E+00
142	1.080E-02	1.111E+01	5.900E-01	5.311E+00
143	1.210E-02	1.103E+01	5.880E-01	5.331E+00

144	1.360E-02	1.111E+01	5.889E-01	5.301E+00
145	1.530E-02	1.266E+01	6.304E-01	4.979E+00
146	1.710E-02	1.274E+01	6.355E-01	4.988E+00
147	1.920E-02	1.367E+01	6.527E-01	4.774E+00
148	2.160E-02	1.251E+01	6.263E-01	5.008E+00
149	2.420E-02	2.198E+01	8.481E-01	3.859E+00
150	2.720E-02	4.077E+00	3.520E-01	8.635E+00
151	3.050E-02	1.049E+01	5.770E-01	5.502E+00
152	3.430E-02	1.136E+01	6.024E-01	5.305E+00
153	3.850E-02	1.583E+01	7.227E-01	4.566E+00
154	4.320E-02	1.387E+01	6.632E-01	4.782E+00
155	4.850E-02	1.759E+01	7.575E-01	4.305E+00
156	5.440E-02	1.696E+01	7.418E-01	4.373E+00
157	6.110E-02	1.774E+01	7.655E-01	4.315E+00
158	6.860E-02	2.183E+01	8.575E-01	3.928E+00
159	7.700E-02	2.055E+01	8.233E-01	4.006E+00
160	8.650E-02	1.673E+01	7.365E-01	4.402E+00
161	9.710E-02	2.190E+01	8.620E-01	3.936E+00
162	1.090E-01	2.341E+01	8.863E-01	3.785E+00
163	1.220E-01	3.249E+01	1.060E+00	3.263E+00
164	1.370E-01	2.118E+01	8.404E-01	3.967E+00
165	1.540E-01	2.688E+01	9.499E-01	3.533E+00
166	1.730E-01	3.026E+01	1.017E+00	3.359E+00
167	1.940E-01	2.809E+01	9.703E-01	3.454E+00
168	2.180E-01	3.266E+01	1.058E+00	3.238E+00
169	2.450E-01	4.055E+01	1.190E+00	2.936E+00
170	2.750E-01	3.794E+01	1.150E+00	3.032E+00
171	3.090E-01	4.299E+01	1.241E+00	2.887E+00
172	3.460E-01	4.698E+01	1.314E+00	2.796E+00
173	3.890E-01	3.734E+01	1.138E+00	3.049E+00
174	4.370E-01	4.619E+01	1.301E+00	2.816E+00
175	4.900E-01	5.385E+01	1.423E+00	2.642E+00
176	5.500E-01	6.057E+01	1.533E+00	2.531E+00
177	6.180E-01	6.478E+01	1.601E+00	2.471E+00
178	6.940E-01	6.894E+01	1.678E+00	2.434E+00
179	7.790E-01	6.347E+01	1.591E+00	2.506E+00
180	8.740E-01	5.738E+01	1.481E+00	2.581E+00
181	9.810E-01	5.287E+01	1.394E+00	2.636E+00
182	1.100E+00	5.940E+01	1.515E+00	2.551E+00
183	1.240E+00	5.786E+01	1.481E+00	2.559E+00
184	1.390E+00	5.749E+01	1.476E+00	2.567E+00
185	1.560E+00	5.377E+01	1.387E+00	2.579E+00
186	1.750E+00	4.980E+01	1.316E+00	2.643E+00
187	1.960E+00	4.794E+01	1.275E+00	2.660E+00
188	2.210E+00	5.258E+01	1.365E+00	2.595E+00

189	2.480E+00	4.724E+01	1.233E+00	2.610E+00
190	2.780E+00	4.006E+01	1.110E+00	2.770E+00
191	3.120E+00	3.269E+01	9.767E-01	2.988E+00
192	3.500E+00	2.809E+01	8.890E-01	3.165E+00
193	3.930E+00	2.537E+01	8.303E-01	3.273E+00
194	4.410E+00	2.100E+01	7.484E-01	3.563E+00
195	4.960E+00	1.488E+01	6.147E-01	4.131E+00
196	5.560E+00	1.102E+01	5.220E-01	4.736E+00
197	6.240E+00	8.076E+00	4.599E-01	5.695E+00
198	7.010E+00	5.918E+00	3.899E-01	6.590E+00
199	7.870E+00	3.649E+00	3.027E-01	8.295E+00
200	8.840E+00	1.888E+00	2.222E-01	1.177E+01
201	9.920E+00	9.831E-01	1.634E-01	1.662E+01
	1.110E+01			

LIST OF REFERENCES

[1] A. W. Decker, “Verification and validation of Monte Carlo N-Particle Code 6 (MCNP6) with neutron protection factor measurements of an iron box,” M.S. thesis, PHY. Dept., AFIT., Wright-Patterson Air Force Base, OH, 2014.

[2] W. J. Erwin, “Verification and validation of Monte-Carlo N-Particle 6 for computing gamma protection factors,” M.S. thesis, PHY. Dept., AFIT., Wright-Patterson Air Force Base, OH, 2015.

[3] A. W. Decker, “Neutron protection factor measurement and simulation for a 2ft armored box at the White Sands Missile Range (WSMR) Fast-Burst Reaction (FBR),” West Point, NY, 2017.

[4] J. L. Hall, S. J. Ha, R. D. Prins and A. W. Decker, “Verification and validation of MCNP6.1 gamma protection factor estimates using an armored box and Phantom,” Journal of Radiation Effects, Research and Engineering, vol. 35, no. 1, pp. 103–110, 2016.

[5] G. F. Knoll, *Radiation Detection and Measurement*, 4th ed., Ann Arbor, MI: John and Wiley & Sons, Inc., 2010.

[6] K. Ferlic, “The phenomenon of pair production,” Releasing Your Unlimited Creativity, 2006. [Online]. Available: http://ryuc.info/creativityphysics /energy/pair_production.htm. [Accessed April 2017].

[7] Los Alamos National Laboratory, “Passive nondestruction assay of nuclear materials,” D. Reilly, N. Ensslin and H. Smith, Eds., Los Alamos, NM: Los Alamos National Laboratory, 1991.

[8] H. Caton, “Radiation transport calculations of a simple structure using the Vehicle Code System with 60-Group Cross Sections and the Monte-Carlo Neutron and Photon Code,” Ballistic Research Laboratory, Aberdeen Proving Ground, Maryland, 1989.

[9] W. A. Rhoades, “Development of a code system for determining radiation protection of armored vehicles (The VCS Code),” Oakridge, TN, 1974.

[11] ICRP, “Conversion coefficients for use in radiological protection against external radiation,” ICRP Publication 74., Ann. ICRP 26 (3-4), 1996.

[12] W. A. Roades, et al., *Vehicle Code System (VCS) User's Manual*, Oakridge National Laboratory, Oakridge, TN, 1974.

[13] M. B. Emmett, et al., *A User's Manual for MASH 1.0 – A Monte Carlo Adjoint Shielding Code System*, Oakridge National Laboratory, Oakridge, TN, 1992.

[14] *MCNP6.1 User's Manual*, 1st ed., Los Alamos National Laboratory, Los Alamos, NM, 2013.

[15] L. E. Peterson and S. Abrahamson, *Effects of Ionizing Radiation: Atomic Bomb Surivors and Their Children (1945–1995)*. Washington, DC: Joseph Henry Press, 1998.

[16] W. A. Rhoades and F. R. Mynatt, "The DOT III Two-Dimensional Discrete Ordinates Transport Code," Oak Ridge National Laboratory, Oak Ridge, TN, 1973.

[17] E. A. Straker, P. N. Stevens, D. C. Irving and V. R. Cain, "The Morse Code – A multigroup neutron and gamma-ray Monte Carlo transport code," Oakridge National Laboratory, Oak Ridge, TN, 1970.

[18] Radiation Safety Information Computational Center (RSICC). (2013). "RSICC Code Package CCC-810. [Online]. Available: https://rsicc.ornl.gov/codes/ccc/ccc8/ccc-810.html. [Accessed March 2017].

[19] Los Alamos National Laboratory. (2017). "A General Monte Carlo N-particle (MCNP) transport code. [Online]. Available: https://laws.lanl.gov /vhosts/mcnp.lanl.gov/references.shtml#mcnp6_refs_h. [Accessed March 2017].

[20] M. S. George and A. F. Spilhaus, "Operation JANGLE – Summary report: weapon effects tests," United States Department of Defense, Washington, D.C., 1952.

[21] R. P. Beckelheimer and R. E. Rexroad, "Attenuation of 1.2 MeV gamma radiation by Soviet and U.S. military vehicles and U.S. rail equipment," United States Army Chemical Center, Maryland, MD, 1953.

[22] R. A. Rydin and H. Caton, "Computational analysis of the effect of holes and gaps on the radiation protection factors of a lined steel box," United States Army Ballistic Research Laboratory, Aberdeen Proving Ground, MD, 1986.

[23] H. Caton and J. A. Morrissey, “Radiation protection factors of selected light vehicles against residual radiation,” United States Army Ballistic Research Laboratory, Aberdeen Proving Ground, MD, 1988.

[24] United States Army, “Army science and technology master plan: Volume I,” Washington, D.C., United States Army, 1992.

[25] C. R. Heimbach, “Research project of the radiation protection of a concrete bunker,” United States Army Ballistic Research Laboratory, Aberdeen Proving Grounds, MD, 2001.

[26] R. Radev, “Neutron spectra, fluence, and dose rates from bare and moderated cf-252 sources,” Lawrence Livermore National Laboratory, Livermore, CA, Tech. Rep. LLNL-TR-688699, Apr. 2016.

[27] *Ludlum Model Model 42–5 Neutron Ball Cart*, Ludlum Inc., Sweetwater, TX, 2015.

[28] *142A, B, and C Preamplifier Brochures*, ORTEC, Oak Ridge, TN, 2016.

[29] M. Reginatto, B. Wiegel, A. Zimbal and F. Langner, “UMG version 3.3: unfolding with MAXED and GRAVEL,” Physikalisch-Technische Bundesanstalt (PTB), Braunschweig, 2004.

[30] Radiation Safety Information Computational Center. (n.d.). “RSICC code package PSR-529,” Physikalisch-Technische Bundesanstalt (PTB). [Online]. Available: https://rsicc.ornl.gov/codes/psr/psr5/psr-529.html. [Accessed 04 May 2017].

[31] E. E. Lewis and W. F. Miller, *Computational Methods of Neutron Transport*. La Grange Park, IL: American Nuclear Society, 1993.

[32] K. Ivanov. (n.d). Chapter 1: The neutron transport equation. [Online]. Available: http://www.engr.psu.edu/cde/courses/nuce521 /nuce521_chapter1_reading.pdf. [Accessed 22 March 2017].

[33] Japan Nuclear Data Center. (n.d.) 26-Fe-56” Iron-56 isotope data. Japan Atomic Energy Agency. [Online]. Available: http://wwwndc.jaea.go.jp/cgi-bin/nuclinfo2014?26%2C56. [Accessed 10 MAY 2017].

[34] A. W. Decker, “The radiation protection factor white paper,” *Countering WMD Journal*, 15, pp. 28–36, 2017.

THIS PAGE INTENTIONALLY LEFT BLANK

INITIAL DISTRIBUTION LIST

1. Defense Technical Information Center
   Ft. Belvoir, Virginia

2. Dudley Knox Library
   Naval Postgraduate School
   Monterey, California